

---

**Granzyme H:**  
**A novel cell-death-inducing serine protease**

---

**Dissertation zur Erlangung des  
Doktorgrades der Naturwissenschaften (Dr. rer. nat.)  
der Fakultät für Biologie  
der Ludwig-Maximilians-Universität München**

Vorgelegt von  
**Edward Fellows**

aus  
**Wesel**

**München 2007**



**Eingereicht am:** 8.9.2007.....

**Mitglieder der Promotionskommission:**

Erstgutachter:           Prof. Dr. Elisabeth Weiß

Zweitgutachter:       Prof. Dr. Charles David

**Tag des Promotionskolloquiums:** 4.12.2007.....

**Doktorurkunde ausgehändigt am:** .....

Die Versuche zur vorgelegten Dissertation wurden in der Zeit vom April 2003 bis März 2007 in der Arbeitsgruppe von Dr. med. habil. Dieter Jenne, Abteilung für Neuroimmunologie am Max-Planck-Institut für Neurobiologie in Martinsried bei München durchgeführt.

Hiermit erkläre ich, daß ich diese Arbeit selbständig und nur unter Verwendung der angegebenen Quellen und Hilfsmittel angefertigt habe.

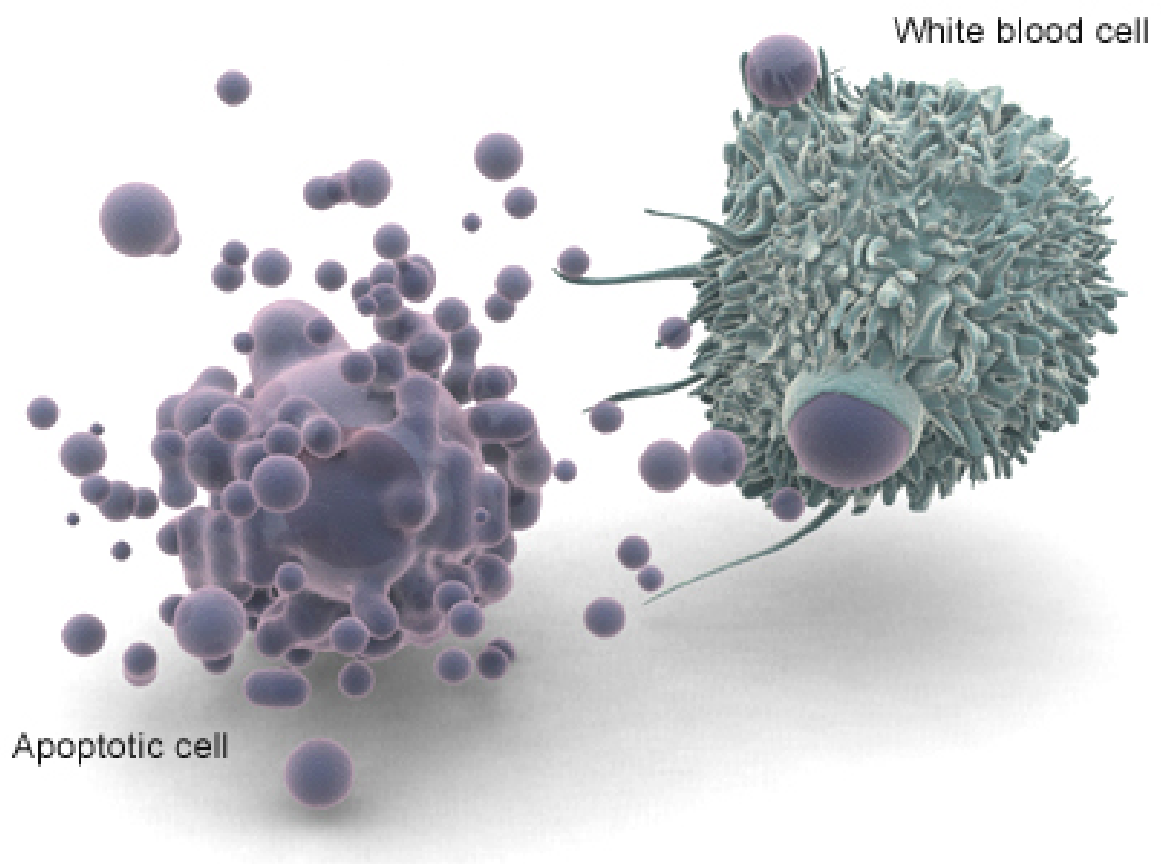
Martinsried, den 5. September 2007



*Dedicated to*

*my mother Patrícia and my father Leslie*

A macrophage engulfs the apoptotic bodies of a diseased cell in the final stages of apoptosis....



U.S. National Library of Medicine

## *Acknowledgements*

I would like to thank, primarily, PD Dr. Dieter Jenne, Dr. Florian Kurschus and Prof. Hartmut Wekerle for making this thesis, here at the Max-Planck-Institute of Neurobiology, possible. I am particularly fortunate to have been supervised and mentored by my boss, Dieter, and my colleague Florian. I am extremely grateful to Dieter for accepting me into his lab and for his continual guidance, support and advice throughout this thesis. Dieter, you are a master of your craft and a true fountain of knowledge! I also greatly acknowledge Florian. I have benefited tremendously from planning, conducting and discussing research with him; I thank him for his patience! Florian, cheers for being a most triumphant colleague but also a good friend. I am also grateful to Prof. Hartmut Wekerle for hosting me in the department of Neuroimmunology and, of course, for his continual interest in my PhD project.

I express my gratitude to Prof. Elisabeth Weiß for accepting to act as my principal supervisor at the biological faculty of the Ludwig Maximilian University here in Munich. Along with Prof. Weiß, I also kindly acknowledge the members of my thesis examination board from the Ludwig Maximilian University, namely Prof. Charles David, Prof. Hugo Scheer, Prof. Heinrich Leonhardt, Prof. Michael Schleicher and Prof. Michael Boshart.

I would also like to thank the members of my thesis committee here at the Max-Planck-Institute, which included Dr. Klaus Dornmair and Dr. Uwe Jacobe, for their helpful discussions and ideas.

I am also thankful to my co-authors. I am extremely grateful to Shirley Gil-Parrado who so willingly offered me her help and experience in the study of caspase activation. Shirley, the good times at Tiers will be remembered! Additionally, I am particularly grateful to Felipe Andrade; I thank him for a successful collaboration but also for widening my interests in the field of granzyme biology.

During my time here, I have benefited greatly from my fellow students and colleagues. I thank each and every one of them for making my experience in, and outside, the department a memorable one. To those of you from the “Jenne group”, namely Elisabeth Stegmann (alias “Lisa Minnelli”), Angelika Kuhl (alias “Ange”), Kai Kessenbrock (alias “K.K.”) and until recently Florian Kurschus (alias “Carlos”), it has been an pleasure working, and laughing, alongside you. In particular, I am indebted to Kai, not only for providing me with support and stimulating discussions during my thesis, but also for his invaluable friendship. Cheers mate for an unforgettable time here in Bavaria; Servus, and be true to the dunkel stuff! Very special thanks also go to some very special friends, namely all the gang from the European School and the Nuneham Courtney countryside mansion; you know who you are! Last, but not least, I thank my dear friends Sophie, Adrian, Simon and Philipp.

Needless to say, this entire exercise would have been an insurmountable task if it were not for my loving family. To my parents, Patricia and Leslie, I thank you for your continual input into my education; thank you for your consistent interest and encouragement but also for your critical advice. Above all, I thank you both for always being there for me. To my sisters, Rebecca and Amelia, I thank you for your love and support.

Finally, I dearly thank my fiancée Denitsa for her unceasing love and care throughout this entire endeavour.

## *Table of content*

<b>I</b>	<b>Summary</b>	<b>1</b>
<b>II</b>	<b>Introduction</b>	<b>3</b>
II.1	<b>Granzymes</b>	<b>3</b>
	Definition	3
II.1.1	<b>Human and mouse granzymes: genetic organization</b>	<b>3</b>
	Nomenclature	3
	Chromosome locations: family clusters and enzyme activities	3
	GzmB, GzmH and murine homologues	5
II.1.2	<b>Granzyme synthesis and storage</b>	<b>5</b>
	Proteolytic processing in three steps	5
	From zymogen to active serine protease, an example chymotrypsin	6
	Secretory granules store subdued active granzymes	7
II.1.3	<b>Structural characteristics of granzymes</b>	<b>7</b>
II.1.4	<b>Enzymes specificity of granzymes</b>	<b>8</b>
	Serine 195 of serine proteases	8
	The Schechter and Berger nomenclature	9
	Enzyme specificity	9
II.2	<b>Cytotoxic effector cells and granzyme cytotoxicity</b>	<b>11</b>
	The granule exocytosis model	11
	Granzyme delivery: where does perforin open the door to death?	13
	Granzymes: natural born killers	15
	Granzyme B	16
	Granzyme A	16
	Orphan granzymes	17
II.3	<b>Granzyme B and its multiple apoptogenic substrates</b>	<b>19</b>
	The caspase-dependent cell death pathway	19
	The caspase-independent cell death pathway	20
II.4	<b>Granzyme H</b>	<b>22</b>
II.5	<b>Granzymes and antiviral strategies</b>	<b>24</b>

---

II.6	<b>In vitro granzyme delivery by alternative pore-forming proteins</b>	25
	Bacterial streptolysin O (SLO)	25
	Mutant streptolysin O	25
	Bacterial Streptolysin O versus human perforin	25
II.7	<b>Aim</b>	26
<b>III</b>	<b>Materials &amp; Methods</b>	27
III.1	<b>Cloning in plasmid vectors</b>	27
	Plasmid DNA purification from E.coli	27
	DNA amplification	27
	DNA restriction digestion	28
	Agarose gel electrophoresis	28
	DNA purification from agarose gels	29
	DNA concentration and purity determination	29
	DNA fragment ligation	29
	Construction of expression plasmids	30
	Expression constructs	30
	DNA sequencing	31
III.2	<b>DNA transformation</b>	31
	Preparation of CaCl <sub>2</sub> competent cells	31
	Transformation of CaCl <sub>2</sub> competent cells	31
III.3	<b>Recombinant protein expression in <i>E.coli</i></b>	32
	The pET expression system	32
	Inclusion body (IB) isolation	34
	Solubilization of inclusion bodies	35
	Renaturation of IB proteins	36
	FPLC protein purification	38
	Granzyme activation: processing by cathepsin C	39
III.4	<b>Protein separation</b>	41
	SDS-polyacrylamide gel electrophoresis (SDS-PAGE)	41
III.5	<b>Protein Detection</b>	42
	Silver nitrate staining of proteins after SDS-PAGE	42

---

SDS-polyacrylamide gel Coomassie-blue staining	42
Western blot analysis: protein detection using chemiluminescence	43
Spectrophotometric determination of protein concentration	44
Colorimetric determination of protein determination	45
<b>III.6 Enzymatic tests</b>	45
Recombinant granzyme H activity assays	45
Recombinant granzyme H inhibition assays	46
<b>III.7 Apoptosis assays</b>	47
Culture of target cells	47
<b>III.7.1 Changes in membrane integrity</b>	47
FITC-annexin V and propidium iodide staining	47
Trypan blue staining	48
<b>III.7.2 Caspase activation</b>	49
Purified recombinant procaspases as potential substrates	49
Caspase activity in living cells	49
DNA laddering	50
Inhibitor of caspase activated DNase (ICAD) cleavage	50
<b>III.7.3 Mitochondrial damage</b>	51
Purified recombinant Bcl-2 family protein Bid	51
Mitochondrial transmembrane potential loss	51
Reactive oxygen species (ROS) production	52
Cytochrome c release	53
<b>III.7.4 Characterization of monoclonal GzmH antibodies</b>	53
<b>III.7.5 Isolation of peripheral blood leukocytes subsets</b>	54
Peripheral blood leukocyte subset isolation	54
Natural killer (NK) cell isolation	54
<b>III.7.6 NK cell cytotoxicity and granzyme release</b>	55
NK cell killing of target cells	55
GzmH release from NK cells	55
<b>III.7.7 Cellular morphology and nuclear fragmentation</b>	56
Apoptotic nuclei	56
Nuclear fragmentation	56
<sup>3</sup> H-thymidine release assay	57

<b>IV</b>	<b>Results</b>	58
<b>IV.1</b>	<b>Construction of the GzmH plasmids</b>	58
	pET24c(+)MKH <sub>6</sub> GzmH	58
	pET24c(+)MKH <sub>6</sub> GzmH <sup>S195A</sup>	58
<b>IV.2</b>	<b>Production of GzmH and variants from inclusion body material</b>	59
	GzmH expression yields high amounts of pure IB material	59
	Interchain disulphide bond rich GzmH IB are efficiently solubilized	60
	Renaturation and dialysis of GzmH results in correctly folded protein	61
	GzmH is efficiently purified via ion exchange FPLC	63
	Pure, converted GzmH variants are stored in physiological conditions	64
	Difference in yields between active and inactive GzmH	65
<b>IV.3</b>	<b>GzmH activity</b>	65
	GzmH has chymotrypsin-like (chymase) activity	65
	GzmH cleaves AMC based substrates	66
<b>IV.4</b>	<b>GzmH inhibition</b>	68
	GzmH is efficiently inhibited by the general protease inhibitor DCI	68
<b>IV.5</b>	<b>GzmH and apoptosis induction</b>	69
<b>IV.5.1</b>	<b>GzmH is a cytotoxic protease able to induce cell death</b>	69
	Sublytic PFN and SLO are essential for Gzm specific killing	69
	SLO delivered GzmH is able to induce cell death	70
	SLO delivered GzmH requires 10 to 12 hrs to efficiently kill target cells	72
	PFN delivered GzmH also efficiently kills K562 and HL60 cells	74
	GzmH triggered cell death is distinguishable under the microscope	75
<b>IV.5.2</b>	<b>GzmH induces nuclear fragmentation and chromosomal condensation</b>	78
	GzmH treated cells display fragmented nuclei with condensed chromatin	78
	GzmH mediated cell death causes a loss of typical cell-cycle peaks	80
	GzmH does not induce DNA laddering or ICAD cleavage	81
	GzmH induces the release of radioactively labeled nuclear DNA	82
<b>IV.5.3</b>	<b>GzmH does not activate main apoptosis executioner molecules</b>	83
	GzmH does not directly cleave recombinant effector caspases or Bid	83
	GzmH induced cell death does not activate initiator or effector caspases	85
	GzmH treatment does not lead to cytochrome c release	86
	GzmH triggered cell death leads to mild caspase 2 activation	87

---

Caspase 2 activity is not required for GzmH cell death	90
Cysteine proteases, the cathepsins, are not mediators of GzmH killing	91
<b>IV.5.4 GzmH induces mitochondrial damage and ROS production</b>	92
GzmH triggers mitochondrial depolarization	92
GzmH induces the release of mitochondrial reactive oxygen species	93
<b>IV.5.5 GzmH expression in NK cells and release during cytotoxic attack</b>	95
GzmH is expressed at high levels in CD3 <sup>-</sup> , CD56 <sup>+</sup> NK cells	95
GzmH is released from NK cells during killer cell attack	97
<b>V Discussion</b>	99
<b>V.1 Recombinant Granzyme production</b>	99
Eukaryotic and prokaryotic host systems	99
What are the advantages of refolding from E.coli IB material?	100
<b>V.2 Cytosolic delivery of granzymes by pore-forming proteins</b>	101
Human perforin versus bacterial streptolysin O	101
SLO is an appropriate substitute for perforin	101
<b>V.3 Cell death induction by GzmH</b>	102
GzmH treated cells are morphologically different	102
GzmH induces cell death independently of caspase activation	103
Is caspase 2 activity a prerequisite for GzmH mediated cell death?	104
Is cathepsin release a hallmark of GzmH induced cell death?	105
Is ROS release essential or an epiphenomenon in GzmH cytotoxicity?	106
Does GzmH trigger a different kind of DNA degradation?	107
GzmH cytotoxicity: an apoptotic or necrotic-like form of cell death?	109
<b>V.4 GzmH and its siblings</b>	111
Is GzmH cell death reminiscent of GzmA cytotoxicity?	111
GzmH and the orphan granzymes	112
Granzyme K	112
Granzyme M	113
<b>V.5 GzmH expression is restricted to NK cells</b>	114
Differential expression of human granzymes in resting lymphocytes	114
GzmH is predominantly expressed by NK cells	115
Does GzmH play a role in innate immunity?	116



---

<b>V.6</b>	<b>GzmH is an antiviral protease</b>	117
<b>V.7</b>	<b>Human and mice granzymes</b>	119
	Human and murine granzyme expression in cytotoxic lymphocytes	120
	GzmA <sup>-</sup> /GzmB <sup>-</sup> deficient mice	121
	Is GzmC the functional murine equivalent to human GzmH?	122
	GzmH homologs from different placental mammals	123
<b>VI</b>	<b>Conclusions and Outlook</b>	126
<b>VII</b>	<b>Literature</b>	128
<b>VIII</b>	<b>Abbreviations and Initialisms</b>	143
<b>IX</b>	<b>Appendix</b>	146
<b>X</b>	<b>Curriculum Vitae</b>	148
<b>XI</b>	<b>Publications and Meetings</b>	149

---

## ***I - Summary***

Cytotoxic lymphocytes are comprised of natural killer (NK) cells, specific to innate immunity, and cytotoxic T lymphocytes (CTLs) which man the adaptive immune response. These two cell types come equipped with an arsenal of cytotoxic granule-enzymes named granzymes (Gzms). Although NK cells and CTLs mediate the elimination of diseased cells in a number of different fashions, e.g. by FAS ligand or TNF $\alpha$  induced receptor-mediated cytotoxicity, the principal cytotoxic mechanism, known as the granule exocytosis pathway, delivers granzymes into the target cell cytosol, in a receptor independent manner, via the membrane perturbing perforin (PFN) of cytotoxic granules.

The human granzyme family is comprised of five members. Of these five, only two, namely granzyme A (GzmA) and granzyme B (GzmB), have received ample attention and are confirmed as being strongly apoptogenic. Of the remaining three, very little is known and, consequently, the trio has been labelled “orphan granzymes”. Recently however, advances in the field have confirmed that granzyme K (GzmK) and granzyme M (GzmM) are cytotoxic. Our granzyme of interest is granzyme H (GzmH). No functional studies have, until now, been performed on the protease and a physiological substrate remains to be found, leaving the question open as to whether the protease is indeed cytotoxic. Additionally, the importance of GzmH is underscored by the fact that structural equivalents are only present in placental mammals. In rodents, multiple copies derived from a common GzmH ancestral precursor do exist, but none of these granzymes can be regarded as a functional equivalent of human GzmH. To accomplish the goals of this thesis, we set out to develop a procedure to produce recombinant GzmH. Our method utilized inclusion body material from *Escherichia coli* (*E. coli*) as the starting material for *in vitro* refolding, a technique which successfully allowed us to purify catalytically active recombinant GzmH, along with its inactive variant, in large quantities and in highly pure form.

Several studies have recently shown GzmH to be constitutively and highly expressed in human NK cells and to possess chymotrypsin-like (chymase) enzymatic activity. In this work, we show for the first time that GzmH efficiently kills cells after entry into the targeted cytosol. Using PFN, but more specifically its bacterial counterpart streptolysin O (SLO), as translocators of granzymes across the target cell plasma membrane, GzmH-induced cell death was characterized by apoptotic morphology such as increased granularity, condensed nuclei, membrane irregularities and phosphatidyl serine externalization. Additional hallmarks, such as mitochondrial depolarization, ROS generation and DNA degradation also defined cell death mediated by this chymotrypsin-like protease. Contrary to GzmB, however, cell death by GzmH did not involve the activation of the executioner caspases, the cleavage of Bid or ICAD, or the release of cytochrome c. During this study, we also verified the expression of

GzmH in various leukocyte populations while attempting to prove that the granule protease is indeed released upon cytotoxic attack into the immunological synapse. As previously reported, we confirm that GzmH is constitutively expressed in NK cells and demonstrate, in a strictly controlled manner, that following target cell attack, GzmH can be detected in the medium supernatant by immunoblotting.

In summary, our data demonstrate that GzmH is a functional cell-death-inducing protease of killer cell granules and its high expression in NK cells and release during target cell killing suggest a pivotal role for the granzyme in innate immunity. In addition, in recent collaborative work, headed by Felipe Andrade, we also demonstrated that GzmB and GzmH have anti-adenoviral activity. Excitingly, the study reveals that both granzymes work in synergy to outsmart viral defense mechanisms. Indeed, in the event of GzmB inhibition GzmH, is not only able to cleave a common vital viral protein, but, interestingly, can also free GzmB from inhibition. It seems, too, that on top of their abilities to mediate cell death, granzymes have also acquired alternative strategies to overcome viral infection.

## ***II - Introduction***

### ***II.1 - Granzymes***

#### ***Definition***

In 1986, while attempting to understand the mechanisms by which cytotoxic lymphocytes achieve target cell lysis, a group from the University of Lausanne in Switzerland, lead by Jürg Tschopp, first employed the term Granzyme (Gzm) to describe the expanding family of Granule-associated Enzymes found uniquely within these cells (Masson et al., 1986).

Granzymes are chymotrypsin (CHT)-like serine proteases expressed in the secretory granules of CTLs and NK cells. Upon the encounter of diseased cells, granzymes are released by exocytosis, along with other granular proteins, into the immunological synapse where they are subsequently taken up into rogue cells via the actions of the pore forming protein perforin (PFN). Once in the target cell cytosol, granzymes proteolytically cleave a variety of death substrates that, in turn, lead to eventual cell suicide.

#### ***II.1.1 - Human and mouse granzymes: genetic organization***

##### ***Nomenclature***

Granzymes are a highly conserved set of serine proteases that are present in all placental mammals. Mice and humans are the most studied species accounting for fourteen members between them, mice possessing a present tally of ten members, while humans have five. Interspecies comparisons between the present mouse and human granzyme cDNA reveal that certain members have near identical nucleotide sequences and, as homologues, should thus share the same alphabetic nomenclature. The human and mouse granzyme homologues are granzymes A, B, K and M. The remaining mouse members include granzymes C, D, E, F, G and N whereas solely granzyme H (GzmH) remains to complete the human family. Coincidentally, the above group of mouse granzymes is linked to GzmH in that they are also referred to as “orphan” granzymes.

##### ***Chromosome locations: family clusters and enzyme activities***

The human and mouse granzyme genes are situated on three separate chromosomes where they are contained within separate clusters named after GzmA, GzmB and GzmM respectively. The GzmA cluster, found on chromosome 5 in humans and on chromosome 13 in mice, harbours GzmA and

GzmK. Both proteases are tryptases indicating their preference to cleave after basic residues such as arginine and lysine. In both species, the second cluster is located on chromosome 14 and is named after the most studied of all granzymes, GzmB. In this tightly linked gene cluster, the GzmB gene is linked with the cathepsin G (CG) and mast cell chymase genes, the only difference between men and mice being the presence of the mouse granzyme genes C, D, E, F, G and N in-between *GzmB* and *CG*, whereas in humans only *GZMH* occupies this space. GzmB cleaves caspase 8-like specific sequences after acidic residues. In contrast, GzmH, like mast cell chymase and CG, has chymotrypsin-like activity with a preference for hydrophobic, aromatic amino acid residues (Phe or Tyr) at the P1 site (Edwards et al., 1999). The proteolytic activities of the mouse orphan granzymes remain unknown. The GzmM gene cluster is the third, and last, granzyme locus, the human granzyme residing on chromosome 19 and the mouse counterpart on chromosome 10. Granzyme M is a metase and prefers to cleave after residues with long, uncharged side chains such as methionine and leucine (Kelly et al., 2004; Smyth et al., 1993). In humans, GzmM is linked to the neutrophil elastase (NE) gene cluster that contains genes such as proteinase 3 (PR3). NE and PR3 are also granular serine proteases that once released from neutrophils are reported to participate in microbial removal and neutrophil migration through the extracellular matrix at sites of inflammation (Jenne, 1994; Pham et al., 1996; Sugawara, 2005).

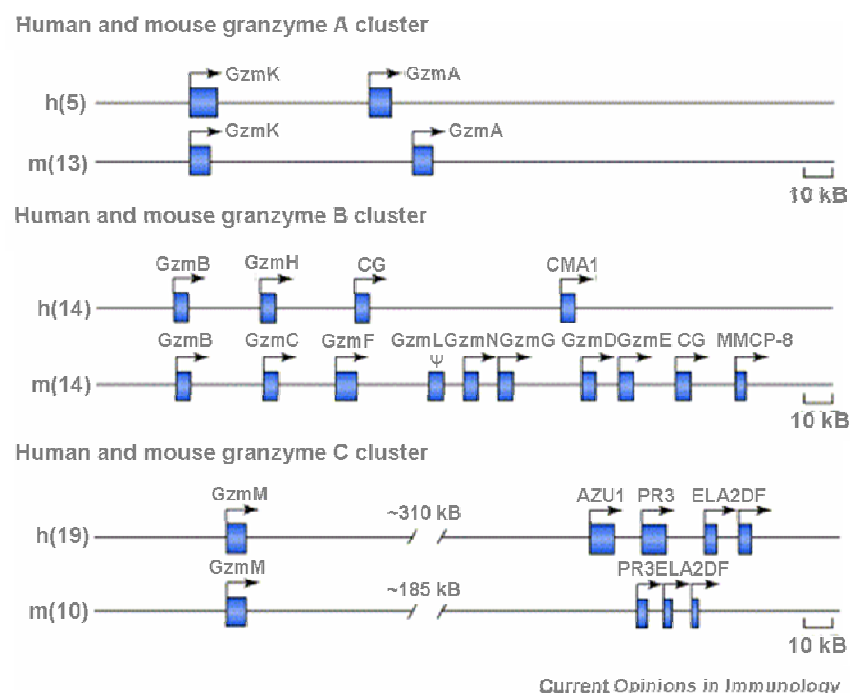


**Figure II.1 - Human and mouse granzyme gene clusters.** Closed boxes represent both exons and introns, and are drawn to scale. Arrows indicate the direction of transcription within the loci. Abbreviations are described as follows:  $\Psi$ , pseudogene; AZU1, azurocidin; CMA1, mast cell chymase 1; DF, D component of complement/adipsin; ELA2, mouse elastase 2; ELA2, human neutrophil elastase; h, human; m, mouse; MMCP-8, mouse mast cell protease 8; PR3, proteinase 3. Taken from "The orphan granzymes of humans and mice" Current Opinions in Immunology (Grossman et al., 2003).

### ***GzmB, GzmH and mouse homologues***

It is the GzmB cluster, on chromosome 14, which is home to our gene of interest, namely *GZMH*. *GZMH* is neighbour to *GZMB*, lying just downstream. Moreover, the two proteases share the highest structural homology (71% amino acid identity) in the human granzyme family and cDNA comparisons between the members of the mouse GzmB gene cluster, reveal that the mouse *GzmB* is also most closely related to its immediate down stream partner, namely *GzmC*. Despite the high sequence homologies between the human and mouse GzmB and their respective downstream neighbours, both enzyme pairs display very distinct enzymatic activities. As described previously, in both humans and mice, GzmB is an aspartase cutting after aspartate residues whereas GzmH is a chymotrypsin-like proteinase. Although the enzymatic activity of GzmC still remains to be determined, a functional study has recently demonstrated that the granzyme is distinct from mouse GzmB in that it is capable of inducing cell death in a caspase-independent manor (Johnson et al., 2003). It has been proposed that *GzmC* is the mouse homologue of *GZMH*. Recently, molecular modelling has predicted GzmC to cleave after asparagine, or serine, at the P1 position, while GzmD through to G are said to prefer leucine, or more interestingly phenylalanine, as is the case for GzmH (Grossman et al., 2003; Trapani, 2001). At present, however, none of these related mouse genes can, as yet, be regarded as functional GzmH homologue.

## ***II.1.2 - Granzyme synthesis of storage***

### ***Proteolytic processing in three-steps***

Granzymes are synthesized in the endoplasmic reticulum (ER) as pre-pro-enzymes and finally reach the status of “active-granular-enzyme” after a three-step conversion process. The signal-peptide, or pre-sequence, is 18 to 24 residues long and is required for the compartmentalization of the nascent granzyme into the ER, following translation. The propeptide, in turn, then ensures that the protease remains inactive during its transport through the ER and Golgi network, thus preventing inappropriate or premature degradation of substrates.

Like other serine proteases of hematopoietic-cell secretory granules, such as the previously mentioned CG, NE and PR3, granzymes are synthesized as zymogens that must be converted to their mature form by intracellular proteolysis. The propeptide consists of very short dipeptides (usually Gly-Glu or Glu-Glu) and is processed by the broadly reactive lysosomal enzyme dipeptidyl peptidase I (DPPI), an exopeptidase otherwise known as cathepsin C (Kummer et al., 1993; McGuire et al., 1993) (refer to *Figure IV.5* page 65 and for a detailed description of cathepsin c to material and methods page 40).

With the exception of GzmM, which carries a hexapeptide, the remaining granzymes all possess dipeptide pro-sequences. Once the propeptide is removed, the granzyme, its N-terminus now starting with the highly conserved sequence Ile-Ile-Gly-Gly (refer to appendix), will finally acquire an active and mature status by undergoing conformational change. Indeed, the catalytic domains of granzymes harbour flexible stretches that only achieve functional conformation by cleavage of the propeptide.

The importance of the amino-terminal propeptide cleavage event has been illustrated experimentally by expressing recombinant GzmB either with or without the amino-terminal dipeptide (Caputo et al., 1993). Furthermore, it has been shown that CTL effector function is impaired in response to inhibition of dipeptidyl peptidase I activity (Thiele et al., 1997). On the contrary though, a study on the cellular consequences of cathepsin C deficiency found in the human Papillon-Lefevre syndrome surprisingly reports that the absence of DPPI is not essential for the activation of GzmA and GzmB, although it is required for the optimal activation and stability of these proteases. The deficiency is also associated with the severe reduction in the activity of the neutrophil-derived serine proteases CG, NE and PR3 (Pham et al., 2004).

Finally, a third, not so well characterized cleavage event has been reported to take place in the processing of the azurophilic granule enzyme neutrophil elastase (NE). In addition to pre-pro sequences, NE also contains a proteolytically processed 19-residue C-terminal extension which is reported not to be required for proteolytic activity and granule localization (Benson et al., 2003; Matsumoto et al., 1995). However, it has recently been shown that some diseases stem from the inability to remove the NE C-terminal extension, thus preventing its interaction with AP3, a trafficking protein, resulting in the misdirection of the protease to membranes, and not granules, the default destination for cargo proteins in the absence of AP3 (Horwitz et al., 2004). The later event has not been reported to take place in granzyme processing.

### ***From zymogen to active serine protease, an example: Chymotrypsin***

The chymotrypsin-like proteases are the most abundant proteases in nature and are unique in that their catalytic domain exhibits allosteric properties, the "activation domain" oscillating between a more loosely folded "inactive" and a compact "active" conformation (Branden and Tooze 1991). Let us take the example of chymotrypsin. Removal of the propeptide sequence is, in this case, managed by trypsin or enterokinase cleavage of the Arg15-Ile16 peptide bond (chymotrypsin numbering), thus resulting in a new N-terminus starting with residue Ile16. Ile16 then proceeds to form a salt bridge with the carboxylate side chain of Asp194, thereby, initiating the formation of the mature, active protease through conformational change. These conformational changes occur in the segment lying between Ser189 and Asp194. As mentioned above, metaphorically, the segment resembles a loop pointing

inwards in the zymogen, but following conversion, then changes to point outwards, towards the solvent, thus forming a reconstructed activation domain which houses a substrate recognition site, oxyanion hole and S1 specificity pocket. Processing and conformational change result in a mature, active chymotrypsin, its N-terminus now protected from any further attack from exopeptidases such as enterokinase and cathepsin C.

### ***Secretory granules store subdued active granzymes***

Following their synthesis and initial processing in the lumen of the ER and Golgi apparatus, granzymes are sent to cytotoxic granules in which they are packaged together with other granule components (Matsumoto et al., 1995). The location of the final processing event, leading to full protease maturation is not yet known. Inhibition of zymogen activation though suggests that secretory proteases only become fully mature in post-Golgi organelles (Benson et al., 2003; Matsumoto et al., 1995; Rao et al., 1996). Indeed, preventing the premature activation of proteases, such as the granzymes, until they reach secretory granules, can only be advantageous to the host cell. To ensure that secretory zymogens arrive at their intended destination they are subject to glycosylation. The added sugars, which include mannose-6-phosphate residues, are important for targeting proteases, such as GzmA and GzmB, to cytolytic granules although other targeting mechanisms are likely to exist (Griffiths and Isaaz, 1993). Indeed, both GzmK and mouse GzmC, which lack consensus sequences for N-glycosylation, are transported via different mechanisms. Once installed, the mature granzymes (overall positively charged) are kept inactive by sitting tightly packed, in favourable ionic conditions, to chondroitin sulfate proteoglycans (negatively charged) in an acidic environment of pH 5.5 (Masson et al., 1990). Whether or not the granzyme-proteoglycan attachment is retained upon cytotoxic stimulation and granule-content release into the immunological synapse remains unclear. However, Spaeny-Dekking et al. in 2000 demonstrated that in patients with various viral diseases and rheumatoid arthritis, GzmA was found at elevated levels and that a certain percentage of GzmA was still found complexed to proteoglycans. It is postulated that this interaction might protect the protease against plasma inhibitors. Furthermore, the results support the notion that granzymes may exert extracellular functions distant from the site of CTL or NK cell interaction with their target cells (Spaeny-Dekking et al., 2000).

### ***II.1.3 - Structural characteristics of granzymes***

Granzymes not only need the precise three-dimensional arrangement of catalytic residues to function, they also rely on nonspecific, main chain substrate interactions and other key structural features such



the previously mentioned oxyanion hole to stabilize transition states of the enzyme-substrate complex. Additionally, residues making up a feature called the specificity pocket determine the protease's specificity or nature of the peptide bond to be cleaved. As we have seen, processing of the maturing granzyme triggers the formation of the precise conformation required to provide these features that together determine the enzyme's specificity (Trapani, 2001).

The activity of granzymes, as with all members of the CHT-like family, depends on the highly conserved amino acid triad, His57 Asp102 and Ser195 (chymotrypsin numbering), otherwise known as the catalytic triad. Other conserved residues include those that are involved in the formation of the oxyanion hole (193 and 195), those involved in nonspecific main chain substrate binding, residues 189, 216 and 226, which are important in determining the specificity pocket, and cysteine residues required for disulphide bridge formation.

Granzymes also display features that are not seen in other CHT-like family members. For instance, the mature enzymes found in granules share a strictly conserved N-terminal sequence from positions +1 to +4 (Ile-Ile-Gly-Gly) and positions +9 to +16 (Pro-His-Ser-Arg-Pro-Tyr-Met-Ala) as well as the previously mentioned propeptide sequence consisting of either Gly-Glu or Glu-Glu. Cysteine (Cys) residues involved in disulphide bond formation are also highly conserved in the granzyme family. Apart from GzmA, most chromosome 14 granzymes characteristically contain three disulphide bridges and lack a bridge between Cys-191 and Cys-220 otherwise present in CHT family members such as CHT, trypsin and elastase. Again, in contrast to other granzymes, GzmA possesses a free cysteine (93) at its carboxyl terminal allowing the protease to exist as a stable, disulphide-linked 60 kDa homodimer (Fink et al., 1993; Hink-Schauer et al., 2003).

### ***II.1.4 - Enzyme specificity of granzymes***

#### ***Ser195 of serine proteases***

Proteases are a group of enzymes that catalyze the hydrolysis of covalent peptide bonds. Indeed, in the case of serine proteases, such as granzymes, once a substrate attaches to the enzyme at the main chain binding site and specificity pocket, with the scissile bond (substrate bond to be cleaved) exposed to the previously mentioned catalytic triad, a nucleophilic attack on the targeted peptide bond is initiated by the triad residue Ser195, explaining the family's nomenclature. In many cases, the nucleophilic property of the group is improved by the presence of a histidine, held in a "proton acceptor state" by an aspartate. Thus, the aligned side chains of His57, Asp102 and Ser195 build the catalytic triad in serine proteases, the serine initiating a nucleophilic attack on the scissile amide bond, a required first

step in the hydrolysis of substrate peptide bonds. The chapter entitled “enzyme specificity” shows the specificity pocket of GzmH, our enzyme of interest. As we shall discuss later, GzmH prefers bulky, hydrophobic amino acids such a phenylalanine (refer to *Figure III.2A*) and tyrosine. The catalytic triad allows the initiation of the proteolytic activity that will also be discussed in the next chapters.

### ***The Schechter and Berger nomenclature***

The active site of serine proteases is shaped as a cleft where the amino acids of polypeptide substrates bind to enzyme subsites. In 1967, Schechter and Berger introduced a nomenclature to describe the interaction between enzyme and substrate. The enzyme subsites were termed S, after subsite and the substrate residues P, after peptide. The amino acids located on either side of the scissile bond, where the cleavage occurs, are named P1 and P1' and those residues leading towards the N-terminus and C-terminus are named P2, P3, P4 etc. and P2', P3', P4' respectively, their respective enzyme subsites numbered accordingly (Schechter and Berger, 1967).

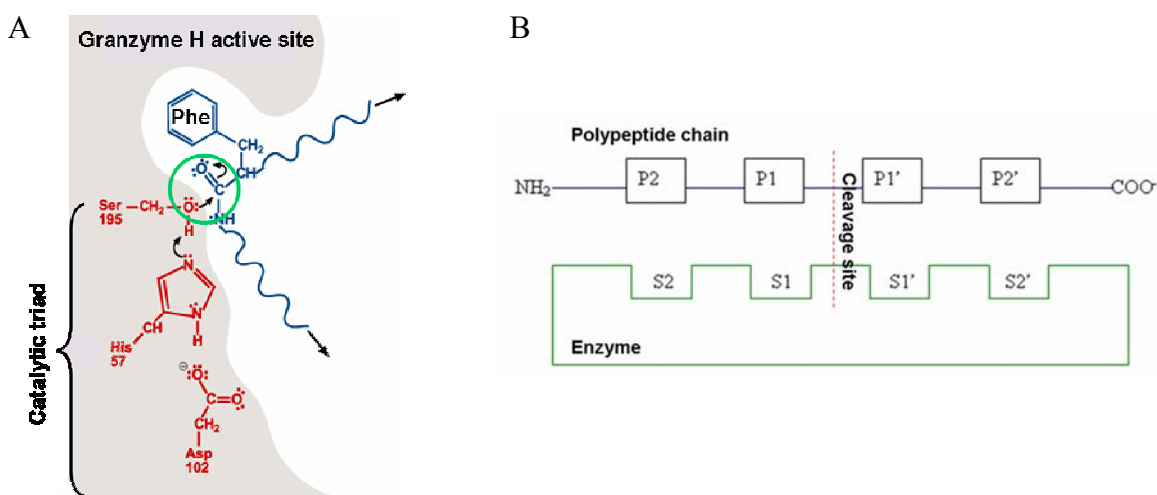


**Figure II.2 – The GzmH active site and the Schechter and Berger nomenclature.** (A) The active site of GzmH prefers bulky, hydrophobic amino acids such a phenylalanine and tyrosine. The catalytic triad allows the initiation of proteolytic activity, serine 195 initiating a nucleophilic attack on the scissile amide bond (green circle). (B) The general nomenclature for the substrate cleavage site positions was formulated by Schechter and Berger in 1967. They designate the cleavage site between P1-P1', the numbering in direction of the N-terminal of the cleaved peptide bond continuing as P2, P3, P4, etc. On the carboxyl side the numbering is notated likewise, P1', P2', P3' etc.

### ***Enzyme specificity***

The serine proteases exhibit different substrate specificities which are related to amino acid substitutions in various enzyme subsites (see nomenclature of Schechter and Berger) interacting with the substrate residues. Some enzymes have an extended interaction site with the substrate, whereas others have a specificity restricted to the P1 substrate residue. The granzyme family members have very similar three-dimensional structures but differ in specificity. Indeed, the 3D structure

determinations by X-ray crystallography of GzmA, GzmB and GzmK have allowed the analysis of their respective active sites. GzmA and GzmB cleave adjacent to positively charged and acidic side chains respectively (Estebanez-Perpina et al., 2000; Hink-Schauer et al., 2003) whereas GzmH has been shown to preferably cleave after bulky aromatic residues (Edwards et al., 1999). The three residues at positions 189, 216 and 226 are responsible for these preferences and together form the biophysical properties of the S1 specificity pocket.

Residues 216 and 226 line the walls of the pocket. In most granzymes, such as GzmA and GzmH, these amino acids are both Gly and because of their small size, allow side chains of the substrate to penetrate easily into the specificity pocket (see *Figure II.3*). GzmB however, preferably accommodates a negatively charged residue such as Asp or Glu at the P1 position forming a salt bridge with the guanidinium group of Arg226 at the top of the S1 pocket (Estebanez-Perpina et al., 2000). This probably explains why bulky residues such as Phe cannot be accommodated.

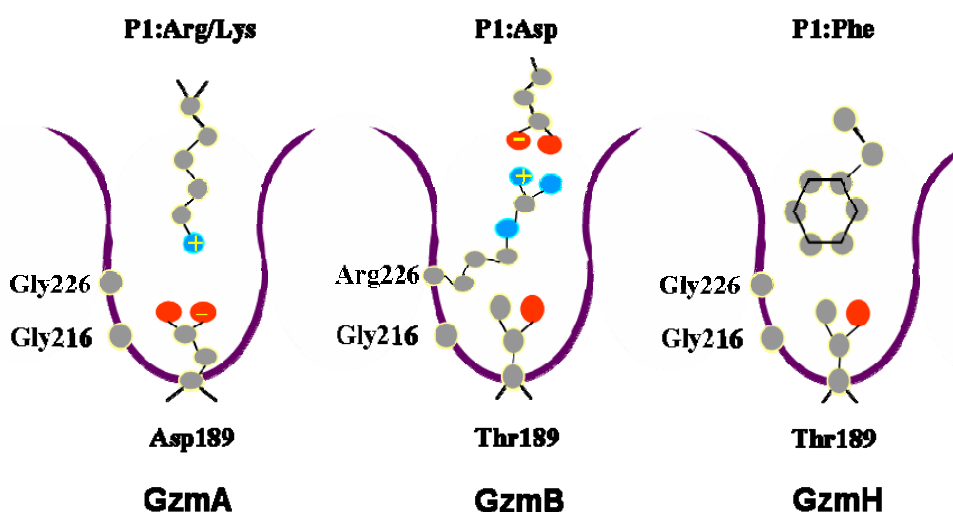


**Figure II.3 - Schematic diagrams of granzyme specificity pockets.** The representations illustrate the preferences of granzymes A, B and H for side chains adjacent to the scissile bond in polypeptide substrates. GzmA prefers a positively charged side chain that can interact with Asp189. GzmB, on the other hand, shows preference for a negatively charged, acidic amino acid, namely Asp, a specificity that is attributed to the Arg in position 226. GzmH, like GzmA displays an open specificity pocket and prefers aromatic side chains such as Phe. The blue circles represent nitrogen and red circles oxygen. Charge is indicated in yellow.

Residue 189 (S1 position) is at the bottom of the specificity pocket and can interact with the P1 residue of the substrate. Indeed, the 189 residue of trypsin, like that of GzmA, is an Asp that interacts positively with the substrate side-chains of Lys or Arg accounting for its cleavage preference. However, in the case of chymotrypsin or GzmH, Ser or Thr can occupy the S1 position, both residues being small and aliphatic except for the presence of a polar hydroxyl group on each. Bulky aromatic P1 side-chains, such as Phe or Tyr, are here preferred as they can fill up the mainly hydrophobic pocket. Interestingly, the preference of GzmB for acidic P1 amino acids such as Asp or Glu is

attributed to Arg226 and not Thr189. Indeed, as previously mentioned, Arg226 is involved with the negatively charged carboxylate group of Asp. Cleavage on the carboxyl side of Asp residues is unique to GzmB in the granzyme family but it is also the requirement of another family of proteases, the caspases, which are intimately connected with cell death (Perfettini and Kroemer, 2003; Wolf et al., 1999).

In some instances, cross-reactivity may be expected at P1. This is the case for GzmA and GzmK, which both show a preference for basic residues such as Lys and Arg, or for the chymotrypsin-like enzymes, such as chymase and GzmH, which tolerate aromatic residues such as Phe and Try. Here, the distinct specificities at P2 to P4, and also at P1'-P4', should further contribute to selectivity.

## ***II.2 - Cytotoxic effector cells and granzyme cytotoxicity***

CTL and NK cells are the two main types of cytotoxic effector cells of the immune system. In recent years, it has become increasingly clear that both cell types share common effector mechanisms, both granule- and receptor-mediated, that induce target cell death. Granule-mediated cell death or “granule exocytosis” destroys unwanted cells by releasing the content of host cytotoxic granules, namely perforin and granzymes, into the immunological synapse before it is then taken up into the target cell. Alternatively, target cells perish through stimulation of cell-surface receptors, such as the members of the tumor-necrosis factor receptor (TNF-R) family, including FAS (CD95). Of these different mechanisms, findings in genetically manipulated mice, human genetics diseases and *in vitro* studies, show that the granule exocytosis pathway has the dominant role in eliminating viral infections, intercellular pathogens and tumor cells (Balkow et al., 2001; Kagi et al., 1994). Indeed, *in vitro* experiments have revealed that effector cells prefer to kill via the granule mediated pathway and that only when the latter is interrupted do levels of FAS stimulation increase. A plausible explanation for this phenomenon might be the fact that CTL and NK cell granules come pre-loaded with cytotoxic proteases, the granzymes, and hence killing through this pathway occurs more rapidly (Barry and Bleackley, 2002).

### ***The granule exocytosis model***

Although granzymes may possess a number of different functions it is now widely accepted that the family's major business lies in the heart of cytotoxic effector cell function and, more specifically, in the granule-mediated response to diseased cells (Griffiths and Isaaz, 1993). The first ideas on how these effector cells achieved cell death were rather simple and it was initially believed that mere

membrane damage would suffice. It has now become evident, however, that this is not the case and that more complex cell death pathways are at work (Shresta et al., 1999).

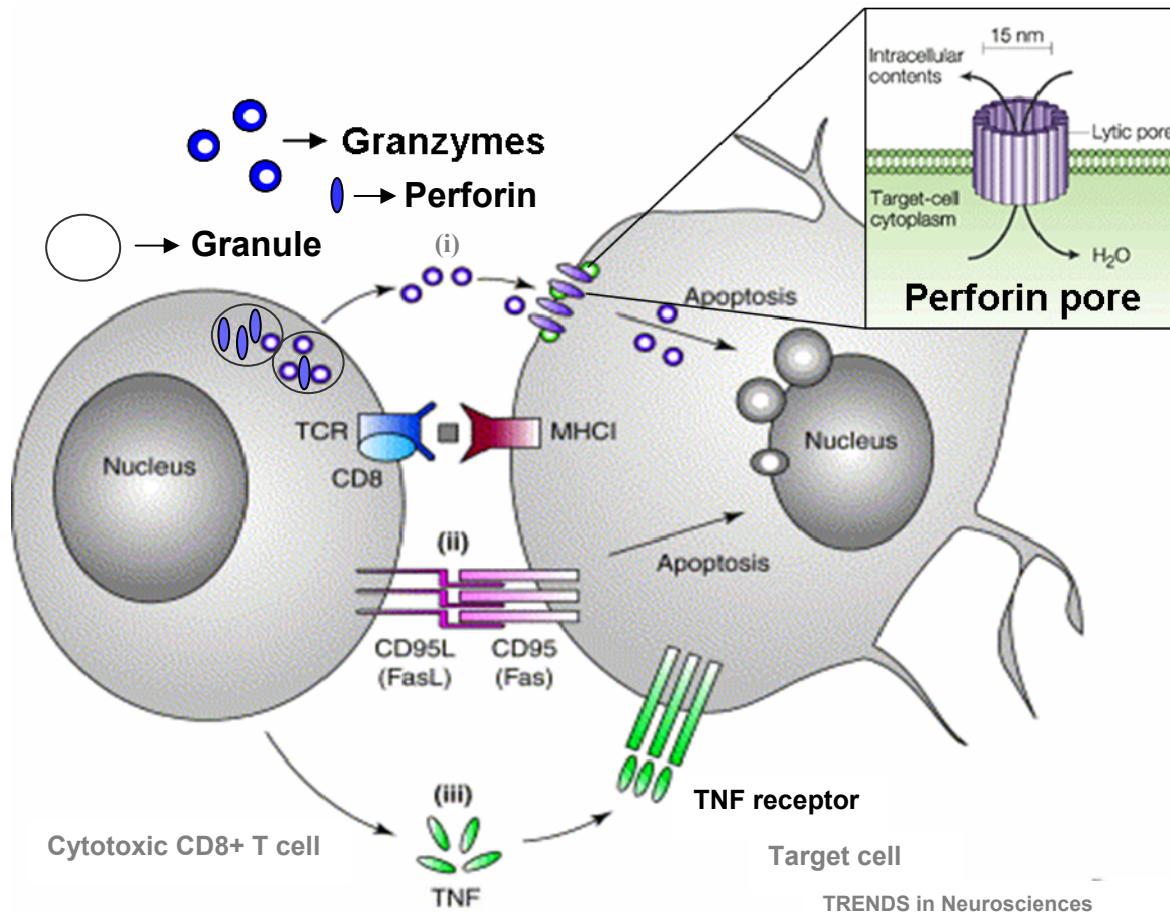


**Figure II.4 - CTLs trigger different pathways to achieve target cell destruction.** CD8<sup>+</sup> CTLs recognize their targets cells by binding of its T-cell receptor (TCR) to the appropriate combination of major histocompatibility complex (MHC I) and peptide (here represented as a square). Destruction of the target, which can also be performed by natural killer (NK) cells (which do not require the TCR-MHC I recognition) is mediated by (i) the secretion of cytotoxic granule content, i.e. perforin and granzymes, resulting in cell death induction once perforin (PFN) allows the passage of granzymes across the plasma membrane. (ii) the activation of FAS/CD95 receptors by FAS ligand/CD95 ligand (FASL) triggering apoptosis, and (iii) the release of cytokines, such as tumor necrosis factor (TNF). Taken from Trends in Neuroscience (Neumann et al., 2002).

Our understanding of how CTL and NK cells deliver their granule content was greatly increased after microscopical analysis, based on effector-target cell interactions, revealed that engagement was transient and sequential. Additionally, it was shown that upon target cell interception, effector organelles, such as the microtubule-organizing centre, the Golgi and the lytic granules began to reorganize, rapidly orientating themselves towards the site of conjunction (Kuhn and Poenie, 2002; Stinchcombe et al., 2001; Stinchcombe and Griffiths, 2006). Furthermore, it was also demonstrated that acid phosphatase, that is normally restricted to lytic granules, was found at the site of site of

effector-target cell engagement (Zagury, 1982). The above observations combined with preliminary data on the content of lytic granules lead to the formulation of the cytotoxic granule exocytosis model (Henkart, 1985; Zagury, 1982) which, although now more complex, remains valid today (Lieberman, 2003). The original description of granule exocytosis suggests that the process involves the rearrangement of the effector cell cytoplasm after which perforin (PFN), a calcium sensitive pore-forming protein, is released and delivered to the target cell. Indeed, PFN was first described as the key effector protein of lytic granules (Henkart, 1985) but the exocytosis model has now become much more complex, the granules harboring other key molecules released upon killer cell attack.

***Granzyme delivery: where does perforin open the door to death?***

Perforin (PFN) was the first component of effector cell lytic granules to be discovered, along with cytolyisin, (Podack and Konigsberg, 1984) and is exclusively found in CTL and NK cells where it plays a pivotal role in the induction of granule mediated cell death. The importance of PFN has been demonstrated with both cytotoxic cells and mice deficient in the protein. Indeed, cytotoxic lymphocytes from PFN deficient mice are unable to efficiently trigger target cell apoptosis and PFN knockout mice are profoundly immunodeficient, showing an enhanced susceptibility to viral infections and tumour growth (Kagi et al., 1994; Rossi et al., 1998; van den Broek et al., 1996). Earlier studies define PFN as a cytotoxic membrane damaging agent that triggers cell death by damaging the target cell plasma membrane (Dennert and Podack, 1983; Dourmashkin et al., 1980; Podack and Konigsberg, 1984). More recent work however, clearly demonstrates that the protein alone is unable of triggering all the features associated with CTL/NK induced cell death (Shresta et al., 1999). As expected, other granule components are involved in the exocytosis pathway, their presence necessary in order to achieve the full array of morphological and biochemical cell death characteristics (Stinchcombe et al., 2001). Granule mediated cell death is therefore a concerted effort which, along with PFN, requires the presence of other granule proteins. The above observations lead to the original hypothesis that PFN allows the entry of cytotoxic granule components into the target cytosol by building multimeric pores on the plasma membrane (Stinchcombe et al., 2001). See *Figure II.4*.

The initial plasma membrane pore model, mentioned above, was put into doubt when a recent study showed that granzymes do not require the presence of PFN to be endocytosed into endosomes despite target cells remaining healthy (Edwards et al., 1999). If PFN is not required for granzyme uptake into endosome-like vesicles, then where does the pore-forming protein act to liberate granzyme into the target cell cytosol? To help answer these questions, PFN was added to target cells which had already internalized granzymes. Soon thereafter, features of CTL induced cell death were detectable. It now seemed likely that granzymes require the actions of PFN once they are safely endocytosed within target cell endosomes (Trapani et al., 1998; Zhang et al., 2001). However, the idea that PFN, acting

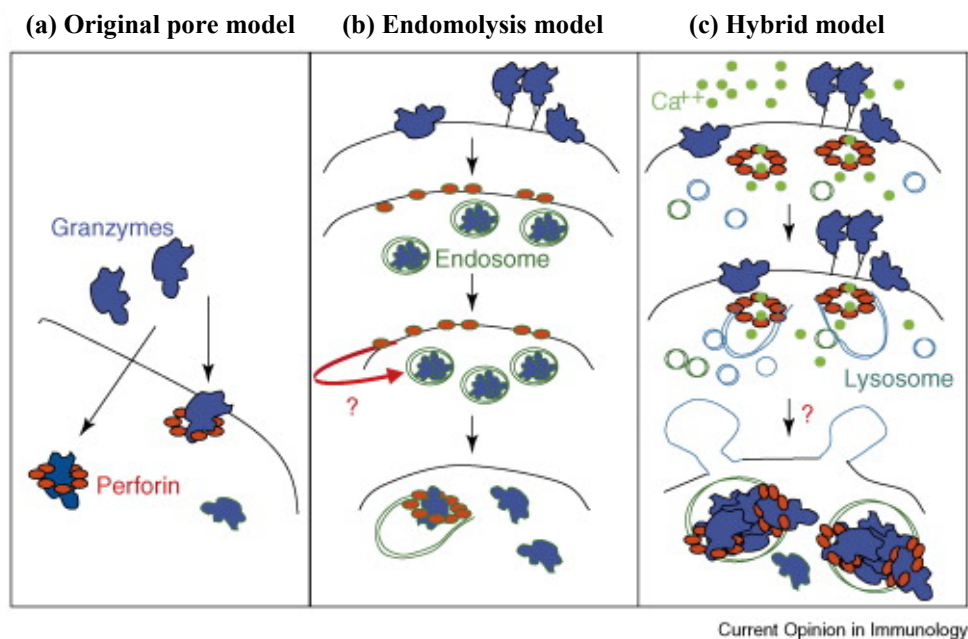
from outside the target cell, could trigger the release of granzymes contained within endosomes seemed somewhat unrealistic. Revised studies revealed that once internalized, if real care is taken in removing all surface-bound GzmB, PFN was actually unable to effectively deliver the previously endocytosed granzymes (Babe et al., 1998) and it was therefore hypothesized that both granzymes and PFN must be eternalized together in order to induce efficient apoptosis. On the other hand, the original model may, indeed, be the actual method of entry. Interestingly, a second study by Lieberman's group in 2005 showed that when cells are incubated with sublytic PFN, granzymes are endocytosed, probably by macropinocytosis, much more rapidly and efficiently than in its absence (Keefe et al., 2005; Sutton et al., 1997).

The second model devised by Froelich and colleagues, mentioned previously, highlights how basic granzymes are, and that removing them from target cell plasma membranes requires a great deal more than simply attempting to wash them off with simple cell culture medium. Surface bound receptors such as the cation-independent mannose-6-phosphate receptor (CI-MPR) and heparin have also been shown to bind GzmB on the cell surface. These receptors are not only considered a method of entry for granzymes but also, when present, are thought to contribute to the enhanced killing of target cells in the presence of PFN (Edwards et al., 1999; Jans et al., 1996; Woodard et al., 1998). Recently, however, the need for membrane receptors was questioned by several studies. In one study, CTLs from patients with I-cell disease, which can not synthesis mannose-6-phosphate-containing GzmB, can nevertheless kill target cells as efficiently as their wild type counterparts (Griffiths and Isaacs, 1993). In another study, the authors demonstrated that target cells that lack heparin receptors are just as efficiently killed by recombinant, unglycosylated GzmB, and conclude that receptors for GzmB are not crucial for killer-cell-mediated apoptosis (Kurschus et al., 2004). Several other studies also argue that receptor mediated uptake is not required for granzyme delivery into the target cell cytosol (Sayers et al., 2001; Smyth et al., 1993).

Most recently, Liebermann and colleagues have published data suggesting a "hybrid" PFN entry model that supports to some extent the previous hypothesis. The work favours a model in which PFN triggers rapid endocytosis of itself and granzymes into large endosome-like vesicles, the pore forming protein then releasing the cytotoxic proteases into the target cell cytosol. The group shows that PFN can form small pores on the plasma membrane but that these pores are, apparently, only large enough to allow the entry of small dyes and calcium, but not granzymes. It appears that, at the right PFN concentration, enough calcium influx is achieved to allow efficient cell death induction while, at the same time, triggering membrane repair responses to avoid eventual necrosis. Exactly how PFN achieves the internalization of granzymes into endosomal vesicles still needs to be resolved, but it is believed that both granzymes and PFN may be endocytosed and that, once inside, the pore-forming



protein damages the vesicular membrane to form large enough pores through which the granzymes can then be released (Pipkin and Lieberman, 2007). Alternatively, PFN may perturb the endosome by forming small pores that disrupt the acidification of the vesicle, thus destabilizing it and causing it to burst (Pipkin and Lieberman, 2007). Taken together, both Froelich's and Lieberman's models seem to agree with one another, but a lot still needs to be done in order to fully understand the actions of PFN. Despite that fact, many think it likely that granzymes do actually enter the target cell cytosol through pores in the plasma membrane, the original model still remaining very much possible.



Current Opinion in Immunology

**Figure II.5 - The three perforin-mediated granzyme entry models.** (a) The initial pore model states that granzymes access the target cell cytosol via PFN that multimerizes on the plasma membrane to form pores. (b) The endomolysis model, proposed by Froelich and colleagues, says that granzymes are endocytosed independently of PFN and that PFN then acts to release the protease as an endomolysin. (c) The hybrid model is the result of much work by Judy Lieberman's group. They propose that PFN causes the influx of calcium and that this triggers a membrane repair response that leads to quick repair of the membrane pores. Thereafter, the previous actions of PFN lead to the endocytosis of both granzymes and PFN together. PFN would then either allow the release of granzymes from the endosomes by the formation of large pores or its action on the endosomal membrane could cause the vesicle to burst also allowing the granzymes to escape into the target cell cytosol. Scheme taken from a review entitled "Delivering the kiss of death: progress on understanding how PFN works", Current Opinions in Immunology (Pipkin and Lieberman, 2007).

### ***Granzymes: natural-born killers***

As discussed in the above chapter on PFN, cytotoxic cells induced target cell death only in the presence of both PFN and other granule components. Indeed, sublytic PFN alone is not a threat to the target cell, but, together with granzymes, is responsible for DNA fragmentation (Duke et al., 1983). Work from Bleackley and colleagues in 1986, focusing on identifying genes involved in CTL induced cell death, singled out two genes, namely B10 and C11, which belonged to a family of serine



proteases. In particular, C11 or cytotoxic cell protease I (CCPI) was found to encode for the now named GzmB, its expression patterns closely correlating with the induction of CTL cytotoxicity (Lobe et al., 1986).

### ***Granzyme B (GzmB)***

GzmB is unique among its kind owing to its ability to activate a family of apoptogenic cysteine proteases named caspases, which, coincidentally, also share the same proteolytic specificity at the P1 position. In the early 90s, it was shown that purified GzmB, from rat natural killer cells, could, along with PFN, induce rapid DNA fragmentation within 1 hour of exposure to target cells (Shi et al., 1992). Exciting research from the Henkart lab then went on to show that, by transfecting a rat basophilic cell line (RBL-1) with GzmB and PFN constructs, RBL-1 acquired cytotoxic activity (Nakajima et al., 1995). Additionally, Ley et al. also made an important step towards understanding the role of granzymes in granule mediated cell death when they generated mice deficient in the GzmB gene. These GzmB-null mice developed normally and had normal hematopoiesis and lymphopoiesis. *In vitro*, however, CTLs derived from the mice displayed a reduced capacity to induce <sup>51</sup>Cr-release from target cells. Furthermore, the cells showed a profound defect in their ability to induce rapid DNA fragmentation and apoptosis in target cells. It was concluded that GzmB had a critical, and none redundant, role in the rapid induction of target cell DNA fragmentation and apoptosis (Heusel et al., 1994). Taken together, the above findings, spanning a decade of research, clearly show that GzmB, in the presence of PFN, is a key player in CTL killing. Indeed, it is now an established fact that GzmB is the most potent granzyme in the family owing to its ability to act at multiple points in the initiation of diseased cell death.

### ***Granzyme A (GzmA)***

Mice deficient in this GzmA have an increased susceptibility towards certain viral infections, despite being able to efficiently eradicate tumors. Additionally, CTLs from these mice have normal cytotoxic responses *in vitro* (Ebnet et al., 1995; Heusel et al., 1994; Mullbacher et al., 1996; Pereira et al., 2000; Shresta et al., 1999; Zajac et al., 2003). In cell death studies using recombinant GzmA, in the presence of sublytic concentrations of PFN, target cells not only undergo rapid cytolysis but also acquire single-strand DNA nicks in a caspase-independent manner (Pinkoski et al., 1998). In addition, it has been observed that GzmB-induced DNA fragmentation is significantly enhanced in the presence of GzmA, indicating that GzmA induces a form of cell death that is distinct from that triggered by GzmB (Browne et al., 1999; Pinkoski et al., 1998; Zajac et al., 2003). GzmA has been demonstrated to cause direct and indirect mitochondrial dysfunction. Indeed, GzmA-treated cells show a loss of transmembrane potential but do not cause the release of proapoptotic intermembrane space proteins such as cytochrome c. More recently, it was shown that GzmA transferred into target cells via PFN,

leads to the fast generation of reactive oxygen species (ROS) which, in turn, then induces the nuclear transfer of the previously described ER-associated SET complex. Once in the nucleus, GzmA relieves the active nuclease NM23-H1 by destroying its bound inhibitor SET (Martinvalet et al., 2005). GzmA is also known to target the DNA-binding protein HMG-2 and the base excision repair enzyme Ape-1 (Lieberman and Fan, 2003). Interestingly, when target cells are preincubated with antioxidants such as Tiron and NAC (N-Acetyl cysteine), GzmA is no longer able to execute its cell-death pathway. Are then reactive oxygen species an absolute necessity for cell death?

### ***Orphan granzymes***

With regard to the remaining three members of the human granzyme family, no concrete, fully explored role in CTL-mediated cell death has yet been established for this trio of proteases known as the orphan granzymes. However, GzmK, a tryptase like its closely linked chromosome neighbour GzmA, has recently been reported to induce a caspase-independent form of cell death defined by phosphatidylserine (PS) externalization, mitochondrial depolarization, nuclear morphological changes and single-stranded DNA nicks. Additionally, GzmK, like GzmA, is also able to cleave the nucleosome assembly protein SET in its recombinant and native forms. Once cleaved, SET is released from the bound nuclease NM23H1 and, in turn, becomes active and goes on to nick chromosomal DNA (Zhao et al., 2007b). Earlier in 2007, however, a second study from the same group further demonstrated that GzmK directly processes the Bcl-2 family member Bid, resulting in the release of cytochrome c and endonuclease G from the mitochondria. (Zhao et al., 2007a). In this same study, ROS was also shown to be released resulting from injury of the mitochondrial respiratory chain. Moreover, the authors reported that the pretreatment of target cells with antioxidants completely blocked GzmK-induced cell death, as was the case with GzmA (above) in a study by Lieberman's group (Martinvalet et al., 2005). These studies suggest that ROS does, indeed, play an essential role in accomplishing target-cell eradication. See the comment in 'Immunity' entitled "Do cytotoxic lymphocytes kill via reactive oxygen species?", (Williams and Henkart, 2005).

GzmM is a metase and prefers to cleave after residues with long, uncharged side chains such as Met and Leu. The protease has also recently been labeled as cytotoxic because of its ability to induce caspase-independent cell death (Kelly et al., 2004). In this report, no target cell substrates were identified, the authors defining GzmM cytotoxicity by significant <sup>51</sup>Cr release (equimolar amounts of GzmB and GzmM triggering similar levels of cell death) and chromosomal condensation. Interestingly, and contrary to GzmA, GzmB and GzmK, the authors report a complete lack of mitochondrial perturbation. Very recently though, a study by Fan and colleagues revealed that, in their hands, the metase initiated caspase dependent apoptosis (Lu et al., 2006). The work goes on to demonstrate how GzmM triggers cell death by DNA fragmentation, but not DNA nicking, and how

the protease can degrade the inhibitor of caspase activated DNase (ICAD) thus releasing the active caspase-activated nuclease (CAD). Finally, the study reveals that GzmM cleaves the DNA damage sensor enzyme poly(ADP-ribose) polymerase (PARP), consequently preventing the target cells from DNA repair (Kelly et al., 2004; Lu et al., 2006). Unlike GzmB, but like GzmA, GzmM has been shown to be constitutively stored at high levels in NK cell granules. Additionally, along with the fact that GzmM appears to trigger cell death in concert with the kinetics of NK cell mediated cytotoxicity (Suck et al., 2005), it has been suggested that GzmM may indeed play a crucial role in NK target cell attack (Kelly et al., 2004). Recently, however, a report on GzmM deficient mice reveals that the mice display normal NK-mediated cytotoxicity against tumor cells, the knock-out mice only troubled by the slow clearance of mouse cytomegalovirus (MCMV) infection. In conclusion, the authors suggest that GzmM is not critical for NK-mediated cell death (Pao et al., 2005).

<b>Table II.1 - Properties of granzymes in humans and rodents</b>		
<b>Protease</b>	<b>Peptide cleavage-site specificity</b>	<b>Species</b>
Granzyme A	Arg/Lys	Mouse, rat, human
Granzyme B	Asp/Glu	Mouse, rat, human
Granzyme C	Asn/Ser	Mouse, rat
Granzyme D	Phe/Leu	Mouse
Granzyme E	Phe/Leu	Mouse
Granzyme F	Phe/Leu	Mouse, rat
Granzyme G	Phe/Leu	Mouse
Granzyme H *	Phe	Human
Granzyme J	Unknown	Rat
Granzyme K	Arg/Lys	Mouse, rat, human
Granzyme M	Met/Leu	Mouse, rat, human

**Table II.1 – Properties of granzymes in humans and rodents.** \* GzmH has chymotrypsin-like proteolytic activity and it has been reported that the protease prefers not only Phe but also Tyr and Met at the P1 position. The red rectangle is indicative of predicted cleavage specificities. This table is taken from a review entitled “Cytotoxic lymphocytes: all roads lead to cell death”, ‘Nature Reviews Immunology’ (Barry and Bleackley, 2002).

Granzyme H, the least studied of the orphan trio and only member of the family to be found exclusively in humans, has yet to be added to the list of cytotoxic proteases. This chymotrypsin-like protease, and “granzyme of interest” in this thesis, will be discussed in more detail in the following chapters.

### ***II.3 – Granzyme B and its multiple apoptogenic substrates***

GzmA and GzmB are the most abundant granzymes in mice and humans and have, therefore, received the most attention, particularly GzmB because of its ability to activate caspase-dependent pathways that lead to the most common type of cell death, otherwise known as apoptosis. Moreover, GzmB can also achieve its cytotoxic goals by triggering caspase-independent pathways, as seen with the cell death pathway triggered by GzmA.

In order to analyze GzmB and its functions, the protease was first purified and activated in its native form and then, soon after, expressed and purified as an active recombinant enzyme (Caputo et al., 1993; Shi et al., 1992). In the mid nineties, Bleackley and colleagues made the first step in identifying the crucial substrate for GzmB. They showed that active, recombinant GzmB cleaves and activates CPP32 or procaspase 3, which, in turn, leads to the cleavage of poly(ADP-ribose) polymerase (PARP) (Darmon et al., 1995). Since then, many more apoptogenic substrates have been found to be cleaved by GzmB. As we shall see, it is the variety of pathways through which GzmB can inflict apoptosis on target cells, and the speed at which this granzyme destroys its prey, that crowns it as the ultimate weapon in granule mediated cytotoxicity. Additionally, purified GzmB, or a recombinant variant of the protease, can also be used as the perfect comparative tool in studies, such as this one, which seek to unravel the possible cytotoxicity of other members of the granzyme family.

#### ***The caspase-dependent cell death pathway***

GzmB is not the only protease that prefers to cleave after aspartic acid residues. Interleukin-1 $\beta$ -converting enzyme (ICE), which also has this specificity, belongs to a family of cysteine proteases called the caspases. ICE, or caspase 1, was found to have high homology with the *C. elegans* Ced 3 protein which is essential in the developmental cell-death program of the worm. This finding led to speculation hinting that the caspase family might also play an important role in mammalian cell death. Indeed, the caspases are now well established in the community of cell-death inducing proteases, especially in the art of DNA fragmentation.

Caspases are synthesized as inactive precursors and acquire active conformation only after cleavage at aspartate residues, suggesting that the family would be excellent substrates for GzmB. This was later confirmed by work from Bleackley and colleagues who demonstrated the cleavage and activation of caspase 3 by GzmB and, furthermore, went on to underline the cytotoxic importance of this caspase in a number of studies. They revealed that the cleavage of caspase 3 results from the action of GzmB, and not from that of GzmA, in target cell lysates. Furthermore, caspase 3 is activated *in vivo* in cells

under attack from CTLs. Additionally, use of GzmB knock-out mice revealed that the cleavage of caspase 3 is specific to the actions of the aspase.

Although other members of the caspase family have been shown to be activated by GzmB, caspase 3 is believed to play the most important role in GzmB-mediated cell death (Froelich et al., 1996b; Shresta et al., 1999). Caspase-3 has recently been shown to cleave a number of proapoptotic proteins such as PARP, mentioned above, ICAD, which leads to DNA fragmentation, and, more recently, gelsolin, a protein involved in the maintenance of the cytoskeleton and also in the loss of aminophospholipid translocase activity, a protein involved in phosphatidylserine (PS) externalization (Kothakota et al., 1997). Together, the cleavage of these substrates results in the hallmarks that currently define the state of apoptosis, namely chromatin condensation, nuclear fragmentation, and PS externalization, among others. The loss of mitochondrial transmembrane potential ( $\Delta\Psi$ ) is another apoptotic hallmark of GzmB-triggered cell death but was thought, initially, to be independent of caspases. Therefore, this phenomenon will be discussed in the following chapter (Beresford et al., 1999; Zhang et al., 2001). Recent studies, however, have revealed that caspase 3 and 8 can cleave and activate a proapoptotic protein, named Bid, a member of the Bcl-2 family of proteins, which leads to the formation of pores in the outer mitochondrial membrane, thus allowing the release of other proapoptotic proteins which, in turn, go on to amplify the apoptotic cascade. Until these observations were made, Bid was thought to be the direct physiological substrate for GzmB. The exact involvement of caspases, under physiological conditions, will require further research (Metkar et al., 2003).

### ***The caspase-independent cell death pathway***

Cell death induced by CTLs can also proceed in the absence of caspases, as demonstrated using peptide caspase inhibitors, or in target cells expressing viral caspase inhibitors such as baculovirus p35 and the poxvirus inhibitor, crmA (Henkart et al., 1997; Sarin et al., 1997). Nuclear changes and other signatures of cell death still occur, even in target cells over-expressing the anti-apoptotic protein Bcl-2 (Chiu et al., 1995; Sutton et al., 1997). Accordingly, many studies report the capacity of GzmB to induce cell death independently of caspase activation, all the substrates mainly being downstream caspase substrates, GzmB here substituting for the blocked initiator or effector caspases (Beresford et al., 1999; Sarin et al., 1997; Trapani et al., 1998). As mentioned above, Bid (BH3-interacting domain death agonist) is one of the most important targets for GzmB. Indeed, once Bid is cleaved and activated, the truncated protein (tBid) damages the integrity of the mitochondrial membrane in concert with two other Bcl-2 family members, BAX and BAK, thereby causing the release of a number of proapoptotic proteins from the organelle's inter-membrane space. Cytochrome c (crucial for activating procaspase 9), endonuclease G (which activates DNA damage) and HtrA2/OMI (a recently identified serine protease that inhibits the inhibitor of apoptosis protein (IAP)) are all released upon GzmB

induced caspase-independent cell death. Interestingly, only the apoptosis-inducing factor (AIF), a fourth mitochondrial inter-membrane space protein (MIMP), is reported to remain contained (Alimonti et al., 2001).

Mitochondrial depolarization has also been shown to occur independently of cytosolic mediators, GzmB reportedly being directly able to act on the mitochondrial membrane (Alimonti et al., 2001; MacDonald et al., 1999). Disruption in the mitochondrial membrane potential is followed by an increase in ROS but the underlying mechanisms remain unknown.

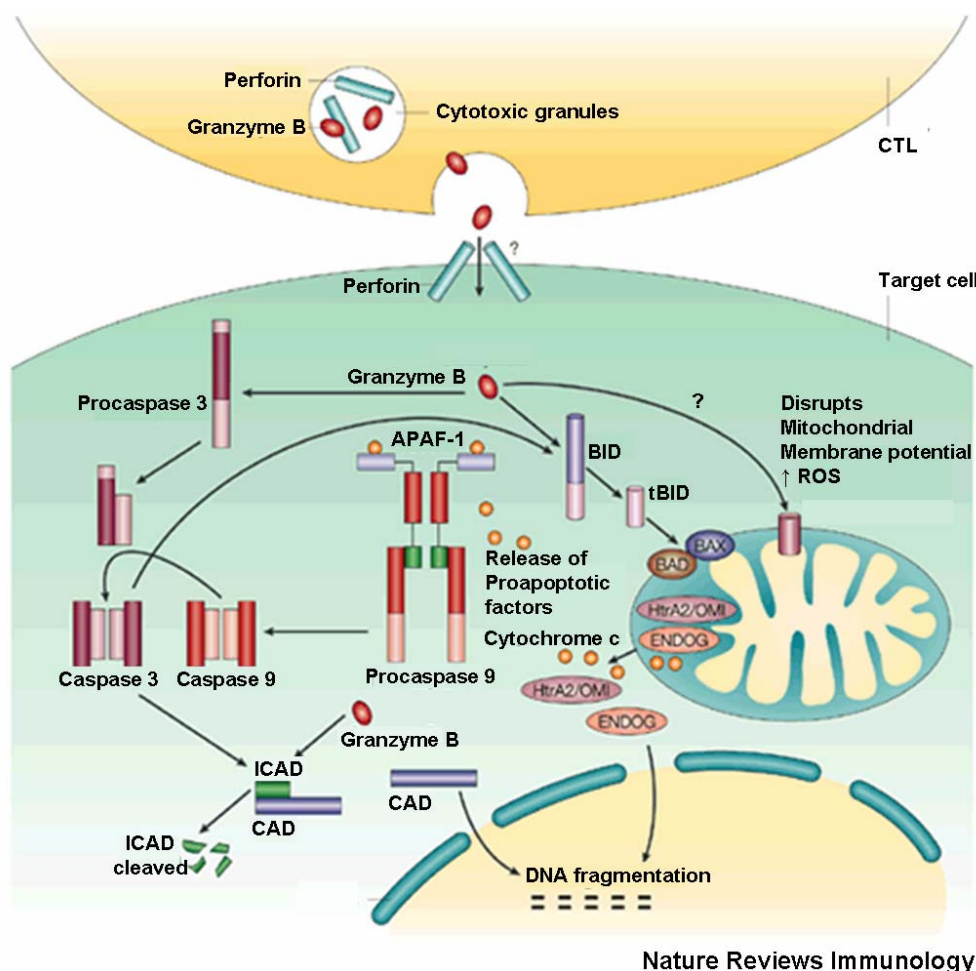


**Figure II.6 - GzmB activates both caspase dependent and independent pathways to achieve death of the target cell.** Two early substrates of GzmB are procaspase 3 and Bid. Truncated Bid (tBid) disrupts the outer mitochondrial membrane to cause the release of cytochrome c and other proapoptotic factors such as endonuclease G (which leads to DNA damage) and HtrA2/OMI (a protein which blocks inhibitors of apoptosis). Importantly, cytochrome c release is an essential event that leads to the formation of the apoptosome through binding to APAF1 and recruitment of procaspase 9. Once assembled, the apoptosome causes the autocatalytic activation of procaspase 9; the active caspase then goes on to activate caspase 3. GzmB is also reported to directly disrupt the mitochondrial membrane although the mechanism by which the caspase achieves this remains unknown. GzmB, along with active caspase 3, cleaves the inhibitor of caspase activated DNase (ICAD) to free CAD. The liberated DNase then causes DNA fragmentation, as seen in the form of DNA laddering. APAF1: apoptotic protease-activating factor 1; BAD: BCL-2 antagonist of cell death; BAX: BCL-2-associated X protein; CTL: cytotoxic T lymphocyte; ROS: reactive oxygen species. Taken from a review entitled “The ABCs of granule-mediated cytotoxicity: new weapons in the arsenal”, ‘Nature reviews Immunology’ (Lieberman, 2003).

In the case of Bid activation and outer membrane perturbation, the escape of cytochrome c (the smallest MIMP) triggers an essential pathway necessary for the amplification of caspase activity. Moreover, if caspases are truly involved in activating Bid, as is suggested in the previous chapter, cytochrome c may also be involved in the amplification of mitochondrial membrane disruption and MIMP release. After its release, cytochrome c binds to APAF1, which, in turn, recruits procaspase 9 to form the apoptosome. Apoptosome assembly ensures the autocatalytic activation of caspase 9 which then goes on to activate procaspase 3. It is also known that partially activated caspase 3 can dimerise and activate itself (Lieberman, 2003).

Finally, GzmB can also directly cleave ICAD in the absence of caspase activation thus ensuring that, along with endonuclease G, these two nucleases fulfill target cell DNA damage (Li et al., 2001; Sharif-Askari et al., 2001; Thomas et al., 2000). Additionally, GzmB has also been shown to cleave a number of downstream caspase substrates such as PARP, the catalytic subunit of DNA-dependent protein kinase (DNA-PKcs), which is involved in repairing double-stranded DNA breaks, and the nuclear-envelope intermediate-filament protein lamin B (Andrade et al., 1998; Froelich et al., 1996a; Zhang et al., 2001).

## ***II.4 - Granzyme H***

Human granzyme H (GzmH) is our serine protease of interest. As a brief reminder, GzmH is a chymase that lies among the members of the GzmB cluster on chromosome 14. GzmH is not the only chymase of the locus and is neighbour to other serine protease genes, namely those of *GZMB*, *CATHEPSIN G* and *MAST-CELL CHYMASE*, the later two also being chymotrypsin-like enzymes. GzmH has the highest amino acid identity with GzmB, over 90%, and in particular with sequences near the N-terminus of the aspase, despite both proteases boasting distinct proteolytic activities. Indeed, it has been suggested that *GZMH* arose by duplication of part of the 5' end of *GZMB*, housing exons 3 and 4, followed by fusion of this segment with the 3' end of another primordial serine protease gene with chymase activity (Haddad et al., 1991). As a reminder, the mouse GzmB locus holds no direct structural equivalent of GzmH but is home to six other granzyme genes, four of which are also predicted to code for functional chymotrypsin-like proteases.

The current state of knowledge on GzmH is, for the most part, based on three papers that span a 14-year period: 1990 to 2004. Haddad, Jenne and colleagues, in 1990, revealed the structure and evolutionary origin of human *GzmH* as described above. Nearly a decade later, two studies from the Trapani lab, in 1999 and 2004, reported upon the expression of GzmH in blood lymphocytes, the

enzyme's proteolytic activity and its uptake into target cell vesicles in the absence of perforin (Edwards et al., 1999; Sedelies et al., 2004).

Using a novel monoclonal antibody raised against the 33 kDa glycosylated recombinant enzyme, Trapani and colleagues showed in greater detail, that GzmH is stored constitutively at high levels in unstimulated natural killer (CD3<sup>-</sup>CD56<sup>+</sup>) cells. GzmB, on the other hand, was much less abundant in unstimulated NK cells but not in stimulated CD4<sup>+</sup> and CD8<sup>+</sup> T cells where the aspartase was very highly expressed. GzmH, in comparison, was hardly detectable in the latter CTLs. Neither was GzmH detectable in NKT cells, monocytes and neutrophils. The work also showed that there was a good correlation between mRNA and protein expression in cells, such as NK cells, that express both GzmB and GzmH, suggesting that both granzyme genes are similarly regulated. The work concludes that, although the genes are tightly linked, the protein expression of these two granzymes differs greatly, GzmH, unlike GzmB, being more frequently abundant in NK cells. It is also interesting to note that, along with GzmH, GzmA and GzmM have also been shown to be expressed at high constitutive levels in NK cells (Bratke et al., 2005; Sayers et al., 2001; Sedelies et al., 2004).

Trapani's team was the first to report the esterolytic (but not amidolytic) activity of glycosylated recombinant GzmH, secreted from baculovirus-infected Sf21 insect cells, by showing cleavage of the thiobenzyl ester Suc-Phe-Leu-Phe-SBzl and suggesting GzmH as a chymotrypsin-like (chymase) serine protease. Additionally, this study also showed that, like fluoresceinated GzmB, fluoresceinated GzmH was also internalized by target cells in a PFN-independent but temperature dependent manner thus suggesting an intracellular function for the chymase-like protease (Edwards et al., 1999).

Most recently, however, a study by Craik and colleagues has compared the extended substrate specificities of all granzymes by using combinatorial libraries of protease substrates. In this work, the optimal P4-P3-P2-P1 substrate specificities, with amide bond hydrolysis occurring following P1, were determined to be IGNR for GzmA, IEPD for GzmB, YRFK for GzmK, KVPL for GzmM and, more importantly for our interests, PTSY for GzmH. The results clearly show that the P4-P1 substrate specificities of the five granzymes are quite distinct from one another. The profiles obtained for Gzms A, B and M largely confirm previous findings based on other positional scanning combinatorial libraries. The P1 preferences for Gzms H and K, however, differ somewhat, Mahrus et al. suggesting that GzmK strongly prefers lysine over arginine and, more interestingly for our purposes, that GzmH in fact exhibits a noticeable preference for tyrosine over phenylalanine and tryptophan. Moreover, the work defines for the first time the P4-P2 substrate specificities for these two granzymes.

Until now, no functional data on GzmH has been reported. The above studies, while raising a number of questions regarding the cytotoxicity of the chymotrypsin-like protease, have probably encountered



various problems in investigating the question, one such problem seemingly being the inability to produce large enough amounts of recombinant active granzyme. Another obstacle could also be the task to produce enough stably active PFN, the natural granzyme translocator. Once these problems are solved, the fact that GzmH is expressed at high constitutive levels in NK cells, where the caspase activating GzmB is present in much reduced amounts, is suggestive of a role for GzmH in innate immunity, a role that probably complements that of GzmB, found at its highest levels in activated CTLs of the adaptive immune system.

## ***II.5 - Granzymes and antiviral strategies***

Apart from the alternative pathways that allow granzymes such as Gzms A and B to efficiently eradicate transformed tumor cells, the family also plays an important role in eliminating host cells infected by intracellular pathogens such as viruses. The mechanisms by which these serine proteases exert their antiviral activity remain elusive. A collaborative study conducted by Felipe Andrade has shed new light on some of these mechanisms. The host-virus relationship is a complex business in which the virus attempts to escape capture and elimination. It achieves this by minimizing its visibility. About a third of the viral genome is devoted to this purpose and immediately after infection numerous viral proteins begin to interfere with host cells defense mechanisms, some inhibiting apoptosis at the mitochondrial level, others removing apoptosis-inducing receptors such as FAS and TNK-related apoptosis inducing ligand (TRAIL). The transport of MHC class I molecules to the cell surface can also be targeted. Andrade and colleagues recently showed that the 100K assembly protein, which has essential functions in the adenovirus life cycle (such as virus assembly and activation of late viral protein synthesis), also directly inhibits GzmB (Andrade et al., 1998; Andrade et al., 2001). In a recent collaboration with Dr. Andrade, we report the new finding that, in cells infected with adenovirus in which GzmB and down stream apoptosis pathways are inhibited, GzmH directly cleaves viral substrates essential for replication of the adenovirus. Moreover, GzmH was also found to cleave the 100K assembly protein, also a major inhibitor of GzmB, an event that leads to the freeing of GzmB from inhibition. These results introduce another granzyme into the battle of “host versus foe” and show that granzymes can act synergistically to outsmart viral defenses. Although, the antiviral properties of GzmH are not the topic of this thesis, our recent publication will be briefly mentioned in more detail during the discussion. Understanding how effector cells tame and eliminate target cells which have been hijacked by viral defense mechanisms is of extremely important if we are to make advances in antiviral treatment.

## ***II.6 - In vitro granzyme delivery by an alternative pore forming protein***

### ***Bacterial streptolysin O (SLO)***

Our experimental approach to deliver proteins does not rely on purified human PFN but upon a bacterial counterpart. The delivery of our recombinant granzymes into target cells is based upon a reconstituted system where entry of our granule enzymes is achieved by a recombinant bacterial substitute for PFN, namely streptolysin O (SLO). SLO and PFN monomers assemble on membranes into pore complexes through which granzymes can illegally enter. Whether PFN monomerises on plasma membranes or with internalized endosomes of target cells to allow granzyme entry is not yet clear. SLO, on the other hand, is reported to act on the plasma membrane (Walev et al., 2001).

### ***Mutant streptolysin O***

Additionally, along with the commercial SLO, which requires the reduction, and hence the presence of reducing agents such as cysteine in the permeabilization buffer, we also use a mutant SLO variant, namely SLO<sup>C530A</sup>. SLO<sup>C530A</sup> is oxygen stable and therefore does not need to be reduced in order to perform its pore-forming duties. Additionally, and more importantly in experiments measuring ROS production, the mutant SLO was used to circumvent the need for prior activation under reducing conditions.

### ***Bacterial streptolysin O versus human perforin***

The decision to use SLO was not only made because of the protein's affordability and availability but also because of its purity and stability in cell death assays. PFN, on the other hand, although being the natural delivery agent of CTL and NK cells, is just the opposite, the commercially available protein is very expensive, its availability, purity and activity uncertain and it is reported to be unstable *in vitro*. Despite the use of a bacterial substitute, our reconstituted system efficiently allows GzmB to induce apoptosis in an identical manner to that observed in studies using purified human PFN. We, therefore, suggest that our reconstituted system is a reliable method with which to question the role of GzmH in the induction of cell death.

## II.7 - Aim

Granzymes (Gzms) are a family of serine proteases which comprise the content of lysosome-like lymphocyte granules. These granule enzymes, of which five are known to date in humans, are of particular interest because of their different proteolytic specificities and potential abilities to trigger cell death in tumour and virally infected cells. Indeed, GzmA and GzmK, both “tryptases”, cleave after basic residues and GzmB, an “aspase” preferring to cleave after acidic residues, have evolved distinct apoptotic pathways. GzmH is referred to as an orphan granzyme because its biological functions and relationship to cell death are still unknown. Recent reports show that the protease is predominantly expressed in natural killer cells and is predicted to have chymotrypsin-like (chymase) activity. Like GzmA, GzmB and GzmM, GzmH has been shown to be taken up by target cells in endosome-like vesicles. How it should then effect the cellular environment upon its release into the cytosol is the underlying interest of this thesis.

So that we might question the possibility that GzmH could be involved in the induction of cell death, our first goal was to establish a procedure allowing the production and purification of large homogenous quantities of uncontaminated granzyme. In order to achieve this, we sought to refold GzmH inclusion body material according to a protocol developed by Wilharm and colleagues in 1999. Wilharm *et al* successfully describe the generation of catalytically active granzyme K in milligram quantities per litre of *Escherichia coli* culture. Additionally, the refolding of catalytically inactive GzmH, GzmH<sup>S195A</sup>, was also attempted in order to appropriately control our apoptosis experiments. Importantly, this inclusion body (IB) refolding method was also adapted to produce catalytically active and inactive GzmB, the granzyme we use as a positive control of apoptosis induction in our experiments.

Before, exploring the potential of GzmH as a cell-death inducing enzyme, we first attempted to confirm the findings of several studies that define GzmH as having chymotrypsin-like (chymase) activity with a preference for hydrophobic, aromatic amino acid residues (Phe or Tyr) at the P1 site. Its esterolytic activity is also reported to be inhibited by 0.1 mM of the general protease inhibitor 3,4-dichloroisocoumarin. Additionally, the GzmH protein has been shown to be predominantly expressed in NK cell lines, but as mentioned its functional role *in vitro* has yet to be determined. Once the latter is achieved, the study of the protease’s possible cytotoxic functions will be possible through the application of the many available apoptotic assays, controlled by the caspase activating GzmB, the proteolytically inactive GzmH, and the two chymotrypsin-like proteases that are neighbours to GzmH on Chromosome 14, namely cathepsin G and mast cell chymase. Additionally, if produced in large enough quantities, an attempt could be made to crystallise active GzmH alone, or, much more elegantly, in complex with a natural inhibitor which is yet to be named.

### ***III – Material & Methods***

#### ***III.1 - Cloning in plasmid vectors***

##### ***Plasmid DNA purification from *E. coli****

A number of methods have been developed that efficiently remove contaminating chromosomal DNA leaving plasmid DNA free in solution. The Qiagen mini and maxiprep systems provide fast and simple protocols designed for the respective preparation of up to 20/500 µg of plasmid DNA from 5/500 ml overnight cultures of *E. coli* in Luria-Bertani (LB) medium (Bacto tryptone 10 g, yeast extract 5 g, NaCl 5 g and deionized (*d*) H<sub>2</sub>O, 1 L) containing the appropriate selective antibiotic. The desired plasmids were isolated using the appropriate Qiagen kits, mentioned above, according to the provided protocols. The resulting plasmid DNA was then used for sequence verification or for further cloning procedures after transformation into the *E. coli* host strain DH5α (Birnboim, 1983; Birnboim and Doly, 1979).

##### ***DNA amplification (PCR)***

The polymerase chain reaction or PCR process, here performed in the PCR-Thermocycler “Trio-Thermobloc” from Biometra, is used to amplify short target segments (100-500 bp) from a longer DNA molecule. A typical amplification reaction includes the sample of target DNA, two oligonucleotide primers, deoxynucleotide triphosphates (dNTPs), reaction buffer, magnesium and a thermostable DNA polymerase, here the PfuTurbo-DNA polymerase (Stratagene Kit with supplied 10x Pfu-buffer). All PCR reactions were started with a preincubation step known as “Hot Start” which denatures the template DNA at 95-100°C so that the primers can anneal after cooling. The second step, otherwise referred to as “touchdown” allows the oligonucleotide primers to anneal to the denatured template by lowering the temperature to 37-65°C depending on the  $T_m$  (annealing temperature) of the primers. The reaction proceeds with the extension, or elongation of the primers at 72°C, the optimal temperature for PfuTurbo-DNA polymerase. The duration of the extension steps can be increased if long amplicons are being amplified, but for the majority of PCRs, times of up to 2 minutes are usually sufficient. Often, the elongation time of the final cycle is longer (up to 10 minutes) in an attempt to ensure that all the product molecules are fully extended. Steps 1-3 constitute one cycle of the PCR, where the number of cycles of the whole reaction is between usually 25-30 cycles. With increasing cycle numbers it is common to observe an increase in the amount of unwanted artifacts and no increase in the desired product.

<b>Typical amplification reaction:</b>	50 ng	Template DNA
	5 $\mu$ l	10x Pfu-buffer (Stratagen kit)
	5 $\mu$ l	2 mM dNTP-Mix
	10 $\mu$ M	Forward primer
	10 $\mu$ M	Reverse primer
	2.5 U	PfuTurbo-DNA polymerase (Stratagen kit)
	Add <i>d</i> H <sub>2</sub> O to 50 $\mu$ l	

### ***DNA restriction digestion***

Restriction digestion of plasmid DNA was performed following a standardized protocol for the use of one or more endonucleases (Ausubel., et al. 1999). The definition of 1 Unit (U) of restriction enzyme activity is the amount needed to completely digest one microgram of substrate DNA (often Lambda DNA) in one hour at the optimal temperature (usually 37°C). Additionally, each reaction is carried out with a buffer that ensures 100% activity of the endonuclease in question. As a rule of thumb, the total volume of restriction enzyme in the digest should not exceed 10% of the total digest volume which also ensures that the glycerol concentration in the reaction mixture remains below 5%. Once all the components, DNA, *d*H<sub>2</sub>O and buffer, have been added to the reaction mix, the endonuclease is then applied, so it enters optimal reaction conditions. Under non-standard conditions, restriction endonucleases are capable of cleaving sequences which are similar but not identical to their defined recognition sequence. This is termed “star” activity. Star activity is completely controllable in the vast majority of cases and is generally not a concern when the enzymes are used under the recommended conditions. Cleaving plasmid DNA with two restriction endonucleases simultaneously (double digestion) is achieved by selecting a buffer that provides reaction conditions that are amenable to both restriction endonucleases. Choosing the optimal buffer for both enzymes should be done carefully under the guidelines supplied by the manufacturer. Alternatively, if no single buffer is available to satisfy the buffer requirements of both enzymes, the reactions should be done sequentially; the salt conditions adjusted in between digestions using a small volume of a concentrated salt solution to approximate the reaction conditions of the second restriction endonuclease. Reactions were brought to a halt either by thermal inactivation or by the addition of loading-buffer in preparation for gel electrophoresis.

### ***Agarose gel electrophoresis***

Agarose gel electrophoresis allows the visualization of a restriction enzyme digestion. The technique enables the user to determine precisely the yield and purity of a DNA preparation or PCR reaction, but

also to size fractionate DNA molecules, which can then be eluted from the gel. Prior to gel casting, dried agarose is dissolved in buffer by heating and is then poured into a self assembled mold into which a comb is fitted while the mixture is still wet. The percentage of agarose in the gel varies. In this work 0.8% agarose was used, 1% agarose gels being necessary for the accurate size fractionation of DNA molecules smaller than 1 kb. Ethidium bromide (EtBr) (end concentration: 1 µg/ml) was included in the gel matrix to enable fluorescent visualization of the DNA fragments under UV light. The gels were then submerged in electrophoresis buffer (TAE) in a horizontal electrophoresis apparatus. After the samples were mixed with gel loading dye and loaded into the sample wells, the electrophoresis was initiated by applying 60 mV for 30 minutes to 1 hour at RT. Size markers are co-electrophoresed with DNA samples for fragment size determination. Two size markers, 1 kb and 50 bp, were used from Peqlab. After electrophoresis, the gel was placed on a UV light box and the fluorescent ethidium bromide-stained DNA pictured using the thermal imaging system FTI-500 from Pharmacia Biotech.

**TAE buffer (10 fold):**            242 g    Tris  
   57.1 ml    Acetic acid  
   100 ml    0.5 M EDTA, pH 8.0  
   H<sub>2</sub>O to 1 L

### ***DNA purification from agarose gels***

After electrophoresis, DNA fragments were visualized on a UV light box before being removed from the gels by the use of scalpels. Once captured, the DNA was eluted from the jellified agarose following the instructions of the “QIAquick Gel Extraction Kits” from Qiagen.

### ***DNA concentration and purity determination***

DNA concentration and purity was determined by using the Eppendorf spectrophotometer “BioPhotometer” (Hamburg, Germany). The concentration was determined by measuring the absorbance at 260 nm and purity was measured by calculating the ratio of absorbance at OD 260/OD280 nm.

### ***DNA fragment ligation***

Purified and restriction-enzyme treated DNA fragments (PCR product) were cloned as described (Ausubel., et al. 1999) into the desired plasmid vectors, also having been digested with the same endonucleases producing compatible overhangs. After the vector and insert DNA have been prepared

and their respective concentration determined, various vector to insert DNA ratios were tested in order to determine the optimum ligation ratio. In most cases a 1 to 3 molar ratio of vector and insert proved successful. All ligations were performed with ATP-dependent T4 DNA ligase and the provided buffer (Boehringer) overnight at 16°C or for 3 hours at RT. Following the reaction, the ligated DNA was transformed into an appropriate host strain, here the *E. coli* strain DH5 $\alpha$ .

### ***Construction of expression plasmids - pET24c(+)*MKH<sub>6</sub>GzmH**

Granzyme H (GzmH) cDNA was amplified from the homo sapiens cDNA clone IMAGE:15434 (vector pT7T3D) using the sense strand primer DJ2715 (5'-GAG GAT ATC ATC GGT GGC CAT GA-3') and the antisense strand primer DJ2716 (5'-GCC TAA CGT TAG AGG CGT TTC ATG GTA CGT TTG ATC C-3'). The resulting PCR product was digested with *Eco* RV and *Hind* III and subsequently cloned into the *Pml* I and *Hind* III (173) cut pET24c(+) *E. coli* expression vector (Novagen). Vector pET24c(+) was previously modified by introducing the codon sequence MKH<sub>6</sub> into the vector's multiple cloning site cleaved at restriction sites *Nde* I and *Bam* HI. The MKH<sub>6</sub> tag was constructed as a duplex with primers DJ2333 (5'-TAT GAA ACA TCA CCA TCA TCA CCA CGT G-3' - introducing codons Met and Lys and the mentioned *Pml* I site) and DJ2334 (5'-GAT CCA CGT GGT GAT GAT GGT GAT GTT TCA-3'). The cloning of modified GzmH cDNA directly upstream from the MKH<sub>6</sub> tag produced a sequence coding for a mature-like GzmH starting with codons Ile-Ile-Gly-Gly.

### ***pET24c(+)*MKH<sub>6</sub>GzmH<sup>S195A</sup>**

The catalytically inactive GzmH<sup>S195A</sup> construct was obtained using pET24c(+)GzmH as a template for the amplification of sense primer DJ 2871 (5'-ACA CAC CGG TTT CAA AGG TGA CGC CGG-3') introducing a 5' *Age* I restriction site, and antisense primer T7-ter from. Sense primer DJ 2871 contains a point mutation which replaces the reactive Ser195 with Ala and rendering the protease unable to act proteolytically. The resulting PCR product was digested with *Age* I and *Hind* III and sub-cloned into the identically cut pET24c(+)MKH<sub>6</sub>GzmH vector. The sequences of positive clones from both constructs were verified by sequencing analyses and transformed into the *E. coli* strain B834 (mentioned later page 32) ready for expression (DE3) (Novagen).

### ***Expression constructs***

Construct	Primer	Restriction Sites	Target DNA	Temp.(AT)
pET24c(+)MKH <sub>6</sub> GzmH	DJ2715/16	<i>Pml</i> I / <i>Hind</i> III	Clone154343(human)	53°C
pET24c(+)MKH <sub>6</sub> GzmH <sup>S195A</sup>	DJ2871/27	<i>Age</i> I / <i>Hind</i> III	pET24c(+)MKH <sub>6</sub> GzmH	58°C

***DNA sequencing***

The sequencing of plasmids and PCR products was performed by Toplab (Martinsried) using fluorescently labeled nucleotides as described by Sanger and colleagues (Sanger et al., 1977).

***III.2 - DNA transformation******Preparation of CaCl<sub>2</sub> competent cells***

A single DH5 $\alpha$  colony was inoculated from an LB plate in 2.5 ml of LB medium and incubated overnight at 37°C with shaking (~225 rpm). On the following day, the entire o/n culture was used to inoculate 250 ml of LB medium (1:100 dilution). The cells were then grown until the OD<sub>600 nm</sub> reached 0.4-0.6 (5-6 hours). In pre-cooled falcon tubes, cells were pelleted by centrifugation (Sorvall GSA) at 3000 rpm (4°C, 7 minutes) before being resuspended in one-fifth of the volume (based on the original culture volume) of ice cold 0.1 M CaCl<sub>2</sub> solution. For the remaining steps, the cells were kept on ice and all flasks, pipettes (Eppendorf, Milan, Italy), and tubes were pre-chilled. Cells were then incubated on ice for 5 minutes at 4°C. After centrifugation at 3000 rpm (5 minutes, 4°C), the cells were gently resuspended in one-twenty fifth of the original culture volume of ice cold 0.1 M CaCl<sub>2</sub> solution. For long term storage of competent cells at -80°C, 20% glycerin was added to the CaCl<sub>2</sub> solution.

**CaCl<sub>2</sub> solution:**            0.1 M    CaCl<sub>2</sub>  
                                      20%    Glycerin (Glycerol)  
                                      10 mM   PIPES [piperazine-N,N'-bis(2-hydroxypropanesulfonic acid)]  
                                      pH 7.0

***Transformation of CaCl<sub>2</sub> competent cells***

An aliquot of 100  $\mu$ l competent cells was thawed on ice to which 10 ng of plasmid-DNA or ligation preparation was added and mixed by gentle swirling of a pipette tip (over 10 ng of DNA may decrease the efficiency with some competent cell preparations). The mixture was incubated on ice for 30 minutes. Thereafter, the tube was transferred to 42°C for 2 minutes before being immediately placed back on ice to cool for 2 minutes. After cooling, 1 ml LB medium (without antibiotic) was added and incubated for 1 h at 37°C with shaking at ~150 rpm. Centrifugation was performed at 6000 rpm for 5 minutes. The bacteria were then resuspended in the remaining supernatant and plated out on kanamycin selection agar destined for overnight incubation at 37°C (Cosloy and Oishi, 1973; Dagert and Ehrlich, 1979).



### III.3 - Recombinant protein expression in *E. coli*

#### *The pET expression system*

The cloning and expression of recombinant GzmH and the inactive variant GzmH<sup>S195A</sup> in *E. coli* was accomplished using the pET system from Novagen. This method is based upon the T7 promoter-driven system originally developed by Studier and colleagues (Moffatt and Studier, 1987; Rosenberg et al., 1987; Studier, 1991). The gene of interest is cloned into a pET plasmid of choice under control of the bacteriophage T7 promoter. Expression is only induced upon providing a source of T7 RNA polymerase in the host cell. The T7 RNA polymerase is so selective and active that, when fully induced, almost all of the cell's resources are converted to target gene expression. The desired product is comprised more than 50% of the total cell protein only a few hours after induction. Although this system is extremely powerful, it is also possible to attenuate the expression level simply by lowering the concentration of inducer. Decreasing the expression level may enhance the soluble yield of some target proteins. Another important benefit of this system is its ability to maintain target genes transcriptionally silent in the uninduced state. Target genes are initially cloned using hosts that do not contain the T7 RNA polymerase gene, in our case the *E. coli* strain DH5 $\alpha$  (genotype: F $\phi$ ,80*dlacZ* $\Delta$ M15,  $\Delta$ (*lacZYA*-argF) U169,*recA1*,*endA1*,*hsdR17* (rK $^-$ ,mk $^+$ ),*supE44*, $\lambda^-$ ,*tfi-1*,*gyrA*,*relA1*, Invitrogen), thus eliminating plasmid instability due to the production of proteins potentially toxic to the host cell. Once established in a non-expression host, target protein expression may be initiated by transferring the plasmid into an expression host containing a chromosomal copy of the T7 RNA polymerase gene under *lacUV5* control. Expression is induced by the addition of IPTG (1 mM) to the bacterial culture (see Figure III.1).

Both GzmH constructs were transformed into the *E. coli* expression host B834 (DE3) (genotype: F $^+$ ,*ompT*,*hsdS<sub>B</sub>*(rB $^-$ mB $^-$ ),*gal*,*dcm*,*met*(DE3), Novagen) which is a protease deficient, methionine auxotroph that, as explained above, bears the T7 RNA polymerase gene ( $\lambda$ DE3 lysogen) under the control of the *lacUV5* promoter. To prevent constitutive expression of the target gene, 2% glucose was added to the overnight pre-culture (400 ml LB-kanamycin) where it acts as a catabolic suppressor. Glucose is then removed by centrifugation (7000 rpm, 15 min, Sorvall Evolution – SLC 6000 rotor) after which the bacteria are resuspended in 80 ml LB containing kanamycin (kana) before being introduced into 10 liters of the above selection medium. The culture then undergoes shaking at 37°C until an OD (600 nm) of 0.6 is reached at which point an end-concentration of 1 mM IPTG is added thus allowing T7 RNA polymerase expression, and shortly thereafter, target gene expression. During this procedure, probes are taken and visualized on silver stained SDS electrophoresis gels in order to define the optimal duration of protein induction. In our case an incubation time of 5-6 h provided sufficient target



***Inclusion body isolation***

As mentioned above inclusion bodies (IB) are large spherical particles obtained by the over-expression of a desired recombinant protein in the cytosol of a transformed microbial host. More precisely, upon high-level expression of heterologous proteins, the natural folding pathway is frequently perturbed and instead of native, soluble protein, large inactive conglomerates (IB) accumulate within the host cell where they eventually come to span the entire diameter of the *E. coli* cell. In fact, IB formation, which is often considered a nuisance, actually has various benefits. On one hand, the resultant conglomerates provide a high enrichment of the desired protein at an early stage of purification while on the other hand, IB formation protects the recombinant protein against proteolysis by intracellular proteases. Additionally, the production of recombinant proteins initially as IB may be the method of choice for proteins that, if active, may be harmful or even lethal to the host cell.

Harvesting IB is made easy due to their relatively high specific density and so following lysis of the host cell, they can be isolated by a series of centrifugation steps which are preceded by lengthy washing in buffers composed of high salt concentrations and detergents such as Triton X-100. Moderate rotor speeds (12000 rpm, 20 minutes, Sorvall Evolution, SLC 6000 rotor) allowed the IB to sediment more rapidly than the bulk of the cell debris and the washing steps further rid the preparation of host contaminants such as cell walls or membrane fragments.

The first step, cell lysis, was performed using a combination of lysozyme (final concentration: 1 mg/ml, Sigma-Aldrich) and DNase (10 µg/ml, Sigma-Aldrich) treatment in a lysis mix (detailed below) containing MgCl<sub>2</sub> but void of EDTA as the chelator scavenges bivalent ion cofactors for metalloproteases and inhibits DNase activity. The lysis mix (25 ml / liter culture) was incubated for 30 minutes while being vigorously shaken after which 5 bursts of sonification (the Output Control and Duty Cycle of the Branson sonifier-450 set to 6) were applied. The mixture was incubated on ice to prevent over-heating. Wash-buffer I (see below) was added to the lysis mix (one-third of the lysate-volume) and shaken again vigorously at RT for an hour. The lysate was then spun down at 12000 rpm for 20' (SLC-1500 rotor, Sorvall). The IB pellet was then resuspended using a Potter-S homogenizer (Sartorius). This cycle of "wash, centrifugation and homogenization" was then repeated three times with Wash-buffer I (30 ml / 4 L culture) and then again three times with Wash buffer II (detailed below, 30 ml / 4 L culture). After the final centrifugation step, the pelleted IB were removed, weighed and stored at -20°C until use. A 10 L culture of GzmH transformed B834 hosts generally producing 4-5 g of IB material.

---

<b>Lysis mix:</b>	50 mM	Tris HCl, pH 7.2
	2 mM	MgCl <sub>2</sub>
<b>Wash buffer I:</b>	50 mM	Tris HCl, pH 7.2
	60 mM	EDTA
	1.5 M	NaCl
	6%	Triton X-100
<b>Wash buffer II:</b>	50 mM	Tris HCl, pH 7.2
	60 mM	EDTA

### ***Solubilization of inclusion bodies***

IB disintegration requires the use of rather drastic denaturants. Indeed, even though IB conglomerates contain relatively high secondary structure content, they do not disentangle under physiological solvent conditions. In our protocol 6 M guanidinium chloride (GdmCl) was chosen as the preferred denaturant due to its ability to solubilise particularly sturdy IB that are often resilient to solubilisation by other chaotrophs such as urea. Another consideration concerning the composition of the solubilisation buffer (SB buffer) was whether or not the recombinant protein in question contains cysteine residues. Isolated IB usually contain a number of interchain disulphide bonds which reduce the solubility of IB in the absence of reducing agents such dithiothreitol or Cleland's reagent (DTT), dithioerythritol (DTE) and glutathione. The addition of these thiol reagents, in combination with the above chaotrophs, results in the reduction of the interchain disulphide bonds by thiol-disulphide exchange. Recombinant GzmH contains 7 cysteine residues, as does GzmB, which were successfully solubilised following a protocol described for GzmK (Wilharm et al., 1999). Here oxidized and reduced glutathione (GSSG and GSH respectively) (Fluka) was the redox-system of choice. Finally, because the reactive species in the thiol-disulphide exchange is the thiolate anion, IB solubilisation in the presence of a reducing agent is usually performed under mildly alkaline conditions and should additionally be carried out in the presence of EDTA to prevent the oxidation of thiols by molecular oxygen and metal ions at neutral to alkaline pH values.

Recombinant GzmH IB were first of all homogenised, as described above, in freshly prepared SB buffer at pH 8 (1 ml per 100 mg IB, composition detailed below). Once well resuspended, the solubilisation mixture was shaken over night in a rotating fashion at RT. Following centrifugation (10' at 4000 rpm, GSA rotor, Sorvall Evolution) the supernatant was prepared for dialysis to rid the solubilise of the redox-system and EDTA. In the case of considerable pellet formation, the remaining IB were homogenised and sonified, as previously explained, before centrifugation. Persistent pellet

formation was dealt with by again resuspending the IB in fresh SB buffer. Dialysis was performed three times and changed every 8 hours, in 6 M GdmCl, pH 5, after which the solubilisate was diluted 1:40 and its concentration measured at 280 nm. Prior to refolding, the solubilisate was filtered (0.22 µm) and stored at 4°C.

**SB buffer:**

6 M	Guanidinium Cl
100 mM	Tris HCl, pH 8.0
20 mM	EDTA
15 mM	GSH
150 mM	GSSG

### ***Renaturation of IB proteins***

Renaturation (or refolding) of solubilised IB proteins was achieved by rapid dilution of the solubilisate in an optimised refolding buffer (RF buffer). This was preferred to refolding by dialysis where, at the stage of folding intermediates, intermediate denaturant conditions lead to high levels of precipitation. The preference of a given protein for refolding by dilution or by dialysis cannot be deduced from its molecular properties. Instead, the optimum procedure has to be determined on a case-by-case basis. Whatever the method of choice, misfolding, as well as aggregation, competes with the correct folding pathway (see *Figure III.2*). The cause of aggregation may be the result of non-specific hydrophobic interactions of predominately unfolded polypeptide chains or even due to incorrect interactions of partially structured folding intermediates. Importantly, aggregation has been shown to be concentration dependent and predominates upon refolding above a “limiting” or “threshold” concentration of solubilisate. Finding the threshold for a given solubilisate is therefore essential for successful dilution refolding.

Another parameter to consider in protein renaturation is the number of disulphide bonds the protein in question possesses. Not only must the correct noncovalent secondary, tertiary, and quaternary structures be regenerated but also the correct disulphide bonds. Disulphide bond formation is aided by exchange reactions with low molecular weight thiols, most commonly oxidised and reduced glutathione otherwise known as “oxido-shuffling” reagents although depending on the protein, other low weight thiols, such as cysteine, may better aid disulphide bond formation as is the case with our granzymes. Importantly, because thiol disulphide exchange proceeds via a nucleophilic attack on the thiolate anion, mildly alkaline conditions are used, the pH in our protocol being set at 7.3. Physical parameters such as pH, ionic strength and temperature are also reported to have a great effect on the folding process. Furthermore, buffer compounds or prosthetic groups may additionally be essential. Indeed, buffering compounds such as Tris buffer and L-arginine have been reported to greatly improve

the stability of certain proteins, again such as the members of the granzyme family, although their exact functions as “folding enhancers” remain unclear.

Finally, after sufficient renaturation time, the refolded material is filtered and concentrated to a volume suitable for dialysis. The correctly refolded protein is repetitively dialysed, following the 1:25 dilution rule, into a suitable, stabilising buffering solution thus separating the protein from RF components such as L-arginine (L-Arg) which if not removed may have an effect on the protein’s purification via cation exchanger columns.

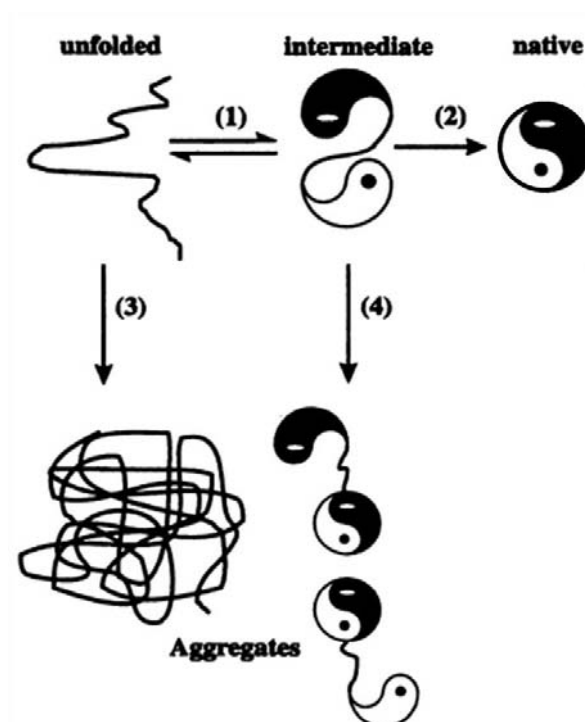


**Figure III.2 - Folding and aggregation during protein renaturation.** Correct folding reactions, leading to the native state [(1) and (2)]. Irreversible aggregation reactions, starting from different conformations during the refolding process [(3) and (4)].

GzmH was purified essentially as described (Wilharm et al., 1999), the limiting solubilisate concentration, as reported for GzmB and GzmK, remaining unchanged at 100 µg/ml. Dilution renaturation was carried out in a final volume of 5 L of RF buffer (see below). Renaturation was performed overnight at 4°C, the solubilised protein added at RT (with light stirring) followed by gradual cooling. Importantly, cysteine (0.5 mM) was given to the RF buffer just before the solubilisate. Alternatively, the solubilisate can be added in pulses every 8 hours (Cysteine always added beforehand) although a single pulse with overnight incubation at 4°C was found to produce

higher yields of correctly folded GzmH. The solubilisate was added to 5 L RF buffer at a concentration of 100 µg/ml.

**RF buffer:**

50 mM	Tris HCl, pH 7.3
0.5 M	L-arginine
1 mM	EDTA
150 mM	NaCl
0.5 mM	cysteine

After overnight incubation at 4°C, the refolding solution was filtered (0.22 µm) and concentrated from 5 L to 1 L using a 10 kDa cut off miniset filter from Palfilltron. Protein concentration was determined spectroscopically using  $\epsilon_{280\text{ nm}} = 24,960\text{ M}^{-1}\text{ cm}^{-1}$ , before and after concentration so as to determine the amount of protein loss. The concentrated inactive GzmH was then dialysed 5 times, in 5 L of 25 mM MES buffer (pH 5.5) containing physiological salt (150 mM NaCl) and 20 mM CaCl<sub>2</sub>. Protein purity can also be checked at this point by SDS-PAGE followed by silver staining (see p 42).

### ***FPLC protein purification***

Following renaturation, concentration and dialysis into a stabilising buffered solution, soluble granzyme is further purified using a technique known as *Fast Protein Liquid Chromatography* or **FPLC**. FPLC is a form of column chromatography used to separate and concentrate proteins from complex mixtures. Columns used with an FPLC can separate proteins based on size (gel filtration), hydrophobic interaction, affinity (ligand affinity, such as a His-tagged protein) and charge distribution (ion exchange, cation or anion).

GzmH was purified using an FPLC system (ÄKTAp<sub>prime</sub>, Amersham, Pharmacia Biotech, Piscataway, NJ, USA) equipped with an ion exchange column. The separation is here based on the reversible interaction between a charged protein and an oppositely charged chromatographic medium. After loading of the desired protein, the elution is usually performed by increases in salt (NaCl) concentration (or changes in pH) in form of a continuous gradient. Target proteins are thus concentrated during binding and collected in a purified, concentrated form. The net surface charge of proteins varies according to the surrounding pH which when above the isoelectric point (pI) of the protein in question will cause it to bind to an anion exchanger, while if the pH is below the pI will force the protein to bind to a cation exchanger. GzmH has a theoretical pI of 9.94 and is buffered in 150 mM NaCl, 25 mM MES at pH 5.5. Following these criteria, the strong cation ion exchanger

Source 15S media (Pharmacia) with a binding capacity of 25 mg protein /ml gel, was chosen and loaded onto a HR 5/5 column (Pharmacia).

Once loaded with the desired packing material, the column must be charged and equilibrated. First the ion exchanger is charged with counter ions (buffer B) and then equilibrated using the buffering solution in which the protein is contained (buffer A). After sample application the column is further washed with equilibration buffer A until the salt gradient is started. GzmH was eluted using buffer B and collected in fractions of 2ml. Fractions were selected and pooled after analysis by both protein determination measurements and SDS-PAGE analysis. Fractions were kept at 4°C.

**Buffer A** (Degassed):    25 mM   MES, pH 5.5  
                                     150 mM   NaCl

**Buffer B** (Degassed):    25 mM   MES, pH 5.5  
                                     2 M     NaCl

Our purification protocol for GzmA, GzmB, GzmH and GzmK uses two ion exchange column steps. First, the proform is purified and concentrated. Next, activation of the granzyme is achieved by the removal of its pro sequence, explained next. Finally, the second FPLC purification step is needed to not only separate any remaining proGzmH from its active counterpart but also to rid the protein of the applied converting agents. Although the size difference between the two forms is very small (8 amino acids) the loss of 6 histidines and a lysine causes enough reduction in positive charge to allow the active form to elute slightly before the proform. Active protein fractions are pooled after SDS-PAGE analysis and dialysed into the appropriate buffering solution. Overnight dialysis against 25 mM MES pH 5.5 and physiological NaCl (150 mM) provided stable one-time-use conditions for storage at -80°C. Under these conditions a final SDS-PAGE analysis revealed the pure and efficient conversion of both GzmH and GzmH<sup>S195A</sup>.

### ***Granzyme activation - processing by Cathepsin C***

The activation of granzymes is achieved by the removal of their prosequences, in our case the MKH<sub>6</sub> tag, creating a N-terminal sequence beginning, as in all granzymes, with the characteristic Ile-Ile-Gly-Gly. As explained, this cleavage allows the granzymes to undergo conformational change resulting in the formation of a salt bridge between the amino group of Ile16 and the carboxylate group of Asp 194, and hence a mature, active protease.



The enzyme responsible for this activation step *in vivo* is cathepsin C, otherwise known as DPPI (dipeptidyl peptidase I). Cathepsin C is a papain family cysteine protease that, at the correct pH (between 6.7 and 7.2) sequentially removes dipeptides from the free N-termini of proteins and peptides. It has broad specificity except that it does not cleave after basic amino acids such as Arg or Lysine (Lys) in the N-terminal position or proline (Pro) on either side of the scissile bond. We have placed a Lys (a stop codon for cathepsin C) after methionine as a protective measure in case of Met removal by bacterial methionine aminopeptidases. Importantly, once the last of the MKH<sub>6</sub> tag's three dipeptides is removed, conformational change and salt bridge formation between Ile16-Asp194 ensures that the new N-terminus is protected from further attack by exopeptidases such as cathepsin C.

Following the purification step, described above, bovine cathepsin C (Sigma-Aldrich) was activated by incubating the desired amount of the enzyme (0.5 U/mg protein) in conversion buffer (detailed below) for 1 h at 37°C. Concentrated proGzmH (500 µg/ml) is then added to the activated cathepsin C along with sodium acetate (50 mM NaOAc, pH 5.5) at one tenth of the total volume. Finally, 1 mM DTE is added ensuring that cathepsin C remains active. As explained above, the pH must be kept in the optimal range and therefore should be checked before leaving the mix for 6-8 hours at 30°C.

**Conversion buffer:**      50 mM   NaOAc, pH 5.5  
                                 100 mM   NaCl  
                                 1 mM   DTE

As mentioned, in our purification protocol, source S15 columns were used to purify both the pro and active forms of GzmH. As a final note, although a H<sub>6</sub> tag was adjoined as a prosequence, the use of a nickel NTA column for proGzmH purification was finally decided against. The source S15 ion exchange media proved to provide much cleaner results. Additionally, it was thought that nickel might interfere with the H<sub>6</sub> tag by attaching to histidine residues and thus interfering with cathepsin C conversion. Elution by imidazol was also thought to interfere directly with cathepsin C, possibly by blocking its active site.

### III.4 - Protein separation

#### ***SDS-polyacrylamide gel electrophoresis (SDS-PAGE)***

Gel electrophoresis is a useful method to separate and identify proteins. In sodium dodecyl sulphate (SDS) polyacrylamide gel electrophoresis (PAGE) or SDS-PAGE, proteins are separated on the basis of polypeptide length, therefore allowing their molecular weight to be estimated. Our protocol uses Laemmli buffer (a denaturing buffer) and a discontinuous gel system composed of both a stacking and separating gel. The stacking gel is slightly acidic (pH 6.8) and has a low acrylamide concentration to make a porous gel. Under these conditions proteins separate poorly but form thin, sharply defined, bands. The separating gel, is more basic (pH 8.8), and has a higher polyacrylamide content (in our case mostly 15%), which causes the gel to have narrower channels. As the protein of interest travels through the separating gel, the narrower pores have a sieving effect on the proteins, allowing smaller proteins to travel more easily and hence rapidly through the matrix (Laemmli, 1970).

#### **SDS polyacrylamide gels (15%): Eight-gel assembly**

	<b>Stacking Gel (20 ml)</b>	<b>Separating Gel (40 ml)</b>
<b>dH<sub>2</sub>O</b>	13.6 ml	9.4 ml
<b>30% acrylamide</b>	3.32 ml	20 ml
<b>1 M Tris HCl, pH 6.8</b>	2.56 ml	-
<b>1.5 M Tris HCl, pH 8.8</b>	-	10 ml
<b>20% SDS</b>	100 µl	200 µl
<b>10% APS</b>	200 µl	400 µl
<b>TEMED</b>	20 µl	16 µl
<b>Bromophenol blue</b>	5 µl	-

Once polymerized, the polyacrylamide gels were next mounted in a Mini-protean II apparatus (Bio-Rad) and covered with 1x running buffer based on glycine (10x running buffer: 250 mM Tris, 1.92 M glycine and 1% SDS in an aqueous solution). The low molecular weight protein marker, Roti-Mark prestained (Roth) was loaded (3 µl for silver staining and 5 µl for coomassie staining) in one of twelve wells during sample preparation. Concentrated Laemmli buffer ((4x denaturing buffer: 200 mM Tris HCl, pH 6.8, 40% Glycerol (denser than water, makes the sample fall to the bottom of the well), 30% β-mercaptoethanol (disulphide bridge reduction), 10% SDS (confers negative charge) and 0.2% bromophenol blue (visualisation)) was added to the samples which were then boiled (95°C, 5 minutes) and loaded. For the best results all samples should be in identical, low ionic strength buffers and

should be loaded in equal volumes. The protein amount per well should not exceed 30-40 µg. Finally, gels were run at a constant voltage (200 mV/s) using a Bio-Rad electrophoresis apparatus.

### ***III.5 - Protein detection***

#### ***Silver nitrate staining of proteins after SDS-PAGE***

After the separation of proteins comes their detection. One of the most popular detection methods is silver staining which can detect as little as 3-10 ng of loaded protein. In fact, while a 100 fold more sensitive than Coomassie blue staining, silver staining comes close to the sensitivity provided by Western Blot analysis.

Following electrophoresis, polyacrylamide gel plates were disassembled and briefly washed in *d* H<sub>2</sub>O. Next, the gels are soaked, while shaking, in a fixing solution composed of 50% Methanol, 12% acetic acid and 0.5 ml 37% formaldehyde (topped up to 1 L with *d* H<sub>2</sub>O) for 1 hour after which 3 baths of 10 minutes in 50% ethanol are required. Thereafter, the gels were introduced into a sodium thiosulphate solution (0.2 g Na<sub>2</sub>S<sub>2</sub>O<sub>3</sub> x 5 H<sub>2</sub>O per litre) for 1 minute before being washed 3 times for 20 seconds in *d* H<sub>2</sub>O. A freshly made silver nitrate solution (2 g AgNO<sub>3</sub> and 750 µl 37% formaldehyde per litre) was then exposed to the gels. After 30 minutes the staining solution is removed by several washing steps in *d* H<sub>2</sub>O. A developing solution (60 g/L Na<sub>2</sub>CO<sub>3</sub>, 4 mg/L Na<sub>2</sub>S<sub>2</sub>O<sub>3</sub> x 5 H<sub>2</sub>O, 0.5 ml 37% formaldehyde/L) is then applied and eventually stopped by thorough washing with *d* H<sub>2</sub>O. Two methanol based washes follow, first a 10 minute incubation in 50% methanol, 12% acetic acid and then a 20 minute bath in 50% methanol. Both solutions were brought to 1 L with *d* H<sub>2</sub>O. The gels were finally stored in *d* H<sub>2</sub>O. The washing procedure is always accomplished by shaking.

#### ***SDS-polyacrylamide coomassie blue staining***

Coomassie blue staining is much less sensitive than silver staining as described above. Its purpose is geared towards simple protein verification but is not intended for monitoring protein purification schemes such as is the case with our granzyme production protocols.

Following SDS-PAGE, the gel was incubated for 1 hour in Coomassie blue solution (25% isopropanol, 10% acetic acid and 0.05% Coomassie Brilliant Blue G per litre) after which it was heated to 60°C, with lid, for 1 minute in a microwave oven. After careful removal, the gel is left to shake in the solution for 5-10 minutes. The Coomassie solution is then removed (back into original bottle) and the gel is bathed in de-staining solution (10% ethanol, 10% acetic acid) until bands appear.

For the efficient removal of excess coomassie staining, absorbing paper can be used along with the exchange of destaining solution. If proteins bands take time to appear, further heating in a microwave can help accelerate development (Meyer and Lamberts, 1965).

### ***Western blot analysis - protein detection using chemiluminescence***

Simply put, Western Blot analysis is a technique used for the determination of relative amounts of proteins from different samples which have been previously separated by SDS-PAGE and thereafter blotted onto a “Hybond ECL” (nitrocellulose) membrane (Amersham-Pharmacia) again by electrophoresis, and reacted with a specific primary antibody. A secondary antibody-enzyme conjugate, which recognises the primary antibody is then added to find the locations where the primary antibody is bound by means of chemiluminescentie. Alternatively, proteins can also be transferred onto a different kind of membrane, a “Immunobilon-PSQ” (PVDF) membrane which can then be used for N-terminal sequencing of the desired protein. Before sequencing however, the membrane is stained very briefly with Coomassie blue and then destained with 30% acetic acid until a strong enough signal is detected (Bronstein et al., 1992; Towbin et al., 1979).

In this work both Wet-Transfer (Bio-Rad apparatus) and Semi-Dry (Biometra) Western blotting (WB) was performed. As a rule of thumb, Semi-Dry WB was used for low molecular weight proteins up to 30-35 kDa. Wet-Transfer WB on the other hand was chosen for proteins exceeding 35 kDa in size. Fresh transfer buffer was made before both procedures and although the Wet Transfer WB also worked well for proteins of low molecular weight, Semi-Dry WB was often the method of choice as much less transfer buffer (25 mM Tris HCl, 200 mM glycine, 20% methanol, 0.1% SDS) is needed along with less Whatman 3 mm paper.

Before the Wet Transfer run is carried out, the SDS polyacrylamide gel and both Whatman and membrane of choice are equilibrated in transfer buffer. Then, after assembly and correct set up of the Bio-Rad Protean apparatus (filled with transfer buffer and containing an ice pack) the transfer is initiated and run for 1 h at 100 V. Constant stirring is applied during the transfer.

The Semi-Dry procedure differs in a number of aspects. Apart from being preferred for low molecular weight proteins, as noted above, the quantity of buffer is largely reduced. Secondly, the sandwich assembly is horizontal, the bottom surface being the cathode. Further differences include the use of fewer Whatman sheets (3 each side as opposed to 5 in Wet-Transfer WB) and importantly, depending on the surface area with the membrane, an increasing surface requires an increase in the voltage applied.

Once the run of choice is through, the transfer is verified by checking the presence of a similarly sized pre-stained marker bands (Roth). Thereafter, the membrane is washed three times in PBS-T (1x PBS, 0.05% Tween) and blocked in a milk solution (PBS-T, 5% non-fat-powered-milk (NFPM)) for 1 h at RT (shaking). The membrane was then washed three times in PBS-T with shaking before being exposed overnight to the desired primary antibody, diluted appropriately in PBS-T containing 5% NFPM, at 4°C with rotation. To save antibody, the membrane was sealed within a tight, special plastic poach. Again, the membrane is washed three times, with shaking in PBS-T. The PBS-T was then drained off before the ECL substrate solution (Amersham Pharmacia), 1 ml of both solutions mixed for a membrane of 5x10 cm in size, was added for 1 min. Finally, the membrane was exposed to X-ray ECL film (Amersham Pharmacia) for 20 seconds to 30 minutes until the expected bands developed.

### ***Spectrophotometric determination of protein concentration***

The concentration of a sample protein in solution can be determined by spectrophotometric methods. Absorbance can be measured at 280 or 215-230 nm, a simple method that can be used for crude lysates or for purified or partially purified proteins. Indeed, proteins have two absorbance peaks in the UV region, one between 215-230 nm, where the peptide bonds absorb, and another at 280 nm where light is absorbed by aromatic amino acids, tyrosine (Tyr), tryptophane (Trp) and phenylalanine (Phe).

Protein concentration was calculated as such:  $c(\text{mg/ml}) = (A_{280} \times \text{MW}) / (\epsilon_{280} \times b)$

where, c is the concentration,  $A_{280}$  is the measured absorbance at this wave length (biophotometer, Eppendorf), MW, the molecular weight of the protein in question,  $\epsilon_{280}$ , the absorption coefficient and b, the path length, which for most spectrometers is 1 cm. Alternatively, a coefficient factor can be calculated,  $\text{MW} / (\epsilon_{280} \times b)$ , that can multiplied against  $A_{280}$ .

Although proteins have little absorbance at 260 nm, both proteins and nucleic acids absorb at 280 nm and therefore, if mixed, their spectra interfere with one another. Because nucleic acids have maximal absorbance at 260 nm, protein purity can be estimated by dividing  $A_{260}/A_{280}$  where a ratio of 0.6 is characteristic of pure protein. Finally, our spectrophotometer (Biophotometer, Eppendorf) also displays a 320 nm reading for protein measurement which should show virtually no absorbance since neither nucleic acids nor proteins absorb at this wave length [Warburg et al., 1942; Layne et al., 1957].

### ***Colorimetric determination of protein concentration***

The colorimetric methods make use of the property that certain ions change in adsorption maximum on binding to other molecules such as proteins. In this work, the colorimetric quantification of proteins was based on the Bradford assay, where instead of Coomassie Brilliant Blue G, a Bio-Rad protein dye equivalent was used which also has absorption maximum shifting from 465 to 595 nm upon binding to proteins. Standard cuvettes were used in this assay. In the cuvettes, different quantities of BSA (1-10 µg) were carefully mixed with 200 µl of Bio-Rad protein dye. Absorption was then measured at 595 nm and the BSA values drawn as a standard curve. The desired protein sample(s) are dealt with as above and their concentration determined against the linear BSA curve (Bradford, 1976).

### ***III.6 - Enzymatic tests***

#### ***Recombinant granzyme activity assays***

The enzymatic analysis of GzmH was performed in 96 well plates and monitored using a Dynatech MR4000 microplate reader. The esterolytic activity of GzmH was previously demonstrated by Edwards and colleagues using a thiobenzyl ester. As reported, the enzymatic hydrolysis of peptide thioester substrate Suc-Phe-Leu-Phe-SBzl was measured in a activity buffer (50 mM Tris HCl pH 8, 150 mM NaCl, and 0.01% X-100) at RT. A 10x assay buffer was made for convenience. From the GzmH stock preparation (500 µg/ml in 25 mM MES, 150 mM NaCl, pH 6), the enzyme was diluted to 300 nM in 1x assay buffer. Ten µl was then added to a well containing 90 µl of 1x activity buffer. A further 50 µl, containing 2.25 µl substrate Suc-Phe-Leu-Phe-SBzl (0.9 mM), 2.25 µl DTNB (0.9 mM) and 45.5 µl 1x assay buffer was then added bringing the final concentrations in 150 µl total volume to 20 nM GzmH (20 nM = 0.5 µg), 0.3 mM substrate and 0.3 mM DTNB. Once the substrate added, its hydrolysis was monitored by absorbance at OD 405 using a Dynatech MR4000 microplate reader. In some assays Cathepsin G or mast cell chymase (both from Merck Biosciences) were used as positive controls.

New peptide substrates H-Pro-Thr-Ser-Tyr-AMC and H-Ala-Thr-Ser-Tyr-AMC, a kind gift from Dr. Doerner (Merck Biosciences) were tested. Both amide substrates were delineated from a peptide substrate library scan PS-SCL, positional scanning synthetic combinatorial libraries, described by Mahrus and Craik in 2005. The substrates were dissolved in 99.5% pure DMSO (Sigma Aldrich) to a concentration of 50 mM and diluted to 250 µM in activity buffer. Fluorescence intensities were recorded with a Fluostar Optima (BMG Labtech, Offenburg, Germany) at RT and evaluated using the Fluostar Optima software.

Enzymatic activity of GzmB (200 nM) was measured using the substrate Ac-IEPD-pNA (10 mM in 99.5% DMSO) at a final concentration of 250  $\mu$ M in 100  $\mu$ l activity buffer. Absorption of the resulting cleavage was again monitored at OD 405 using the above reader.

### ***Recombinant GzmH inhibition assays***

Inhibition by DCI (3,4-Dichloroisocoumarin), a highly reactive, potent irreversible general serine protease inhibitor and the phosphonate inhibitors from J.C. Powers, were measured as described above. Inhibition was measured by incubating 4.5  $\mu$ l GzmH (11.11  $\mu$ M) with 0.5  $\mu$ l inhibitor (10 mM) for 20 min at room temperature. The 5  $\mu$ l was then transferred to 166.6  $\mu$ l of buffer bringing down the molarity to 300 nM. After mixing, 3x 10  $\mu$ l was immediately added to 90  $\mu$ l buffer triplicates. The substrate, DTNB, and buffer were added to assay the residual enzyme activity as described above. As a note, the incubation of enzyme (E) and inhibitor (I) was performed at stock concentrations thus increasing E-I interaction instead of previous dilution in an assay buffer; DCI is not so very stable in aqueous solutions. Finally, for optimal E-I interaction a physiological salt concentration of 137 mM and of pH 7.4 is optimal.

### **Reagents:**

- Suc-Phe-Leu-Phe-SBzl (Bachem) for GzmH. Stock solution: 20 mM in 99.5% pure DMSO (Sigma). Final concentration in test: 0.3 mM
- H-Pro-Thr-Ser-Tyr-AMC and H-Ala-Thr-Ser-Tyr-AMC (Merck Biosciences) for GzmH. Stock solutions: 50 mM in 99.5% pure DMSO (Sigma). Final concentration in test: 0.25 mM
- Ac-IEPD-pNA (Calbiochem) for GzmB. Stock solutions: 10 mM in 99.5% pure DMSO (Sigma). Final concentration in test: 0.25 mM
- DCI (Sigma). Stock solution: 10mM in 99.5% pure DMSO (Sigma). Final concentrations in test: 1 and 10 mM
- DTNB (Sigma). Stock solution: 20mM in 99.5% pure DMSO (Sigma). Final concentration in test: 0.3 mM.
- Assay buffer: 50 mM Tris HCl pH 8, 150 mM NaCl, and 0.01% Triton X-100

### ***III.7 - Apoptosis assays***

#### ***Culture of target cells***

K562 (immortalized erythroleukemia cells derived from a patient with chronic myelogenous leukemia, initialised CML), HL-60 (Human Caucasian promyelocytic leukaemia cell line) and U937 (Human leukemic monocyte lymphoma cell line) cells were cultured in RPMI 1640 supplemented with 10% fetal bovine serum (FBS), 2 mM L-glutamine, 100 U/ml penicillin/ streptomycin (Gibco) in a humidified atmosphere at 37°C with air containing 5% CO<sub>2</sub>. The NK cell lines, YT, NK92 and NKL were also maintained in RPMI containing GlutaMax, 15% FBS, 100 U/ml penicillin/streptomycin and 200 U/ml interleukin-2 (IL-2).

#### ***Changes in membrane integrity***

##### ***FITC- annexin V & propidium iodide staining***

Killing assays and target cell staining with annexin V-FITC (AV) and propidium iodide (PI) were performed in triplicates in 96-microwell plates (NUNC #163320, Wiesbaden, Germany) using  $1 \times 10^5$  cells in 50  $\mu$ l ( $2 \times 10^6$ /ml) per well in serum free, 0.5% BSA RPMI GlutaMax medium. All assays were performed in 50  $\mu$ l total volume (100,000 cells) unless indicated. GzmB and GzmH (both at stock concentrations of 500  $\mu$ g/ml) were added to the cells at the indicated final concentrations (see figure legends) before the addition of translocator proteins, namely perforin (PFN) and Streptolysin O (SLO). SLO, but not perforin, was activated prior to use in medium containing 40  $\mu$ M cysteine for 10 minutes at RT, diluted and freshly added to the cells at a final concentration which depended on the cells type. Indeed, sublytic concentrations of every new batch of perforin (a generous gift from C. J. Froelich, Evanston, IL), SLO (Sigma-Aldrich) were determined separately for K562, U937 and HL60 cells and were defined as the concentration required to induce cell death in 10% to 20% of all cells. PFN was used at final concentrations of 75-80 ng/ml with HL60 cells and 200-225 ng/ml with K562 cells. SLO was used at 75 ng/ml and 125-175 ng/ml respectively.

After the necessary incubation period, cells were washed twice in 1x PBS. Cells were then stained for 15 minutes in a volume of 25  $\mu$ l at RT with fluorescein isothiocyanate (FITC)-annexin V (15  $\mu$ M, recombinantly produced and FITC labeled) at 1:100 and propidium iodide (BD biosciences, stock concentration 1 mg/ml) 1:20 in annexin binding buffer (BD biosciences). Following this, the cells were diluted in binding buffer and analysed by fluorescence activated cell sorter (FACS) with CellQuest software (BD Biosciences, Heidelberg, Germany). In some experiments the caspase inhibitors zVAD-FMK, zDEVD-FMK and zVDVAD-FMK (Bachem, Bubendorf, Switzerland) were



applied at a final concentration of 50  $\mu$ M from 50 mM stock solutions resuspended in 99.5% pure DMSO (Sigma) (Kurschus et al., 2004; Kurschus et al., 2005).

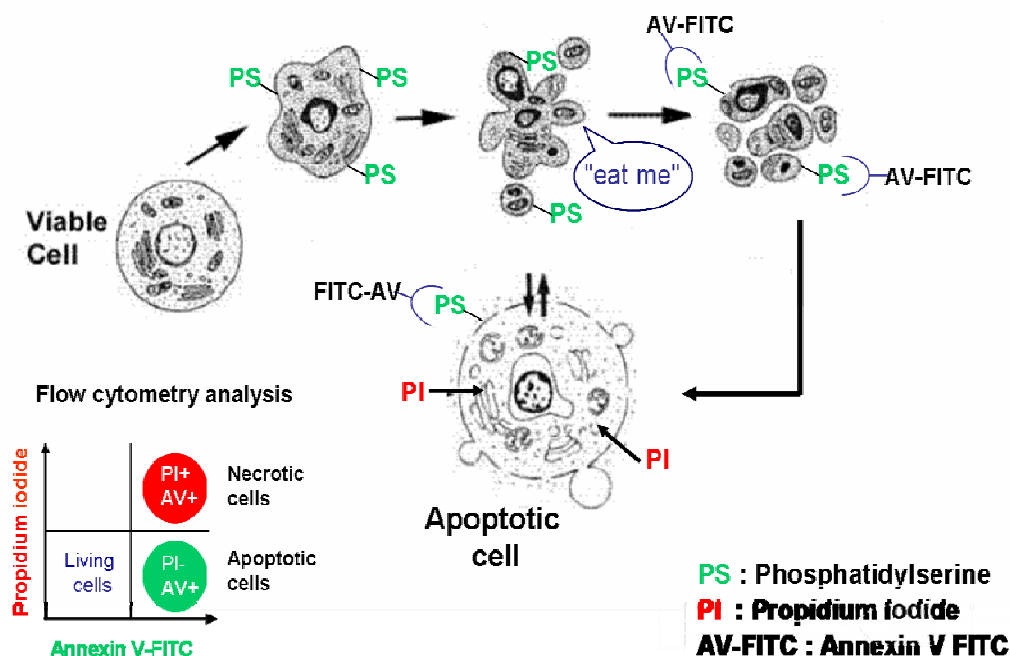


**Figure III.3 - The annexin V-FITC, propidium iodide assay.** Propidium iodide (PI) intercalates into the major groove of double-stranded DNA and produces a highly fluorescent adduct that can be excited at 488 nm with a broad emission centered around 600 nm. Annexin V-FITC (AV), on the other hand detects the relocation of membrane phosphatidylserine from the intracellular surface to the extracellular surface. Following one hour of GzmB treatment K562 cells, for example, display apoptotic features, many of which can be detected by flow cytometry. Following staining with AV and PI, a dot plot would display living cells as AV negative and PI negative, whereas apoptotic but not dead cells would be defined by an AV<sup>+</sup> and PI<sup>-</sup> population while necrotic cells would be displayed as being AV<sup>+</sup> and PI<sup>+</sup>.

### Trypan blue staining

Trypan blue is so-called because it can kill trypanosomes, the parasites that cause sleeping sickness. The dye is also known as diamine blue and Niagara blue. Trypan blue is a vital dye. The reactivity of trypan blue is based on the fact that the chromophore is negatively charged and therefore does not interact with the cell unless the membrane is damaged allowing the researcher to distinguish between viable and non viable cells. Trypan blue staining of K562 and HL60 cells was performed by mixing equal volumes of cell suspension with a 0.4% trypan blue solution diluted to 0.1% (T8154, Sigma-Aldrich). Cells were then counted using a hemocytometer. The percentage of trypan-blue-positive cells was then scored.

## ***Caspase activation***

### ***Purified recombinant pro-caspases as potential substrates***

Caspases are synthesized as inactive pro-enzymes and are activated by cleavage at specific aspartate cleavage sites to release an N-terminal pro domain, leaving two subunits (p20 and p10) to heterodimerise. Since all caspases are cleaved at specific aspartate residues, it raises the possibility that some caspases sequentially activate others thereby establishing a hierarchy of caspases. A distinctive feature of caspases is the absolute requirement of aspartate residue in the P1 position. The carboxylate side chain of the substrate P1 Asp is tethered by four residues in caspase 1 (Arg179 and Gln238 from p20; Arg341 and Ser347 from p10) that are well conserved in all family members. The P4 residue is important in substrate recognition and specificity (caspase-1 prefers a hydrophobic tyrosine whereas caspase 3 prefers an anionic aspartic acid residue). Generally, the catalysis involves a cysteine proteinase mechanism. The tetrapeptides used in this work to identify differential caspase activities correspond to the substrate P4-P1 residues.

Catalytically inactive human procaspases 3 and 7 (5  $\mu$ M), in which the active site Cys285 was replaced by an Ala residue (Riedl et al., 2001; Riedl et al., 2005), were used to avoid auto-activation (a gift of Stefan Riedl). The procaspases were incubated with either recombinant GzmH or GzmB for 1 h at 37°C in activity buffer (50 mM Tris HCl pH 8, 150 mM NaCl, and 0.01% TX-100) in a final volume of 10  $\mu$ l. Refer to figure legends for GzmB and GzmH final concentrations. Samples were boiled in reducing Laemmli buffer, loaded and separated on an 18% polyacrylamide gel. Electrophoretically separated bands were visualized by silver staining.

### ***Caspase activity in living cells***

Caspase activity can be assayed using either a fluorophore (AMC, AFC) or a chromophore (pNA) attached to a substrate sequence although fluorogenic substrates offer a greater sensitivity of detection compared to colorimetric substrates. To increase the cell permeability of caspase substrates, aspartate residues were esterified (OMe).

Caspase activity, in intact (non-lysed) target cells, was measured with fluorogenic substrates. The cells were mixed with the substrates acDEVD-AMC, acLEHD-AMC or zVDVAD-AFC (Merck Biosciences) at a final concentration of 100  $\mu$ M in RPMI 1640 medium (without phenol red). This medium contained 0.5% BSA (Sigma-Aldrich), hepes (25 mM), 100 U/mL of both penicillin and streptomycin and 2 mM L-glutamine (Invitrogen, Karlsruhe, Germany). Each mix was then plated on a 96-well plate, with flat bottom, for 1 hour at 37°C in a 5% CO<sub>2</sub> atmosphere. In several experiments caspase inhibitors were included in the cell culture medium before treating the cells with granzymes

and sublytic concentrations of PFN or SLO. Substrate hydrolysis was directly monitored using a Wallac Victor 2 multi-label counter, model 1420, (Perkin Elmer, Fremont, CA) at 37°C. AMC was monitored by excitation at 380 nm and emission at 460 nm, AFC by excitation at 420 nm and emission at 520 nm.

### ***DNA Laddering***

A caspase-3-activated DNase, most likely caspase activated DNase (CAD), produces internucleosomal DNA cleavage, otherwise known as DNA laddering. GzmB is also reported to directly cleave the inhibitor of CAD. Apoptotic DNA-laddering was done as described by Hermann *et al.*, in 1994. After treatment with GzmB (10 µg/ml) or GzmH (20 µg/ml) K562 cells were pelleted and treated for 10 minutes in lysis buffer (1% NP-40 in 20 mM EDTA, 50 mM Tris HCl, pH 7.5). Ten µl of lysis buffer was used per 10<sup>6</sup> cells (e.g. 5x10<sup>6</sup> in 50 µl). After 5 minutes of centrifugation at 3000 rpm, the supernatant was collected and the extraction is repeated with the same volume of lysis buffer. The supernatants (and the resuspended nuclei as control for the complete recovery of apoptotic DNA fragments) are brought to 1% SDS (20% stock) and treated for 2 h with RNase A (stock concentration 10 mg/ml, final concentration 100 µg/ml) at 56°C. Digestion with proteinase K (stock concentration 10 mg/ml, final concentration 100 µg/ml) followed for 2 hours at 37°C. After the addition of half the volume of 10 M ammonium acetate, the DNA was precipitated with 2.5 volumes of 100% ethanol. Pellets were collected and dried before being dissolved in 20 µl TE buffer (10 mM Tris HCl, pH 7.5 1 mM EDTA) and separated by electrophoresis in 1% agarose gels (Herrmann *et al.*, 1994).

### **Assay Scheme:**

- K562 cells (5x10<sup>6</sup> in 50 µl total vol.) were treated with GzmB (10 µg/ml) and GzmH (20µg/ml).
- After treatment for 4 & 12 hours, cells were pelleted and lysed in lysis buffer (10 µl per 10<sup>6</sup> cells).
- After 10 minutes, cells were again pelleted (3000 rpm, Eppendorf) and the supernatants collected.
- Supernatants were treated with SDS (1%) and RNase A (100 µg/ml) for 2 h at 56°C.
- Proteinase K (100 µg/ml) was added for additional 2 h at 37°C.
- A half vol. of 10 M NH<sub>4</sub>-acetate is added and the DNA precipitated with 2.5 vol. of 100% ethanol.
- Finally, the pellets were dried, dissolved in 20 µl TAE buffer and separated by electrophoresis.

### ***ICAD cleavage***

Caspase activated DNase is constitutively inhibited by the inhibitor of CAD (ICAD), which can be cleaved by active caspase 3 or directly by GzmB. The inhibitor-enzyme complex then dissolves and CAD executes DNase activity leading to DNA fragmentation (Enari 1998). Cleavage of endogenous ICAD was analyzed after K562 cells were incubated with GzmB or GzmH and SLO (see figure

legend). At defined time points, 100  $\mu$ l of cells at  $1 \times 10^5$  were harvested and washed in PBS before being directly boiled in reducing Laemmli buffer. After SDS-PAGE on a 15% gel, protein bands were blotted on nitrocellulose (Amersham Biosciences) and probed with the anti-human ICAD polyclonal rabbit antibody (eBioscience, San Diego, CA). The anti-actin mouse monoclonal antibody (clone JLA20 from Calbiochem) at a 1:5000 dilution was used to control loading.

### ***Mitochondrial damage***

#### ***Purified recombinant Bcl-2 family protein Bid***

A number of different proapoptotic signals trigger mitochondrial membrane permeability (MMP). One such stimulus is provided by GzmB which can cleave the Bcl-2 family protein Bid to a truncated proapoptotic form, namely t-Bid. The truncated form then translocates from the cytosol to the mitochondrial outer membrane resulting in the formation of pores. MMP culminates in the complete loss of the barrier function of the outer mitochondrial membrane and the subsequent release of proapoptotic proteins such as cytochrome c.

As reported for the analysis of recombinant procaspases, purified recombinant human Bid (5  $\mu$ M, a kind gift from Shirely Gil-Parrado) was incubated with nM concentrations of either recombinant GzmH or GzmB for 1 h at 37 °C in activity buffer (50 mM Tris HCl pH 8, 150 mM NaCl, and 0.01% triton) in a final volume of 10  $\mu$ l. Refer to figure legend for final GzmB and GzmH concentrations. Samples were boiled in reducing Laemmli buffer, loaded and separated on an 18% polyacrylamide gel. Electrophoretically separated bands were visualized by silver staining.

#### ***Mitochondrial trans-membrane potential loss***

The loss of mitochondrial membrane potential ( $\Delta\Psi$ ) is a hallmark in apoptosis. It is an early event that precedes phosphatidylserine (PS) externalization and that is thought to coincide with caspase activation, although this is not always thought to be the case (Balasubramanian et al., 2001; Savill et al., 2002). JC-1 is a cationic dye that measures the mitochondrial membrane potential in cells. Indeed, in non-apoptotic cells JC-1 (5,5',6,6'-tetrachloro-1,1',3,3'-tetraethylbenzimidazolyl-carbocyanine iodide) exists as a monomer in the cytosol (green) and accumulates as aggregates in the mitochondria which stain red. Here, the negative charge established by the intact mitochondrial membrane potential allows the lipophilic dye, bearing a delocalized positive charge, to enter the mitochondrial matrix where it accumulates. Finally, when the critical concentration is exceeded, J-aggregates form which become fluorescent red. In apoptotic and necrotic cells however, the mitochondrial membrane

collapses subsequently leading to the release of the dye into the cytosol where it assumes its monomeric form and becomes green. The aggregate red form has an absorption/emission maxima of 585/590 nm whereas the green form has an absorption/emission of 510/527 nm. For the measurement of mitochondrial depolarization our target cells were prepared for staining as explained in the AV/PI method. The cells were then stained with JC-1 (Merck Biosciences) at a final concentration of 10  $\mu\text{g/ml}$  in PBS for 15 min and directly analyzed by FACS.

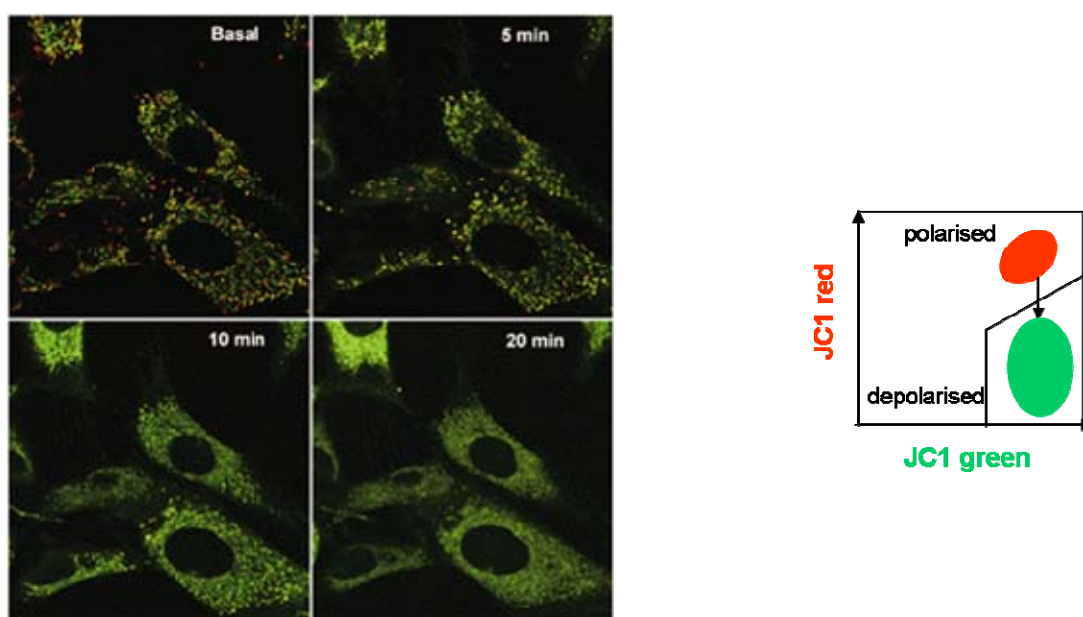


**Figure III.4 - Mitochondrial depolarization.** NIH 3T3 fibroblasts stained with JC-1 following exposure to hydrogen peroxide. JC-1 is a cationic dye that produces two emissions depending on the mitochondrial membrane potential. Red indicates polarized mitochondria (the dye is aggregated) and green depolarized mitochondria (the dye is found as a monomer). Taken from the Perugia University Medical School library.

### ***ROS production***

Mitochondria play a central role in the regulation of apoptosis and in ROS generation. It remains unclear, however, how mitochondrial ROS production is regulated during apoptosis and if ROS generation is at all necessary for the completion of cell death.

In this work intracellular ROS production was monitored by adding 2  $\mu\text{M}$  DHE (Molecular Probes, Eugene, OR) just before FACS analysis to cells treated at 37°C with GzmH (20  $\mu\text{g/ml}$ ), the inactive variant (20  $\mu\text{g/ml}$ ) or GzmB (10  $\mu\text{g/ml}$ ) every 5 minutes up to 90 minutes. For ROS measuring experiments, SLO<sup>C530A</sup>, a SLO variant mutated at the activating residue Cys530 was used to circumvent the need for prior activation under reducing conditions. In these cases mercaptoethanol (ME) was omitted from RPMI GlutaMax medium containing 0.5% BSA as well as 100 U/ml penicillin

and streptomycin. As a positive control, cells were exposed to 1 to 3% H<sub>2</sub>O<sub>2</sub> (hydrogen peroxide, Merck, Darmstadt, Germany).

### ***Cytochrome c release from mitochondria***

Digitonin is a weak nonionic detergent that, at low concentrations, selectively renders the plasma membrane permeable, releasing cytosolic components from cells but leaving other organelles intact (Heibei et al., 1999). This is an ideal compound with which to study the release of mitochondrial inter membrane space proteins (MIMPs) such as cytochrome c, the smallest members of the proapoptotic MIMPs.

Following treatment with GzmH (20 µg/ml) or GzmB (10 µg/ml) after 1, 2 and 6 hours, K562 cells ( $1 \times 10^5$  / 50µl) were washed twice with 1x PBS and resuspended in 200 µl digitonin lysis buffer (75 mM NaCl, 1 mM NaH<sub>2</sub>PO<sub>4</sub>, 8 mM Na<sub>2</sub>HPO<sub>4</sub>, 250 mM sucrose, 190 µg/ml digitonin, pH 7.4). After 5 min on ice, cells were spun for 5 min at 14,000 rpm at 4 °C. Supernatants were transferred to fresh tubes, and the pellets resuspended in Triton lysis buffer (25 mM Tris HCl, pH 8.0 , 0.1% Triton X-100). Aliquots of both pellet and supernatant for each sample were added SDS-loading buffer and boiled for 5 min. Boiled samples were then loaded onto 15% polyacrylamide gels followed by electrophoresis and transfer to nitrocellulose membranes, membranes were blocked overnight at 4°C in PBS-T, 5% milk. Blocked membranes were incubated with a monoclonal anti-human cytochrome c antibody (Clone JLA20, Merck Biosciences, 1:2000 dilution) in PBS-T containing 5% milk for 1 h at room temperature. Membranes were washed three times (5 min each) with PBS-T. The anti-actin mouse monoclonal antibody (clone JLA20 from Calbiochem) at a 1:5000 dilution was used to control loading. Specific mouse and rabbit antibodies were detected with goat anti-mouse (1:2000, Perbio Science, Bonn, Germany) or goat anti-rabbit antibodies (1: 5000, Jackson Immunoresearch, Hamburg, Germany) conjugated to horseradish peroxidase (HRP) respectively. Bound HRP antibody conjugates were visualized with the SuperSignal West Pico substrate (Perbio Science) (Heibei et al., 1999).

### ***Characterization of monoclonal GzmH antibodies***

ELISA (Enzyme-Linked Immunosorbent Assay) can be performed in a number of ways. One of the most useful methods is the two antibody “sandwich” ELISA which requires two antibodies that bind to epitopes which do not overlap on the antigen of interest. In our method however recombinant GzmH was directly coated to special immuno absorbent plates. Unbound products are removed with a

washing step and then labeled with the specific antibody or “detection” antibody.” Thereafter, the primary antibody specificity is measured through the use of a colorimetric substrate.

Indeed, to evaluate the specificity of monoclonal antibodies, purified recombinant GzmB and GzmH at a final concentration of 2.5 µg/ml were coated in a buffer containing 0.01 M Na<sub>2</sub>CO<sub>3</sub>, 0.04 M NaHCO<sub>3</sub>, 0.02% NaN<sub>3</sub>, pH 9.6 over night (100 µl / well). After washing and blocking with 0.05% Tween 20 and 2% caseine in PBS, the primary antibody against human GzmH (MAB1377, R&D Systems) or a mouse isotype control antibody (BD #553447) was added at a final concentration of 1 µg/ml. The solid phase ELISA was developed with peroxidase-conjugated goat anti-mouse antibodies and 3,3',5,5'-tetramethylbenzidine (TMB) as a chromogenic substrate (GE Healthcare Europe, Munich, Germany). Optical density of the reaction product was measured at 405 nm using the Dynatech MR4000 plate reader.

### ***Isolation of peripheral blood leukocyte subsets and NK cells***

#### ***Peripheral blood leukocyte subsets***

Monocytes were obtained from the remaining CD56-negative cell population by depletion of the nonmonocytic cells using a cocktail of biotin-conjugated antibodies (Miltenyi Biotec, Bergisch-Gladbach, Germany, catalog no. 130-091-153). CTLs were purified from PBMCs by positive selection with anti-CD8 dynabeads, and activated and expanded using anti-CD3/anti-CD28 dynabeads, overnight without the addition of IL-2. (refer to CD3/CD28 T-cell expander kit PDF from Invitrogen). For Western blot analyses, cells were lysed (50 µl / 3 x 10<sup>6</sup> cells) in a buffer containing 150 mM NaCl, 20 mM Tris HCl pH 7.2, 1% Triton X-100 (“lysis buffer”). A volume of 10 µl of lysis supernatant was loaded per lane.

#### ***NK cell isolation***

CD56 positive cells were purified from human PBMC by positive selection with the CD56 MultiSort Kit (Miltenyi Biotec, Bergisch-Gladbach, Germany, catalog no. 130-055-401) and thereafter used for GzmH and GzmB detection by western blot analysis. NK cells for killing assays were purified from fresh PBMCs using the Dynal® NK cell negative isolation kit (Invitrogen, Karlsruhe, Germany). Negatively isolated NK cell purity was assessed by FACS analysis with the PE-labelled CD16 and CD56 antibodies but also with the FITC labeled CD3 antibody (Immunotools, Friesoythe, Germany). Following FACS analysis, NK cell purity was found to be greater than 90% (see *Figure III.5*).

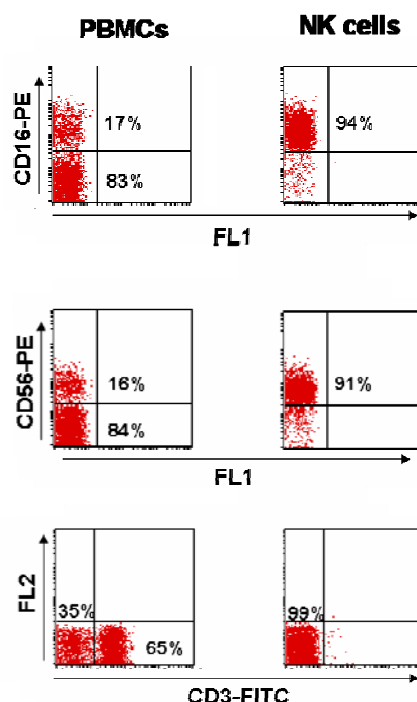


**Figure III.5 - Purity of negatively isolated Natural Killer cells.** Naive NK cells were isolated using the Dynal Negative selection kit to avoid any kind of activation and hence up-regulation of granzymes. PBMCs and NK cells were stained for NK cell markers CD16 (FL2) and CD56 (FL2) and the T-cell lineage marker CD3 (FL1) after which they were analysed by FACS.

### *NK cell cytotoxicity and granzyme release*

#### *NK cell killing of target cells*

Killing assays were performed for 4 hours in RPMI 1640 supplemented solely with 100 U/mL penicillin/streptomycin and 2 mM L-glutamine and IL-2 100 U/ml (Roche) in small cell culture flasks in a volume of 8 ml containing  $8 \times 10^6$  NK cells and  $4 \times 10^6$  K562 cells. Killing efficiency of target cells was determined by FACS after AV/PI staining using specific forward/sideward scatter characteristics which permitted us to discriminate between NK and K562 cells. Refer to *Figure IV.31*.

#### *GzmH release from NK cells*

Following killing verification, the culture supernatants were collected by sequential centrifugation (500 g for 10 min following by 20000 g for 15 min at 4 °C) and concentrated 40-fold (5 KNMWL ultrafree, Millipore, Schwalbach, Germany). FBS was not used during NK killing as we had encountered problems during the gel run, the FBS being too concentrated and thus blocking normal protein migration. Twenty microlitres of the concentrated supernatant was loaded and immunoblotted against GzmH (monoclonal antibody MB1377, R&D systems) or GzmB (monoclonal antibody GB11,



Hiss Diagnostics GmbH). Mouse isotypes controls were also used, namely #553447 and #557351 (BD biosciences) for the granzymes respectively. In some cases concentrated supernatants were pretreated with hyaluronidase (Sigma-Aldrich) at 80 µg/ml for 30 min at RT. Hyaluronidase was added to supernatants in an attempt to release GzmH from proteoglycans.

### ***Cellular morphology and nuclear fragmentation***

#### ***Apoptotic nuclei***

To distinguish living cells from those with apoptotic nuclei, bright field pictures were taken with an inverted microscope (Zeiss, Axiovert 200M, 40x objective, numerical aperture 0.6) connected to a Coolsnap-HQ camera (Photometrics, Roper Scientific, Ottobrunn, Germany). Additionally, staining of GzmH and GzmB treated cells for apoptotic nuclei was done in solution in annexin V binding buffer with annexin V-FITC (30 nM) and the Hoechst dye 33342 (Merck Biosciences) at 4 µg/ml for 10 min at RT. Cells were washed, bound on poly-L-lysine (Sigma Aldrich) coated coverslips, fixed with 2% formaldehyde, washed and mounted with Moviol (Sigma Aldrich). Fluorescent pictures were taken with an inverted microscope (Zeiss, Axiovert 200M) using a 40x objective or a 63 x oil objective (Zeiss) and processed using MetaMorph software (Visitron Systems, Puchheim, Germany). For quantification one half of a visual field showing about 50 to 200 cells was evaluated.

#### ***Nuclear fragmentation***

The DNA content of K562 target cells and the rate of apoptotic cells that appear in the sub-G1 peak of DNA histograms were analyzed by FACS after staining with PI (Sigma-Aldrich). After DNA fragmentation, the sub-G1 method relies on a series of simple steps. Cells are first fixed in EtOH before being rehydrated. Membrane poration for PI entry is then performed using a detergent, a process in which cleaved apoptotic DNA is lost. RNA is also removed as it is also stained by PI. FACS analysis then reveals that in cells undergoing cell death, which have lost DNA, less PI is taken up and thus appear on the left of the G1 peak.

Treated cells ( $1 \times 10^5$  cells / well) were first spun down (3000 rpm, Eppendorf) and resuspended in PBS (300 µl) before 100% ice cold ethanol (900 µl, from -20 °C) was added drop wise using a vortex. Samples were then kept at -20°C for 15 minutes (for up to several weeks) before being centrifuged (6000 rpm) and the pellet resuspended in 0.5 ml PBS, 0.1% NP-40 and left on ice for 10 minutes. After another spin down, the pellet was resuspended in PBS (279 µl) to which 6 µl RNase A (10

mg/ml) was added. The samples were then left at RT for 15 minutes before PI was added to a final concentration of 50 µg/ml and left in the dark for up to an hour. FACS analysis followed.

### ***<sup>3</sup>H-Thymidine release assay***

The <sup>3</sup>H-Thymidine assay allows the determination of the amount of DNA that is degraded upon treatment of cells with cell death causing agents such as our granzymes. The principle of this assay is to radioactively label the target cell DNA by growing the cells in presence of <sup>3</sup>H-Thymidine. The radioactive <sup>3</sup>H-Thymidine is then incorporated into the host DNA. After exposure of cells to GzmB and GzmH, the target cells are harvested and the release of radioactively labeled DNA measured. To calculate the percentage of DNA fragmentation the counted radioactivity (counts per minute = cpm) of cells that were not treated is compared with the cpm in cells that were treated.

Target cells were labeled by adding 5 µCi/ml [methyl-<sup>3</sup>H] thymidine (Amersham Biosciences, Freiburg, Germany) for 20 h to cell cultures in the logarithmic growth phase. The cells ( $1 \times 10^5$  / 50 µl) were then washed three times with RPMI GlutaMax medium (0.5% BSA and 100 U penicillin/streptomycin) and prepared for exposure to GzmB and GzmH in a final volume of 50 µl of medium. After the indicated times of incubation at 37°C the cells were lysed with an equal volume (50 µl) of 1% Triton X-100 in 100 mM Tris, 50 mM EDTA, transferred to 1.5 ml Eppendorf tubes, vortexed, and centrifuged for 10 min at 4 °C at 15,000 x g to pellet intact nuclei. For analysis of total DNA labeling, the respective samples were lysed with an equal volume of 2% SDS in 0.1 M NaOH and vigorously vortexed. Thereafter, 25 µl of supernatant was removed to scintillation plates, mixed with 100 µl of scintillation mixture (PerkinElmer Life Sciences), and counted on a Wallac MicroBeta Trilux counter. The specific <sup>3</sup>H release was calculated as:  $[(\text{sample cpm} - \text{spontaneous cpm}) / (\text{total cpm} - \text{spontaneous cpm})] \times 100$ .

## IV - Results

To assist in our functional studies on recombinant GzmH and its role, among other granzymes such as GzmB, in immune surveillance, we took to the parallel production of both active and inactive variant of the protease. Inactive GzmH resulted from a modification made in the enzyme's catalytic triad, the main player in the catalytic mechanism, where the serine (Ser) residue, at position 195, was replaced with an alanine (Ala).

### IV.1 - Construction of the *GzmH* plasmid and Variants

The expression cassettes of GzmH and the point-mutated inactive GzmH<sup>S195A</sup> were all cloned into the pET24c(+) plasmid (Invitrogen) (refer to the appendix), sequenced and subsequently transformed in to an appropriate expression host.

#### *pET24c(+)*MKH<sub>6</sub>GzmH

GzmH cDNA was amplified from the *homo sapiens* cDNA clone IMAGE: 15434 (vector pT7T3D) using the sense-strand primer DJ 2715 (5'-GAG GAT ATC ATC GGT GGC CAT GA-3') and the antisense-strand primer DJ2716 (5'-GCC TAA CGT TAG AGG CGT TTC ATG GTA CGT TTG ATC C-3'). The resulting PCR product was digested with *Eco* RV and *Hind* III and subsequently cloned into the *Pml* I and *Hind* III (173) cut pET24c(+) *E. coli* expression vector. The pET24c(+) plasmid vector was previously modified by introducing the codon sequence MKH<sub>6</sub> into the vector's multiple cloning site cleaved at restriction sites *Nde* I and *Bam* HI. The MKH<sub>6</sub> tag was constructed as a duplex with primers DJ2333 (5'-TAT GAA ACA TCA CCA TCA TCA CCA C/GT G-3' introducing codons Met and Lys and the mentioned *Pml* I site) and DJ2334 (5'-GAT CCA CGT GGT GAT GAT GGT GAT GTT TCA-3'). The cloning of modified GzmH cDNA directly upstream from the MKH<sub>6</sub> tag produced a sequence coding for a mature-like GzmH starting with codons Ile-Ile-Gly-Gly. Refer to the GzmH amino acid sequence in the appendix page 146.

#### *pET24c(+)*MKH<sub>6</sub>GzmH<sup>S195A</sup>

The catalytically inactive GzmH<sup>S195A</sup> construct was obtained using pET24c(+)GzmH as a template for the amplification of sense primer DJ 2871 (5'-ACA CA/C CGG TTT CAA AGG TGA CGC CGG-3') introducing a 5' *Age* I restriction site, and antisense primer T7-ter from. Sense primer DJ 2871 contains a point mutation which replaces the reactive Ser195 with Ala and rendering the protease unable to act proteolytically. The resulting PCR product was digested with *Age* I and *Hind* III and sub-

cloned into the identically cut pET24c(+)MKH<sub>6</sub>GzmH vector. The sequences of positive clones from both constructs were verified by sequencing analysis and transformed into the *E. coli* strain B834 (mentioned later page 32) ready for expression (DE3) (Novagen). Refer to the GzmH amino acid sequence in the appendix page 146. Serine 195 in highlighted in bold.

The pET24c(+) based constructs with the incorporated GzmH variants: MKH<sub>6</sub>GzmH and MKH<sub>6</sub>GzmH<sup>S195A</sup> were separately transformed into the *E. coli* strain DH5 $\alpha$ , the plasmid DNA purified and their sequences sent for verification analysis. Correct sequence readings for the wild-type (WT) GzmH cDNA and both of the inactive and tagged counterparts allowed us to then to think towards protein production and the selection of an appropriate expression hosts.

## ***IV.2 – Production GzmH and Variants from inclusion body material***

### ***GzmH expression yields high amounts of pure inclusion body material***

In the next paragraphs, and as an example of the procedure followed to produce the two GzmH variants, I report, in a step wise fashion, the production and purification of WT recombinant GzmH from inclusion body (IB) material. The data shown here is based upon an optimised protocol used for both constructs. The following results were obtained from a single procedure and are representative of the many individual batches, regardless of the variant in question, produced throughout the study.

The expression of recombinant GzmH and the inactive variant GzmH<sup>S195A</sup> in *E. coli* was accomplished under the guidelines of the pET system from Novagen. This method uses the bacteriophage T7 promoter to direct expression of target genes (see detailed explanation of the system in materials and methods, pages 32 & 33). It was therefore important to transform our established plasmids into an expression host bearing the T7 RNA polymerase gene ( $\lambda$ DE3 lysogen). Knowing that the production of both GzmK (Wilharm et al., 1999), and later GzmB (Kurschus et al., 2004; Kurschus et al., 2005), had been successfully performed in our lab using the *E. coli* expression host B834 (DE3), this previous work provided us with enough reassurance for the use of B834 (DE3) in our initial attempts to express and purify GzmH IB material. Indeed Wilharm and colleagues clearly demonstrated that the B834 (DE3) strain yielded larger amounts of IB protein over other strains, even the B834 derived host BL21, also a methionine auxotroph deficient in harmful proteases.

GzmH expression in B834 (DE3) and purification of inclusion body material was successful; the IB yield resulting in quantities of almost 1 g/l culture medium as previously described (Wilharm et al., 1999). Cultures (B834 in 10 L LB) of correct density (0.6 OD at 595 nm) and under the correct

selective pressure (kanamycin), were exposed to IPTG. Samples, taken before and after expression initiation, were then analysed by SDS-PAGE thus providing confirmation of protein expression (*Figure IV.1*). After extensive washing and centrifugation, the resulting aggregated IB protein was again denatured and analysed by SDS-PAGE. *Figure IV.2* shows a silver stained SDS-PAGE analysis combining both the expression of the GzmH precursor and purification of the resulting inclusion body material for bacterial debris. On average, a 10 L culture yields roughly 6 g (wet weight) of GzmH IB material.

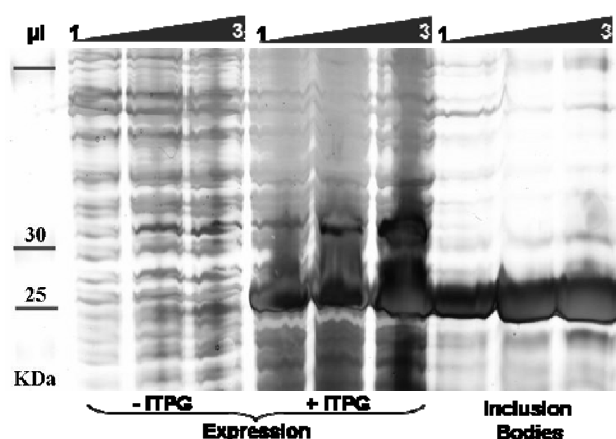


**Figure IV.1 - Silver stained SDS-PAGE analysis combining both the expression of the GzmH precursor and the purification of the resulting inclusion body material for bacterial debris.** Samples of 1ml (from the 10 L culture) were taken before and after 6 hours of IPTG induction. Thereafter, the samples were spun down at 6000 rpm, the supernatant discarded, and the pellet resuspended with PBS and Laemmli buffer (4x). Boiling at 95°C for 5 minutes was then followed by loading 1 to 3  $\mu$ l of sample on a 15% SDS polyacrylamide gel. Inclusion body visualisation was performed in a similar manner, 50  $\mu$ l of IB material (in 75 ml Wash II buffer, see methods p 34) being resuspended in PBS, boiled in presence of Laemmli buffer and loaded. The thick IB bands reveal a pure IB preparation.

### ***Interchain disulphide bond rich GzmH inclusion bodies are efficiently solubilised***

Recombinant wild type (WT) GzmH contains 7 cysteine residues. Solubilisation (SB) of the 6 g of IB aggregates was carried out in SB buffer (60 ml) containing oxidised and reduced glutathione as a redox system (1 ml/ 100 mg IB). The addition of these thiol reagents in combination with the chaotroph guanidinium chloride (GdmCl) allowed the reduction of the protease's interchain disulphide bonds by thiol-disulphide exchange. Homogenisation of the IB in solubilisation buffer, followed by over night stirring, resulted in the efficient solubilisation of GzmH IB material. The redox system was then removed by a series of dialysis steps against the GdmCl at pH 5.5, the low pH stabilising the deformed mixed disulphides. After 3 changes every 8 hours, the concentration of the solubilised protein was determined spectroscopically using  $\epsilon_{280\text{nm}} = 24,960 \text{ M}^{-1} \text{ cm}^{-1}$ . Following homogenization and dialysis, 90 ml of the solubilisate contained a total of 1.15 g precursor GzmH (12.8 mg/ml).

***Renaturation and dialysis of GzmH results in correctly folded soluble protein***

Renaturation was performed in 5 L of refolding buffer (RF buffer) in which GzmH solubilisate was added at the optimal final concentration of 100 µg/ml (Wilharm et al., 1999). In comparison to the RF buffers used for the production of our GzmB and GzmK, the composition of the GzmH RF buffer included the addition of 20 mM calcium chloride (CaCl<sub>2</sub>), reported to improve refolding by stabilizing the protein in question (Rudolph and Lilie, 1996). Other components known to aid refolding were also tested. Polyethylene glycol (PEG), thought to improve *in vitro* structure formation by preventing aggregation at stiochiometric amounts (1%), unfortunately showed no improvement while elevating sodium chloride (NaCl) concentrations from 0.15 to 0.5 M also revealed no amelioration in yield. Variations in temperature, pH and duration of renaturation were also tested without amelioration. Finding the optimal refolding conditions is crucial, if one is to obtain high yields of the desired protein but unfortunately, despite numerous trials with the above components, we could not reach the high yields obtained in the case of GzmB (Kurschus et al., 2004). Satisfactory yields of pure, active GzmH were nevertheless obtained using a RF buffer based on work of Wilharm and colleagues (Wilharm et al., 1999). The addition of 20 mM CaCl<sub>2</sub>, adjustment of the pH to 7.3 and reduction of the refolding period to over night incubation (begun at room temperature and cooled down to 4°C by incubation in a cold chamber) were the modifications made to the refolding procedure. Filtration of the RF buffer was thereafter performed to rid the protein solution of precipitates which, if left, are known to encourage further precipitation as well as clog up wide-surface filtering membranes used to concentrate the 5 L preparation (Rudolph and Lilie, 1996).

Dialysis into an appropriate buffer is a crucial step if protein purification is to succeed, providing a stable environment for the desired protein. MES [2-(N-Morpholino)-ethanesulfonic acid] buffer at pH 6, again complimented with 20 mM CaCl<sub>2</sub> and 0.15 M NaCl, provided the most stable conditions for GzmH. Tris [Tris-(hydroxymethyl)-methane] and PBS (phosphate buffered saline) based buffers both caused much higher degrees of precipitation to occur after 5 rounds of dialysis. The five exchanges were necessary to efficiently remove the positively charged arginine which could later have an effect during ion exchange purification, possibly competing with the granzyme for binding in a column packed with cation exchange media. Sodium chloride was kept at physiological concentrations, throughout the procedure, an essential requirement for all future cell-based apoptosis assays.

*Figure IV.2* shows the loss of refolded protein, subject to precipitation, that occurs during renaturation and especially during dialysis, despite the optimized conditions mentioned above. Roughly 40 ml of solubilisate (12.8 mg/ml) was added to the RF buffer (5 L), thus diluting the protein to the optimal concentration of 100 µg/ml (Wilharm et al., 1999). After overnight renaturation and subsequent filtration, protein concentration was measured spectroscopically at 280 nm against RF buffer alone.

From the 512 mg of protein added (40x 12.8 mg/ml), only 145 mg remained in solution. Protein concentration was again measured after the 5<sup>th</sup> round of dialysis. At this stage 30 mg of soluble granzyme remained, thus a loss of almost 95% of the total amount initially added to the RF buffer. Interestingly, when all of the above samples were analysed side by side by SDS-PAGE, the four precursor GzmH bands appeared in a step-like fashion, suggesting that the presence of 0.6 M arginine (Arg), which influences ionic charge, might cause the bands to run incorrectly. Once Arg was fully removed by dialysis, however, MKH<sub>6</sub>GzmH ran at the correct molecular weight position of 26 kDa.

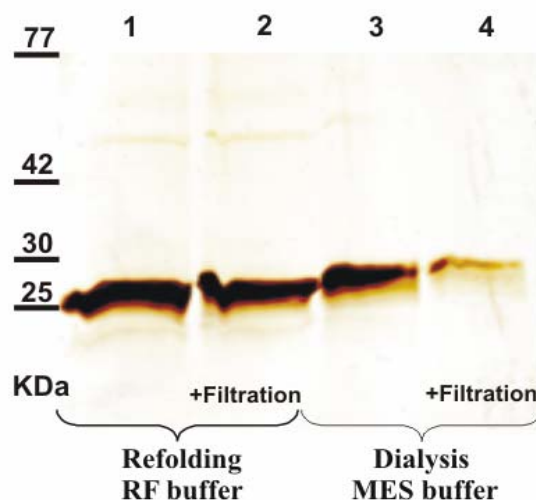


**Figure IV.2 - Silver stained SDS-PAGE analysis showing WT GzmH and the loss of partially refolded protein yield that occurs between renaturation and dialysis.** In all cases, 25 µl of proGzmH (in lanes 1 and 2 proGzmH was taken from 5 L refolding (RF) buffer and lanes 3 and 4 from 1 L 25 mM MES buffer containing 150 mM NaCl) was added to (4x) Laemmli, boiled and loaded onto 15% acrylamide SDS gels. Lane one represents proGzmH in refolding solution and lane two, proGzmH in filtrated RF solution. Lane 3 shows the concentrated, dialysed RF material whereas in lane 4 the latter has been filtered (0.22 µm). ProGzmH appears to run at different sizes on the gel due to the high concentration of arginine (0.6 M) in the RF buffer.

### *GzmH is efficiently purified via ion exchange FPLC*

GzmH was purified using a fast protein liquid chromatography (FPLC) system from Pharmacia equipped with an ion exchange column. Protein separation was based on the reversible interaction between the charged granzyme and an oppositely charged chromatographic medium “Source 15S”. Elution of both proform and active GzmH was performed by an increase in NaCl concentration in form of a continuous gradient, while protein elution was monitored by a UV detector.

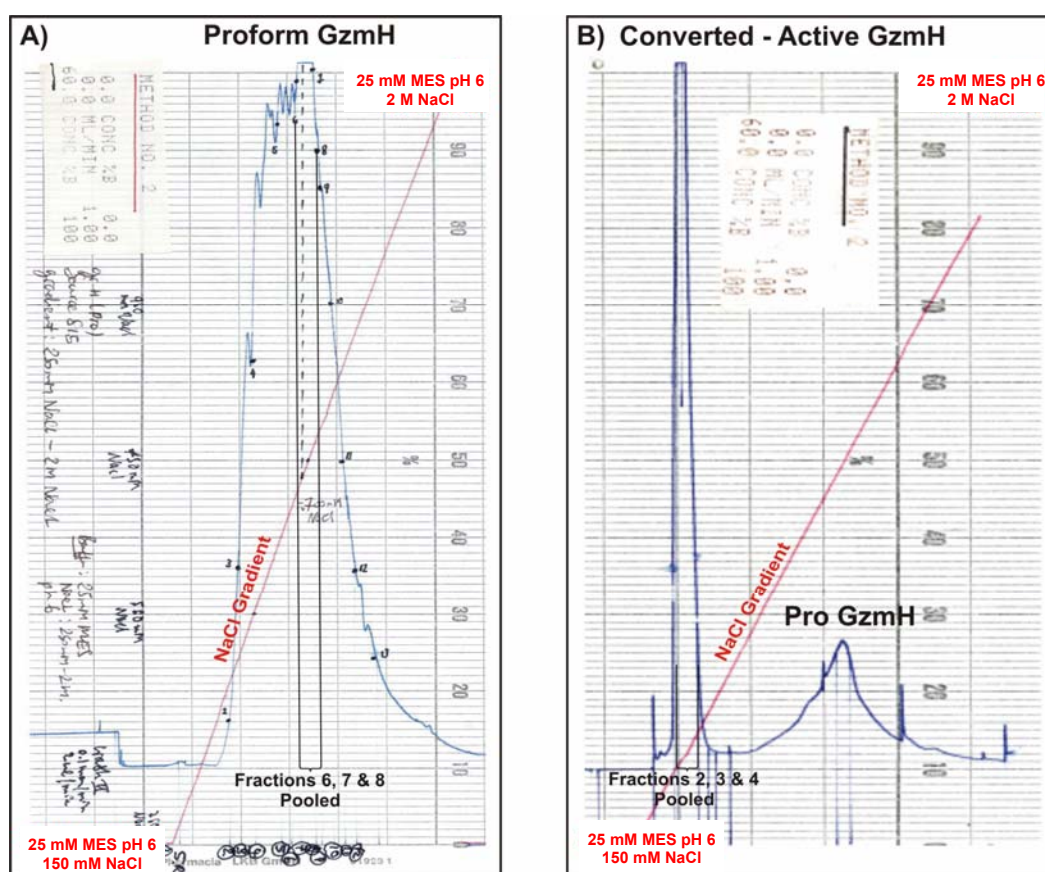


**Figure IV.3 - WT GzmH purification via ion exchange FPLC.** Precursor GzmH, dialysed into 25 mM MES buffer (pH 6) containing 150 mM NaCl and 20 mM  $\text{CaCl}_2$ , was loaded onto a Source S15S based column and eluted by a salt gradient ranging in concentrations from 0.15 to 2 M NaCl. **(A)** At 700 mM, Fractions 6, 7 and 8, of correct size and purity, were pooled and further converted by cathepsin C (0.5 U/mg) overnight at 30°C. **(B)** Converted GzmH was then again purified over a second identical column where at 250 mM, fractions 2, 3 and 4 containing the active enzyme were pooled and verified for their purity and activity. As expected, the remaining precursor GzmH eluted at NaCl concentrations just short of 1 M.

Following dialysis and filtration, proGzmH, contained within approximately 1 L of buffer A (25 mM MES pH 6, 150 mM NaCl and 20 mM  $\text{CaCl}_2$ ), was successfully loaded onto the ion exchange SOURCE 15S packed column. After lengthy washing in buffer A, devoid of  $\text{CaCl}_2$ , a 60 minute salt gradient (0 to 100% buffer B, 1 ml/min) was initiated feeding from both buffers A and B (25 mM



MES pH 6, 2 M NaCl). Absorbance at 280 nm reached its highest readings at approximately 700 mM NaCl, defining the peak of the elution curve (*Figure IV.3A*). Once collected, all fractions were analysed spectroscopically but also visually after SDS-PAGE and silver staining. As expected, gel analysis of fractions flanking the elution peak revealed pure bands running between the 25 and 30 kDa marker proteins at a molecular weight (MW) of 26,247 kDa (pI: 10.0), representative of unglycosylated recombinant precursor GzmH. Once pooled, the proenzyme fractions were concentrated to 0.5 mg/ml and appropriately converted to their active conformation by DTE-pre-activated bovine cathepsin C before undergoing a second round of purification over a Source 15S ion exchange column. Following dilution in 25 mM MES buffer, necessary to lower salt concentrations to gain physiological conditions, converted GzmH was again loaded and eluted as described above. This second purification step efficiently separated the active GzmH from cathepsin C and other applied converting agents as well as remaining precursor enzyme (*Figure IV.3B*).

Because cathepsin C action removes the adjoined eight amino acid residues MKH<sub>6</sub>-tag and because of the basic nature of the histidine (His) residue, the resultant active GzmH was on the whole less basic than its precursor counterpart (which at pH 6,0 carries 6 protons more than active GzmH) and hence less able to compete for binding to the column media in the presence of increasing salt concentrations. Elution of active GzmH therefore occurred at the considerably lower NaCl concentration of roughly 250 mM, the remaining pro-form following suit at concentrations of NaCl just below 1 M (*Figure IV.3B*).

#### ***Pure, converted active and inactive GzmH are stored in physiological buffering conditions***

To ensure that mature GzmH was stored in the correct buffering environment at physiological salt concentrations, converted GzmH fractions were first of all analysed by SDS-PAGE. Fraction samples revealing pure and efficiently converted GzmH were then pooled and dialysed into an appropriate stabilising buffer, here 25 mM MES pH 6 complimented with 150 mM NaCl, to ensure uniform physiological salt conditions. Thereafter, the recombinant protease was concentrated and measured spectroscopically at 280 nm until a final concentration of 500 µg/ml was obtained. The concentration of converted GzmH was measured using the following formula:  $c \text{ (mg/ml)} = (A_{280} \times \text{MW}) / (\epsilon_{280} \times b)$  where the molecular weight of converted GzmH is 25165.35 kDa and the extinction coefficient 25110 (ExPASy ProtParam tool); b represents the path length, which for most spectrometers is 1 cm. Converted GzmH was subsequently aliquoted, in stable conditions, into one-time-use volumes of 20 µl and stored at -80°C. *Figure IV.4* shows proform, active and inactive GzmH on a silver-stained SDS-PAGE. Clean bands with the expected sizes of 26 and 25-kDa respectively demonstrate the 8 amino acid (1100.2 Daltons) shift from proform to mature GzmH.

### ***Difference in yields between active and inactive GzmH***

On average, a total amount of 3 mg precursor GzmH was obtained from 500 mg solubilised GzmH (renaturation being performed with a protein concentration of 100 µg per ml RF buffer). After removal of the MKH<sub>6</sub> tag by cathepsin C treatment and further purification over ion exchange columns, a total of 1.3 mg of converted GzmH remained. In comparison to the yields of active WT GzmH, yields of the converted inactive variant were noticeably higher. Indeed, after renaturation of GzmH<sup>S195A</sup>, a marked decrease in precipitation was observed throughout the dialysis procedure, probably due the lack of proteolytic activity acquired following cleavage of the MKH<sub>6</sub> tag.

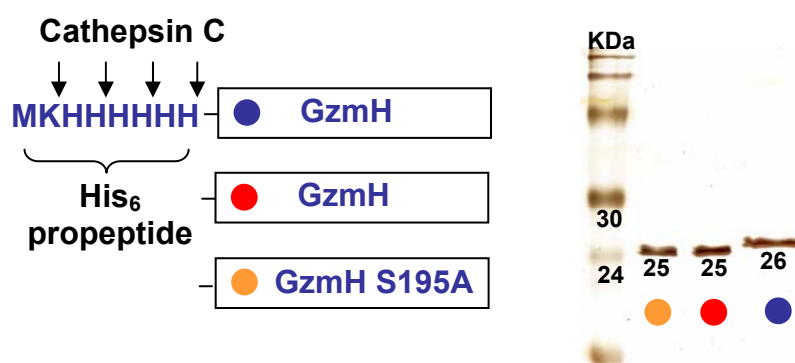


**Figure IV.4 - Pure, recombinant unglycosylated GzmH variants.** SDS-PAGE allowed the visualization of the two correctly folded and converted GzmH constructs along with the GzmH precursor.. The SDS gel was run at 200 mV until the 17 kDa marker band reached the extremity of the 15% acrylamide matrix. Thereafter, silver staining revealed clean bands representing, in order from top to bottom, proGzmH in blue (precursor protein of 26 kDa with the adjoined N-terminal MKH<sub>6</sub> peptide), wild-type GzmH (Red, 25 kDa) and inactive GzmH<sup>S195A</sup> (Yellow, 25 kDa). Each protein band represents 50ng of loaded sample. All proteins were of expected size as indicated.

## ***IV.3 - GzmH Activity***

### ***GzmH has chymotrypsin-like (chymase) activity***

Edwards and colleagues were the first to report the esterolytic but not amidolytic activity of glycosylated recombinant GzmH secreted from baculovirus-infected Sf21 insect cells (Edwards et al., 1999). The authors nicely demonstrate that their recombinant GzmH processed chymotrypsin-like (chymase) activity by showing the efficient cleavage of the thiobenzyl ester Suc-Phe-Leu-Phe-SBzl. Furthermore, testing with numerous other thiobenzyl esters, such as Z-Lys-SBzl (tryptase), revealed that that GzmH has no tryptase or aspartase activity. The group then measured GzmH activity against a more comprehensive panel of synthetic oligopeptide thiobenzyl esters and aminomethylcoumarin (AMC). Although none of the AMC substrates were hydrolyzed, the thiobenzyl ester substrate Boc-Ala-Ala-Met-SBzl, was hydrolysed at the second best rate demonstrating that GzmH can also tolerate

aliphatic residues such as methionine (Met) at the P1 position. Here we confirm the above finding, with regard to the thiobenzyl ester Suc-Phe-Leu-Phe-SBzl as a good GzmH substrate, by demonstrating that enzymatic hydrolysis of the tripeptide thioester substrate (with GzmH at 20 nM) is indeed efficient. Suc-Phe-Leu-Phe-SBzl is reported to be an excellent substrate for Cathepsin G which was therefore used to control the procedure (*Figure IV.5*) (Edwards et al., 1999). In contrast to the WT GzmH, the Ser-to-Ala mutant showed no proteolytic activity towards the thiobenzyl ester substrate.

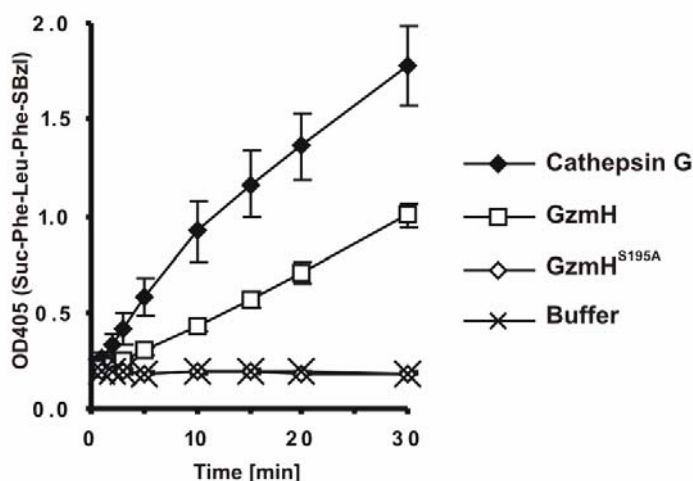


**Figure IV.5 - GzmH cleaves the thioester substrate Suc-Phe-Leu-Phe-SBzl.** Enzymatic hydrolysis of the peptide thioester substrate Suc-Phe-Leu-Phe-SBzl (30 mM) by GzmH (20 nM) was measured at RT in activity buffer (50 mM Tris-HCl pH 8, 150 mM NaCl, 0.01% Triton X-100) containing 0.3 mM 5,5'-dithiobis-2-nitrobenzoic acid (DTNB). Once the substrate added, its hydrolysis was monitored by measuring the absorbance at OD 405 using a Dynatech MR4000 microplate reader. Cathepsin G (20 nM) was used as positive control.

### ***GzmH cleaves AMC based substrates***

Two GzmH specific tetrapeptide sequences, based on a study by Mahrus et al. in which all human granzymes were compared at positions P1 to P4 by using combinatorial libraries of protease substrates, were kindly synthesized and adjoined to AMC groups by Novabiochem (Laufelfingen, Switzerland) (Mahrus and Craik, 2005) (refer to *Figure IV.6*). For the first time we were able to show that GzmH was able to cleave amide bonds by the hydrolysis of the above predicted peptide substrates, namely Pro-Thr-Ser-Tyr-AMC and Ala-Thr-Ser-Tyr-AMC. GzmH showed a marked preference for a proline at the P4 position over an alanine which occupies the same site in the alternative tetrapeptide (*Figure IV.7*). Yet again, cathepsin G was clearly the more efficient enzyme when exposed to Pro-Thr-Ser-Tyr-AMC or Ala-Thr-Ser-Tyr-AMC. Expectedly, like GzmH, cathepsin G also preferred proline at the P4 position. GzmB was also included as a control, showing that the two substrates were specific for chymotrypsin-like enzymes. It would of course be of interest to compare the above tetrapeptide sequences with the tripeptide sequence Phe-Leu-Phe also attached to an AMC group.

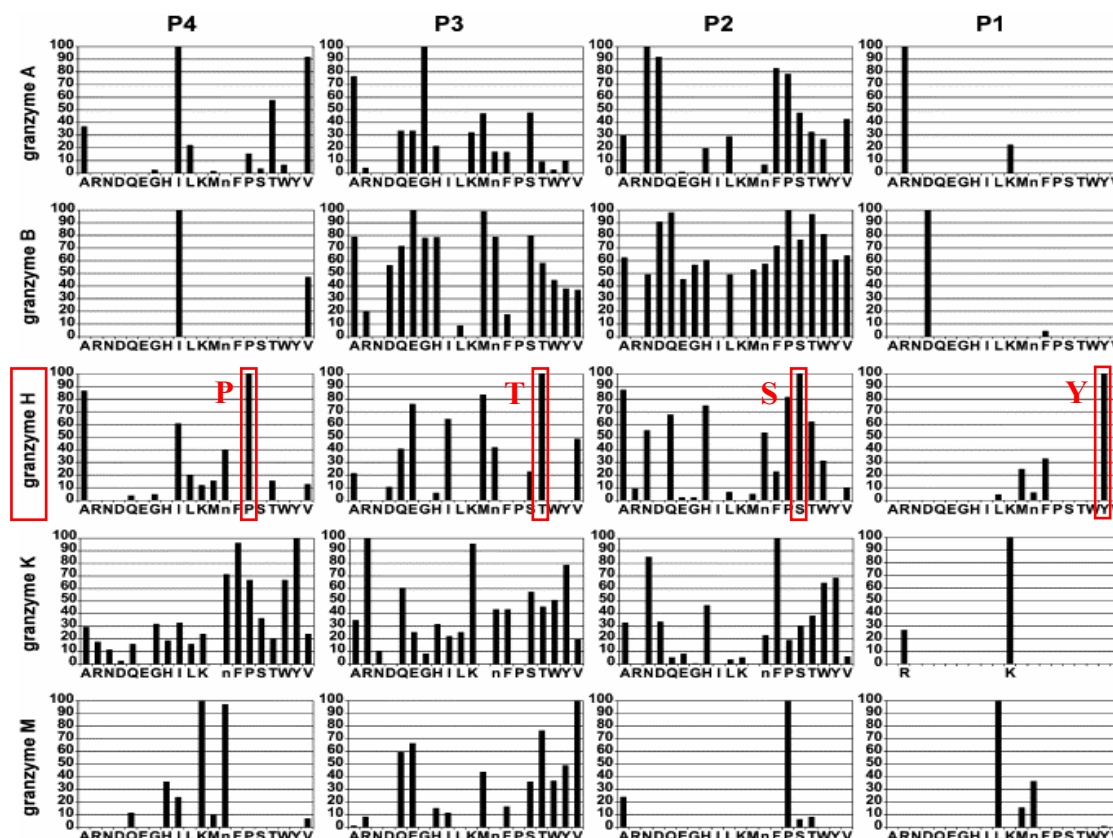


**Figure IV.6** - Figure showing the substrate specificity of human granzymes (Mahrus *et al.* 2005). Recombinant GzmA, GzmB, GzmH (outlined in red) and GzmM were profiled at positions P4-P2. The y axis represents relative activity, and the x axis represents the fixed P4, P3, P2 or P1 amino acids (with norleucine represented by n). Activities for each granzyme are relative to the highest activity at each of the four substrate positions. The library profiles indicate, contrary to previous work, that GzmH exhibits a strong preference for tyrosine over phenylalanine and tryptophane at the P1 position, the preferred P4 to P1 sequence being **PTSY** (see Figure IV.8 below). Taken from Mahrus *et al.* Chemistry and Biology, vol. 12, 567-577, 2005.

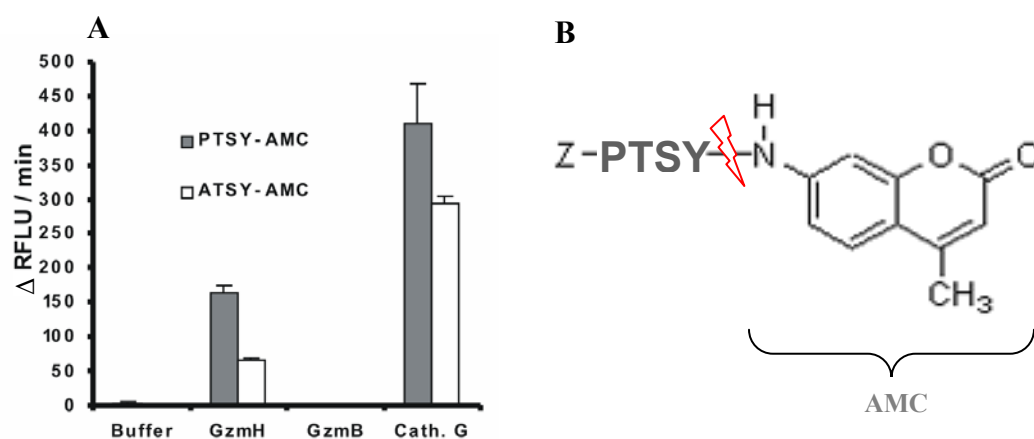


**Figure IV.7** - GzmH cleaves amide bonds in synthetic peptides. (A) The new peptide substrates H-Pro-Thr-Ser-Tyr-AMC (PTSY-AMC) and H-Ala-Thr-Ser-Tyr-AMC (ATSY-AMC) are a kind gift from Dr. Doerner (Merck Biosciences, L  ufelfingen, Switzerland). They were dissolved in DMSO and applied at 250  $\mu$ M in activity buffer. All proteases were added at end concentrations of 20 nM, Fluorescence intensities were recorded with a Fluostar Optima (BMG Labtech, Offenburg, Germany) at RT and evaluated using the Fluostar Optima software. (B) Fluorescent dye based peptide substrates are synthesized by coupling the carboxy group of the desired peptide of a specific sequence to the amine group of a dye, in this case AMC (7-amino-4-methylcoumarin). Before enzymatic hydrolysis, these substrates have no or very weak fluorescence. On enzymatic hydrolysis, the dye is released, greatly increasing the fluorescence.

#### IV.4 - GzmH inhibition

We were interested in pursuing work on GzmH inhibition as it is in our plans to attempt the crystallization of GzmH bound to a specific inhibitor, the inhibitor here rendering the active enzyme more stable in general while teaching us more about the specificity of the enzyme. Furthermore, and in line with the main theme of this study, a specific, efficient, non toxic and cell permeable inhibitor (such as phosphonates) would allow us to learn about the potential contribution GzmH makes, among other released granzymes, towards the death of target cells. A study from Sedelies and colleagues in 2004 already point towards GzmH being frequently more abundant than GzmB in natural killer (NK), a finding that suggests a role for GzmH in complementing the proapoptotic function of GzmB (Sedelies et al., 2004).

##### *GzmH is efficiently inhibited by the general protease inhibitor DCI*

Edwards and colleagues also attempted to inhibit GzmH with inhibitor compounds such as isocoumarins, peptide chloromethyl ketones, and peptide phosphonates. The most effective inhibitor reported was the general protease inhibitor 3,4-dichloroisocoumarin (DCI) with PMSF also providing some inhibition but at concentrations of 1 mM in comparison to 0.1 mM DCI. The peptide phosphonates with the Phe-Leu-Phe sequence also provided moderate inhibition at 0.1 mM concentration, the most effective being interestingly FTC-Aca-Phe-Leu-Phe(p)(OPh)<sub>2</sub> indicating that GzmH may have a remote subsite for very hydrophobic structures. Again, we were able to confirm that GzmH was completely inhibited by DCI at the even lower end concentration of 1 and even 0.1  $\mu$ M of the general protease inhibitor (*Figure IV.8*).

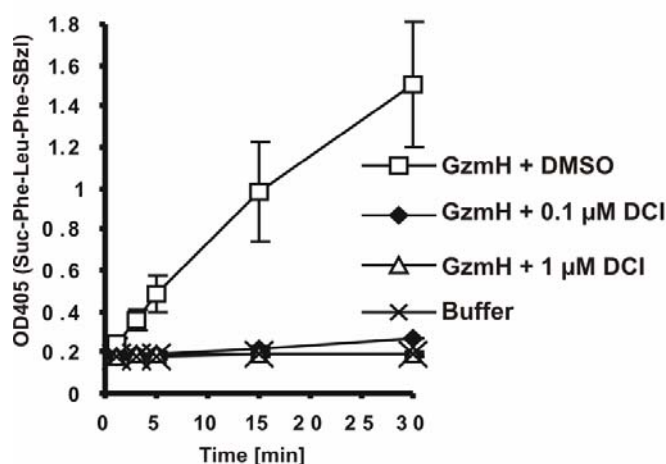


**Figure IV.8 – GzmH inhibition.** Inhibition was measured by incubating 4.5  $\mu$ l Gzm (4.44  $\mu$ M) with 0.5  $\mu$ l inhibitor (4 mM) for 20 min at room temperature (see materials and methods). The substrate, DTNB, and buffer were added to assay the residual enzyme activity as described above. At a enzyme ratio of 1:100, DCI nearly completely inhibited GzmH. Complete inhibition was accomplished at the lower enzyme:inhibitor ratio of 1:10.

## ***IV.5 - GzmH and Apoptosis Induction***

### ***IV.5.1 - GzmH is a cytotoxic protease able to induce cell death***

The cell death inducing potential of GzmH, in comparison to that of GzmB, was assessed in an effector cell-independent system. Recombinant granzymes were used in combination with purified perforin (PFN), the natural pore forming protein of CTL and NK cell secretory vesicles, and as an alternative the PFN substitute, streptolysin O (SLO), a bacterial cholesterol-binding exotoxin (Walev et al., 2001). Pooled, pure active GzmH was prepared for cell culture experiments by dialysis into 25 mM MES pH 5.5, 150 mM NaCl followed by high speed centrifugation (14000 rpm) and filtration (0.22  $\mu$ m). Enzyme concentration was measured spectroscopically at 280 nm and the active protease was stored at -80°C at a stock concentration of 500  $\mu$ g/ml.

#### ***Sublytic concentrations of PFN and SLO are essential for Gzm specific killing***

In an initial attempt to study the possibility of GzmH possessing cytotoxic potential, we first defined the sublytic window for the pore forming protein SLO in combination with GzmB, a known potent apoptosis inducer. Sublytic perforin concentrations, which were also tested similarly, followed at a later time point during this work. The sublytic window is defined as the concentration of pore forming protein required to produce maximum cell death, induced here by GzmB, while maintaining background levels of cell death (10-15% AV<sup>+</sup>/PI<sup>+</sup> cells), in the presence of the translocator alone. Cell death was monitored using annexin V FITC (AV) and propidium iodide (PI), the percentage of cytotoxicity defined as the sum of both apoptotic and dead cells (AV<sup>+</sup>/PI<sup>-</sup> + AV<sup>+</sup>/PI<sup>+</sup> cells).

Sublytic SLO concentrations were determined with target cells K562, HL60 and U937 whereas the sublytic PFN window was only defined for both K562 and HL60 cells. PFN usage was limited to two cell lines due to the cost and availability of recombinant translocator. In the presence of GzmB, cell death levels (AV<sup>+</sup>/PI<sup>+</sup> cells) of K562 cells were at their highest at PFN and SLO concentrations of 200 and 150 ng/ml respectively (refer to *Figure IV.9A* and *C* respectively). Importantly, background death levels, for both translocators, were optimal (under 10-15% AV<sup>+</sup>/PI<sup>-</sup> + AV<sup>+</sup>/PI<sup>+</sup> cells). As for HL60 cells, concentrations of 75 and 100 ng/ml of PFN and SLO respectively provided the optimal window for specific GzmB killing (refer to *Figure IV.9B* and *D* respectively). Cell death studies with U937 cells were only performed in combination with SLO where the most efficient “translocator background” versus “cell death” ratio was achieved using SLO concentrations in the range of 150 ng/ml.

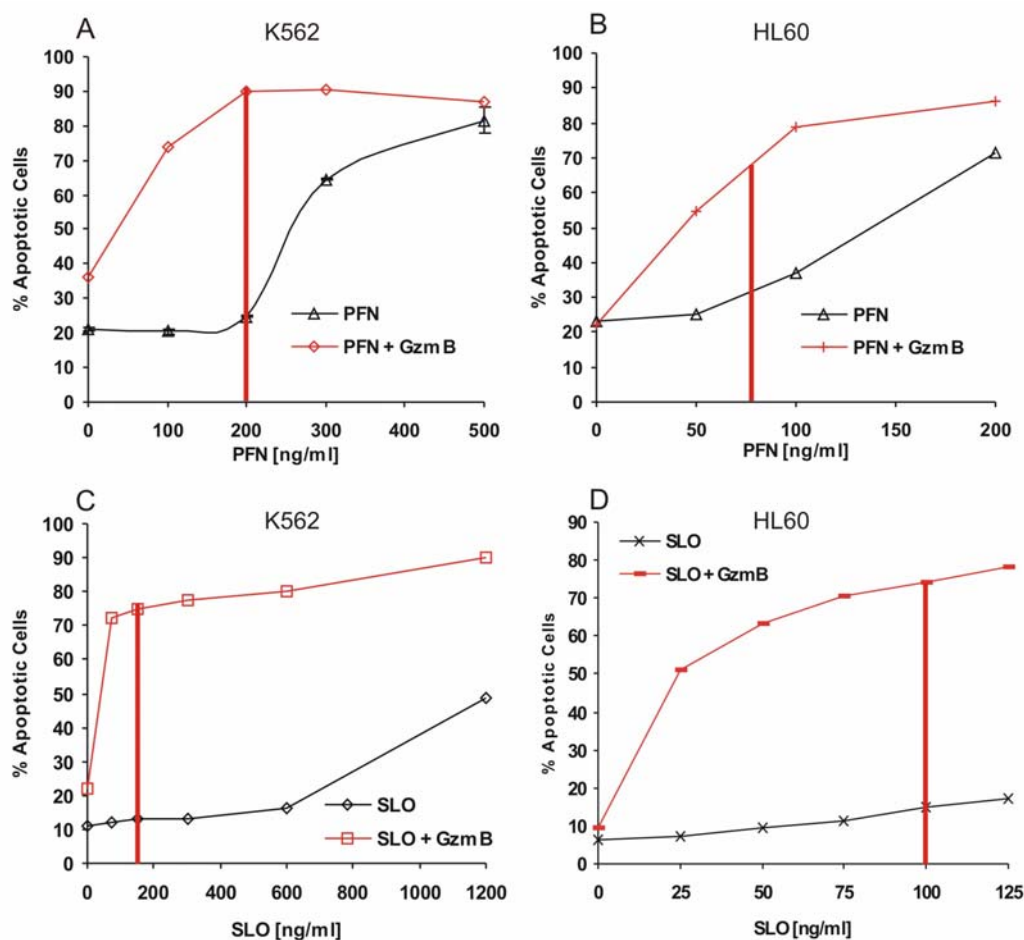


**Figure IV.9 - Sublytic concentrations of PFN and SLO are essential for Gzm specific killing.** (A and C) K562 cells ( $1 \times 10^5$  / 50  $\mu$ l) were exposed to varying concentrations of SLO (A) and PFN (C). (B and D) HL60 cells were also exposed to different concentrations of SLO (B) and PFN (D). In all cases, GzmB was previously added to the cells at a final concentration of 10  $\mu$ g/ml. GzmB is known to efficiently induce apoptosis within one hour of exposure at sublytic concentrations of pore forming proteins such as SLO and PFN. Cells were incubated for 2 hours and then analysed by FACS after Annexin V-FITC and propidium iodide staining. Apoptotic cells are here defined as AV<sup>+</sup>/PI<sup>-</sup> + AV<sup>+</sup>/PI<sup>+</sup> cells. The red line present in each graph represents the sublytic concentration of pore-forming protein chosen for our apoptosis assays.

### ***SLO delivered GzmH is able to induce cell death***

With the sublytic window set for each cell line with regards to PFN and SLO, the next step was to address the question of whether GzmH is indeed able to induce cell death. To address this question, we used GzmB to control our experiments. Work from our lab by Kurschus and colleagues, has indeed shown that unglycosylated recombinant GzmB is potently apoptogenic, killing various target cell lines within an hour (Kurschus et al., 2004; Kurschus et al., 2005). We also set out to determine the range of extracellular concentrations necessary if GzmH were indeed to efficiently trigger cell death. Therefore, GzmH dilutions, reaching final concentrations of between 1-20  $\mu$ g/ml, were applied to K562 and HL60 cells before sublytic concentrations of SLO were respectively applied (Figure IV.10). Analysis after 24 hours of incubation revealed that GzmH had reached maximal killing efficiency killing 70 to 80% of K562 or HL60 cells. Killing was achieved with final GzmH concentrations of 15-20  $\mu$ g/ml



with K562 cells and slightly lower concentrations of 10-15  $\mu\text{g/ml}$  with HL60 cells. GzmB however, achieved comparable levels with both cell lines already at a concentration of 10  $\mu\text{g/ml}$ . Importantly, inactive GzmH, in combination with sublytic SLO, revealed similar levels of cell death obtained with SLO alone. U937 cells were also efficiently killed by GzmH. *Figure IV.10B* shows the percentage of dead cells after 12 hours of exposure to GzmH and GzmB in the presence of sublytic SLO. Cell death was here separately monitored by PI and trypan blue staining.

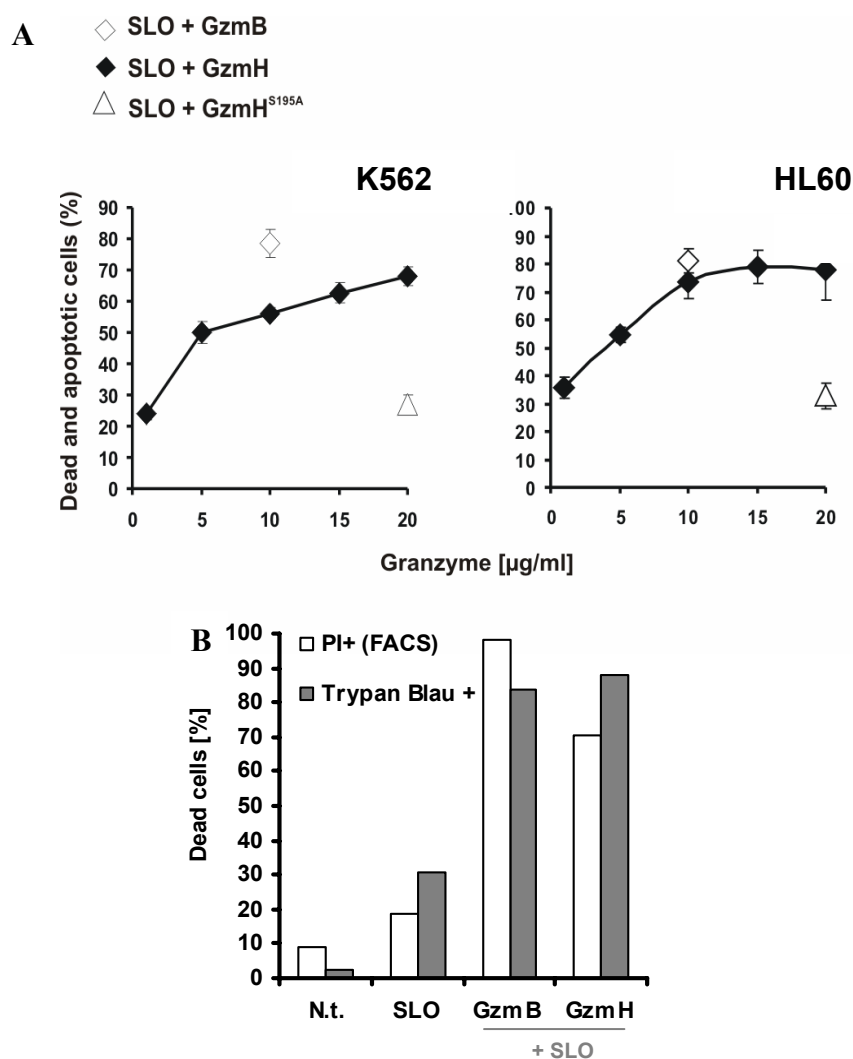


**Figure IV.10 - Cell death induced by recombinant GzmH.** (A) Effective ranges of GzmH concentrations that induced cell death in K562 or HL60 cells. The cells ( $1 \times 10^5 / 50 \mu\text{l}$ ) were analysed after 24 hours having been treated with sublytic SLO (125 ng/ml and 75 ng/ml respectively) and GzmH (20  $\mu\text{g/ml}$ ), GzmH<sup>S195A</sup> (20  $\mu\text{g/ml}$ ) or GzmB (10  $\mu\text{g/ml}$ ). GzmB was used at 10  $\mu\text{g/ml}$ , a concentration at which the protease efficiently induced cell death. Importantly, inactive GzmH (20  $\mu\text{g/ml}$ ) was applied at the highest concentration of Gzm used, only caused background levels of cell death. Cells were analysed after Annexin V-FITC/Propidium iodide staining by FACS, the graphs showing the sum of dead and apoptotic cells ( $\text{AV}^+/\text{PI}^- + \text{AV}^+/\text{PI}^+$  cells). The experiment shows the mean of triplicates,  $\pm$  standard deviations (SD) and is representative of two independent experiments. (B) GzmH triggered cell death of U937 cells ( $1 \times 10^5 / 50 \mu\text{l}$ ). U937 cells were exposed to GzmH (25  $\mu\text{g/ml}$ ) and GzmB (10  $\mu\text{g/ml}$ ) in the presence of sublytic SLO concentrations for 12 hours. In this combined graphic both propidium iodide and trypan bleu stainings were performed. PI staining was performed and analysed by FACS. Trypan blue staining was analysed under the microscope. The experiment represents single measurements. N.t: non-treated.



### ***SLO delivered GzmH requires 10 to 12 hours to efficiently kill target cells***

To better define the time required for optimal GzmH triggered killing, we performed a time course killing assay in which treated K562 cells were analysed every two hours after the addition of sublytic concentrations of SLO. The experiment was performed with SLO and not PFN due to limited PFN availability, the experiment still giving us an impression of the time required for GzmH to reach optimal killing efficiency. Ten hours after GzmH delivery, the percentage of apoptotic and necrotic cells reached a plateau, an effect GzmB achieved within only two hours. The percentage of spontaneous cell death is also shown to indicate the minimal contribution of sublytic SLO (see red arrow in *Figure IV.11*) to the total background values. After several repetitions we were reassured that GzmH, at least delivered with sublytic SLO, could efficiently kill K562 cells within 10 to 12 hours after delivery.

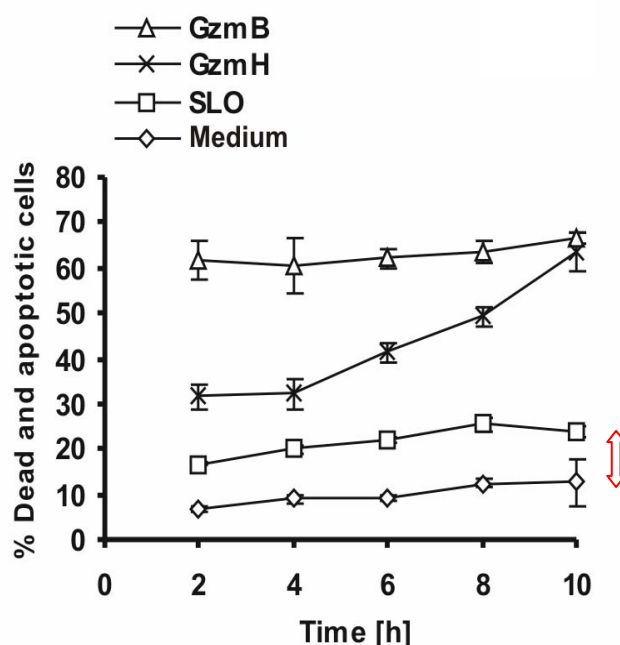


**Figure IV.11 - Cell death induced by recombinant GzmH.** Time course of GzmH killing in K562 cells (shown is the mean of triplicates, representative of two independent experiments). GzmH (20  $\mu\text{g/ml}$ ), induced cell death within 10 hours. GzmB (10  $\mu\text{g/ml}$ ) was used to control the efficiency of SLO delivery. Sublytic SLO at 125 ng/ml induced an additional 10% cell death on top of the natural background values obtained for untreated cells (red double headed arrow). Cells were analysed after Annexin V-FITC/Propidium iodide staining by FACS, the graphs showing the sum of dead and apoptotic cells ( $\text{AV}^+/\text{PI}^- + \text{AV}^+/\text{PI}^+$  cells).

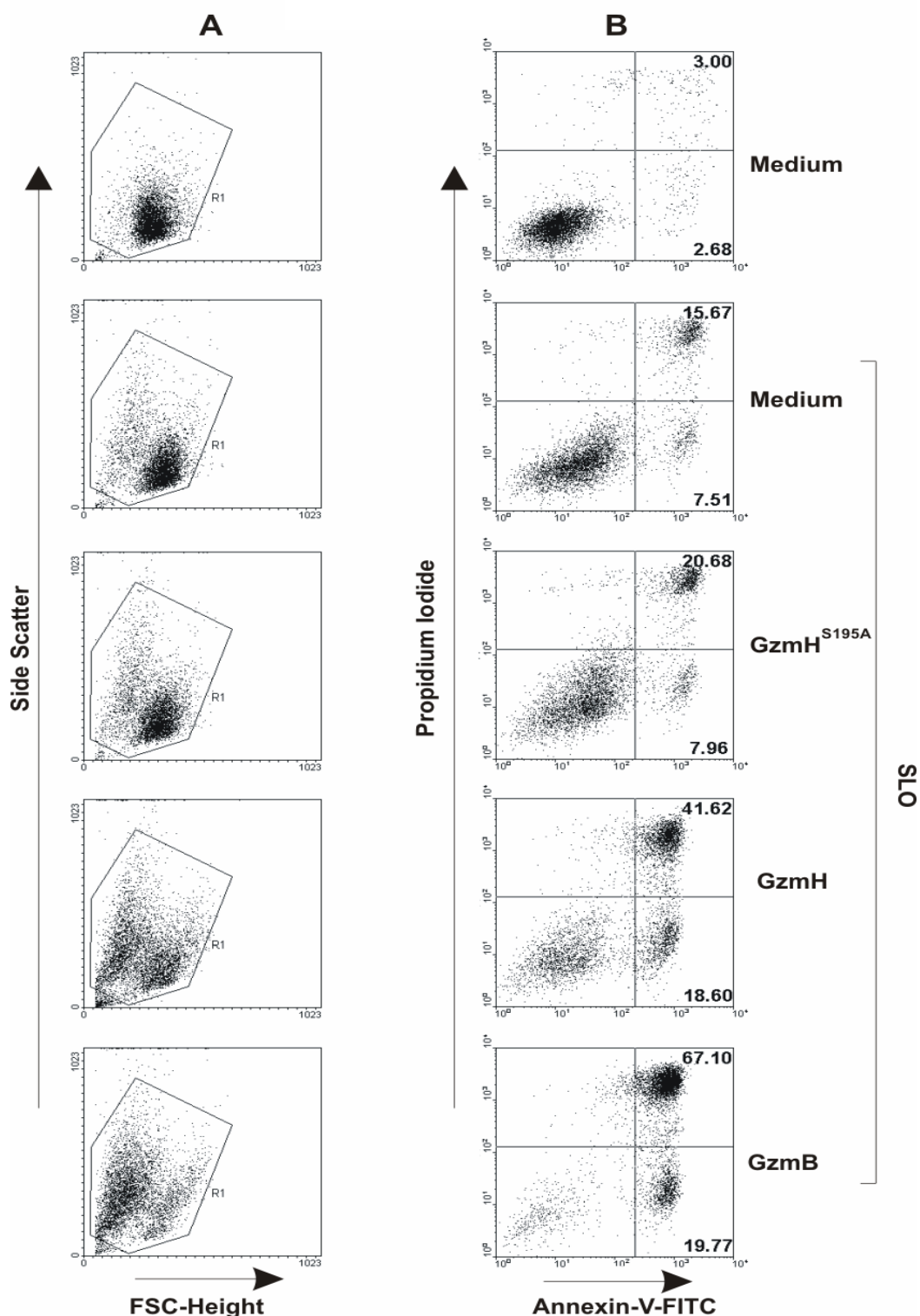


**Figure IV.12 - Raw FACS data demonstrating the capacity of GzmH to trigger cell death.** Representative FACS data for K562 cells ( $1 \times 10^5$  / 50 $\mu$ l), twelve hours after treatment in medium alone, in medium containing sublytic SLO and finally medium containing SLO plus the following proteases: GzmH<sup>S195A</sup> (15  $\mu$ g/ml), GzmH (15  $\mu$ g/ml) and GzmB (7.5  $\mu$ g/ml). Apoptotic and dead cells were identified by annexin V and PI staining. Dead cells are characterized by low FSC and high SSC signals. (A) Plots showing forward scatter (FCS) versus side scatter (SSC) signals. (B) Dot plots showing how GzmB and GzmH induced killing as deduced by the presence of high percentages of apoptotic (AV<sup>+</sup>/PI<sup>-</sup>) and necrotic (AV<sup>+</sup>/PI<sup>+</sup>) cells.

*Figure IV.12* shows representative FACS data of AV/PI stained K562 cells 12 hours after treatment with the indicated proteases. The right column shows how active GzmH and GzmB strongly induced killing as deduced by the presence of high percentages of apoptotic and necrotic cells. The left column of plots, forward scatter (FSC) versus side scatter (SSC) signals showed similar changes that occurred in both GzmH- and GzmB-treated cells. The dying apoptotic cells, here characterized by low FSC and high SSC signals, are typical of apoptotic cells.

### ***PFN delivered GzmH also efficiently kills K562 and HL60 cells***

We next performed a series of experiments analysing K562 and HL60 cells 10 to 12 hours after treatment with GzmH and sublytic Streptolysin O (SLO) or Perforin (PFN). In accordance with the 24 hour killing assay results mentioned above, pooled data from three independent experiments revealed that GzmH can indeed efficiently kill both cell types after this reduced incubation period (*Figure IV.13A*). Importantly GzmH was also able to trigger cell death after the addition of PFN as the delivery agent with cell death levels reaching 70% ( $AV^+/PI^- + AV^+/PI^+$  cells) after 24 hours (*Figure IV.13B*), GzmH<sup>S195A</sup> clearly demonstrating the importance of protease's proteolytic activity with regard to cell death induction.

It is important to note that the values representing PFN/SLO alone were only 5-10% higher than the natural cell death background observed in untreated cells. To ascertain the unique apoptosis-inducing specificity of GzmH, K562 cells were additionally treated with mast cell chymase, a closely related chymotrypsin-like serine protease and a member of the GzmH-GzmB gene cluster on chromosome 14q11.2. Although mast cell chymase efficiently cleaved our chymase substrates, the enzyme was not able to induce SLO mediated target cell death. Indeed, the percentage of  $AV^+/PI^- + AV^+/PI^+$  cells reached levels similar to those observed after being exposed to GzmH<sup>S195A</sup> (*Figure IV.13A*).

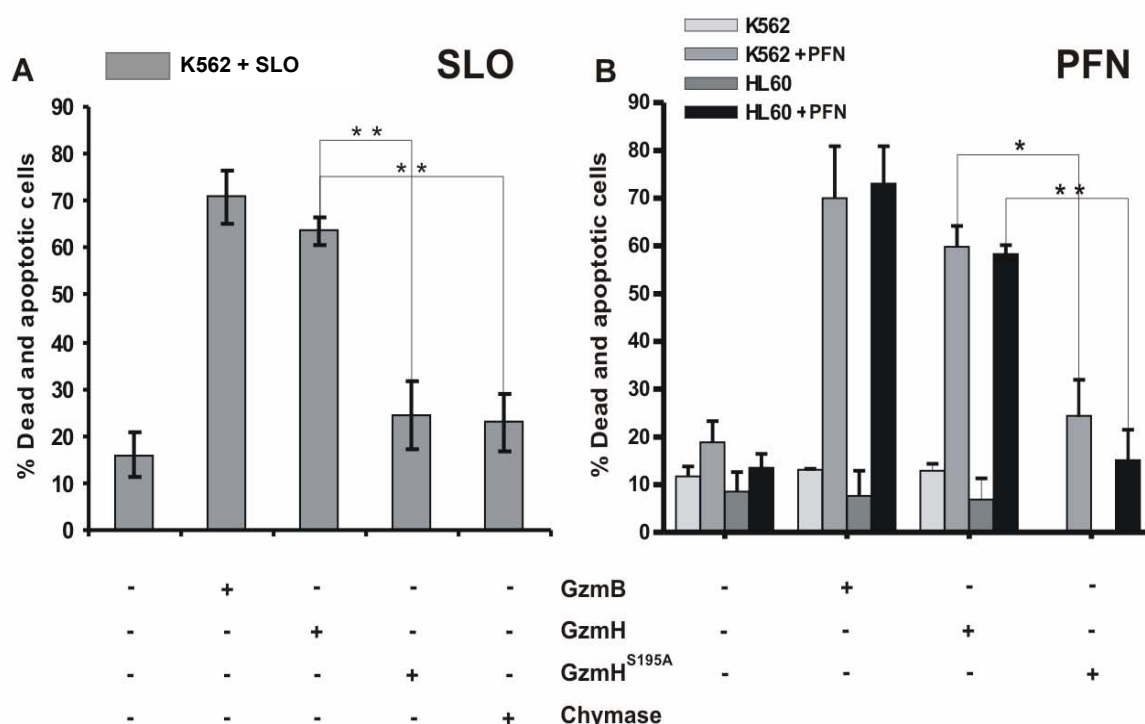


**Figure IV.13 - Cell death induced by recombinant GzmH.** K562 or HL60 cells exposed to GzmH and sublytic concentrations of PFN or SLO resulted in near complete cell death. Viability of K562 and HL60 cells was examined by annexin V-FITC (AV) and propidium iodide (PI) staining 10-12 (SLO) and 24 (PFN) hours after the indicated treatments. Depending on the translocator of choice, graphic A showing SLO and graphic B showing PFN, GzmB or GzmH, were used at final concentrations of 5/10  $\mu\text{g/ml}$  or 5/20  $\mu\text{g/ml}$  respectively, the lower concentration used in combination with perforin. GzmH<sup>S195A</sup> and mast cell chymase were used at 25  $\mu\text{g/ml}$ . Presented, for both perforin and SLO mediated experiments, is the sum of apoptotic (AV<sup>+</sup> and PI<sup>-</sup>) and necrotic (AV<sup>+</sup> and PI<sup>+</sup>) cells from 3 pooled independent experiments (n=3,  $\pm$  standard deviations (SD)). Statistical significance is shown as \* representing p<0.005 (significant) and \*\* p < 0.001 (very significant). In contrast to GzmH, mast cell chymase did not induce cell death.

### *GzmH triggered cell death is distinguishable from GzmB cell death*

To assess the morphological changes triggered by GzmH, we performed live cell imaging of GzmH and GzmB treated cells. GzmH, similar to GzmB, induced many of the typical morphologic changes that occurred during apoptotic cell death, such as high granularity, nuclear condensation, apoptotic body formation and irregularities of the cell surface membrane. Importantly, inactive GzmH<sup>S195A</sup> together with SLO did not elicit any of the above changes (*Figure IV.14*). Despite the lack of morphological differences spotted after exposure of target cells to GzmH or GzmB, GzmH treated cells, stained with trypan blue (a technique used to monitor cell membrane integrity and the emergence of cell necrosis), did reveal a marked difference in the percentage of positively stained cells. Samples were assayed every two hours after GzmH or GzmB loading. Surprisingly, GzmH triggered the accumulation of trypan blue in target cells relatively quickly (45% of cells were positive after 4 hours),

whereas the percentage of secondary cell necrosis was only 30% at the 4 hour time point (*Figure IV.15*) in GzmB experiments. Membrane integrity was lost at a later time in response to GzmB, but GzmH required more time to induce noticeable cell death in the majority of target cells. On the basis of these initial findings, the cell death programs triggered by GzmH and GzmB appeared to be clearly distinguishable.

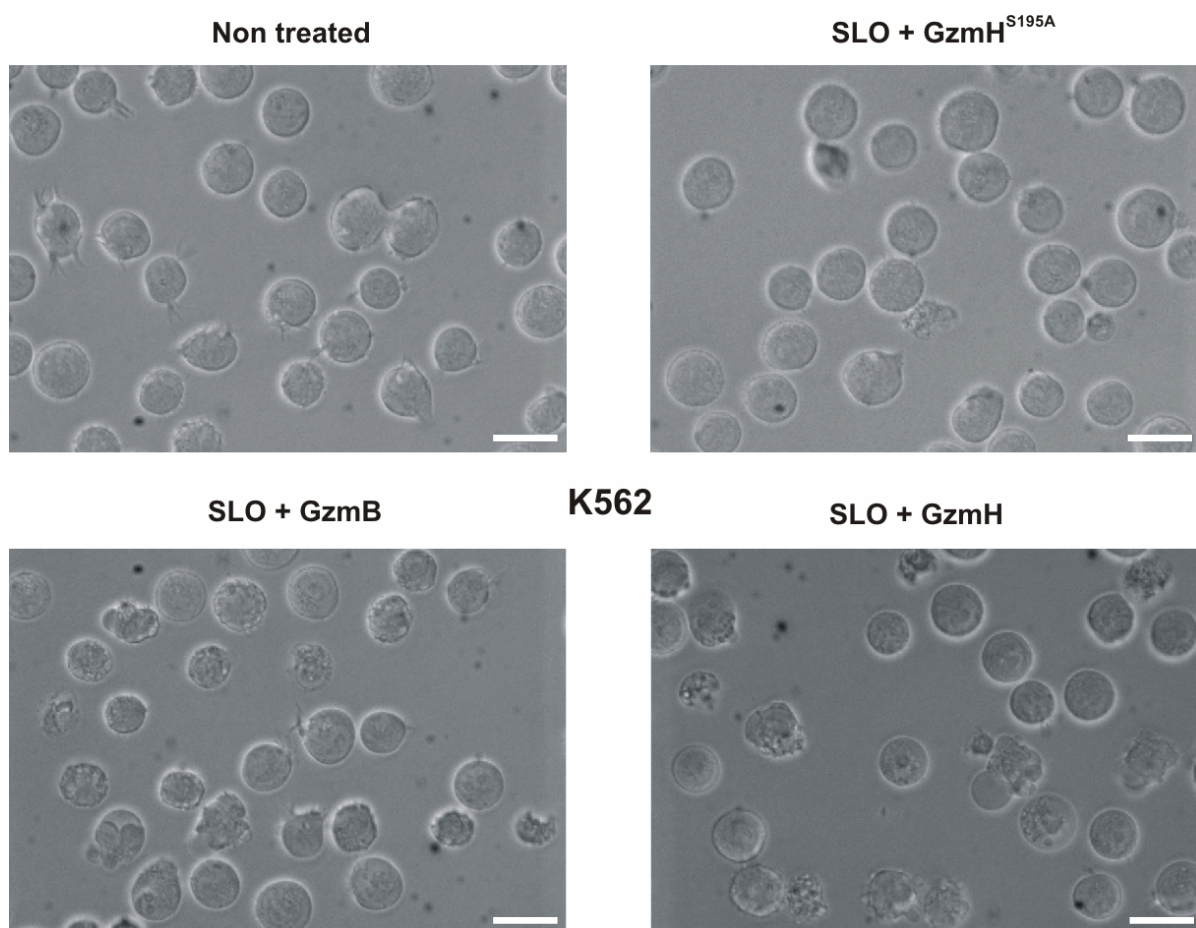


**Figure IV.14 - GzmH treated K562 cells displayed many of the typical apoptotic morphological changes.** To distinguish living cells from those with apoptotic nuclei, bright field pictures were taken with an inverted microscope (40x magnification). Ten hours after GzmH (20 µg/ml) treatment, K562 cells displayed a characteristic morphology with increased granularity, condensation of nuclei and membrane irregularities. GzmB was used at a final concentration of 10 µg/ml. Importantly, inactive GzmH<sup>S195A</sup> (25 µg/ml) together with sublytic SLO did not trigger similar changes. Scale bar equals 20 µm.

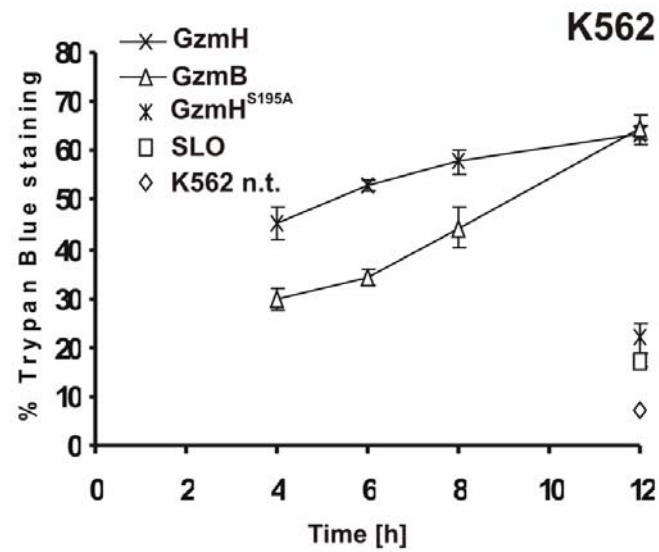


**Figure IV.15 - GzmH induced cell death leads to the quick loss of membrane integrity.** GzmH/SLO treated K562 cells were stained with trypan blue at various time points ( $n=3$ ,  $\pm$  SD). In contrast to GzmB, GzmH induced a much more pronounced trypan staining, with nearly 50% of cells positive after 4 hours. At this time point GzmB treated cells, in late phase apoptosis, accounted for only 30%.

### ***IV.5.2 - GzmH induces nuclear fragmentation & chromosomal condensation***

#### ***Cells treated with GzmH display strongly fragmented nuclei with condensed chromatin***

To further investigate GzmH induced cellular changes, 10 to 12 hours after treatment with the protease and sublytic SLO, K562 cells were stained with the Hoechst dye 33342 and annexin V-FITC and then subsequently analysed by immunofluorescence microscopy after fixation (see materials and methods).

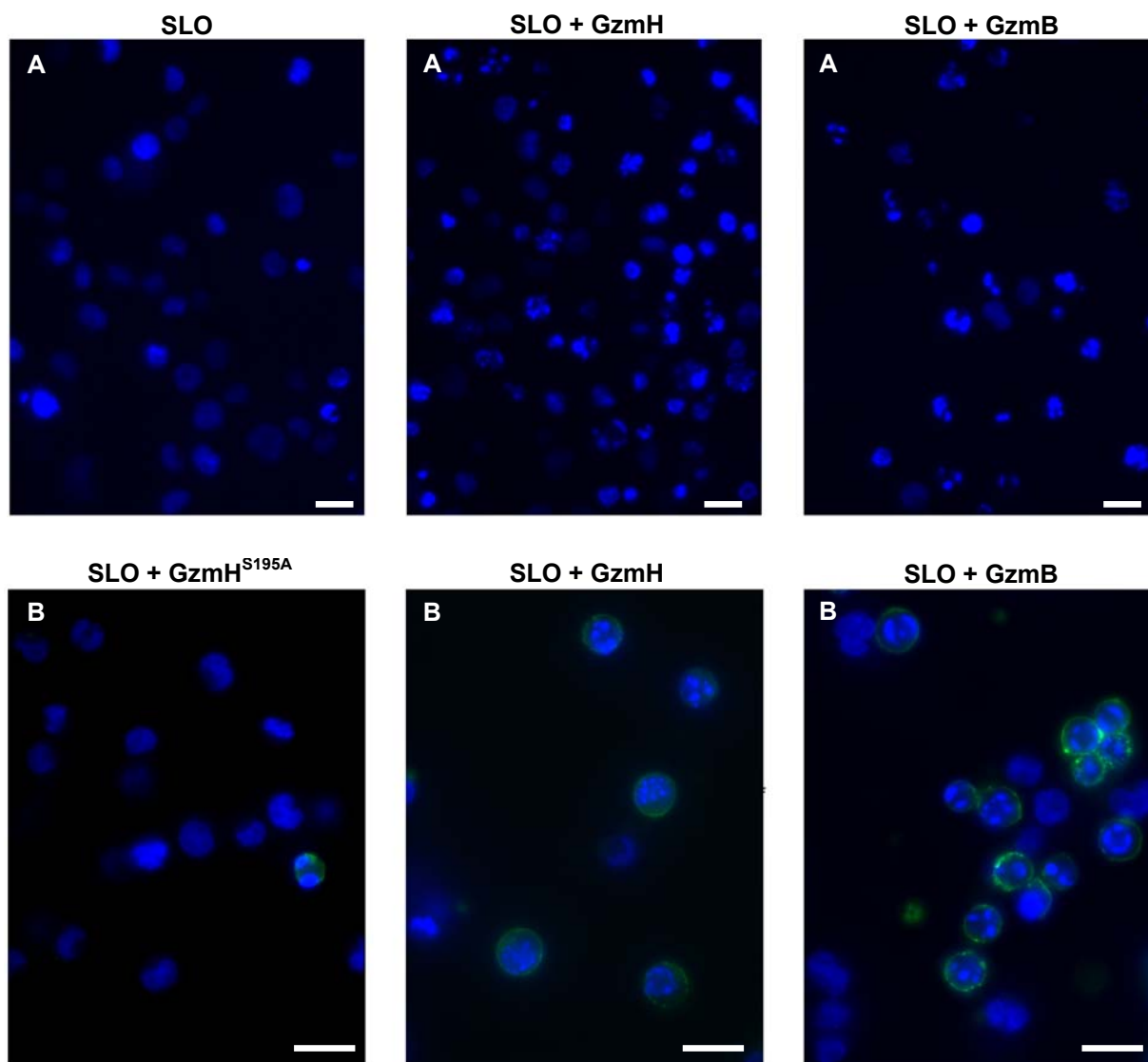


**Figure IV.16 - Nuclear fragmentation of K562 cells treated with GzmH or GzmB and sublytic SLO for 12 hours.** (A) Cells were stained either with the Hoechst dye 33342 alone (40x magnification) or (B) in combination with annexin V-FITC (63x magnification). After fixation fluorescent signals were analysed by microscopy. In contrast to treatment with GzmB (7.5  $\mu\text{g/ml}$ ) and GzmH (15  $\mu\text{g/ml}$ ), cells treated with SLO alone or in conjunction with GzmH<sup>S195A</sup> (15  $\mu\text{g/ml}$ ), (A-B, left) did not show fragmented nuclei with condensed chromatin or phosphatidylserine externalization. Hoechst stainings are representative of 5 independent experiments. Scale bar indicates 20  $\mu\text{m}$ .



In contrast to cells treated with GzmH<sup>S195A</sup>, most cells stained positive for annexin V (dead and apoptotic cells or AV<sup>+</sup>/PI<sup>-</sup> and AV<sup>+</sup>/PI<sup>+</sup> populations) and displayed strong fragmented nuclei with condensed chromatin (*Figure IV.16*). Interestingly, in comparison to GzmB, GzmH treated cells showed nuclei with a higher degree of fragmentation. The GzmB pathway is known to lead to the activation caspase activated DNase (CAD) which results in the cleavage of host DNA into segments of approximately 180-200 bps in length. The mechanism by which GzmH triggers eventual DNA cleavage has not been investigated so far, the presence of much smaller fragmented nuclei, compared to that induced by GzmB, pointing towards the possibility that GzmH mediated cell death results in the activation of endonucleases which cleave DNA into much shorter double-stranded pieces.

In a separate experiment the nuclei of K562 cells treated with GzmH or GzmB in the presence or absence of the general caspase inhibitor zVAD-FMK, were analysed 4 and 12 hours after Hoechst 33342 staining with the aim to acquire a better understanding of the speed with which GzmH harms the host cell's nuclei. After 4 hours of exposure to GzmH, the nuclei of K562 cells still appeared normal under the microscope. Cells exposed to GzmB however already revealed maximum apoptotic nuclei (*Figure IV.17*). After 12 hours though a different story emerged, with most GzmH treated cells displaying apoptotic nuclei thus fitting well to the delayed killing capacity of GzmH (refer to *Figure IV.13*). GzmB-induced nuclear fragmentation, on the other hand, was strongly inhibited by zVAD-FMK after 4 (94% inhibition) and 12 hours (70% inhibition). The latter GzmB induced phenomenon was thus caspase dependent. In contrast, in the presence of zVAD-FMK the effects of GzmH, after 12 hours, were only moderately inhibited by about 30% indicating a caspase independent pathway for the protease.

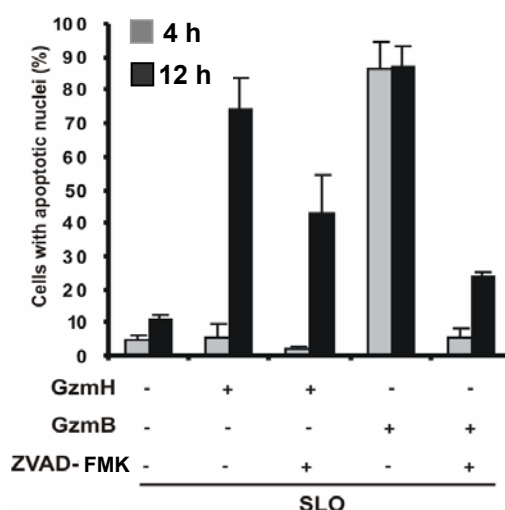


**Figure IV.17 - Apoptotic nuclei induction by GzmH.** Quantification of apoptotic nuclei, following Hoechst 33342 staining, 4 and 12 hours after treatment with GzmB or GzmH and sublytic SLO. GzmH was used at a final concentration of 20 µg/ml and GzmB at 10 µg/ml. Additionally, the general caspase inhibitor zVAD-FMK (100 µM) was used as a probe for caspase activation. The columns represent the mean with its standard deviation from triplicate measurements.



### *GzmH mediated cell death causes a loss of typical cell cycle peaks*

To explore GzmH induced damage of cellular nuclei more explicitly, DNA analysis of the cell cycle was performed. As expected, K562 cells, treated with sublytic amounts of SLO and GzmH<sup>S195A</sup>, revealed the characteristic peaks of proliferating cells in the G<sub>1</sub>, S and G<sub>2</sub> phases with no sub-G<sub>1</sub> peaks visible indicating the absence of double-stranded fragmented apoptotic DNA. On the other hand, cells treated with either active GzmB, or GzmH, eventually lost the characteristic cycle peaks of living cells while the number of cells located in the sub-G<sub>1</sub> area (M1) increased (*Figure IV.18A*).

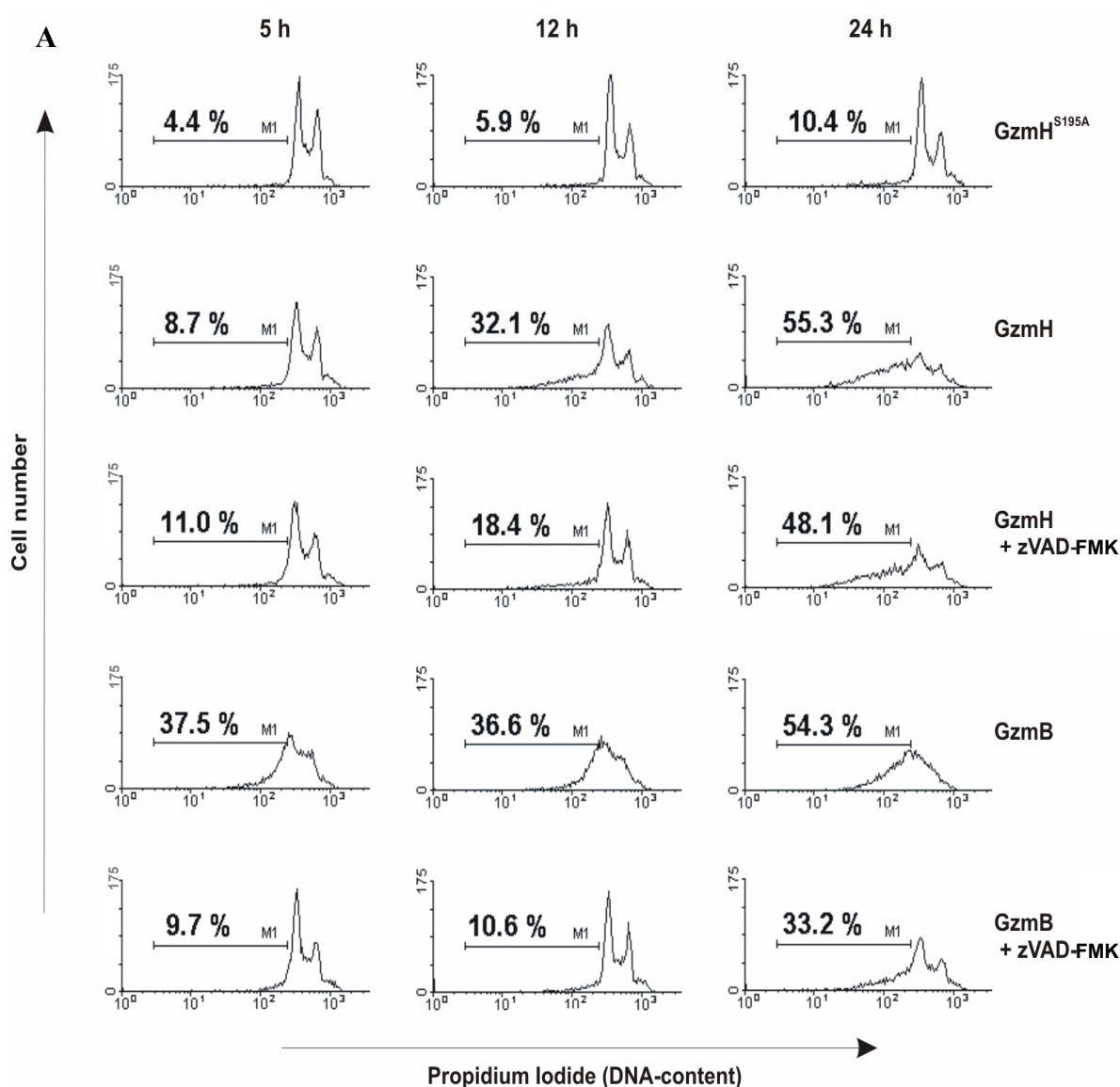


**Figure IV.18A** - DNA content analysis of differentially treated K562 cells after 5, 12 and 24 hours. Following the exposure of K562 cells (  $1 \times 10^5$  / 50  $\mu$ l) to GzmB (10  $\mu$ g/ml) or GzmH (20  $\mu$ g/ml), the two characteristic peaks (G<sub>1</sub> and G<sub>2</sub>M, left and right peaks, respectively) of dividing cells were gradually lost (see time points), while cells with lower DNA content values in the so-called sub-G<sub>1</sub> area appeared (indicated by M1). Importantly, inactive GzmH (20  $\mu$ g/ml) did not cause a loss of the normal cell cycle peaks, G<sub>1</sub> and G<sub>2</sub>M. The pan-caspase inhibitor zVAD-FMK was used at 100  $\mu$ M.

Although both enzymes did lead to an increase in the percentage of cells containing a reduced DNA content, the GzmH mediated cell population in the sub-G1 area was only evident after 12 hours. In the case of GzmB, similar values of approximately 35% were already present at the 5 hour time point. After 24 hours however, the percentage of DNA contained within the sub-G1 area was the same. Consistent with the differential effects of zVAD-FMK on the nuclear morphology of GzmB- and GzmH-treated cells, the pan-caspase inhibitor also moderately prevented GzmH triggered DNA degradation, whereas inhibition by zVAD-FMK was highly efficient in protecting GzmB-treated target cells. *Figure IV.18B* is a quantitative presentation of our FACS observations in *Figure IV.18A*, specifying the percentage of sub-G1 cells (marker M1) after treatment under the above conditions.

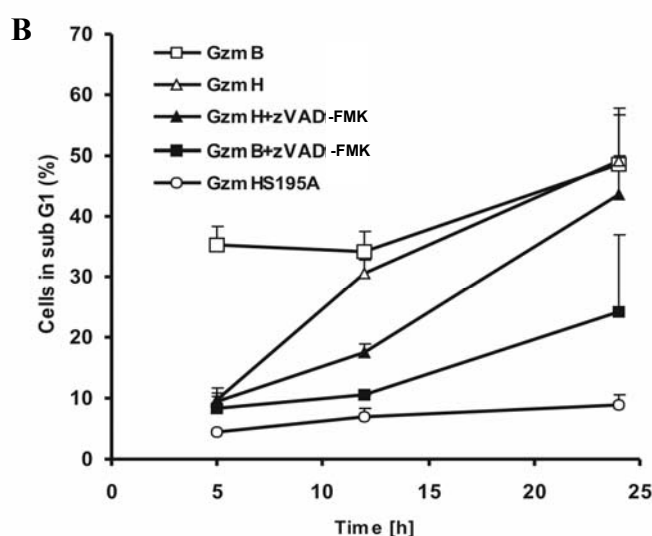


**Figure IV.18B** - DNA content analysis of differentially treated K562 cells after 5, 12 and 24 hours. Quantitative representation (n=3, +/- SD) of experiment A. Following the same trends as seen in the FACS data, GzmB treated cells show early DNA degradation while GzmH works a slow, but progressive diminution of DNA, the percentage of Sub-G1 cells matching that induced by GzmB at the 24 h time point.

### ***GzmH does not induce DNA laddering or ICAD cleavage***

Nuclear disintegration was analysed by agarose gel electrophoresis (*Figure IV.19A*). After 4 hours no laddering was detected in postnuclear lysates of GzmH treated cells although a slight background smear did become apparent at the 12 hours time-point. This background could be due to unspecific GzmH events which occur before the 12 hour, a time point when 70-80% of cells are already dead. On the other hand GzmB, which efficiently activates procaspase 3 and in turn the caspase activated DNase CAD, revealed a clear-cut laddering pattern after the 4 hours time point. To back up these observations, we decided to analyse levels of ICAD, the inhibitor of caspase activated DNase (CAD). As implied above, this DNase is thought to be largely responsible for the caspase induced laddering effect seen in many apoptotic pathways. In the case of GzmH induced cell death however, ICAD

remained untouched during time course experiments with minimal decline only detectable at the 12 hour time point (*Figure IV.19B*). Our observations strongly indicate that CAD activation does not take place during GzmH induced cell death and suggest the late decline in ICAD is the result of secondary, indirect events. The absence of CAD activation during GzmH mediated cell death provides yet more evidence, along with the ineffectiveness of the general caspase inhibitor, zVAD-FMK, that the pathway triggered by this protease is indeed caspase independent.

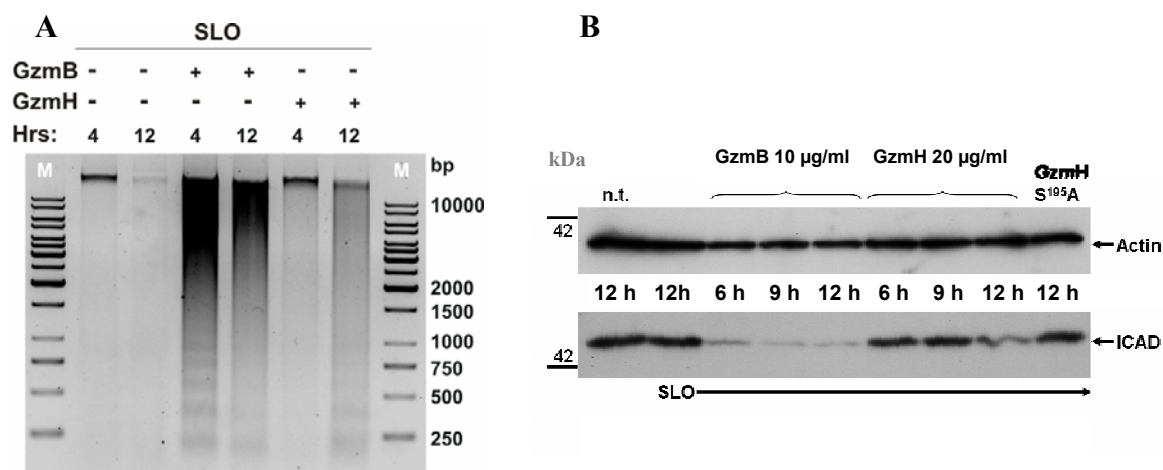


**Figure IV.19 - GzmH treatment does not cause apoptotic DNA laddering or activate caspase activated DNase (CAD) via ICAD cleavage.** (A) K562 cells ( $1 \times 10^5$  / 50 µl) were treated for 4 and 12 hours as indicated with GzmH (20 µg/ml) or GzmB (10 µg/ml) in the presence of sublytic concentrations of SLO. Cellular DNA was analysed on a 1% agarose gel and the experiment repeated three times. Lanes 2 and 3 (from left to right) show the intact cellular DNA from non treated K562 cells. Lanes 4 and 5 are representative of the GzmB effect on cellular DNA, showing DNA degradation and low molecular weight fragments differing by 200 bps in length. In lanes 6 and 7, GzmH treatment shows control-like results, with only a slight background after 12 hours. (B) K562 cells ( $1 \times 10^5$  / 50 µl) were exposed to GzmB or GzmH. At the above defined time points, 100 µl of cells,  $1 \times 10^6$  / 50 µl, were harvested and washed in PBS before being directly boiled in reducing Laemmli buffer and loaded onto SDS gels. Following transfer, blots were then analysed for the presence of ICAD by immunoblotting (see materials and methods page 50 and 51). The blot was stripped and then analysed with an anti-actin antibody to control loading (see materials and methods page 50/51).

### *GzmH induces the release of radioactively labeled nuclear DNA*

Degradation and release of radioactively labeled nuclear DNA into the cytosol was monitored by the  $^3\text{H}$ -thymidine release assay (refer to *Figure IV.20*). In line with the above experiments, GzmH induced slower  $^3\text{H}$ -thymidine release than GzmB, reaching maximum levels 24 hours after cell death induction. By contrast the catalytically inactive GzmH<sup>S195A</sup> mutant did not induce any significant effects above background levels. Again treatment with zVAD-FMK totally abolished the initial effects of GzmB after 4 hours again emphasizing the essential role caspases play in the GzmB death pathway. After 12 and 24 hours, however, cells treated with zVAD-FMK and either GzmB or GzmH displayed consistent  $^3\text{H}$ -thymidine release at similar levels. Contrary to previous experiments demonstrating the absence of caspase involvement in GzmH triggered cell death, here the general caspase inhibitor diminished  $^3\text{H}$ -

thymidine release by approximately 40% at the 12 hour time point. This observation lead us to consider the possibility that zVAD-FMK might indeed be inhibiting other intracellular proteases such as the lysosomal cathepsin family. Indeed, members of this cysteine protease family have not only been reported to be irreversibly inhibited by most caspase inhibitors, especially zDEVD-CMK/FMK, acYVAD-CMK/FMK and zVAD-FMK (Rozman-Pungercar et al., 2003), but also to be involved in triggering various apoptosis pathways (Guicciardi et al., 2004). It was therefore conceivable that GzmH might be involved in unleashing these lysosomal proteases (*Figure IV.26*). In summary, GzmH induced a slow form of DNA-degradation, distinct from that of GzmB, which was only partially inhibited by zVAD-FMK.

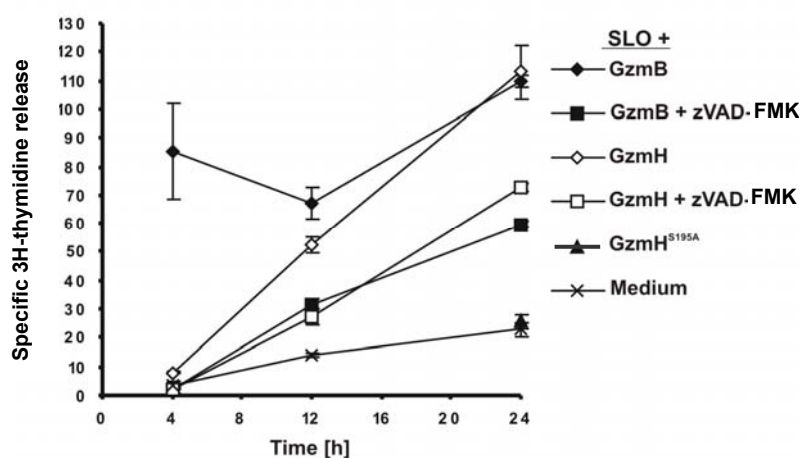


**Figure IV.20 - GzmH induces DNA fragmentation monitored by the  $^3\text{H}$ -thymidine release assay.** After 4, 12 and 24 hours, K562 cells ( $1 \times 10^5 / 50 \mu\text{l}$ ), which had incorporated  $^3\text{H}$ -thymidine and been treated with SLO and the indicated proteases (GzmH at  $20 \mu\text{g/ml}$  and GzmB at  $10 \mu\text{g/ml}$ ) were monitored for fragmented DNA release into the supernatant. The caspase inhibitor zVAD-FMK ( $50 \mu\text{M}$ ) only partially inhibited both proteases after 12 and 24 hours. The data points represent the average of triplicate measurements  $\pm$  SD.

### IV.5.3 - GzmH does not activate main apoptosis executioner molecules

#### *GzmH does not directly cleave recombinant effector caspases or recombinant Bid*

Executioner caspases are potent coordinators of apoptosis. Catalytically inactive variants of main executioner caspases 3 and 7 (C285A mutants), kindly provided by G. Salvesen and S. Riedl, allowed us to verify if GzmH could directly cleave these essential coordinators of apoptosis. Recombinant GzmB was used as a positive control, the aspartase widely reported to directly target executioner caspases 3 and 7 and the Bcl-2 family member Bid after entry into the cytosol (Barry et al., 2000; Metkar et al., 2003).

GzmB modifies procaspases by cleaving after aspartic acid residues. This then results in the liberation of the prodomain and the generation of a small and a large fragment. The smaller fragment, namely p10 or p11, p10 referring to the molecular weight of the caspase 3 fragment and p11 to that of caspase 7. The remaining p22/24 fragment, or large fragment, goes on to form a heterodimer with fragment p10/11 which in combination with a second heterodimer produces an active tetramer (refer to *Figure IV.21A*). In contrast to GzmB, which efficiently cleaves both procaspase 3 and 7 even after 5 minutes incubation at 37°C, incubation with GzmH for 1 hour resulted in no cleavage whatsoever, both procaspase bands identical to the controls in lanes 1 and 2 (*Figure IV.21B*). Likewise, recombinant Bid was also not cleaved after exposure to GzmH (*Figure IV.21C*). Indeed, truncated Bid (t-Bid) is another potent coordinator of apoptosis which damages the mitochondrial outer membrane and which, moreover, is another direct substrate of GzmB.

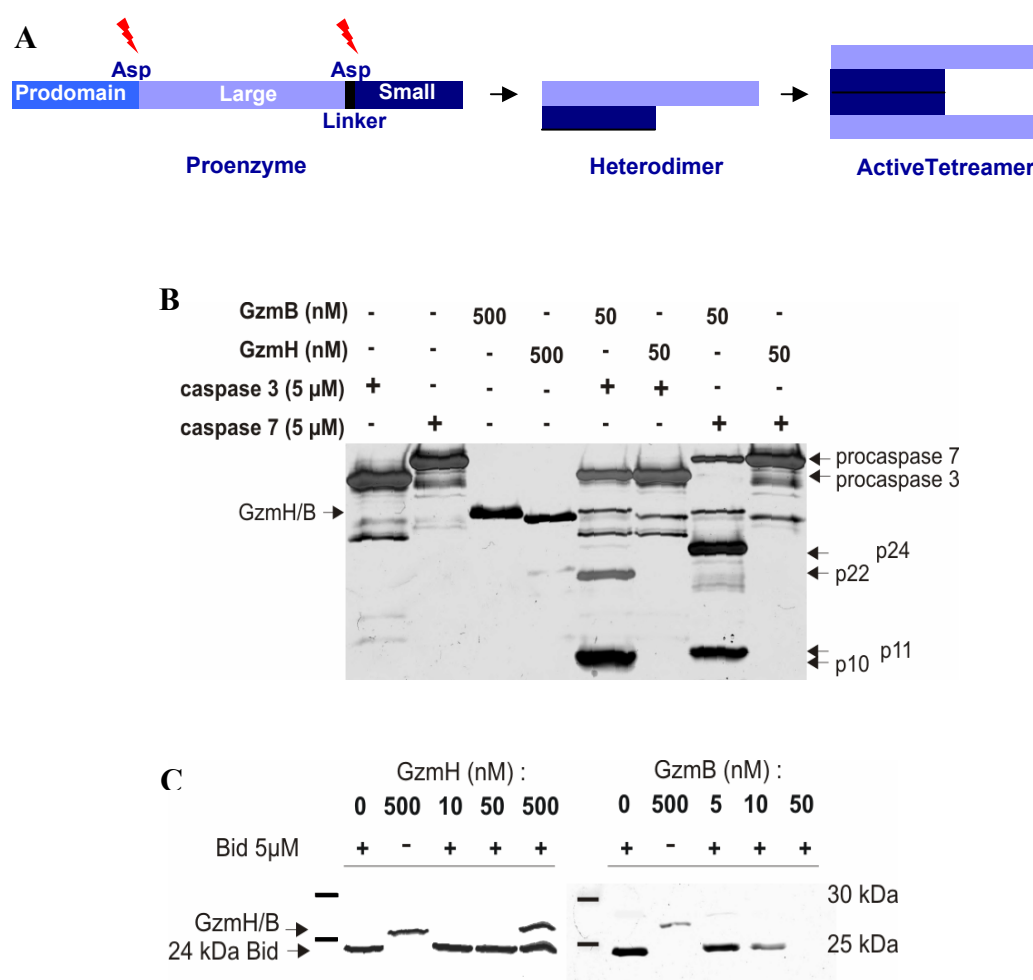


**Figure IV.21 - GzmH does not cleave recombinant procaspases 3 and 7 or recombinant Bid.** (A) Scheme representing procaspase cleavage and activation. (B) The catalytically inactive human procaspases 3 and 7 (5  $\mu$ M), with the active site Cys285 replaced by an Ala residue to avoid autoactivation, and (C) recombinant Bid (5  $\mu$ M), were incubated with either recombinant GzmH (50 nM) or GzmB (50 nM) for 1 h at 37°C in activity buffer. Samples were boiled in reducing Laemmli buffer, loaded and separated on a 18% polyacrylamide gel. Electrophoretically separated bands were visualized by silver staining.

### *GzmH induced cell death does not activate initiator or effector caspases*

To investigate GzmH-related caspase involvement more thoroughly, we continuously monitored the activity of caspases 3, 6, 7, 8 and 10 in living cells for up to 10 hours using the cell penetrating fluorogenic substrate acDEVD-AMC (see handbook on caspase inhibitors and substrates from Calbiochem).

Figures IV.22A and B show the efficient cleavage of acDEVD-AMC in response to GzmB, after K562 cells were exposed to both sublytic concentrations of SLO or PFN respectively. Conversely, GzmH or GzmH<sup>S195A</sup> resulted only in baseline readings. To rule out any late surge in caspase activity, prolonged measurements, of up to 15 hours, were performed but no increase was observed. As expected, the addition of the general caspase inhibitor zVAD-FMK completely inhibited GzmB induced executioner caspase activity.

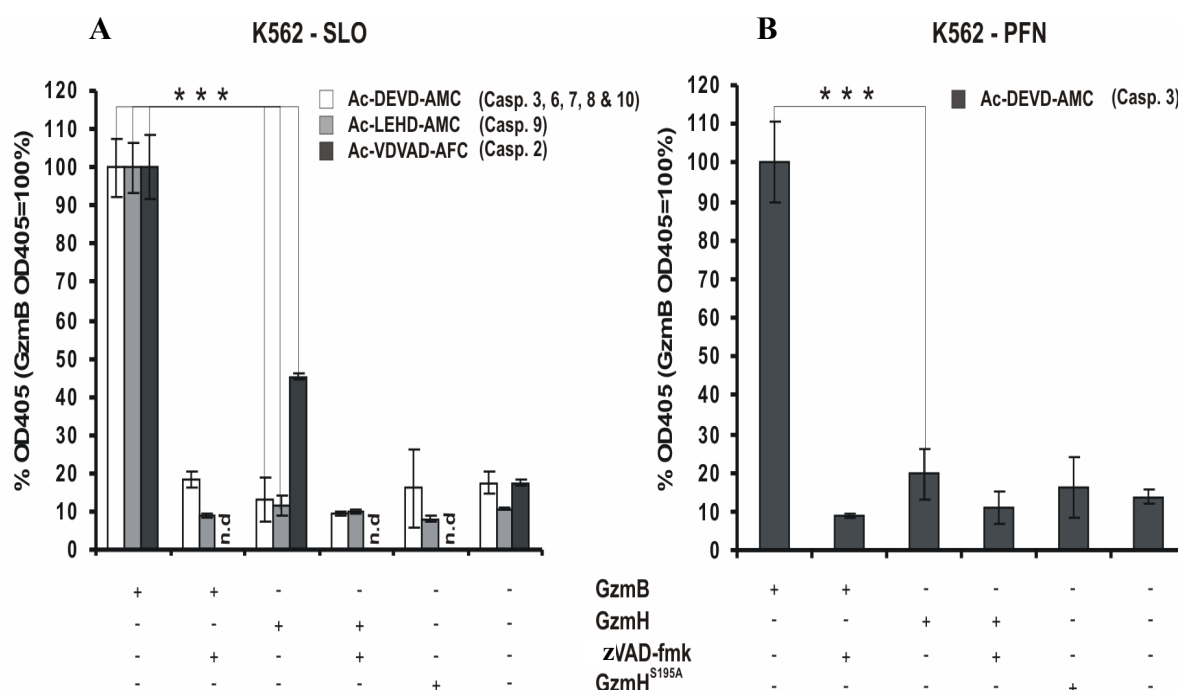


**Figure IV.22 - GzmH does not activate effector caspases in living cells.** Using cell penetrating caspase substrates we analysed caspase activities in living cells ( $1 \times 10^5$  / 50  $\mu$ l) 10 hours after granzyme treatment. Data was normalized to GzmB and pooled from 3 (A) and 2 (B) independent experiments,  $\pm$  SD. In contrast to cell death mediated by sublytic concentrations of perforin (B) or SLO (A), GzmH (20  $\mu$ g/ml) did not induce cleavage of acDEVD-AMC which monitors the activities of caspases 3, 6, 7, 8 and 10. Addition of zVAD-FMK (50  $\mu$ M) completely blocked the activation of caspases by GzmB (10  $\mu$ g/ml). The same observations were seen with the caspase 9 substrate, acLEHD-AMC, here only monitored using SLO as a translocator. Cleavage of the caspase 2 substrate, acVDVAD-AFC, was observed in both GzmB and GzmH-SLO treated K562 cells, where in comparison to GzmB, the effect of GzmH was weaker, but clearly above the background levels caused by sublytic SLO alone. N.d.: not determined.

### ***GzmH mediated cell death does not lead to apoptosome formation and cytochrome c release***

We also measured caspase 9 activity using the fluorogenic substrate acLEHD-AMC (*Figure IV.22A*). Whereas caspase 9 activity was easily detected in GzmB-treated K562 cells over time, no activity towards ac-LEHD-AMC was found after SLO mediated delivery of GzmH or GzmH<sup>S195A</sup>. Despite the lack of caspase 9 activity after GzmH treatment, we nevertheless chose to verify cytochrome c release, the smallest of the proapoptotic mitochondrial intermembrane space proteins. If the outer mitochondrial membrane were damaged by GzmH, cytochrome c would be expected to be released into the cytosol thereby triggering the formation of the apoptosome complex and procaspase 9 activation (Zou et al., 1999).

To ascertain the lack of cytochrome c release, cytosolic fractions of GzmH treated K562 cells were prepared and analysed at different time points following cell death induction. Digitonin, a weak nonionic detergent that selectively renders the plasma membrane permeable, releasing cytosolic components from cells but leaving other organelles intact (Heibei et al., 1999), was used at low concentrations (see materials and methods) to monitor the release of cytochrome c. Digitonin is an ideal compound with which to study the release of mitochondrial inter membrane space proteins (MIMPs) such as cytochrome c, the smallest members of the proapoptotic MIMPs. Following treatment with GzmH or GzmB after 1, 2 and 6 hours, K562 cells were washed and resuspended in digitonin lysis buffer. Supernatants and pellets loaded onto polyacrylamide gels followed by electrophoresis and transfer to nitrocellulose membranes for Western blot analysis. GzmH treated target cells did not show any detectable cytochrome c loss from the inner membrane space of mitochondria (*Figure IV.23*). As expected, cytosolic levels of cytochrome c did increased over time in K562 cells that had been treated with GzmB, while levels of the cytochrome declined in the respective membrane fractions.

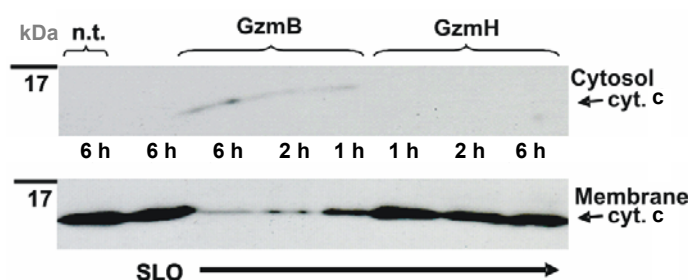


**Figure IV.23 - GzmH mediated cell death does not result in the release of cytochrome c.** Western blot analysis (representative of 2 independent experiments) reveals that cytochrome c release is not a hallmark of GzmH induced cell death. K562 cells ( $1 \times 10^5$  / 50  $\mu$ l) were exposed to GzmH (20  $\mu$ g/ml) or GzmB (10  $\mu$ g/ml) and sublytic SLO for the indicated times. After cytosolic and membrane supernatant preparation, cytochrome c, in the case of GzmH treatment, could only be detected in the membrane fraction. The membrane fractions prepared, 1, 2 and 6 h after exposure to GzmB show a gradual decline of cytochrome c, and gradually reappear in the cytosolic fractions.

***GzmH induced cell death leads to weak caspase 2 activation***

As previously demonstrated the use of the zVAD-FMK during GzmH triggered cell death resulted in a slight decrease of the protease's cytotoxic ability. Using recombinant effector caspases as well as cell penetrable, caspase specific peptides, we showed that the mechanisms underlying GzmH induced cell death were indeed independent of caspase activation. Recently, interest has been mounting regarding the role of caspase 2 in cell death with various studies by Sten Orrenius and colleagues suggesting that caspase 2 is activated in response to DNA damage and genotoxic stress. Thereafter an alternative cell death pathway is induced based on damage to the mitochondria (Robertson et al., 2004; Zhivotovsky and Orrenius, 2005) although the exact mechanism by which the cysteine protease executes cell death still remains obscure. Therefore, we investigated whether caspase 2 activity might contribute towards GzmH mediated cell death.

Caspase 3 has been shown to cleave the caspase 2 specific sequence, VDVAD (refer to *Figure IV.24C and D*). Since we demonstrated the lack of caspase 3 activity in response to GzmH induced cell death (refer to *Figure IV.24Ai*), cleavage of the fluorogenic acVDVAD-AFC substrate should uniquely monitor caspase 2 activity in GzmH treated cells. Interestingly, GzmH, delivered to K562 cells with sublytic SLO concentrations, generated some acVDVAD-AFC cleaving activity, whereas GzmB again showed a much greater effect at every recorded time-point (*Figure IV.24Aiii*). In experiments repeatedly performed with GzmH<sup>S195A</sup>, only background signals were recorded, whereas the caspase 2 inhibitor zVDVAD-FMK, as well as zVAD-FMK, completely prevented GzmH dependent caspase 2 like activity. GzmH apparently does not activate caspase 2 directly, or in a protease mediated manner, since, in contrast to GzmB, activity against acVDVAD-AFC was not induced in a cytosolic (S100) K562 lysate after GzmH addition (*Figure IV.24B*).



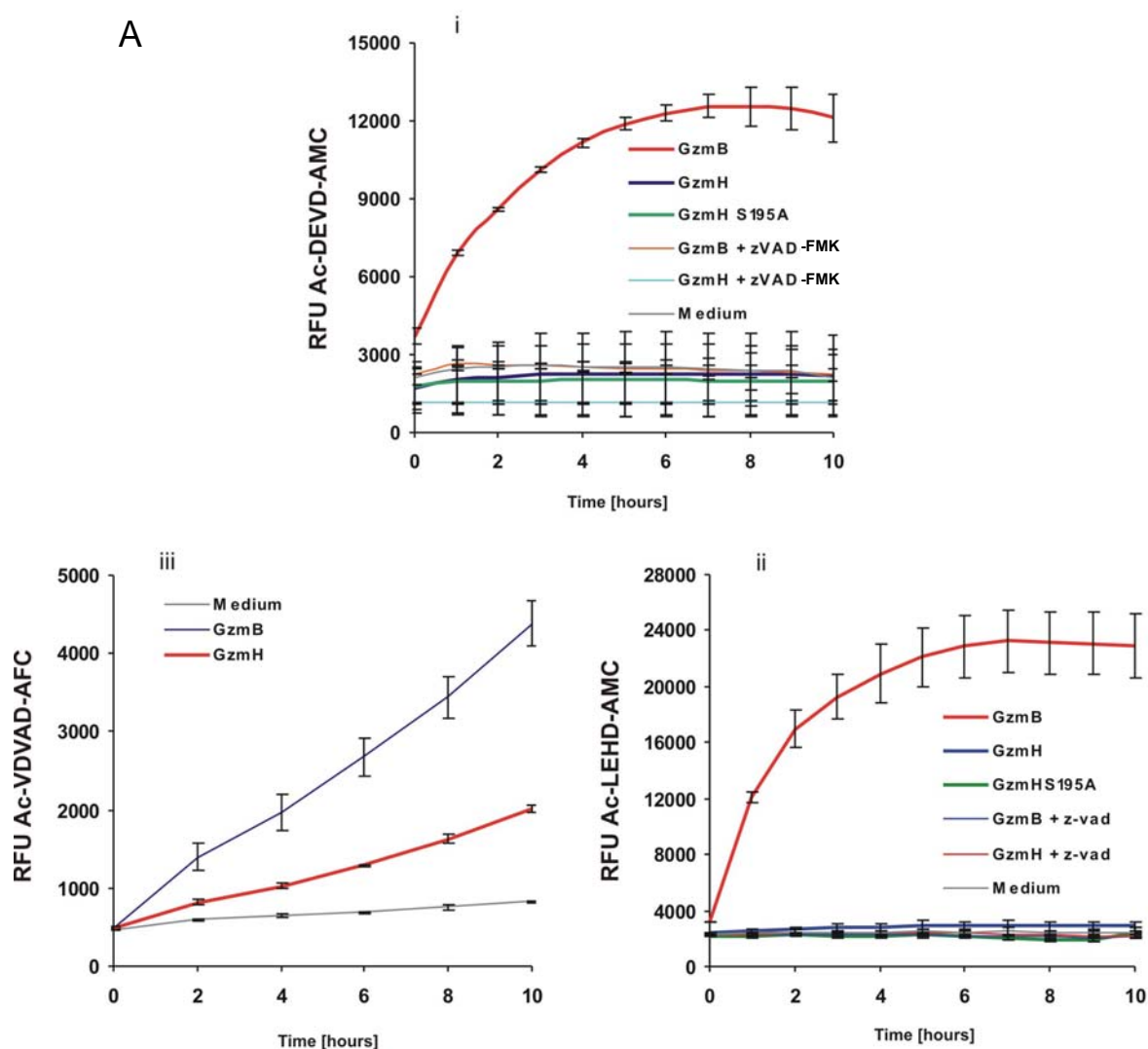


**Figure IV.24A - Cytotoxic activity of GzmH does not depend on caspases.** Full time-lapse immunofluorescence analysis of the 10 hour time point experiments summarized in *Figure IV.22A* (Refer to *Figure IV.22A* experimental details). The curves represent the average fluorescence signals of individual, triplicate measurements taken at 5-min intervals (1 h intervals presented). Each graph is representative of three independent experiments.

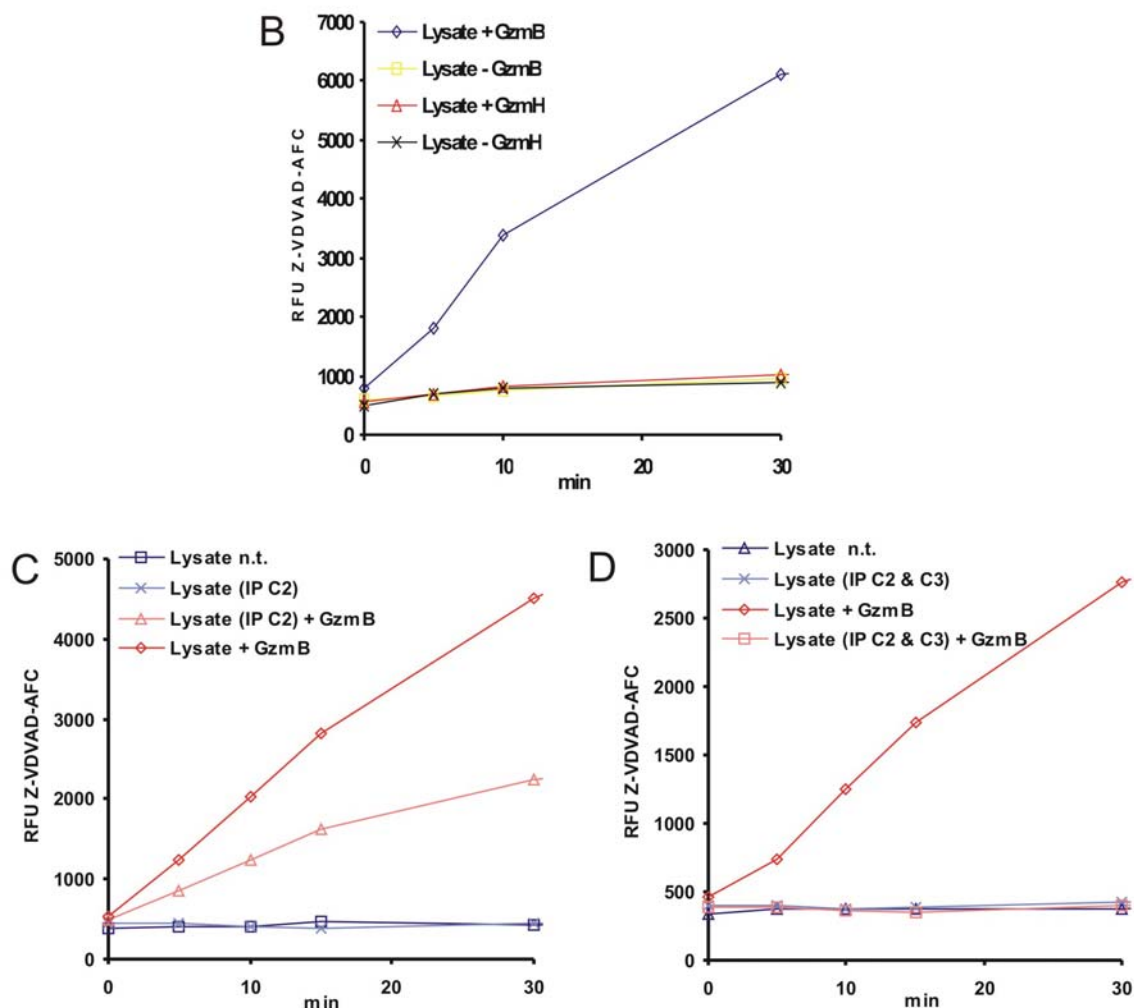


**Figure IV.24B, C and D - Cytotoxic activity of GzmH does not depend on caspases.** Cytosolic fractions from K562 cells ( $1.5 \mu\text{g}/\mu\text{l}$ ,  $20 \mu\text{g}$  total in  $100 \mu\text{l}$ ) were exposed to GzmB ( $10 \mu\text{g}/\text{ml}$ ) or GzmH ( $25 \mu\text{g}/\text{ml}$ ). Caspase 2 activity was measured by the hydrolysis of the fluorogenic caspase 2 substrate acVDVAD-AFC (final concentration  $200 \mu\text{M}$ ). **(B)** Unlike, GzmB, GzmH does not lead to caspase 2 substrate cleavage in a direct or protease mediated fashion. **(C and D)** To ensure that acVDVAD-AFC was truly monitoring caspase 2, and no other caspase activity, the immunoprecipitation (IP) of caspase 2 (C), and both caspases 2 and 3 (D) from cytosolic fractions of untreated K562 cells was tested using specific caspase 2 and caspase 3 monoclonal antibodies from Alexa. Key: lysate, cytosolic fraction; IP, immunoprecipitation; C2 and C3, caspases 2 and 3; n.t., not treated.

***Caspase 2 activity, along with all apoptotic caspases, is not required for GzmH cell death***

Finally, to investigate whether or not the observed caspase 2 activation was essential for GzmH induced cell death, we pretreated K562 or HL60 cells with various concentrations (5, 25, 50  $\mu$ M) of zVDVAD-FMK, a specific caspase 2 inhibitor. Additionally, we also treated cells with other caspase inhibitors, namely zVAD-FMK (a pan-caspase inhibitor) and zDEVD-FMK (inhibiting the initiator caspase 8 and 10 and the executioner caspases 3, 6 and 7) and monitored cell survival by AV/PI staining after 10 hours of incubation (*Figure IV.25*).

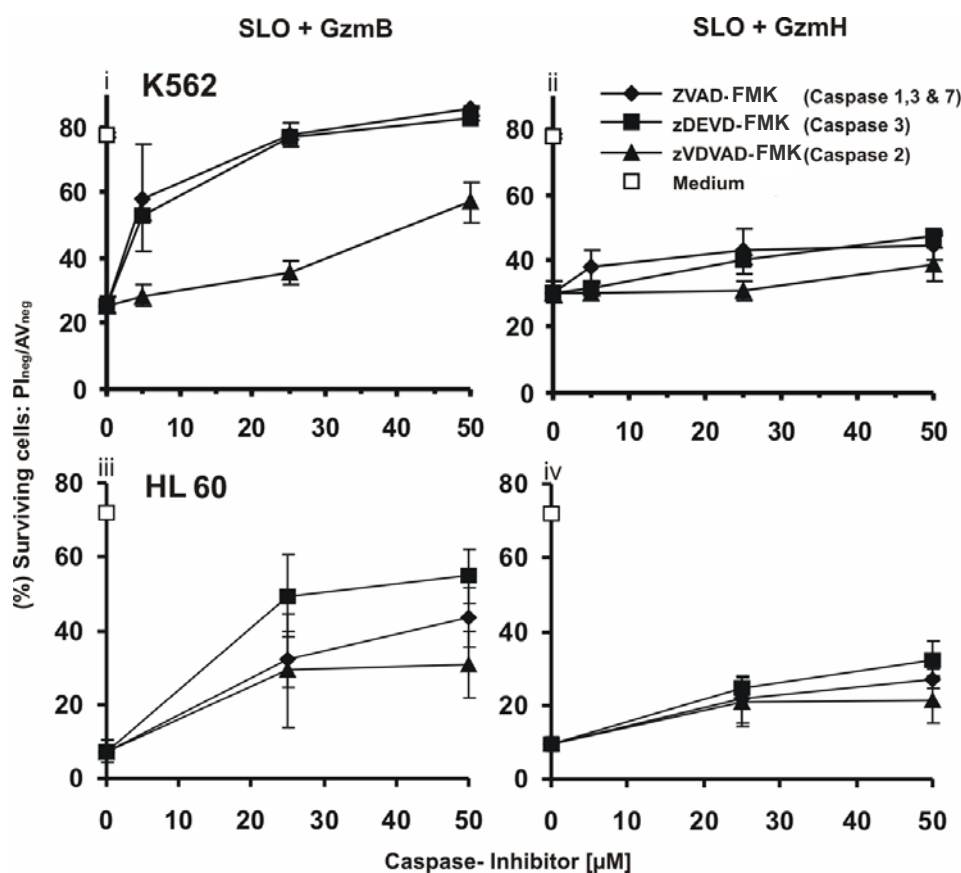


**Figure IV.25 – GzmH kills independent of caspases in K562 and HL60 cells.** Shown is the percentage of surviving cells (Annexin V-FITC/propidium iodide) which had been treated with sublytic SLO and GzmB (10  $\mu$ g/ml) (refer to graphs i and iii) or GzmH (20  $\mu$ g/ml) (refer to graphs ii and iv) for 12 hours. Prior to granzyme and SLO treatment, K562 cells ( $1 \times 10^5$  / 50  $\mu$ l) had been separately exposed to the caspase inhibitors zVAD-FMK (Caspases 1, 3, 7), zDEVD-FMK (Caspase 3) and zVDVAD-FMK (Caspase 2) for 30 minutes. Values represent the average of three independent experiments  $\pm$ SD. The caspase inhibitors zVAD-FMK and zDEVD-FMK rescued cells from GzmB induced apoptosis in a dose dependent fashion, whereas killing by GzmH was minimally affected. Notably, the caspase 2 inhibitor, zVDVAD-FMK did not protect the cells against the actions of GzmH.

In GzmB treated cells, zVAD-FMK and zDEVD-FMK restored the percentage of surviving cells to the level of untreated cells (*Figure 25i and iii*), while none of these inhibitors, even at the highest concentration of 50  $\mu$ M were able to offer protection against GzmH after 10-12 hours. By contrast,

progression of GzmH induced cell death, as monitored by the reduction of surviving cells after 10-12 hours, was poorly affected by all three inhibitors implying that caspase activation, and especially caspase 2 activity, was not crucial for GzmH mediated cell death (*Figure IV.25 ii and iv*).

### ***Cysteine proteases, the cathepsins, are not mediators of GzmH killing***

Our observation that the general caspase inhibitor zVAD-FMK offered slight degrees of protection against various GzmH mediated effects (*Figures IV.17, 18 and 20*) lead us to investigate the possible impact of lysosomal cysteine proteases (cathepsins) in this death cascade.

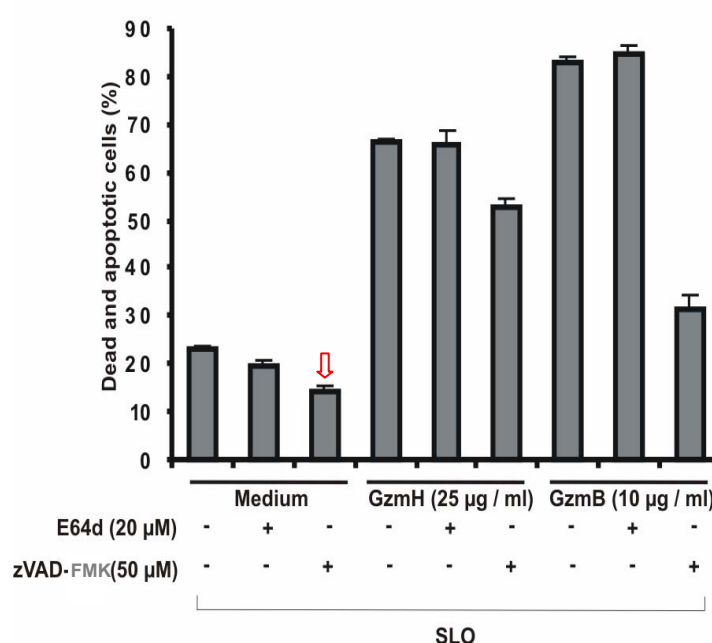


**Figure IV.26 - Lysosomal cathepsins are not mediators of GzmH killing.** Treatment of K562 cells ( $1 \times 10^5$  / 50 µl) with the cell permeable general cathepsin inhibitor E64d (20 µM) provides no protection against sublytic SLO and GzmH (20 µg/ml) or GzmB (10 µg/ml) induced cell death after 12 h. Additionally, the general caspase inhibitor zVAD-FMK was used at a final concentration of 50 µM. Cells were analysed by FACS after annexin V FITC (AV) and propidium iodide (PI) staining. The red arrow indicates the effect of zVAD-FMK on sublytic SLO concentrations, the pan caspase inhibitor most likely mitigating the unspecific sublytic effects of SLO.

Cathepsins are inhibited by a number of irreversible caspase inhibitors including zVAD-FMK (Rozman-Pungercar et al., 2003). We therefore compared the death inhibiting effects of the cell permeable general cysteine protease inhibitor E64d with that of zVAD-FMK in GzmH and GzmB treated target cells (*Figure IV.26*). E64d did not result in any reduction of cell death that occurred within 12 hours after exposure of GzmB or GzmH to K562 cells. We, therefore, conclude that the GzmH triggered cell death is not mediated by lysosomal breakdown and concomitant release of lysosomal proteases into the cytosol.

#### ***IV.5.4 - GzmH induces mitochondrial damage and ROS production***

With the indication that cytochrome c (15 kDa), the smallest of the pro-apoptotic mitochondrial intermembrane space proteins (MIMPs), was not released during GzmH mediated cell death (see *Figure IV.23*), the likelihood that others MIMPS, such as the apoptosis inducing factor (AIF) at 57 kDa and endonuclease G (endo G, 30 kDa), should exit into the cytoplasm is very slim (Barry et al., 2000; Heibein et al., 1999). Mitochondrial depolarization however, if observed, could occur if damage to the inner membrane of the mitochondria is sustained.

##### ***GzmH triggers mitochondrial depolarization***

Using the green fluorescent probe JC-1, which accumulates and aggregates in the inner membrane space and appears red in intact mitochondria, we monitored the depolarization and potential loss ( $\Delta\Psi_m$ ) of inner mitochondrial membranes in K562 cells. As expected, GzmB exerted its strong depolarizing effect on mitochondria already after 4 hours with a near complete loss of red fluorescence visible by FACS analyses after 24 hours (*Figure IV.27 A and B*). GzmH treated cells displayed a similar loss of the membrane potential within 24 hours, but this effect occurred with some delay (*Figure IV.27A and B*). Treatment of K562 cells with GzmH<sup>S195A</sup> clearly confirmed that the decline was due to the proteolytic activity of GzmH.

Regarding GzmB mediated cell death, it is well documented that the aspase is able to induce caspase independent mitochondrial damage by two distinct pathways. One, requires the cleavage and activation of Bid, at a site distinct from that of caspase 8, leading to the release of MIMPS, the release of ROS and the loss of  $\Delta\Psi_m$  (Alimonti et al., 2001; Barry et al., 2000; Heibein et al., 1999; Sutton et al., 2000). The other, whose molecular basis is unknown, involves direct action on mitochondria to induce increased ROS and loss of  $\Delta\Psi_m$  but not release of cytochrome c and other MIMPs (Heibein et al., 1999; MacDonald et al., 1999; Sutton et al., 2000; Thomas et al., 2000). Indeed, treatment of K562 cells with the general caspase inhibitor zVAD-FMK prior to the addition of GzmB and sublytic SLO concentrations, confirmed that, after 24 hours, mitochondrial depolarization by GzmB can occur independently of caspase activation. Unlike the values observed at the 24 hour time point, at the 4 hours, a 20% reduction in depolarization was measured in the presence of zVAD-FMK demonstrating that at early time points caspases do play a role in GzmB triggered mitochondrial depolarization. Importantly though, this was not found to be the case for following GzmH addition to K562 cells. At the 4 hour time point, and in the presence zVAD-FMK, no difference was seen in mitochondrial depolarization values. At 24 hours, however, and under the same conditions, a 15% decrease was measured although at this late time point it is possible that unspecific caspase activation can occur. Additionally, we performed a time course experiment and analysed  $\Delta\Psi_m$  for up to 8 hours (*Figure*

IV.27B). Compared to GzmB, mitochondrial depolarization induced by GzmH is less efficient but nevertheless is closely correlated, time-wise, with the extent of cell death (also see *Figure IV.13*).

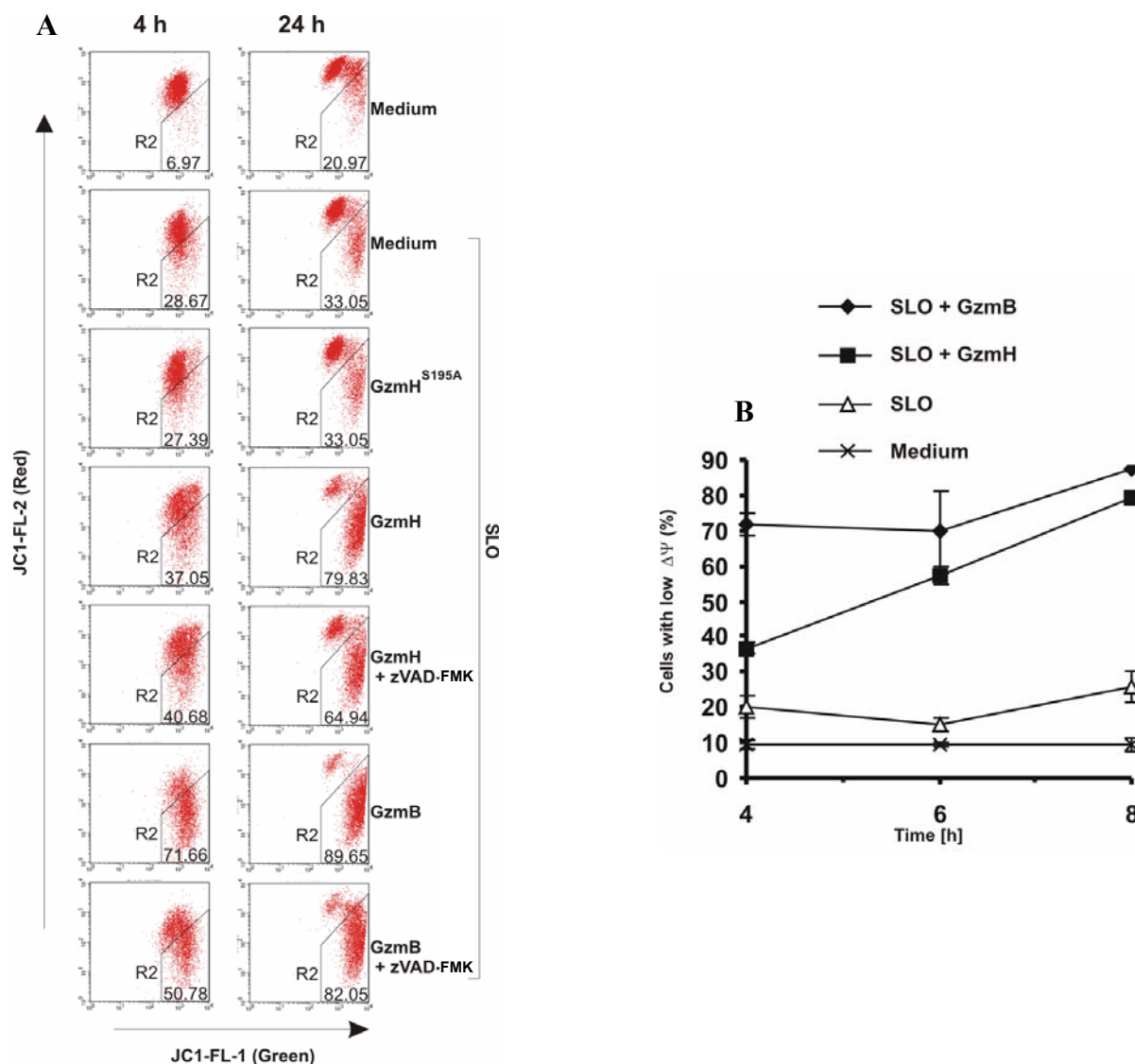


**Figure IV.27 - GzmH induces a loss of the mitochondrial membrane potential  $\Delta\Psi_m$ .** (A) K562 cells ( $1 \times 10^5$  / 50  $\mu$ l) were treated with GzmH (20  $\mu$ g/ml) or GzmB (10  $\mu$ g/ml) in the presence or absence of the zVAD-FMK inhibitor (50  $\mu$ M) for 4 or 24 hours and analysed by flow cytometry after JC-1 staining. The loss of  $\Delta\Psi_m$  is detected by a decrease of red fluorescence (FL2), and has been quantified by the percentage of cells appearing in the R2 region. (B) Accumulation of cells with loss of  $\Delta\Psi_m$  over time. The experiment shows the mean of triplicates ( $\pm$  SD) and is representative of two experiments. Depolarization in most cells was already observed at the 4 hour time point after GzmB treatment; comparable effects were visible after 8 hours in GzmH-treated cells.

### *GzmH triggers the release of mitochondrial reactive oxygen species (ROS)*

To test whether mitochondrial dysfunction, as indicated by  $\Delta\Psi_m$  loss, was associated with increased ROS formation, we stained K562 cells with the oxidation sensitive fluorogenic probe dihydroethidium (DHE, hydroethidine), which is oxidized by ROS, particularly superoxide ( $O_2^-$ ) to

products with strong red fluorescence, namely 2-hydroxyethidium or 2-OH-E<sup>+</sup> (Zhao et al., 2005). We found that GzmH, in the presence of the redox insensitive SLO<sup>C530A</sup>, induced an early, but partially transient ROS increase (indicated by region R2 in *Figure IV.28A*) which peaks at 30 minutes after SLO addition (*Figure IV.28B*). Conversely, GzmH<sup>S195A</sup> triggered a much reduced transient ROS increase (*Figure IV.28A*). Thereafter, ROS declined to slightly elevated levels but gradually increased from 4 hours onwards as cell death became more apparent.

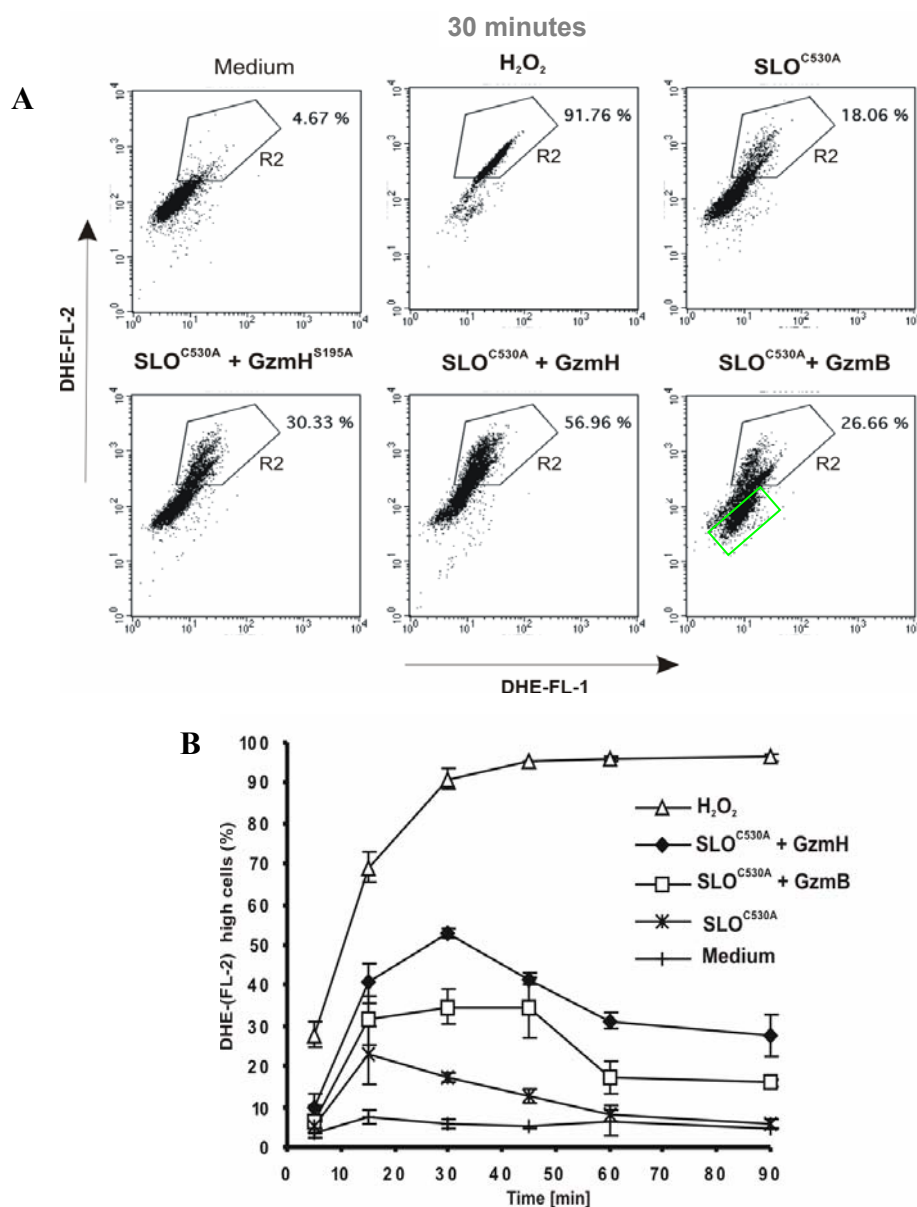


**Figure IV.28 - GzmH induces ROS formation in target cells.** (A) ROS levels measured by DHE staining in GzmH (20 µg/ml) and GzmB (10 µg/ml) treated K562 cells after 30 min and over the first 90 min. As in the previously described cell death assays, K562 cells (1 × 10<sup>5</sup> / 50µl) were treated with the indicated granzymes and sublytic SLO<sup>C530A</sup> (redox insensitive SLO) and then analysed by FACS. The dye is oxidized by ROS to the strongly red fluorescent ethidium (R2 in the dot-blots). H<sub>2</sub>O<sub>2</sub> (1%) was used as positive control. The green rectangle is explained on p 95. (B) GzmH induced a rapid, but transient ROS increase which peaked after 30 minutes. The data represent the average percentage of cells in area R2 of the raw FACS data. Shown is the mean of triplicates ±SD of one experiment representative for two experiments.

Whereas GzmH mediated ROS production, as defined by cells present in the R2 region, was demonstrated by the reaction between DHE and  $O_2^-$  (producing 2-OH- $E^+$ ), GzmB treated cells were displayed in a different fashion on the FACS dot-plot (*Figure IV.28A*). Indeed, GzmB treated cells present in R2 were reduced by more than half in comparison to those treated with GzmH. Interestingly, GzmB treatment additionally formed another distinct population of cells, this time the dye oxidizing two products with green fluorescence (see green region). Zhao and colleagues recently reported that DHE can be oxidized by oxidants other than  $O_2^-$ , such as cytochrome c which do not generate 2-OH- $E^+$  as an end-product (Benov et al., 1998; Zhao et al., 2003a). We speculate that because GzmB mediates the rapid release of cytochrome c, a product from the mitochondrial respiratory chain, this new population of cells could indeed mark cytochrome c release, an event which is absent in GzmH triggered cell death. If this is indeed the case, the cytochrome c generated population (in green) would be another proof that GzmH does not lead to the release of the 15 kDa heme protein.

#### ***IV.5.5 - GzmH expression in NK cells and release during cytotoxic attack***

Natural killer (NK) cells were shown to be the major source of GzmH in the lymphocyte population, where GzmB was interestingly found to be less abundant (Sedelies et al., 2004). Because it has been postulated that GzmH plays an important role in the innate immune response (Sedelies et al., 2004), the fact that we now show that GzmH is an alternative cytotoxic effector protease, prompted us to complement our data with evidence, that GzmH is indeed released from NK cells during effector cell attack. This fact still remains to be demonstrated in the field of granzyme biology.

##### ***GzmH is expressed at high levels in CD3<sup>-</sup>, CD56<sup>+</sup> NK cells***

The specificity of a new monoclonal antibody (R&D systems) against GzmH was first confirmed in Western blots and ELISA using all known human granzymes produced in our lab (*Figure IV.29A and B*). We next analysed the expression of GzmH in different human cell lines and purified cell populations. Unfortunately, only the YT cell line, which is reported to be a poor killer, was found to express relatively high levels of GzmH. Using two different isolation methods (positive selection by MACS beads or negative selection by Dynal beads) we confirmed the recent findings that NK cells are the major GzmH expressing human lymphocyte population (Sedelies et al., 2004). Neither monocytes, nor activated CD8-positive CTLs showed any GzmH expression. In the residual cell population, after depletion of monocytes and NK cells, a weak GzmH signal was observed (*Figure IV.30*) probably corresponding to the weak expression of GzmH in CD4<sup>+</sup> T cells reported by Sedelies and colleagues.



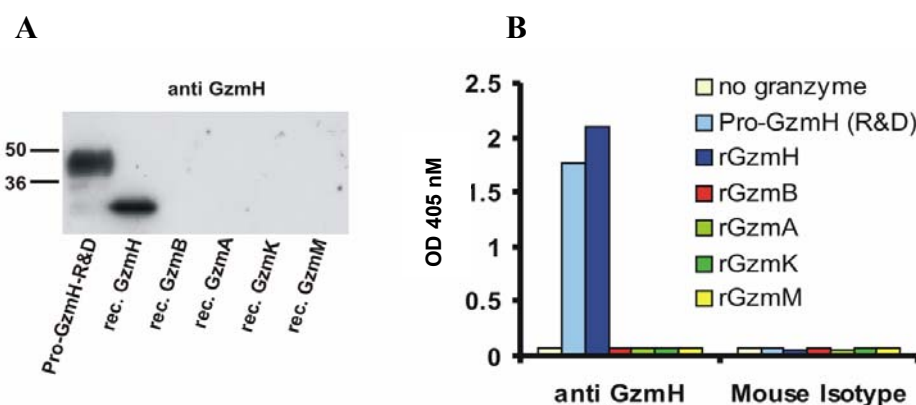


**Figure IV.29 - Specific detection of GzmH by immunoblotting and ELISA.** (A) Purified human granzymes prepared in our lab (lanes 2 to 6) along with a commercial preparation of recombinant proGzmH (lane 1) were separated by SDS PAGE and immunoblotted. Prior to transfer, all granzymes (100 ng) were analysed by SDS-PAGE. Silver staining revealed that all granzymes were indeed present in equal amounts. The mouse monoclonal antibody MAB1377 specifically recognizes proGzmH and GzmH (A, lanes 1 and 2). The N-terminally tagged ProGzmH generated in NS0 cells is glycosylated and migrates as several bands with apparent molecular masses between 38 and 42 kDa. The secreted GzmH proform, moreover, carries 20 artificial glutamate residues at the N-terminus and is, therefore, larger than the bacterially expressed recombinant granzymes. (B) The specificity of the anti-GzmH antibody was also tested against all human granzymes in a solid phase ELISA. Granzymes were coated on microtiter plates and incubated with either MAB1377 or an isotype control antibody. The means shown were calculated from duplicate measurements.

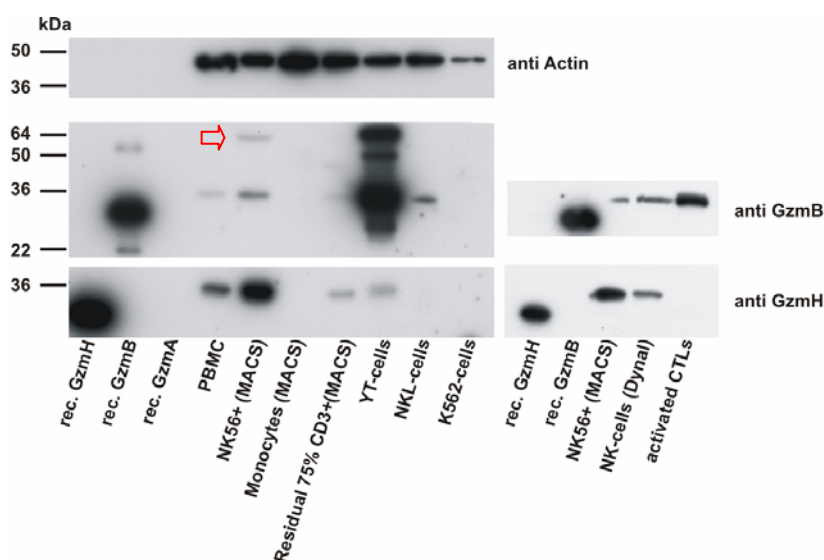


**Figure IV.30 - Specific detection of GzmH in leukocyte subsets.** Expression of GzmB and GzmH in leukocyte subsets of human peripheral blood and tumor cell lines (for the preparation of all leukocyte subsets see materials and methods) was assessed by immunoblotting after SDS-PAGE. Loading of cellular lysates was controlled by immunostaining of actin after antibody stripping (C upper panel). Purified recombinant granzymes (50 ng left panels; 20 ng right panels) and lysates of different human leukocyte populations or cell lines (10 µg) were probed against GzmB (using monoclonal antibody 2C5) or GzmH (MAB1377). GzmB blots also showed some high molecular mass bands between 60 and 70 kDa (red arrow). These bands are suggested to represent covalently linked GzmB complexes that are artificially formed between the GzmB and its serpin inhibitor, PI-9, in the lysates.

### *GzmH is released from NK during killer cell attack*

At an effector to target ratio of 2:1, NK cells freshly isolated by negative selection were capable of killing K562 cells in IL-2 containing medium free of FCS and BSA. In comparison to the necessary controls, *Figure IV.31A* shows how NK cells efficiently kill K562 after 4 hours of incubation. The raw FACS data in *Figure IV.31B* depicts in more detail how the populations of NK and K562 cells were counted. Additionally, the dot plots show that after 4 hours incubation without FCS or BSA, both unchallenged cell populations remain healthy (AV<sup>-</sup>, PI<sup>-</sup>).

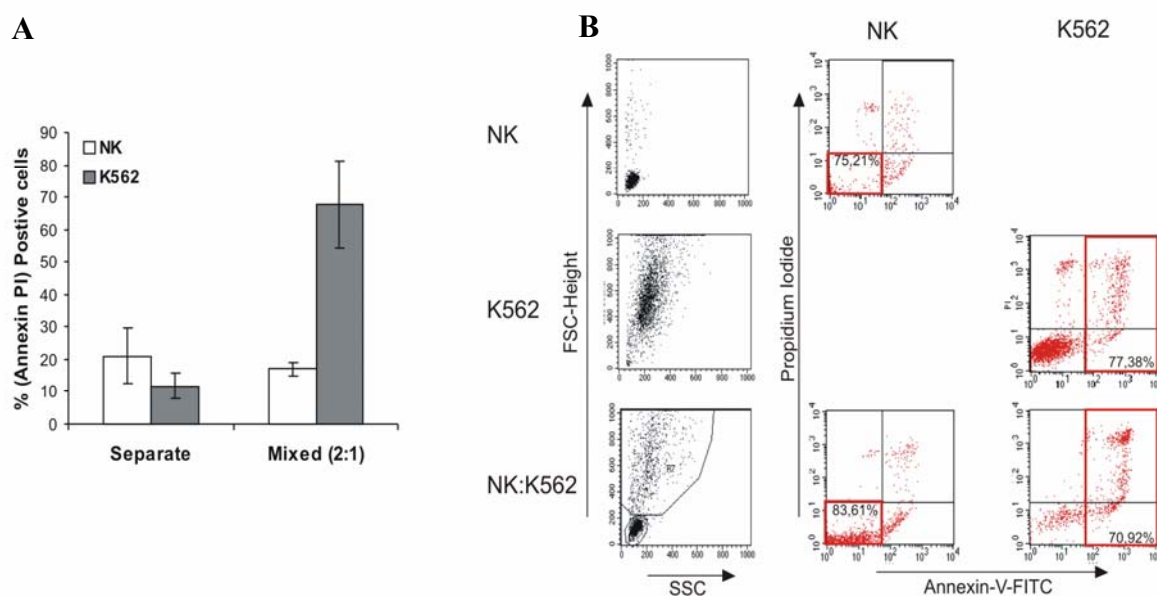


**Figure IV.31 - NK cells efficiently kill K562 cells in the absence of FCS or BSA.** (A) Freshly isolated and purified human naïve NK cells were incubated with K562 cells at a ratio of 2:1 in protein free IL-2 (100 U/ml) containing medium for 4 hours. (B) Killing of K562 cells was evaluated by flow cytometry and was found to exceed 60% in all experiments. Importantly NK cells did not die in response to activation by IL-2 and K562 cells.

The culture supernatant of effector and target cells were concentrated and immunoblotted after SDS-PAGE (*Figure IV.32*). Specific GzmH signals were only found in co-incubations of NK and K562 cells (*Figure IV.32*, lanes 5, 7 and 9). Recombinant GzmH (*Figure IV.32*, lane 9) was added to the concentrated culture supernatant to ensure that the native GzmH was running at the correct position as expected (*Figure IV.32*, lanes 2 and 3). Treatment with hyaluronidase which removes glycosaminoglycans from potential SDS stable complexes (Metkar et al., 2002; Raja et al., 2002), did not increase the recovery of soluble, extracellular GzmH (refer to lanes 3, 4 and 7, *Figure IV.32*). In addition to the band of native glycosylated GzmH running as high as GzmH in the NK cell lysates, other higher molecular weight bands were observed. Since NK and K562 lysates alone did not yield such signals on the blots, covalently linked and partially degraded complexes between a cytosolic serpin and GzmH may have formed in K562 cells during killer cell attack (*Figure IV.32*, lane 5, 7 and 9, see red arrows).

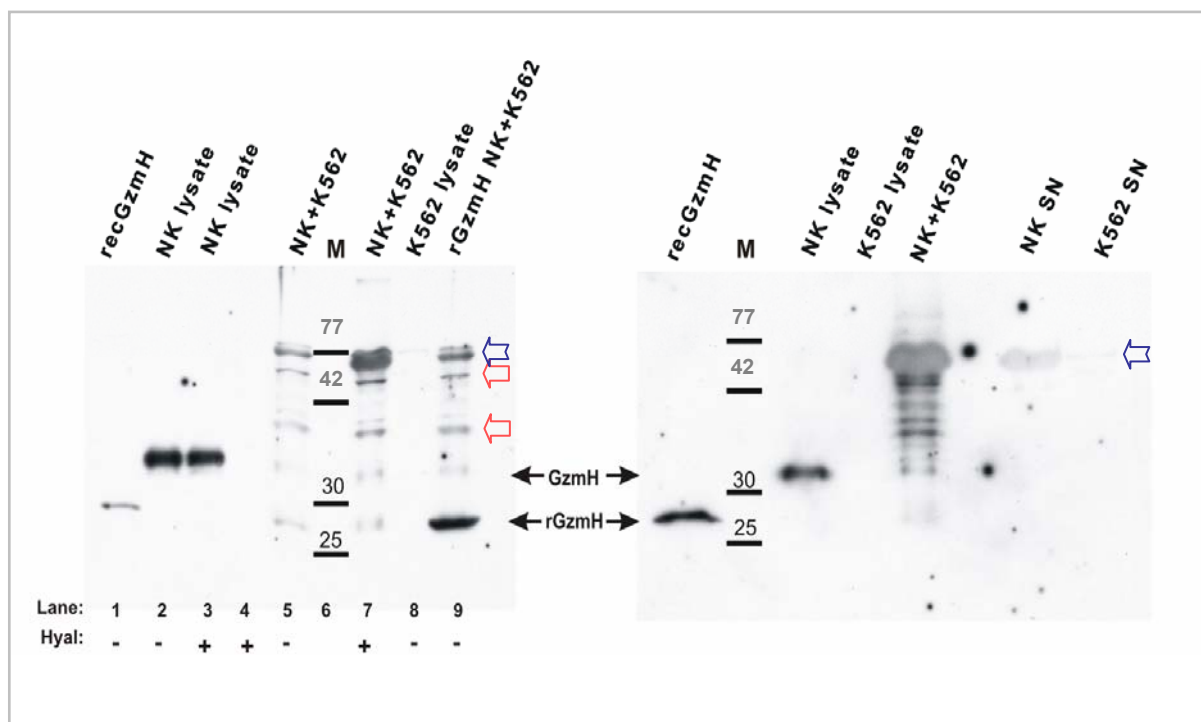


**Figure IV.32 - Release of GzmH from NK cells during cytotoxic attack.** Concentrated supernatants from NK ( $8 \times 10^6$  / 8ml) and target ( $4 \times 10^6$  / 8ml) cell mixtures (see materials and methods p 55) were analysed by SDS PAGE and immunoblotting using a monoclonal antibody against GzmH and compared to those from NK cell and K562 lysates (5  $\mu$ g total protein). To confirm the migration behavior of GzmH, recombinant GzmH (rGzmH, 5 ng) was added to the concentrated supernatant. Recombinant GzmH ran at the expected position (right lane). GzmH immunoreactivity was only found in supernatants of NK cells mixed with K562 cells, but not in supernatants of NK or K562 cells alone. Staining of high molecular weight bands may represent covalently linked complexes between GzmH and as yet undefined serpins which appeared to be partially degraded (red arrows). Despite the lack of FCS or BSA used during NK cell attack of K562 cells, it is possible that during the purification of NK cells and the culturing of the K562 cell line, albumin (65 kDa) could have stuck to the surface of both cell types (refer to blue arrow). Alternatively, albumin could have been endocytosed by the cells. Hyaluronidase was added to supernatants in an attempt to release GzmH from proteoglycans.

---

## ***V - Discussion***

Among the mechanisms used by cytotoxic T lymphocytes (CTLs) and natural killer (NK) cells to destroy their targets, the granule exocytosis pathway is by far the most critical in the host's defence against intracellular pathogens and transformed tumor cells. Once released, these granules eliminate rogue cells by unleashing their content which, through the aid of perforin (PFN), achieves entry into the target cell cytosol. Granzymes differ from one another through their unique proteolytic specificities. Although GzmA and GzmB have been reported to be potent inducers of cell-death (Barry and Bleackley, 2002; Lieberman and Fan, 2003), whether this stands true for the so-called "orphan granzymes" is still not known (Grossman et al., 2003). So too does the answer to the question of whether granzymes use additional mechanisms against pathogens that hijack the cellular apoptosis machinery, thus avoiding or resisting immune attack. In this work, we have shown that granzyme H (GzmH), known previously as an orphan granzyme, is a novel cytotoxic protease which induces an alternative, caspase independent cell death pathway. Dying cells showed typical hallmarks of programmed cell death such as mitochondrial depolarization, reactive oxygen species (ROS) generation, DNA degradation, and chromatin condensation. Moreover, in collaboration with Felipe Andrade from the Department of Medicine, at the John Hopkins hospital in Baltimore, we demonstrated that GzmH is an antiviral protease which directly and efficiently cleaves vital viral proteins. The first biological substrates for the enzyme will, in this discussion, be briefly addressed in more detail.

### ***V.1 - Recombinant granzyme production***

#### ***Eukaryotic and prokaryotic host systems***

Granzyme isolation was first reported in the late eighties. At the time, granzymes were purified from cultures of cytotoxic lymphocytes in small quantities which hindered the comprehensive studies of their biological functions. Indeed, these preparations, although extremely pure, were burdened by contamination with enzymes with different specificities, namely the other members of the granzyme family (Smyth et al., 1993; Woodard et al., 1998). Additionally, the inability to assess the effects of site-specific mutations using this method prevented progression. Only in the last decade has it become possible to express and purify granzymes from recombinant sources. As a result, the study of granzyme function, both biochemical and biological, was greatly facilitated by the ability to work with uncontaminated preparations of both active and inactive granzymes. Indeed, independent studies by Smyth, Pham and Xia led to the first reports of the expression of recombinant, active GzmB in

mammalian, yeast and baculovirus-infected insect cells, respectively (Pham et al., 1997; Smyth et al., 1995; Xia et al., 1998). Around this time, proGzmA was being purified from the bacterial periplasmic space of *Escherichia coli* (*E. coli*) and, thereafter, activated with enterokinase in work by Lieberman and colleagues (Beresford et al., 1997). In 1999, work from our laboratory by Wilharm *et al.* showed the generation of catalytically active GzmK from *E. coli* inclusion bodies (IB) (Wilharm et al., 1999). IB preparations, which differ from the above preparations that produce active granzymes by secretion and transport of precursor forms carrying signal sequences, were here chosen as a starting material for *in vitro* folding. Refolded precursor molecules of IB material were then converted to their active form, following treatment by cathepsin C.

In the late nineties, Trapani and colleagues first demonstrated the production of the active GzmH in the supernatant of baculovirus-infected Sf21 insect cells, but were unsuccessful in expressing soluble GzmH in yeast or bacterial expression systems (Edwards et al., 1999). Nevertheless, with this recombinant insect cell based method, Edwards *et al.* were able to report the esterolytic activity of glycosylated recombinant active GzmH by showing cleavage of the thiobenzyl ester Suc-Phe-Leu-Phe-SBzl, thereby suggesting, for the first time, that GzmH had chymotrypsin-like (chymase) esterase activity.

#### ***What are the advantages of refolding from E.coli inclusion body material?***

Our laboratory focused on *E. coli* as an expression host for the expression and purification of human granzymes, three of which had already been produced and studied, namely GzmA, GzmB and GzmK (Hink-Schauer et al., 2003; Kurschus et al., 2004; Wilharm et al., 1999). *E. coli* is one of the most frequently used prokaryotic expression systems (Hannig and Makrides, 1998) and, despite the complexities encountered upon refolding of the desired protein outside the host, once the optimal conditions are found, the cytosolic formation of IB expression is largely beneficial. Indeed, the formation of IB is favourable for the host as they protect the bacteria from the harmful effects of biologically active recombinant proteases, while at the same time sheltering the protein of interest from degradation by cytosolic host proteases. These advantages, however, are not present during the periplasmic expression of recombinant proteases in *E. coli*. Here, not only may the active granzyme be destructive for the bacterial host but once in the periplasmic space the recombinant granzyme, itself, would be exposed to bacterial proteases and, thus, to a potentially harmful environment. In additional support of inclusion bodies as the method of choice, is the fact that high levels of pure, active, homogeneous recombinant proteins can be obtained and purified at concentrations well inside the milligram per millilitre range. Such quantities are sufficient to attempt formal structural analysis of granzymes by crystallography, although the sample must be extremely pure and void of aggregates.

Thus, to obtain milligram amounts of highly active and pure GzmH for functional tests and possible crystallization trials, we expressed the human GzmH with a cathepsin C cleavable pro-sequence in *E. coli* and developed an optimized refolding and purification protocol by modifying previously established procedures for GzmA, GzmB and GzmK. Compared with preparations of GzmH produced by baculovirus-infected cells in Trapani's lab, our bacterially expressed GzmH was not modified by heterologous and heterogeneous carbohydrates or a His-tag at the C-terminus which may alter the enzyme's interactions with the target cell surface and, furthermore, its internalization.

## ***V.2 - Cytosolic delivery of granzymes by pore-forming proteins***

### ***Human perforin versus bacterial streptolysin O***

To avoid any interference by other granzymes, the cell death inducing properties of GzmH were demonstrated in an effector cell-independent system using purified human perforin (PFN), but principally bacterial streptolysin O (SLO), as a translocator, with recombinant GzmH and GzmB as the effector proteases. SLO and PFN monomers assemble on target-cell membranes into multimeric complexes and enable granzymes to cross the cellular membrane (Tschopp et al., 1986; Walev et al., 2001). Whether PFN oligomerises on plasma membranes or on membranes of internalized endosomes of nucleated cells to allow granzyme entry is not yet clear (see introduction on perforin). SLO, however, is reported to act on the plasma membrane and is known to trigger a plasma membrane repair response which, as in the case of PFN, is characterized by the exocytosis and fusion of lysosomes with the plasma membrane (Keefe et al., 2005; Rodriguez et al., 1997; Walev et al., 2001). The decision to use SLO as the main translocator was taken not only because of the protein's stability in cell death assays but also because of its affordability and availability. Perforin, on the other hand, although the natural delivery agent of CTL and NK cells, is expensive, while its purity and activity are uncertain.

### ***SLO is an appropriate substitute for perforin***

Our cellular model system allowed SLO delivered GzmB to induce apoptosis efficiently, in a highly reproducible manner identical to that observed in studies using purified human perforin (Fellows et al., 2007; Martinvalet et al., 2005; Pinkoski et al., 1998). The delivered recombinant GzmB led to the observation of typical apoptotic hallmarks such as rapid fragmentation of target cell DNA, caspase activation and phosphatidyl serine externalization. Hence, our results obtained with SLO and both GzmB and GzmH can be regarded as a homologous experimental approach to deliver both proteases from the extracellular space into the cytosol.

In collaboration with Christopher Froehlich from the Evanston Northwestern Research Institute, we managed to obtain enough pure, highly active perforin to perform a crucial number of basic apoptosis assays. As expected, in the presence of sublytic concentrations of PFN, GzmH induced cell death in a comparable fashion to that analyzed in combination with SLO (refer to *Figures IV.13*). Indeed, after 10 hours of exposure to GzmH concentrations of 25 µg/ml (about 1 nM) and sublytic SLO, target cells underwent biological and morphological changes indicative of nuclear damage and both plasma and mitochondrial membrane perturbation. Importantly, these effects were triggered neither by GzmH<sup>S195A</sup> nor the neighbouring chromosome 14 chymotrypsin-like proteases cathepsin G or chymase. No additional effect by GzmH was observed in the absence of translocators, implying that GzmH-induced cell death required the limited proteolysis of intracellular substrates that are accessible only after membrane translocation (refer to *Figure IV.13*).

### ***V.3 – Cell death induction by GzmH***

Our work on GzmH was continuously controlled with GzmB. GzmB has received unparalleled attention in the granzyme field due to its ability to trigger fast and efficient cell death. Indeed, the aspartase is particular in its ability to directly and indirectly activate caspase mediated apoptosis but also death pathways independent of caspase activation (Barry et al., 2000; Barry and Bleackley, 2002; Heibein et al., 1999; Metkar et al., 2003; Sutton et al., 1997). In this work, GzmH was found to efficiently induce cell death of a range of target cells in a novel, caspase independent manner. Indeed, as opposed to GzmB, GzmH induced cell death did not require the cleavage of Bid, the release of cytochrome c or the degradation of ICAD, but depended on common events such as mitochondrial depolarization, ROS generation, chromatin condensation and DNA degradation.

#### ***GzmH treated cells are morphologically different from those exposed to GzmB***

The first evidence that cells treated with GzmH were undergoing a different, caspase independent type of cell death came from microscopical observations. Indeed, GzmH induced cell death displayed unique morphological characteristics that were not previously observed in target cells treated with GzmB. GzmB cytotoxicity was characterized by cellular transparency, shrinkage, fragmentation and apoptotic body formation. Additionally, membrane irregularities were observed, along with nuclear fragmentation and condensed chromatin, all typical hallmarks of apoptosis and arguably caspase activation.

Interestingly, apoptotic body formation was more visible in experiments in which cells had been exposed to medium containing fetal calf serum (FCS), indicating that apoptotic events are indeed ATP

dependent. However, because FCS contains potent serine protease inhibitors, such as  $\alpha_1$ -antitrypsin and  $\alpha_1$ -antichymotrypsin, all of our assays were performed in FCS free RPMI medium supplemented with BSA. BSA was not found to interfere with the activity of our granzymes. Of additional interest is the finding that GzmB suffered minimal activity loss in the presence of serum levels of  $\alpha_1$ -antitrypsin, a requirement necessary for the success of GzmB based immunoconjugates (Kurschus et al., 2004).

Conversely, target cells treated with GzmH displayed unique morphological features. After 1 hour of incubation, when maximum apoptotic nuclei were already visible for GzmB, cells exposed to GzmH still possessed normal nuclei only acquiring certain morphological similarities after approximately 4 hours. These similarities included cellular transparency, membrane irregularities and the apparition of fragmented nuclei with condensed chromatin. After 12 hours, most cells displayed apoptotic nuclei, fitting well to the delayed killing capacity of GzmH. Importantly, cellular swelling was a unique characteristic of GzmH treated cells, which, in contrast to GzmB treated cells, were not subject to shrinkage, fragmentation and apoptotic body formation.

In this study, cellular changes were additionally analyzed by immunofluorescence. The Hoechst dye 22242 and annexin V-FITC were used to visualize both nuclear fragmentation and phosphatidyl serine (PS) externalization, respectively. After 12 hours, both proteases caused considerable nuclear fragmentation in nearly all cells. GzmH treatment, however, lead to the formation of considerably smaller bodies, suggesting that the cell death pathway triggered by GzmH involves the direct or indirect cleavage of substrates distinct from those cleaved by GzmB (refer to *Figure IV.16*). PS externalization is a hallmark of apoptosis and is otherwise known as an “eat me” signal for macrophages, which possess specific receptors towards the phospholipid. PS externalization was much less obvious on the plasma membranes of cells exposed to GzmH after 10-12 hours, an event that has been repeatedly reported to be a consequence of executioner caspase activation such as caspase 3 (Diaz et al., 1999; Martin et al., 1996; Naito et al., 1997). More recently, however, a number of studies have demonstrated that PS externalization can be regulated independently of caspases, and may in fact result from oxidative stress, such as the formation of reactive oxygen species (ROS). Indeed, work by Kagan and colleagues has demonstrated that the prevention of PS oxidation by the use of antioxidants inhibits PS externalization (Kagan et al., 2002; Tyurina et al., 2004). Interestingly, although GzmH did not activate executioner caspases, both GzmB and GzmH did lead to ROS generation, which could explain the difference in intensity in PS externalization observed after treatment with the two granzymes.



***GzmH induces cell death independently of caspase activation***

This work defines GzmH as a caspase independent cell-death inducing protease. The occurrence of caspase activity was mainly controlled using the general caspase inhibitor zVAD-FMK which along with zDEVD-FMK (caspase 3 inhibitor) and zLEHD-FMK (caspase 9 inhibitor), efficiently blocked GzmB induced apoptosis. Although the major caspase inhibitors did not halt the progression of GzmH triggered cell death (refer to *Figure IV.26*), an approximate 10% reduction was often observed, 10 to 12 hours after exposure to GzmH. Propidium iodide (PI) and annexin V-FITC (AV) staining was used to differentiate between apoptotic cells (PI<sup>-</sup>/AV<sup>+</sup>) and necrotic cells (PI<sup>+</sup>/AV<sup>+</sup>). In particular, annexin V-staining, without PI uptake, indicated strong PS externalization and caspase dependence (Diaz et al., 1999; Martin et al., 1996; Naito et al., 1997). FACS analysis of both GzmH and GzmB treated cells revealed that cells exposed to GzmH were mainly PI<sup>-</sup>/AV<sup>-</sup> regardless of the length of exposure to the granzyme. Cells exposed to GzmB, however, were first clustered in an exclusively annexin-positive-only population and shifted to a PI-positive-only cluster in the well-advanced stages of cell death. In the case of GzmH induced cell death, the appearance of a minor PI<sup>+</sup>/AV<sup>+</sup> population after 10-12 hours could well be explained by the observed damage to the inner mitochondrial membrane and the release of reactive oxygen species (ROS), the latter which have been implicated in the translocation of phosphatidylserine (PS) (refer to *Figure IV.12*). However, in the presence of zVAD-FMK, an overall reduction of 10% in GzmH triggered cell death was observed, the reduction being primarily noticed in the PI<sup>-</sup>/AV<sup>+</sup> cluster. A similar reduction was also found in cultured cells that were treated with SLO alone, zVAD-FMK most likely mitigating the unspecific sublytic effects of SLO rather than the genuine downstream effects of GzmH (refer to *Figure IV.26* – red headed arrow). Nevertheless, to completely exclude the involvement of caspases, the activation of caspase 2 was investigated which has recently been reported to trigger cell death.

***Is caspase 2 activity a prerequisite for GzmH mediated cell death?***

The activation of caspase 2 has recently been shown to induce an alternative cell-death pathway in response to cytotoxic stress such as DNA damage. Additionally, caspase 2 is also thought to be implicated in mitochondrial permeabilization and possible ROS generation leading to the amplification of caspase activity (Lassus et al., 2002; Zhivotovsky and Orrenius, 2005). In these studies, caspase 2 activity was investigated using the fluorogenic, cell permeable caspase 2 specific substrate acVDVAD-AFC. Although, the major executioner and initiator caspases had previously been tested, caspase 2 activity was nevertheless observed following GzmH delivery, although at a much more reduced level than that triggered by GzmB (refer to *Figures IV.22 and 24iii*).

The preparation of S100 (cytosolic) and nuclear fractions from untreated K562 cells allowed us to address whether caspase 2 was being directly cleaved by GzmH. Whereas the exposure of both

cytosolic and nuclear fractions to GzmB resulted in the cleavage of acVDVAD-AFC, GzmH exposure did not yield any activity indicating that GzmH can not cleave procaspase 2 directly or in a protease mediated indirect manner (*Figure IV.24B*). To ensure that the VDVAD sequence was truly monitoring the activity of caspase 2 and no other caspase, immunoprecipitation (IP) of caspase 2 (*Figure IV.24C*), and both caspases 2 and 3 (*Figure IV.24D*) from S100 fractions of untreated K562 cells was performed. The S100 lysate-containing acVDVAD-AFC was then exposed to GzmB which can directly activate caspase-3. In cell lysates depleted of caspase 2, substrate cleavage was subsequently reduced by more than two thirds, whereas acVDVAD-AFC cleavage in lysates lacking both caspase 2 and 3 was completely abolished. These results suggested that caspase 3 is the only other protease with a strong preference for acVDVAD-AFC cleavage in K562 cells. Because caspase 3 is not activated in GzmH triggered cell death (refer to *Figures IV.22 and 24*), acVDVAD-AFC can, indeed, be efficiently used in our system to test caspase-2 activity.

To investigate whether caspase 2 activity was at all necessary for GzmH induced cell death, the caspase 2 specific inhibitor zVDVAD-FMK was preincubated with cells prior to GzmH treatment. In line with our overall findings, GzmH cell death was not suppressed by zVDVAD-FMK. ZVDVAD-FMK, however, only weakly inhibited GzmB triggered apoptosis suggesting that the activity of caspase 2 is not essential for the progression of cell death (refer to *Figure IV.25*). As a final note, one could speculate that because caspase 2 activation is reported to lead to mitochondrial damage, and possibly the generation of ROS (Lassus et al., 2002), the indirect activation of caspase 2, observed in GzmH mediated cell death, may indeed also contribute towards the externalization of PS and hence the population of annexin V single positive cells noticeable from the FACS data (refer to *Figure IV.12*).

### ***Is lysosomal rupture and cathepsin release a hallmark of GzmH induced cell death?***

This work demonstrates that GzmH mediated cell death is mediated by several key events, namely, mitochondrial depolarization, ROS generation, chromatin condensation and DNA degradation. In particular, mitochondrial damage and the release of ROS have recently received much attention. Indeed, as it has just been discussed, it has been suggested that ROS play an essential role in lymphocyte cytotoxicity (Martinvalet et al., 2005; Zhao et al., 2007a). Additionally, it has recently been suggested that the release of ROS contributes towards the oxidation of PS and its externalization (Kagan et al., 2002; Tyurina et al., 2004). Lysosomal destabilization and disruption is thought to be yet another early consequence of oxidative stress. Whether ROS are the cause of lysosomal rupture or arise as a consequence of lysosomal breakage and act as an amplifying loop causing further lysosomal breach remains unknown (Brunk et al., 2001; Zhao et al., 2003b). This work widely uses the pan-caspase inhibitor zVAD-FMK to control the involvement of caspase involvement. Interestingly,

various caspase specific inhibitors, such as zVAD-FMK and zDEVD-FMK, have been reported to potently inhibit cathepsins (Rozman-Pungercar et al., 2003), namely lysosomal cysteine proteases that have been implicated in the activation of apoptosis (Stoka et al., 2001; Turk et al., 2000). Various cathepsin family members have been reported to be involved in both caspase dependent and independent cell death (Michallet et al., 2003; Stoka et al., 2001). The slight inhibition (approximately 10%) conferred upon GzmH mediated cell death by zVAD-FMK prompted us to investigate the possibility that cathepsin activity might account for this discrepancy and might also, in fact, play a role in GzmH induced cell death. The general cathepsin inhibitor E64d, however, did not provide any protection to cells exposed to GzmH or GzmB. GzmH mediated cell death, thus, seems to be mediated independently of lysosomal rupture and cathepsin activity (refer to *Figure IV.26*), although it must be stated that we did not test the effect of E64d on recombinant cathepsins as a positive control.

### ***Is ROS release essential or an epiphenomenon for GzmH induced cell death?***

As observed in GzmB cytotoxicity, GzmH triggered cell death was marked by a prompt increase of intracellular ROS levels and gradual mitochondrial depolarization. Contrary to GzmB, GzmH did not cleave Bid, both *in vitro* (human recombinant Bid) and *in vivo* (western blot analysis), nor did the granzyme lead to the release of cytochrome c, the smallest of the mitochondrial intermembrane space proteins (MIMPs). Recent work by Martinvalet and colleagues highlighted the importance of ROS by demonstrating that both GzmB and GzmA can directly trigger the release of ROS and the loss of  $\Delta\Psi_m$  when exposed to isolated mitochondria. We therefore set out to investigate whether the direct addition of GzmH or GzmB to freshly isolated and energized mitochondria from mouse liver would induce potential loss ( $\Delta\Psi_m$ ). Although the toxin valinomycin/oligomycin easily induced  $\Delta\Psi_m$  loss, as seen by the instant decrease of rhodamin 123 fluorescence, the direct addition of GzmH, or our control granzyme, GzmB, to the mitochondria did not induce any potential loss at all (data to be reported elsewhere). Mitochondrial membrane specific substrates for GzmH, such as components of the permeability transition pore that, once cleaved, may lead to ROS generation and  $\Delta\Psi_m$  loss, have therefore not been identified in these experiments.

GzmH triggered ROS release initially surged within 30 min of exposure to the protease, an accumulation more intense than that seen in cells exposed to GzmB (refer to *Figure IV.28*). However, at later time points, GzmH mediated a surge in ROS accumulation that was slower than in GzmB-treated cells but occurred with kinetics similar to the mitochondrial membrane depolarization observed in target cells. In order to completely exclude caspase involvement during GzmH induced ROS formation, the general caspase inhibitor zVAD-FMK was used. As expected, no effect on ROS induction was observed.

To further evaluate the causative role of ROS in cell-death induction, we preincubated several antioxidants, including Tiron, D1417 and MnTBAP [Mn(III)tetrakis(4-benzoic acid) porphyrin chloride], a cell-permeable superoxide dismutase (SOD) mimetic, with target cells, before exposing them to recombinant GzmH and GzmB. In the presence of antioxidants, the target cells survived the usual menace presented by both granzymes. It is, however, possible that the above antioxidants may, in fact, be interfering with the delivery of GzmH and GzmB, the survival of the target cells therefore not being due to the antioxidative effect of the applied compounds (data to be reported elsewhere).

At first glance, our observations are in line with studies by the groups of Lieberman and Fan. Recent work by Martinvalet et al. allegedly demonstrated that GzmA induced cell-death requires the generation of ROS to eradicate diseased cells, although GzmA has previously been shown to directly cleave a number of proapoptotic substrates. Even though the authors suggest that ROS production is required for nuclear localization of the SET complex, which harbours components that mediate GzmA induced DNA degradation, the suggestion that ROS inhibition by antioxidants should then alleviate the effects of GzmA treatment should be treated with utmost caution. Recently, Zhao *et al.* again confirmed the critical role attributed to ROS in caspase independent cell-death. Indeed, the group showed that GzmK is also able to provoke rapid ROS generation and that the blockade of ROS, by preincubating target cells with N-acetyl cysteine (NAC) or Tiron, abolishes GzmK induced cell death (Zhao et al., 2007a). Mark Williams and Pierre Henkart discussed the necessity of ROS generation in lymphocyte cytotoxicity in a comment to ‘Immunity’ entitled “Do cytotoxic lymphocytes kill via ROS” (Williams and Henkart, 2005). In line with our ongoing experiments, we suspect that these antioxidants, some of which were applied at concentrations as high as 40 mM, might actually perturb PFN and SLO oligomerisation and, hence, reduce the entry of granzymes into the target cell cytosol.

#### ***Does GzmH trigger a different kind of DNA degradation?***

DNA damage is a key feature of programmed cell-death. GzmA and GzmK, along with murine GzmC, have been reported to cause DNA nicks (Johnson et al., 2003; Shi et al., 1992), whereas GzmB and GzmM appear to inflict double stranded DNA fragmentation upon target cells (Lu et al., 2006; Trapani and Sutton, 2003). GzmH-mediated DNA degradation is at present relatively undefined, but occurs independently of caspase activation. Indeed, executioner caspase activity was not found *in vitro* or in target cells treated with GzmH. In this work, DNA fragmentation was investigated using GzmB as a control. GzmH did not, however, cleave ICAD in target cells, which unleashes the caspase activated DNase CAD, nor did the granzyme trigger DNA laddering at various time-points leading up to 12 hours (refer to *Figure IV.20*). This outcome is reminiscent of GzmA and GzmK cytotoxicity, both proteases solely causing single-stranded DNA nicks.

GzmH DNA damage was analyzed by monitoring the DNA content of cells as they progress through the G1, S, and G2 phases of the cell cycle. In this method, cells undergoing cell-death lose a large portion of their DNA and, when analyzed by FACS, are clearly distinguishable as a separate population, termed sub-G1. The method uses PI for nuclear staining. Interestingly, after 12 hours of incubation, target cells treated with either GzmH or GzmB displayed sub-G1 populations that differed in appearance. Cells that had been exposed to GzmH retained noticeably less DNA than those that had been treated with GzmB, displaying a weaker hypodiploid (sub-G<sub>1</sub>) peak in height, but still easily discriminative from the narrow peaks of cells with normal (diploid) DNA content. Nevertheless, both GzmH and GzmB populations accounted for roughly 35% of the total cell population analyzed at 12 hours (refer to *Figure IV.18A*). GzmH-mediated cell death is suggestive of a different DNA degrading mechanism to that triggered by GzmB and, hence, the targeting of different DNA-degrading substrates. One could interpret these results by suggesting that the oligonucleosomal double-stranded DNA fragments, mediated by GzmB and produced for example by CAD, do not as readily exit target cells following treatment in PBS buffer containing low detergent concentrations. GzmH does not lead to GzmB-like DNA double-stranded fragmentation, the sub-G1 data hinting possibly towards nuclear disintegration and DNA loss due to loss of membrane integrity (refer to GzmH triggered cell death analyzed by trypan blue staining, *Figure IV.15*).

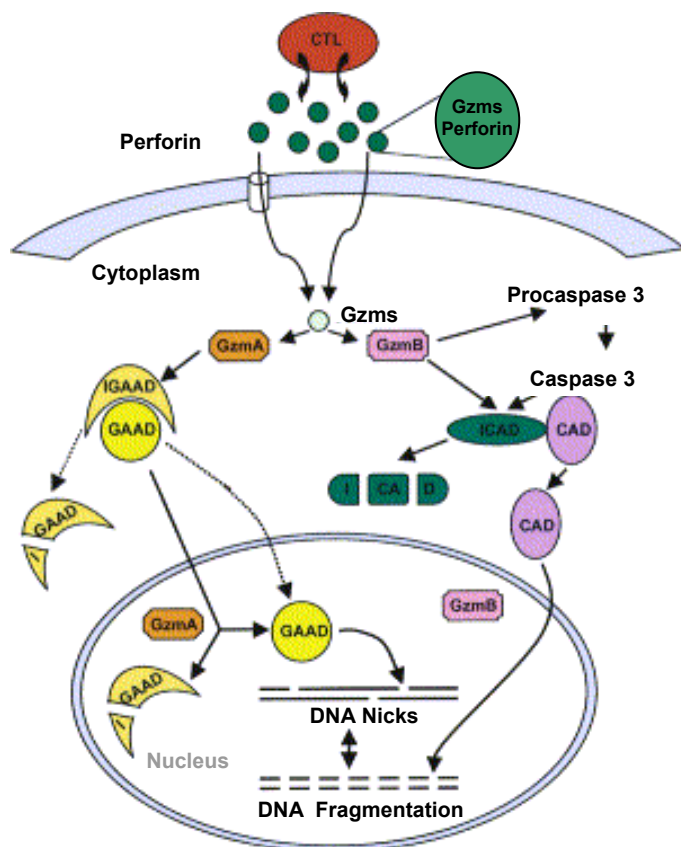


**Figure V.1 – Model for DNA damage during CTL-Mediated cell-death.** Model for DNA Damage during CTL-mediated apoptosis, CTL granules containing perforin and granzymes are released into the synapse formed with the target cell. Gzms enter the target cell cytoplasm either via perforin-induced perturbation of the plasma membrane or through endocytosis. GzmA cleaves IGAAD (SET) which then no longer binds and inhibits GAAD (NM23-H1). It is not known whether SET is cleaved in the cytoplasm or nucleus or both. Uninhibited GAAD in the nucleus makes single-stranded DNA nicks. GzmB, directly or indirectly via caspases destroys the CAD (caspase activated DNase) inhibitor ICAD. Cleaved ICAD no longer binds CAD, which then moves to the nucleus to cause double-stranded breaks. Figure taken from Fan et al. 'Cell' 2003 (Fan et al., 2003).

Following granzyme treatment, DNA degradation was also addressed by estimating the release of DNA fragments labelled with  $^3\text{H}$ -thymidine (refer to *Figure IV.20*). This technique, along with the method above, uses mild detergent concentrations to liberate  $^3\text{H}$ -thymidine-labelled DNA fragments from target cells. As expected, GzmB-induced fragmentation was observed at near maximum levels following analysis at the first time point of 4 hours. GzmH treated cells, however, triggered a much reduced  $^3\text{H}$ -thymidine release, reaching significant levels only after 12 hours, a time point, however, which runs in line with maximum cell-death achieved by the protease (refer to *Figure IV.11*). In the previous paragraph, it was suggested that GzmH triggered nuclear disintegration and that DNA loss might account for the reduced DNA content of the GzmH sub-G1 population. The Sub-G1 data collected at both 12 and 24 hours show that both GzmH and GzmB have near identical percentages of cells in the Sub-G1 population. However, GzmH-mediated  $^3\text{H}$ -thymidine release at the 12-hour time point was considerably lower than that induced by GzmB. Because cells treated with GzmH reached the maximum percentage of cell-death at the 10-12 hours mark, if GzmH-mediated cell death does lead to nuclear disintegration and DNA loss, one would expect the percentage of  $^3\text{H}$ -thymidine release to be more prominent (refer to *Figure IV.20*).

DNA degradation is a well known hallmark of programmed cell death (PCD) and the underlying mechanisms that govern the GzmH-triggered cell death pathway need to be studied in greater detail. Indeed, whether GzmH treatment mediates single-stranded DNA nicking similar to that caused by GzmA (Beresford et al., 1999; Fan et al., 2003) remains to be studied. However, one cannot exclude the possibility that GzmH cytotoxicity may, in fact, not lead to DNA damage by the direct or indirect activation of DNA degradation enzymes. Indeed, at the 10-12 hour mark, the observed damage inflicted upon the DNA of GzmH-treated cells might be the result of secondary necrosis that occurs *in vitro* as a result of cells not being cleared by macrophages. Secondary necrosis is defined by presence of nuclear condensation and/or fragmentation along with the loss of membrane integrity and, consequently, PI uptake (Kelly et al., 2003). It is interesting to note that, although GzmH triggered cell death lacks typical apoptotic hallmarks such as caspase activation, GzmH cytotoxicity does lead to caspase independent PS externalization. Whether or not GzmH-induced cell death should be defined as “apoptotic-like” in the absence of caspases, or rather “necrotic-like” because of its morphological features will be discussed in the following chapter.

### ***GzmH cytotoxicity: an apoptotic or necrotic-like form of cell death?***

Morphologically, necrosis is distinctly different from apoptosis. For a long time, necrosis was considered as an alternative to PCD. Cells rapidly swell followed by plasma membrane collapse and cell lysis. During apoptosis or PCD, however, a classical example being the actions of GzmB, cells first shrink and their nuclei condense. Target cells then further disintegrate into well-enclosed smaller

apoptotic bodies. The biochemical hallmarks of apoptosis such as activation of pro-caspases and oligonucleosomal DNA fragmentation are usually absent in necrosis. However, recent improvements in the techniques used to distinguish between these two forms of cell-death have revealed that some biochemical and morphological characteristics of both modes can be detected in the same cell. This indicates that there may be a spectrum of suicidal programs in cells, and that “classical” necrosis, defined by the rapid efflux of cell constituents, and apoptosis, defined by the rapid, ATP-dependent elimination of target cells without disruption of the plasma membrane, are the extremes of this spectrum. Necrosis, then, may not simply be the result of extreme conditions but, in context, may be a normal, physiological and regulated (programmed) event. Indeed, various stimuli (e.g. cytokines, heat, irradiation and pathogens) can cause both apoptosis and necrosis-like symptoms in the same cell population. Furthermore, signalling pathways such as death receptors, kinase cascades and mitochondria have been found to participate in both processes, and by modulating these pathways, it is possible to switch between apoptosis and necrosis (Proskuryakov et al., 2005). The consequences of “classical” necrotic and apoptotic cell-death are well distinct from one another, necrosis provoking an inflammatory response because of spillage of cellular constituents, while apoptosis attracts the attention of macrophages which safely engulf the cellular content concealed within apoptotic bodies. The inflammatory response caused by necrosis may, however, have obvious adaptive significance under some pathological conditions such as cancer and infection. On the other hand, disturbance of the fine balance between the two types of cell-death may be a key element in the development of some diseases.

In contrast to GzmB cytotoxicity, GzmH does not induce typical apoptotic hallmarks and, consequently, does not display the typical apoptotic morphology mentioned above. Similarly to GzmB cytotoxicity, GzmH-triggered cell-death leads to PS externalization and probably other lipid-based “eat-me” signals, deemed important for the removal of intact diseased cells by macrophages (Lauber et al., 2003; Lauber et al., 2004). Annexin V- FITC labels PS sites on target-cell membranes. Although PS externalization is thought to be mainly the result of executioner caspase activation, our study showed that, despite the lack of caspase activation, GzmH does trigger PS externalization, mitochondrial dysfunction and the release of ROS being the likely stimuli (Kagan et al., 2002; Tyurina et al., 2004). Indeed, ROS generation peaked after 30 minutes of GzmH treatment, an event which could trigger the externalization of various essential phospholipids involved in macrophage-mediated clearance (Lauber et al., 2003). However, despite 15-20% of GzmH treated cells appearing annexin V-FITC positive at the 4 hours time point, in an independent experiment, and at the same time point, 30% of cells were also positive for trypan blue, indicating a loss of membrane integrity (refer to *Figure IV.15*). Morphologically, the plasma membranes of target cells at this stage appeared normal but the cells had become transparent, their nuclei clearly visible. GzmB-treated cells required only 1-2

hours to achieve maximum death and so the trypan blue and PI staining at 4 hours (45-50% and 60-80% respectively) is already indicative of secondary necrosis.

In cells exposed to GzmH prior to the 4 hour mark, mitochondria, monitored by JC-1 staining, appeared mostly intact. Thereafter, depolarization became apparent and continued to increase, reaching maximal levels, already obtained by GzmB at the 4-hour time point. Although an initial ROS surge was observed, levels quickly declined, only to increase again from the 4 hours time point when cell death became more apparent. This suggests that prior to the 4 hour mark putative ATP-dependent processes of GzmH cytotoxicity would most likely not be impaired. Morphologically, GzmH induced cell death became increasingly apparent from 4 hours onwards and, at 10-12 hours, cells appeared rather swollen with membrane irregularities, again indicative of necrosis. However, cells still displayed PS on their plasma membranes. Furthermore, target cell nuclei were noticeably condensed and fragmented and in a manner quite different from that observed post GzmB treatment (refer to *Figure IV.16*).

Taken together, GzmH-induced cell death is not reminiscent of typical necrosis or of classical apoptosis. Instead, GzmH triggers a lengthy form of programmed cell death, cells reaching maximum cell death after 10-12 hours, which displays both apoptotic and necrotic features. Furthermore, the high expression levels of GzmH in naive NK cells strongly support the role of the granzyme in triggering an alternative cell death pathway in innate immunity. GzmH is most likely contained within granules rich in other NK cell associated granzymes, such as GzmA and GzmM. Contrary to our observations *in vitro*, our NK killing experiments showed that 70-80% of target cells die within 4 hours of exposure to freshly isolated and primed NK cells (refer to *Figure IV.31A*). It is highly unlikely that NK cell cytotoxic granules contain only one type of granzyme and, hence, it is the combined work of the family rather than the exploits of one particular member which accounts for the efficient eradication and clearance of diseased cells in a non-inflammatory fashion.

#### ***V.4 – GzmH and its siblings***

##### ***Is GzmH cell death reminiscent of GzmA cytotoxicity?***

Work by the Lieberman group has characterized GzmA, the second most studied family member, as a caspase-independent cell-death inducing protease (Beresford et al., 1999; Lieberman and Fan, 2003; Martinvalet et al., 2005). Like GzmA, GzmH-triggered cell death does not require caspase activation but leads to mitochondrial damage and DNA degradation, with affected cells showing apoptotic morphology such as PS externalization. Furthermore, both granzymes lead to ROS generation and loss



of mitochondrial membrane potential. Like GzmB, GzmA destroys the nuclear envelope by targeting lamins, and opens up DNA for degradation by targeting histones, but, conversely, GzmA, like GzmH, does not cleave initiator or executioner pro-caspases, Bid or ICAD, and does not lead to the release of proapoptotic intermembrane space proteins such as cytochrome c.

GzmA is reported to target and cleave three substrates which form the SET complex, a complex associated with the endoplasmic reticulum. These substrates are the nucleosome assembly protein SET, the DNA binding protein HMG-2 and the base excision repair enzyme Ape-1 (Lieberman and Fan, 2003). The SET complex also contains the tumor suppressor protein pp32 and the GzmA-activated DNase NM23-H1, which is inhibited by SET. In a manner reminiscent of the activation of CAD by cleavage of its inhibitor ICAD, GzmA cleavage of SET unleashes NM23-H1 which goes on to nick single-stranded chromosomal DNA (Fan et al., 2003). Whether or not GzmH mediated cell death also leads to single-stranded DNA nicks by targeting SET, or whether GzmH might cleave other members of the SET complex, remains to be tested.

### ***GzmH and the orphan granzymes***

Along with GzmK and GzmM, GzmH was previously referred to as an orphan granzyme (Grossman et al., 2003). However, these three granzymes have recently received much attention, and with our latest contribution to the field, it is now quite clear that all five human granzymes are truly a family of cytotoxic proteases. It is fascinating to note that each granzyme possesses unique proteolytic specificities, a property that probably accounts for their individual cell death pathways. Indeed, GzmA, a tryptase which cleaves after basic residues and GzmB, an aspartase, preferring acidic residues, have evolved distinct cell death programs. Compared to GzmA and GzmB, the most widely studied granzymes of the family, the ex-orphan human granzymes still require significant attention. Indeed, as we shall see, studies on GzmM come into conflict with one another, introducing doubt into the mechanisms proposed by these authors (Kelly et al., 2004; Lu et al., 2006). Regarding the third orphan, GzmH, this work represents the first functional study on the protease's involvement in target cell death.

### ***Granzyme K (GzmK)***

GzmK appears to kill in a manner very similar to GzmA. The two tryptases both induce cell death marked by single stranded DNA nicks, mitochondrial depolarization, ROS generation and PS externalization, in a pathway independent of caspases activation. Initially, like GzmA, GzmK was also shown to target the nucleosome assembly protein SET resulting in the release of DNase NM23HI and single-stranded nicking (Zhao et al., 2007b). More recently, the same group showed that GzmK can directly cleave Bid in a cell death pathway characterized by the disruption of the outer mitochondrial

membrane and the release of cytochrome c and endonuclease G, the only similarities with GzmA and GzmH being ROS generation, collapse of  $\Delta\Psi_m$  and the absence of caspase activity (Zhao et al., 2007a). The authors report that both GzmK and GzmB process Bid in a similar manner and that the 14 kDa truncated Bid (tBid) is able to recruit Bax to the mitochondrial membrane through a caspase independent mechanism (Heibein et al., 1999; Heibein et al., 2000). Cytochrome c release however is a crucial event in the activation of downstream caspases (Yang et al., 1997); the heme protein acts as a cofactor in conjunction with Apaf-1, procaspase-9 and ATP to form the apoptosome. The lack of caspase activation reported by the authors is probably a result of potent mitochondrial damage and lack of ATP without which the apoptosome cannot form. Collectively, these studies suggest that although GzmA and K prefer to cleave after the basic residues Arg or Lys, their distinct specificities at positions P2 and P4 (Mahrus and Craik, 2005) contribute to the cleavage of different substrates and, hence, to the induction of distinct cell death pathways.

### ***Granzyme M (GzmM)***

How GzmM mediates cytotoxicity remains unclear. One study claimed that the metase, like GzmA, GzmK and GzmH, was also able to induce cell death in a caspase independent manner but, unlike the above granzymes, did so with no damage inflicted upon mitochondria. Like GzmH, GzmM did not trigger chromosomal DNA fragmentation (Kelly et al., 2004). A more recent work, however, demonstrated just the opposite, showing that GzmM initiates caspase-dependent cell death with typical apoptotic nuclear morphology. Moreover, this study showed that GzmM can directly cleave both ICAD and the DNA repair sensor PARP, leading to DNA fragmentation without DNA nicking (Lu et al., 2006). The authors show that the pan-caspase inhibitor (zVAD-FMK) completely blocked cell death marked by DNA fragmentation and procaspase 3 processing, indicating that, although the enzyme can directly cleave both ICAD and PARP *in vitro*, caspase activation is likely to be required for such events to occur within target cells. Taken together, these two studies are in serious disagreement with each other, a situation which highlights the urgent need for further investigation into the true identity of GzmM's cytotoxic abilities.

In summary, unlike GzmB and possibly GzmM, GzmH belongs to the group of granzymes which inflict death upon diseased cells independently of caspase activation by targeting and damaging mitochondria and DNA. Indeed, as is the case with GzmA and, most likely, GzmK, GzmH cell death was defined by PS externalization, interruption of the inner mitochondrial respiratory chain resulting in ROS formation and depolarization and DNA degradation that did not involve the formation of oligonucleosomal double-stranded breaks. GzmH cytotoxicity, like that of GzmA, did not, however, lead to the cleavage of Bid and ICAD as has been reported for GzmB, GzmK and GzmM. GzmH-mediated cell death, like GzmA-mediated cell-death, occurred without the release of MIMPs, although

GzmA was reported to directly damage isolated mitochondria, a feat that still needs to be thoroughly addressed for GzmH. GzmH triggered DNA degradation also requires more detailed studies if the underlying processes are to be clearly understood. Although much more work is needed to understand the pathways that govern GzmH-induced cell death, it is now becoming clearer from work by Mahrus and Craik, who have recently confirmed the P4 to P1 substrate specificities of the five granzymes, that each granzyme most likely targets a differential set of substrates. Indeed, as more functional data are gathered on the orphan granzymes, and their substrates, we will soon also be able to distinguish more clearly the unique traits which characterise each of their respective cell death pathways.

### ***V.5 – GzmH expression is restricted to NK cells***

#### ***Differential expression of human granzymes A, B, K and M in unstimulated lymphocytes***

In contrast to GzmA and GzmB, the study of orphan granzyme expression in human lymphocytes has been restricted because of the lack of appropriate antibodies. Recently, specific monoclonal antibodies (mAbs) have been generated against human GzmK, GzmM and GzmH (Bade et al., 2005; Sedelies et al., 2004). In one study, the cytometric analysis of unstimulated human peripheral blood lymphocytes revealed that GzmA, GzmM and PFN showed a similar distribution, being expressed in CD3<sup>-</sup>CD16<sup>+</sup>CD56<sup>+</sup> NK cells, CD3<sup>+</sup>CD56<sup>+</sup> NKT cells and various T cell sub-populations (refer to *Table V.1*). GzmK, on the other hand, was markedly absent in the highly toxic CD3<sup>-</sup>CD16<sup>+</sup>CD56<sup>+</sup> NK cells and was preferentially expressed in the T cell lineage (refer to *Table V.1*). Interestingly, though, GzmK was found to be expressed in CD3<sup>-</sup>CD56<sup>bright+</sup> cells, a small subset of NK cells which express very little CD16 and has been shown to be poorly cytotoxic. The majority of human peripheral NK cells display a CD3<sup>-</sup>CD16<sup>+</sup>CD56<sup>+</sup> phenotype. However, according to the expression density of CD56, NK cells can be divided into CD56<sup>dim</sup> and CD56<sup>bright</sup> subsets, the CD56<sup>dim</sup> cytotoxic population representing the vast majority (90%) of human NK cells (Jacobs et al., 2001).

In another study by the same group, GzmA, GzmK, and, this time, GzmB expression was also analyzed by cytometry in human resting peripheral blood lymphocytes (Bratke et al., 2005). In agreement with Bade et al. and Grossman et al., GzmA, GzmB and GzmK expression was mainly detected in T cells subsets, namely CD8<sup>+</sup>, CD56<sup>+</sup> and TCRγδ<sup>+</sup> T cells and, to a lesser extent, in CD4<sup>+</sup> T cells (Bade et al., 2005; Grossman et al., 2004). With regard to NK cell expression, the authors found that GzmA and GzmB were detectable at high concentrations in cytotoxic CD3<sup>-</sup>CD16<sup>+</sup> and CD3<sup>-</sup>CD56<sup>dim</sup> NK cells. Additionally, and again in agreement with Bade et al., GzmK was again found to be

highly expressed in CD3<sup>-</sup>CD56<sup>bright</sup> cells. This was not the case for GzmB which was found at low levels (refer to *Table V.1*).

Lymphocyte subset	GzmA	GzmB	GzmK	GzmM
<b>B cells (CD19<sup>+</sup>CD3<sup>-</sup>)</b>	n.d.	n.d.	n.d.	n.d.
<b>CD8 T cells (CD8<sup>+</sup>CD3<sup>+</sup>)</b>	Med	Low	Low	Med
<b>TCRγδ cells (TCRγδ<sup>+</sup>CD3<sup>+</sup>)</b>	High	Med	Med	High
<b>T helper cells (CD4<sup>+</sup>CD3<sup>+</sup>)</b>	Very Low	Very Low	Very Low	Very Low
<b>NKT cells (CD3<sup>+</sup>CD56<sup>+</sup>)</b>	High	Var	Var	High
<b>NK cells (CD3<sup>-</sup>CD16<sup>+</sup> CD56<sup>+</sup>)</b>	High	High	Low	High
<b>NK cells (CD3<sup>-</sup>CD56<sup>dim</sup>)</b>	High	High	Low	n.d.
<b>NK cells (CD3<sup>-</sup>CD56<sup>bright</sup>)</b>	Med./high	Low	Med./High	Med./High

**Table V.1 – Granzyme expression in unstimulated human lymphocytes.** N.d., not detected; very low, <10%; low, 10-50%; med (medium), 50-70%; high, >75% and var (variable), 0-100%. The symbols given represent percentages found in the respective cell populations of most donors. The table is fused from two independent studies from the same group. The authors agree on the expression patterns for both GzmA and GzmK in the above subpopulations (Bade et al., 2005; Bratke et al., 2005).

### ***GzmH is predominantly expressed by NK cells and is stored in secretory granules***

GzmH protein expression in blood leukocytes was first studied by Sedelies et al. (Sedelies et al., 2004). Here, GzmH was reported to be considerably more abundant than GzmB in naïve CD3<sup>-</sup>CD56<sup>+</sup> NK cells (purified from PBMCs) despite there being a good correlation between GzmB and GzmH mRNA expression. Since the majority of human peripheral NK cells are of the highly cytotoxic phenotype (CD3<sup>-</sup>CD56<sup>dim</sup>), this study is in sharp contrast with the recent work from Bratke and Grossman who report that the GzmB protein is highly expressed in unstimulated human CD3<sup>-</sup>CD56<sup>dim</sup> NK cells (Bratke et al., 2005; Grossman et al., 2004). Upon stimulation of NK cells, however, Sedelies et al. show that GzmB protein expression was strongly upregulated although the same stimuli had no effect on GzmH protein levels. In the same study, GzmH expression was also distinct from that of GzmB in peripheral blood T lymphocytes. Various stimuli led to a marked induction of the GzmB protein, both in CD4<sup>+</sup> and CD8<sup>+</sup> PBMCs. However, the GzmH protein was expressed at low levels in CD4<sup>+</sup> T cells but was not detected in CD8<sup>+</sup> T cells, and was not induced upon T cell activation. Additionally, GzmH protein expression was completely absent in NKT cells and monocytes (Sedelies et al., 2004). Taken together, Sedelies et al. report that although both GzmB and GzmH are the products of tightly linked genes, they are regulated in distinct ways.

Because we have recently demonstrated that purified GzmH can induce cell death in an alternative, caspase-independent pathway, we sought, in comparison with GzmB, to strengthen our *in vitro* observations by supporting the results shown by Sedelies et al. Our results confirm that naïve NK (CD3<sup>-</sup>, CD56<sup>+</sup>) cells are the major GzmH-expressing lymphocyte population of the peripheral blood (refer to *Figure IV.30*). Additionally, we also confirm that neither monocytes nor activated CD8<sup>+</sup> CTLs show any presence of GzmH. Neutrophils were also found to lack GzmH expression. We did however find some GzmH protein expression in CD3<sup>+</sup> T-cells, the CD4<sup>+</sup> population most likely to account for this expression as previously shown by Sedelies et al. The fact that the GzmH protein is constitutively expressed at high levels in resting NK cells strongly suggests a central role for the protease in innate immunity.

Interestingly, the Ley group has recently addressed granzyme and perforin expression in murine NK cells. They showed that, although unstimulated NK cells came pre-loaded with the GzmA protein, very little GzmB or perforin protein was present despite the cells expressing abundant mRNAs of the three genes (Fehniger et al., 2007). Once stimulated with cytokines, the minimally cytotoxic NK cells became potent killers with increased perforin and GzmB protein. Messenger RNA levels, however, remained unchanged. The study suggests that resting murine NK cells are minimally cytotoxic because of a block in gene translation that is released following activation, and that NK-receptor ligation probably represents the trigger required to direct granule release at the immunological synapse. The abundant levels of GzmA protein in resting NK murine cells is reminiscent of the high levels of GzmH found in unstimulated human NK cells which also contain very little GzmB protein (Sedelies et al., 2004). Despite the presence of the preloaded GzmA protein, murine NK cells deficient in GzmA, target and kill tumors equally as well as their wild-type counterparts (Ebnet et al., 1995). However, NK cells from GzmA and GzmB double deficient mice kill less efficiently than NK cells deficient in GzmA alone, suggesting that GzmA is a “fail-safe” granzyme, a role that GzmH might also fulfill in human NK cells.

### ***Does granzyme H play a vital role in innate immunity?***

Our study shows that freshly purified CD3<sup>-</sup>CD16<sup>+</sup>CD56<sup>+</sup> NK cells also contained low amounts of GzmB protein and that, upon stimulation with IL-2, the cells were able to kill K562 cells efficiently at a 2:1 effector target ratio (refer to *Figure IV.31*). As a result, both soluble GzmH and GzmB (data not shown) was detectable in the culture supernatant (refer to *Figure IV.32*). This observation strongly suggested the involvement of GzmH during the innate response. Evidence for the delivery of GzmH into the cytosol of target cells is, moreover, provided in a collaborative study (Andrade *et al.* 2007), showing that an adenovirally transduced protein in the cytosol of K562 cells is cleaved at GzmH specific sites following LAK cell attack. LAK cells (lymphokine activated killers) are lymphokine (IL-

2) activated adherent NK and T cells which have enhanced cytolytic activity, and which contain all granzyme activities at different ratios (Ortaldo et al., 1986; Phillips and Lanier, 1986). Andrade et al. confirmed the presence of GzmH using the recently described GzmH specific monoclonal antibody (4G5) (Sedelies et al., 2004).

The observation that resting, highly cytotoxic NK cells, which constitute the first line of defence in innate immunity, come preloaded with GzmA, GzmH and GzmM, and suggests the view that the orphan human granzymes play critical roles in the innate immune response. Moreover, the fact that the five human granzymes each process distinct substrate specificities and now have all been shown to induce cell death in alternative, mostly caspase-independent manners, sheds light on the combinatorial mechanisms used by the granule exocytosis pathway to circumvent evasion strategies developed by viruses and tumor cells which are initially resistant to one or more particular granzymes. Our next task lies, then, not only in fully understanding the exact extent to which granzymes are expressed in the different subsets of cytotoxic lymphocytes, but also in understanding the individual substrates granzymes have evolved to target.

### ***V.6 - GzmH is an antiviral protease***

A recent collaborative work with Felipe Andrade demonstrated that granzymes do indeed work in synergy to outsmart adenoviral defence strategies. In this work, we discovered the first two biological substrates for GzmH, namely the adenoviral DNA binding protein (DBP), and the L4-100K assembly protein (100K) which potently inhibits GzmB (Andrade et al., 2001; Andrade et al., 2007). We demonstrated that, in target cells infected with adenovirus, in which GzmB and downstream caspases are inhibited, GzmH directly cleaves the adenoviral DBP protein. The generation of a mutant adenovirus virus that encodes a GzmH resistant DBP protein allowed us to address the functional consequences of DBP cleavage by GzmH, an event which is responsible for the decay in viral DNA load after effector cell attack.

Site-directed mutagenesis was used to determine the site where GzmH cleaved the IVTT (*in vitro* coupled transcription/translation) generated DBP protein. Initially, Phe 121 was changed to Gly but this substitution did not result in DBP cleavage by recombinant GzmH. However, when Met 118 was replaced by Val, the generation of the 47 kDa cleaved product (see *Figure V.3*) was greatly reduced. Moreover, when a double mutant containing both substitutions was exposed to GzmH, cleavage was completely abolished. The generation of a mutant virus containing the double substitution was thereafter attempted to directly address the functional consequences of DBP cleavage by GzmH during

target cell attack. By assaying the quantity of viral DNA load in infected cells at 12 hours, we were able to show that, in comparison to cells infected with the wild type adenovirus, the DNA load of the mutant virus was minimally affected (refer to *Figure V.2*) (Andrade et al., 2007).

In experiments using the mutant virus, we found that, after 12 hours, viral DNA replication swiftly declined, suggesting that another antiviral force was at work. Because GzmH and GzmB both cleave the DBP protein, we wondered whether GzmH might be involved in the inactivation of another protein, namely the 100K assembly protein, a recently described GzmB substrate that potently inhibits GzmB mediated cell death (Andrade et al., 2001). Interestingly, when 100K, generated by IVTT, was preincubated with GzmH, the inhibitor blocked GzmB activity at early time points. At later time points, however, inhibition of GzmB by 100K was lost, allowing the recovery of caspase 3 activation. In conclusion, this work convincingly shows that in the case of GzmB inhibition, GzmH can equally contribute to DBP cleavage while also being able to relieve GzmB from inhibition by 100K protein. It remains to be seen, however, if granzymes other than GzmH aid in the cleavage of the 100K protein and recovery of GzmB activity. It is necessary to point out though that our study did not include the generation of an adenovirus encoding both DBP and 100K GzmH resistant proteins. Nevertheless, this study identifies the first evidence that granzymes do indeed work in synergy to overcome viral defences involved in blocking granzyme function. Furthermore, the study also sheds light not only on the amino acids after which GzmH prefers to cleave *in vivo*, here Met118, but also opens our eyes to putative P4 to P4' sequences preferred by GzmH.

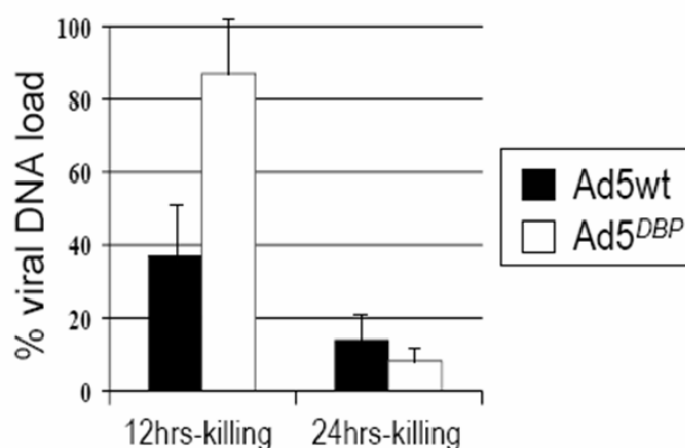


**Figure V.2 - Adenovirus DNA replication and cleavage of DBP during LAK-mediated cell death.** Wild-type (Ad5wt) and mutant (Ad5<sup>DBP</sup>) adenoviruses were co-incubated in the absence (control) or presence of LAK cells at a effector:target ratio of 8:1. After 12 and 24 hours, genomic DNA was purified and the DNA viral load quantified by real-time PCR as described (see paper). Values are shown as percentages in which 100% represents the total viral DNA load in control, non treated cells at 12 or 24 h. The error bars represent the standard deviation. Taken from a study by Andrade et al. entitled “GzmH destroys the function of critical adenoviral proteins required for viral DNA replication and granzyme B inhibition”, EMBO J. (Andrade et al., 2007).

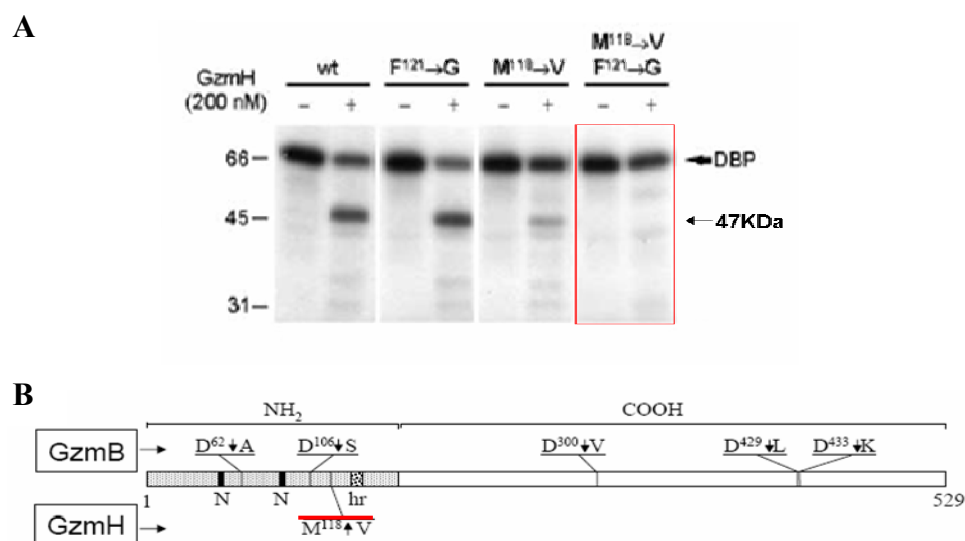


**Figure V.3 - DBP is cleaved by GzmH *in vitro*.** (A) GzmH cleavage sites in DBP were defined by mutating P1 residues Phe 121 to Gly, Met 118 to Val and in a double mutation, Phe 121 to Gly and Met 118 to Val. Wild-type and the mutated [<sup>35</sup>S] methionine-labelled products were incubated with or without GzmH for 60 min at 37°C. The 47 kDa bands are the product of GzmH action upon the DBP protein. The minor bands that appear below the 47 kDa cleavage product are minor DBP fragments. (B) Schematic representation of the functional domains and the GzmB and H cleavage sites in DBP. DBP consists of a N-terminal domain (NH<sub>2</sub>) containing residues 1-173 and a C-terminal domain (COOH) from residues 174 to 529. The N-terminal domain contains 2 nuclear localization signals (N) and a host range (hr) region. The anti-DBP monoclonal antibody recognizes residues 131-174 (Cleghon et al., 1993). Taken from a work in collaboration with Felipe Andrade and colleagues entitled “GzmH destroys the function of critical adenoviral proteins required for viral DNA replication and GzmB inhibition”. EMBO Journal 2007 (Andrade et al., 2007).

### V.7 - Human and mice granzymes

The five human granzyme genes (*GZMA*, *GZMB*, *GZMH*, *GZMK* and *GZMM*) are clustered on three different chromosomes (Trapani and Smyth, 2002). GzmB and GzmH share high structural homology (71% amino acid identity) and belong to a tightly linked gene cluster (GzmB cluster) on chromosome 14, which also harbors cathepsin G and mast cell chymase. Despite their high sequence homology both enzymes bear very distinct enzymatic activities. In the rodent GzmB cluster, a highly variable number of paralogous genes were identified in the region bordered by cathepsin G and GzmB. No structure activity relationships have so far been determined experimentally. Molecular modelling has predicted that the orphan murine granzymes D, E, F and G, but not GzmC which lies directly upstream and adjacent to murine GzmB on its 5' side, will cleave after Phe similarly to GzmH in humans (Grossman et al., 2003; Kam et al., 2000). The GzmH gene has been shown to be the result of a recent intergenic recombination event between a chymase-like ancestor and GzmB (Haddad et al., 1991). Since this gene conversion occurred in the primate lineage after mammalian radiation, a genuine ortholog with conserved substrate specificity is unlikely to exist in rats and mice.



Leukocyte subset	GzmC	GzmD	GzmE	GzmF	GzmG
Resting CD4 <sup>+</sup> Tcells	-	-	-	-	-
Activated CD4 <sup>+</sup> Tcells	+	+	+	+	+
Resting CD8 <sup>+</sup> Tcells	-	-	-	-	-
Activated CD8 <sup>+</sup> Tcells	+	++	++	+	++
CTL cell line	++	++	++	+++	+++
NK cell lines	++	+	+	+	+
GMG cells		+	+	+	+
LAK cells	+++	++	+	++	+
Thymocytes - cultured	++	++	++	+++	+
Thymocytes - cell line	+				
Activated B cells	+	-	-	-	-
Activated macrophages	-	-	-	-	-

**Table V.2 – Relative levels of murine orphan granzyme gene expression.** +/++/+++, relative RNA expression; -, none detected; blank, not determined; LAK, lymphokine activated killer; GMG, granulated metrial gland. Table adapted from the following works: (Grossman et al., 2003; Jenne et al., 1988b; Jenne et al., 1988a; Jenne et al., 1989; Jenne et al., 1991; Mullbacher et al., 1999; Pham et al., 1996)

### ***Human and murine granzyme expression in cytotoxic lymphocytes***

Our study on GzmH cytotoxicity shows that naïve NK (CD3<sup>-</sup>, CD56<sup>+</sup>) cells are the major GzmH expressing lymphocyte population, confirming recent findings by Sedelies and colleagues. Whether granzymes D, E, F or G, the potential candidates for a genuine GzmH homolog in mice, are also mainly expressed at the protein level in unstimulated NK cells remains to be clarified. However, several studies have examined the mRNA expression pattern of murine orphan granzymes in a variety of different cell types, relying on northern blots, RNA protection assays, and/or RT-PCR analysis, to define the cellular expression patterns. The results of these studies are summarized in *Table V.2* (Garcia-Sanz et al., 1990; Jenne et al., 1988b; Jenne et al., 1988a; Jenne et al., 1989; Jenne et al., 1991; MacIvor et al., 1999; Pham et al., 1996). The majority of studies suggest that high-level expression of murine orphan granzymes is restricted to unstimulated LAK cells, NK cell lines, a subset of NK cells known as granulated metrial gland (GMG) cells, and thymocytes. In T cells (both CD4<sup>+</sup> and CD8<sup>+</sup>), the expression of most orphan granzymes is activation-dependent and is much lower than that of GzmA or GzmB (refer to *Table V.2*).

The systematic knockout of individual granzymes genes, including the remaining murine orphan group (granzymes D, E, F, G, K and M), should allow the thorough analysis of their individual functional importance. Because mice do not have a single GzmH ortholog, the identification of the closest functional GzmH equivalent among the various paralogs is essential for the design of appropriate knockout studies.

***GzmA<sup>-</sup>/GzmB<sup>-</sup> deficient mice***

In vitro cytotoxicity assays, using immune effector cells from GzmA<sup>-</sup> or GzmB<sup>-</sup> deficient mice, have indicated that GzmB, but not GzmA, is required for the fast and efficient induction of target-cell apoptosis (Ebnet et al., 1995; Heusel et al., 1994; Shresta et al., 1995), although GzmA can compensate for GzmB deficiency with delayed kinetics (Shresta et al., 1999). Moreover, effector cells deficient in both GzmA and GzmB have been reported to be as defective as perforin null cells in mediating target-cell cytotoxicity (Mullbacher et al., 1999; Shresta et al., 1999; Simon et al., 1997). For instance, Mullbacher and colleagues report that their GzmA<sup>-</sup>/GzmB<sup>-</sup> mice were as incapable as perforin null mice of controlling primary infections by the natural mouse pathogen ectromelia, a poxivirus.

Interestingly, the original GzmB<sup>-</sup> deficient mice (which were a mixed B6/129 background) were later found also to have downregulated expression of the downstream orphan granzymes, C, D, E, F and G owing to a neighborhood effect caused by retention of a PGK-Neo cassette in the GzmB gene (Pham et al., 1996). These mice are, therefore, more accurately described as GzmB-cluster-deficient mice which had previously been crossed with GzmA<sup>-</sup> null mice to produce GzmA and GzmB double knockouts. Subsequent generation of the same mutation on a pure 129/SvJ background revealed restriction of the neighbourhood effect to granzymes C and F. Furthermore, removal of the PGK-Neo cassette eliminated this effect, resulting in mice deficient only in GzmB. Recent studies comparing CTLs from GzmB-cluster and GzmB<sup>-</sup> null mice show that GzmB-cluster deficient mice have a more severe defect in the cytotoxicity of their effector cells compared to those derived from GzmB null mice (Davis et al., 2001; Revell et al., 2005; Smyth et al., 2003; Waterhouse et al., 2006). Indeed, Waterhouse and colleagues demonstrated that murine GzmA<sup>-</sup>/GzmB<sup>-</sup> deficient CTLs induced cell death in a different manner to their wild-type counterparts or target cell death by perforin mediated lysis. Indeed, CTLs from GzmA<sup>-</sup>/GzmB<sup>-</sup> mice induced a novel form of programmed cell death (PCD) which shared similar features with, but was distinct from, apoptosis. Although, overall, the morphology of cell death in response to GzmA and GzmB null CTLs was similar to classic apoptosis, the simultaneous staining of Annexin V, and PI was reminiscent of perforin lysis. Additionally, PS externalization occurred, in parallel to the loss of membrane integrity, suggesting that these cells would not be efficiently engulfed by macrophages and, thus, may be perceived by the immune system as having undergone necrosis. Also, no DNA fragmentation was observed, which is typical of the actions of GzmB (Waterhouse et al., 2006). Taken together, these studies suggest that the murine orphan granzymes encoded in the GzmB-cluster might well play an essential role in effector-cell cytotoxicity.

Recently, GzmC, GzmK, GzmH and GzmM have been shown to be proapoptotic when delivered into target cells by perforin and other means of translocation (Fellows et al., 2007; Johnson et al., 2003; Lu et al., 2006; Zhao et al., 2007b; Zhao et al., 2007a). Therefore, cell death induced by CTLs and NK cells from mice deficient in GzmA and GzmB may not only be caused by perforin-mediated delivery of the GzmB-cluster orphan granzymes, many of which, like GzmH, are predicted to cleave after phenylalanine, but also by granzymes K and M.

As previously mentioned, in a collaborative work with Felipe Andrade, we recently demonstrated that both GzmB and GzmH can work together to outsmart adenoviral defenses (Andrade et al., 2007). In support of our data, which shows that granzymes other than GzmA and GzmB can regulate viral infection, Loh and colleagues demonstrate that orphan granzymes, encoded in the GzmB gene cluster, are critical in the control of the latency of the murine gammaherpesvirus 68 ( $\gamma$ HV68) (Loh et al., 2004). The study shows that GzmA, and especially GzmB through the use of caspase 3 substrates, are important for regulating the early form (16 days post infection, dpi) of  $\gamma$ HV68 latency. Additionally, GzmA<sup>-</sup>/GzmB<sup>-</sup> mice (which are not affected by the downregulation of downstream granzymes C, D, E, F and G) are indistinguishable from their wild-type counterparts at late time points (42 dpi), suggesting that at this stage only orphan granzymes are required. Perforin-null mice failed to control viral latent infection at both early and late time points. Importantly, GzmB-cluster knockout mice were used to demonstrate the role the murine orphan granzymes, but not granzymes K and M, had on regulating  $\gamma$ HV68 latent infection. The authors were unable to determine which specific granzymes were responsible since mice deficient for individual orphan granzymes were not available, but were able to rule out caspase 3 activation. The study suggests that the requirement for specific granzymes differs for early versus late forms of latent infection, and that different granzymes play distinct roles in regulating  $\gamma$ HV68 infection.

Understanding the exact mechanisms by which GzmA<sup>-</sup>/GzmB<sup>-</sup> CTLs kill their targets will be important in furthering our knowledge of how effector cell-induced target cell killing helps prevent infection. Also, such studies will help unmask the key granzymes, other than GzmA and GzmB, in maintaining the relatively healthy immune status of GzmA<sup>-</sup>/GzmB<sup>-</sup> mice compared with perforin-deficient mice.

### ***Is GzmC the functional murine equivalent to human GzmH?***

GzmH-induced cell death displayed several features which are reminiscent of murine GzmC cytotoxicity, although, on a molar basis, the kinetics of cell death of the murine protease showed greater similarity to those observed for GzmB (Johnson et al., 2003). Indeed, after 12 hours of GzmH exposure (1  $\mu$ M), but not before 4 hours, K562 cell nuclei appeared condensed and fragmented, a feat achieved by GzmC after only 1 hour at the same molarity. Similarities also include the externalization

of phosphatidyl serine (PS) and lack of initiator and effector caspase activation. Furthermore, the morphological changes of cellular nuclei were paralleled by the loss of mitochondrial membrane potential. As expected, zVAD-FMK did not prevent the loss of membrane potential following exposure to both GzmC and GzmH, with only a moderate protecting effect observed during the later stages in the case of GzmH mediated cell death (Fellows et al., 2007).

Additionally, both proteases are similar in that, during their respective cell death pathways, neither of the enzymes caused the release of the smallest of the mitochondrial inter-membrane space proteins (MIMPs), namely cytochrome c. Cytochrome c release is an event which marks the actions of both murine and human GzmB (see *Figure IV.23*). Interestingly, a feature that was not observed in the case of GzmH was the direct swelling and membrane depolarization seen in isolated mitochondria exposed to recombinant GzmC. Although we set out to investigate whether the direct addition of GzmH or GzmB to freshly isolated and energized mitochondria from mouse liver would induce potential loss, no effect was seen as monitored by decrease in rhodamin 123 fluorescence. The addition of the toxin valinomycin/oligomycin did, however, easily induce  $\Delta\Psi_m$  loss. In conclusion, although murine GzmC and GzmH share many of the same cell death hallmarks, substrates involved in their respective cytotoxic pathways have yet to be uncovered. Despite the above similarities, comparing the nature of the function relationship between these proteases in a convincing manner is a difficult issue, as activity for GzmC has not been found. It is interesting to note, however, that GzmH shares more key amino acids, predicted to influence cleavage specificity, with murine granzymes D and E (see *Figure V.4*).

### ***GzmH homologs from different placental mammals***

The biological importance of the human GzmH gene is underscored by the fact that structural equivalents exist in all placental mammals. Primates like chimps and macaques, but also dogs and rabbits possess a single copy GzmH gene on the 5' side of the GzmB gene. The structural hallmarks of all GzmH homologs are Thr (Ser, Ala)189, Lys (Arg)192 and Gly226 which determine the S1 subsite and Phe99 affecting S2 (see *Figure V.5*). GzmB homologs of all these species differ from GzmH by Arg226, but otherwise are identical with GzmH at positions 192 and 99 (see *Figure V.4*). Indeed, replacement of Arg226 by Gly226 converted human GzmB into a GzmH-like variant which cleaved Suc-Ala-Ala-Pro-Phe-SBzl and Boc-Ala-Ala-Phe-SBzl like the wild type GzmH (Caputo et al., 1994).

GzmH-like equivalents have not yet been identified unambiguously in the genomes of rodents (rats, mice) and artiodactyls (cattle). Local gene duplications and conversions generated a highly diverse and much greater repertoire of paralogous genes in these species (Gallwitz et al., 2006; Haddad et al., 1991). Owing to a sequence transfer from the adjacent GzmB locus to the ancestral GzmH locus affecting residues 63 to 142, similarity between human GzmH and human GzmB is very high.



predicted to cleave after asparagine or serine at the P1 position (Barry and Bleackley, 2002; Trapani, 2001). Interestingly, like GzmH, recombinant GzmD (R&D systems) is predicted, along with murine granzymes E and G, to cleave after bulky, aromatic amino acids such as phenylalanine at the P1 site and is, indeed, active against Suc-Phe-Leu-Phe-SBzl. To see if this recombinant murine GzmD could induce apoptosis in a similar fashion to GzmH, we analyzed GzmD-exposed K562 cells after 12 and 24 hours by FACS after annexin V FITC and PI staining. Unfortunately, nothing came of these experiments. A personal communication from R&D systems informed us that two thirds of the purified GzmD possessed N-terminal sequences starting with HVVKPHS instead of the correct sequence IIGGHVVKPHS. Consequently, only a third of the proteases in the preparation would be active, Ile16 having correctly formed a salt bridge with the carboxylate side chain of Asp194, so initiating the formation of the mature, active protease through conformational change. As substrate specificities and cleavage activities of purified GzmC and Gzms D to G have not yet been strictly determined, it remains to be proven whether any of the rodent granzymes fulfil the same molecular functions as human GzmH.

Interestingly, although the chain of cause and effect has not yet been reconstructed for any of the known granzymes, cytotoxic activities of GzmA, GzmB, GzmH, GzmK and murine GzmC appear to converge and culminate in irreversible mitochondrial damage. Mitochondrial damage was observed with all of these granzymes in the absence of caspase activation, despite the broad diversity in cleavage specificities with chymase-, tryptase- and caspase-like activities. Thus, the initial chain of proteolytic events in the cytosol of target cells is most likely to be distinct for each granzyme, and may hit on different cell death pathways.

---

## ***VI - Conclusions and Outlook***

Because activated CD3<sup>+</sup>CD16<sup>+</sup>CD56<sup>+</sup> NK cells express the strongly proapoptotic GzmA and GzmB along with perforin (Bade et al., 2005; Bratke et al., 2005; Grossman et al., 2004), the other granzymes of NK cells, namely GzmH, GzmK and GzmM, have until recently received little attention as genuine cell death inducing effector proteases. Several studies, however, conclude that granzymes may possibly be involved in a number of extra-cellular activities. Indeed, GzmA (Kramer and Simon, 1987) and GzmB (Buzza et al., 2005) have been suggested to play a role in matrix remodeling and killer cell migration at the site of target cell attack. Similar extracellular functions may easily be envisaged for the cathepsin G-related GzmH. Hence, it was also important to explore the death-inducing potential of the last true orphan of the granzyme family by means of a well-controllable delivery system. Our findings clearly indicate the importance of GzmH as a novel, alternative cytotoxic effector protease. Although we were unable to find a cell-death related substrate for GzmH, our study is strongly suggestive of target cell death defined by not only caspase independent apoptotic-like morphology, but also caspase independent damage inflicted upon DNA and mitochondria. This initial study on the cell-death inducing properties of GzmH is most reminiscent of human GzmA, but also murine GzmC triggered cytotoxicity.

The biological value and niche of GzmH, which was added to the arsenal of natural killer cells late during mammalian evolution, have just begun to be deciphered. Once clarified, however, they will contribute to a broader understanding of NK cell function, not only in tumour elimination and viral clearance, but also as a regulator of inflammation and tissue repair (Zong and Thompson, 2006). Indeed, together with Andrade and colleagues, we recently demonstrated the anti-adenoviral activity of both GzmB and GzmH (Andrade et al., 2007) thereby providing the first evidence that granzymes can act in synergy to outflank viral defenses.

These initial studies set the scene for GzmH as an important protease in innate immunity, while also setting the foundations for exciting further work on this chymotrypsin-like protease. Indeed, in collaboration with JPT peptide technologies, who offer a protease substrate set consisting of a selection of 360 peptides, we will attempt to better decipher the protease's cleaving specificity, and also cytotoxicity, by searching for GzmH specific substrates. These peptide derivatives contain the cleavage site sequences from P4 to P4' and are flanked by DABCYL and Glu(EDANS)-amide moieties at the N and C-termini respectively. Therefore, upon incubation with GzmH, cleavage of any of the given sequences between the fluorophore and the quencher moiety will be detected using a microtiter fluorescence reader.

The search for cell-death related GzmH substrates has prompted us to attempt the structural analysis of the chymotrypsin-like enzyme in collaboration with Wolfram Bode from the MPI of Biochemistry, Martinsried. Our recombinant, non-glycosylated GzmH appears to be a perfect candidate for crystallization, not only because we are able to produce high quantities of inclusion body based protease, but also because pure recombinant GzmH lacks N-linked carbohydrates which facilitates crystallization. N-linked glycosylation can hinder crystallization because of its bulkiness, flexibility and heterogeneity. The three-dimensional crystal structure of active GzmH would be an extremely helpful tool in our efforts to understand better the protease's overall structure, its substrate specificity (and therefore aid in the search for GzmH specific substrates) and to develop highly specific inhibitors.

As a last remark, since the animal models of choice, namely the mouse or rat, do not possess a function equivalent to the human GzmH gene, functional studies on GzmH by knock-out methodology are not possible. As we learn more about the specificity of GzmH, either through the manipulation of synthetic peptides, the use of peptide substrate libraries, or the discovery of novel protein substrates such as DBP and 100K, the design of tailored GzmH inhibitors will dramatically improve our understanding of GzmH function. Indeed, specific inhibitors against the enzyme will allow us to study its biological importance in cell death induction and in the mechanisms of granzyme-pathogen interaction.



---

## ***VII – Literature***

- Alimonti, J. B., L. Shi, P. K. Baijal, and A. H. Greenberg. 2001. Granzyme B induces BID-mediated cytochrome c release and mitochondrial permeability transition. *J. Biol. Chem.* 276:6974-6982.
- Andrade, F., H. G. Bull, N. A. Thornberry, G. W. Ketner, L. A. Casciola-Rosen, and A. Rosen. 2001. Adenovirus L4-100K assembly protein is a granzyme B substrate that potently inhibits granzyme B-mediated cell death. *Immunity* 14:751-761.
- Andrade, F., E. Fellows, D. E. Jenne, A. Rosen, and C. S. H. Young. Granzyme H destroys the function of critical adenoviral proteins required for viral DNA replication and granzyme B inhibition. *EMBO J.* 2007.  
Ref Type: In Press
- Andrade, F., S. Roy, D. Nicholson, N. Thornberry, A. Rosen, and L. Casciola-Rosen. 1998. Granzyme B directly and efficiently cleaves several downstream caspase substrates: implications for CTL-induced apoptosis. *Immunity* 8:451-460.
- Babe, L. M., S. Yoast, M. Dreyer, and B. F. Schmidt. 1998. Heterologous expression of human granzyme K in *Bacillus subtilis* and characterization of its hydrolytic activity in vitro. *Biotechnol. Appl. Biochem.* 27 ( Pt 2):117-124.
- Bade, B., H. E. Boettcher, J. Lohrmann, C. Hink-Schauer, K. Bratke, D. E. Jenne, J. C. Virchow, Jr., and W. Luttmann. 2005. Differential expression of the granzymes A, K and M and perforin in human peripheral blood lymphocytes. *Int. Immunol.* 17:1419-1428.
- Balasubramanian, K., E. M. Bevers, G. M. Willems, and A. J. Schroit. 2001. Binding of annexin V to membrane products of lipid peroxidation. *Biochemistry* 40:8672-8676.
- Balkow, S., A. Kersten, T. T. Tran, T. Stehle, P. Grosse, C. Museteanu, O. Utermohlen, H. Pircher, F. von Weizsacker, R. Wallich, A. Mullbacher, and M. M. Simon. 2001. Concerted action of the FasL/Fas and perforin/granzyme A and B pathways is mandatory for the development of early viral hepatitis but not for recovery from viral infection. *J. Virol.* 75:8781-8791.
- Barry, M. and R. C. Bleackley. 2002. Cytotoxic T lymphocytes: all roads lead to death. *Nat. Rev. Immunol.* 2:401-409.
- Barry, M., J. A. Heibey, M. J. Pinkoski, S. F. Lee, R. W. Moyer, D. R. Green, and R. C. Bleackley. 2000. Granzyme B short-circuits the need for caspase 8 activity during granule-mediated cytotoxic T-lymphocyte killing by directly cleaving Bid. *Mol. Cell Biol.* 20:3781-3794.
- Benov, L., L. Szejnberg, and I. Fridovich. 1998. Critical evaluation of the use of hydroethidine as a measure of superoxide anion radical. *Free Radic. Biol. Med.* 25:826-831.

- Benson, K. F., F. Q. Li, R. E. Person, D. Albani, Z. Duan, J. Wechsler, K. Meade-White, K. Williams, G. M. Acland, G. Niemeyer, C. D. Lothrop, and M. Horwitz. 2003. Mutations associated with neutropenia in dogs and humans disrupt intracellular transport of neutrophil elastase. *Nat. Genet.* 35:90-96.
- Beresford, P. J., C. M. Kam, J. C. Powers, and J. Lieberman. 1997. Recombinant human granzyme A binds to two putative HLA-associated proteins and cleaves one of them. *Proc. Natl. Acad. Sci. U. S. A* 94:9285-9290.
- Beresford, P. J., Z. Xia, A. H. Greenberg, and J. Lieberman. 1999. Granzyme A loading induces rapid cytolysis and a novel form of DNA damage independently of caspase activation. *Immunity.* 10:585-594.
- Birnboim, H. C. 1983. A Rapid Alkaline Extraction Method for the Isolation of Plasmid Dna. *Methods in Enzymology* 100:243-255.
- Birnboim, H. C. and J. Doly. 1979. A rapid alkaline extraction procedure for screening recombinant plasmid DNA. *Nucleic Acids Res.* 7:1513-1523.
- Bradford, M. M. 1976. A rapid and sensitive method for the quantitation of microgram quantities of protein utilizing the principle of protein-dye binding. *Anal. Biochem.* 72:248-254.
- Bratke, K., M. Kuepper, B. Bade, J. C. Virchow, Jr., and W. Luttmann. 2005. Differential expression of human granzymes A, B, and K in natural killer cells and during CD8+ T cell differentiation in peripheral blood. *Eur. J. Immunol.* 35:2608-2616.
- Bronstein, I., J. C. Voyta, O. J. Murphy, L. Bresnick, and L. J. Kricka. 1992. Improved chemiluminescent western blotting procedure. *Biotechniques* 12:748-753.
- Browne, K. A., E. Blink, V. R. Sutton, C. J. Froelich, D. A. Jans, and J. A. Trapani. 1999. Cytosolic delivery of granzyme B by bacterial toxins: evidence that endosomal disruption, in addition to transmembrane pore formation, is an important function of perforin. *Mol. Cell Biol.* 19:8604-8615.
- Brunk, U. T., J. Neuzil, and J. W. Eaton. 2001. Lysosomal involvement in apoptosis. *Redox. Rep.* 6:91-97.
- Buzza, M. S., L. Zamurs, J. Sun, C. H. Bird, A. I. Smith, J. A. Trapani, C. J. Froelich, E. C. Nice, and P. I. Bird. 2005. Extracellular matrix remodeling by human granzyme B via cleavage of vitronectin, fibronectin, and laminin. *J. Biol. Chem.* 280:23549-23558.
- Caputo, A., R. S. Garner, U. Winkler, D. Hudig, and R. C. Bleackley. 1993. Activation of recombinant murine cytotoxic cell proteinase-1 requires deletion of an amino-terminal dipeptide. *J. Biol. Chem.* 268:17672-17675.
- Caputo, A., M. N. James, J. C. Powers, D. Hudig, and R. C. Bleackley. 1994. Conversion of the substrate specificity of mouse proteinase granzyme B. *Nat. Struct. Biol.* 1:364-367.

- Chiu, V. K., C. M. Walsh, C. C. Liu, J. C. Reed, and W. R. Clark. 1995. Bcl-2 blocks degranulation but not fas-based cell-mediated cytotoxicity. *J. Immunol.* 154:2023-2032.
- Cleghon, V., A. Piderit, D. E. Brough, and D. F. Klessig. 1993. Phosphorylation of the adenovirus DNA-binding protein and epitope mapping of monoclonal antibodies against it. *Virology* 197:564-575.
- Cosloy, S. D. and M. Oishi. 1973. Genetic transformation in *Escherichia coli* K12. *Proc. Natl. Acad. Sci. U. S. A* 70:84-87.
- Dagert, M. and S. D. Ehrlich. 1979. Prolonged incubation in calcium chloride improves the competence of *Escherichia coli* cells. *Gene* 6:23-28.
- Darmon, A. J., D. W. Nicholson, and R. C. Bleackley. 1995. Activation of the apoptotic protease CPP32 by cytotoxic T-cell-derived granzyme B. *Nature* 377:446-448.
- Davis, J. E., M. J. Smyth, and J. A. Trapani. 2001. Granzyme A and B-deficient killer lymphocytes are defective in eliciting DNA fragmentation but retain potent in vivo anti-tumor capacity. *Eur. J. Immunol.* 31:39-47.
- Dennert, G. and E. R. Podack. 1983. Cytolysis by H-2-specific T killer cells. Assembly of tubular complexes on target membranes. *J. Exp. Med.* 157:1483-1495.
- Diaz, C., A. T. Lee, D. J. McConkey, and A. J. Schroit. 1999. Phosphatidylserine externalization during differentiation-triggered apoptosis of erythroleukemic cells. *Cell Death. Differ.* 6:218-226.
- Dourmashkin, R. R., P. Deteix, C. B. Simone, and P. Henkart. 1980. Electron microscopic demonstration of lesions in target cell membranes associated with antibody-dependent cellular cytotoxicity. *Clin. Exp. Immunol.* 42:554-560.
- Duke, R. C., R. Chervenak, and J. J. Cohen. 1983. Endogenous endonuclease-induced DNA fragmentation: an early event in cell-mediated cytolysis. *Proc. Natl. Acad. Sci. U. S. A* 80:6361-6365.
- Ebnet, K., M. Hausmann, F. Lehmann-Grube, A. Mullbacher, M. Kopf, M. Lamers, and M. M. Simon. 1995. Granzyme A-deficient mice retain potent cell-mediated cytotoxicity. *EMBO J.* 14:4230-4239.
- Edwards, K. M., C. M. Kam, J. C. Powers, and J. A. Trapani. 1999. The human cytotoxic T cell granule serine protease granzyme H has chymotrypsin-like (chymase) activity and is taken up into cytoplasmic vesicles reminiscent of granzyme B-containing endosomes. *J. Biol. Chem.* 274:30468-30473.
- Estebanez-Perpina, E., P. Fuentes-Prior, D. Belorgey, M. Braun, R. Kiefersauer, K. Maskos, R. Huber, H. Rubin, and W. Bode. 2000. Crystal structure of the caspase activator human granzyme B, a proteinase highly specific for an Asp-P1 residue. *Biol. Chem.* 381:1203-1214.

- Fan, Z., P. J. Beresford, D. Y. Oh, D. Zhang, and J. Lieberman. 2003. Tumor suppressor NM23-H1 is a granzyme A-activated DNase during CTL-mediated apoptosis, and the nucleosome assembly protein SET is its inhibitor. *Cell* 112:659-672.
- Fehniger, T. A., S. F. Cai, X. Cao, A. J. Bredemeyer, R. M. Presti, A. R. French, and T. J. Ley. 2007. Acquisition of murine NK cell cytotoxicity requires the translation of a pre-existing pool of granzyme B and perforin mRNAs. *Immunity*. 26:798-811.
- Fellows, E., S. Gil-Parrado, D. E. Jenne, and F. C. Kurschus. 2007. Natural killer cell-derived human granzyme H induces an alternative, caspase-independent cell death program. *Blood*.
- Fink, T. M., P. Lichter, H. Wekerle, M. Zimmer, and D. E. Jenne. 1993. The human granzyme A (HFSP, CTLA3) gene maps to 5q11-q12 and defines a new locus of the serine protease superfamily. *Genomics* 18:401-403.
- Froelich, C. J., W. L. Hanna, G. G. Poirier, P. J. Duriez, D. D'Amours, G. S. Salvesen, E. S. Alnemri, W. C. Earnshaw, and G. M. Shah. 1996a. Granzyme B/perforin-mediated apoptosis of Jurkat cells results in cleavage of poly(ADP-ribose) polymerase to the 89-kDa apoptotic fragment and less abundant 64-kDa fragment. *Biochem. Biophys. Res. Commun.* 227:658-665.
- Froelich, C. J., K. Orth, J. Turbov, P. Seth, R. Gottlieb, B. Babior, G. M. Shah, R. C. Bleackley, V. M. Dixit, and W. Hanna. 1996b. New paradigm for lymphocyte granule-mediated cytotoxicity. Target cells bind and internalize granzyme B, but an endosomolytic agent is necessary for cytosolic delivery and subsequent apoptosis. *J. Biol. Chem.* 271:29073-29079.
- Gallwitz, M., J. M. Reimer, and L. Hellman. 2006. Expansion of the mast cell chymase locus over the past 200 million years of mammalian evolution. *Immunogenetics* 58:655-669.
- Garcia-Sanz, J. A., H. R. MacDonald, D. E. Jenne, J. Tschopp, and M. Nabholz. 1990. Cell specificity of granzyme gene expression. *J. Immunol.* 145:3111-3118.
- Griffiths, G. M. and S. Isaaz. 1993. Granzymes A and B are targeted to the lytic granules of lymphocytes by the mannose-6-phosphate receptor. *J. Cell Biol.* 120:885-896.
- Grossman, W. J., P. A. Revell, Z. H. Lu, H. Johnson, A. J. Bredemeyer, and T. J. Ley. 2003. The orphan granzymes of humans and mice. *Curr. Opin. Immunol.* 15:544-552.
- Grossman, W. J., J. W. Verbsky, B. L. Tollefsen, C. Kemper, J. P. Atkinson, and T. J. Ley. 2004. Differential expression of granzymes A and B in human cytotoxic lymphocyte subsets and T regulatory cells. *Blood* 104:2840-2848.
- Guicciardi, M. E., M. Leist, and G. J. Gores. 2004. Lysosomes in cell death. *Oncogene* 23:2881-2890.
- Haddad, P., D. Jenne, J. Tschopp, M. V. Clement, D. Mathieu-Mahul, and M. Sasportes. 1991. Structure and evolutionary origin of the human granzyme H gene. *Int. Immunol.* 3:57-66.

- Hannig, G. and S. C. Makrides. 1998. Strategies for optimizing heterologous protein expression in *Escherichia coli*. *Trends Biotechnol.* 16:54-60.
- Heibei, J. A., M. Barry, B. Motyka, and R. C. Bleackley. 1999. Granzyme B-induced loss of mitochondrial inner membrane potential ( $\Delta\Psi_m$ ) and cytochrome c release are caspase independent. *J. Immunol.* 163:4683-4693.
- Heibei, J. A., I. S. Goping, M. Barry, M. J. Pinkoski, G. C. Shore, D. R. Green, and R. C. Bleackley. 2000. Granzyme B-mediated cytochrome c release is regulated by the Bcl-2 family members bcl-2 and bax. *J. Exp. Med.* 192:1391-1402.
- Henkart, P. A. 1985. Mechanism of lymphocyte-mediated cytotoxicity. *Annu. Rev. Immunol.* 3:31-58.
- Henkart, P. A., M. S. Williams, C. M. Zacharchuk, and A. Sarin. 1997. Do CTL kill target cells by inducing apoptosis? *Semin. Immunol.* 9:135-144.
- Herrmann, M., H. M. Lorenz, R. Voll, M. Grunke, W. Woith, and J. R. Kalden. 1994. A rapid and simple method for the isolation of apoptotic DNA fragments. *Nucleic Acids Res.* 22:5506-5507.
- Heusel, J. W., R. L. Wesselschmidt, S. Shresta, J. H. Russell, and T. J. Ley. 1994. Cytotoxic lymphocytes require granzyme B for the rapid induction of DNA fragmentation and apoptosis in allogeneic target cells. *Cell* 76:977-987.
- Hink-Schauer, C., E. Estebanez-Perpina, F. C. Kurschus, W. Bode, and D. E. Jenne. 2003. Crystal structure of the apoptosis-inducing human granzyme A dimer. *Nat. Struct. Biol.* 10:535-540.
- Horwitz, M., K. F. Benson, Z. Duan, F. Q. Li, and R. E. Person. 2004. Hereditary neutropenia: dogs explain human neutrophil elastase mutations. *Trends Mol. Med.* 10:163-170.
- Jacobs, R., G. Hintzen, A. Kemper, K. Beul, S. Kempf, G. Behrens, K. W. Sykora, and R. E. Schmidt. 2001. CD56bright cells differ in their KIR repertoire and cytotoxic features from CD56dim NK cells. *Eur. J. Immunol.* 31:3121-3127.
- Jans, D. A., P. Jans, L. J. Briggs, V. Sutton, and J. A. Trapani. 1996. Nuclear transport of granzyme B (fragmentin-2). Dependence of perforin in vivo and cytosolic factors in vitro. *J. Biol. Chem.* 271:30781-30789.
- Jenne, D., C. Rey, J. A. Haefliger, B. Y. Qiao, P. Groscurth, and J. Tschopp. 1988a. Identification and sequencing of cDNA clones encoding the granule-associated serine proteases granzymes D, E, and F of cytolytic T lymphocytes. *Proc. Natl. Acad. Sci. U. S. A.* 85:4814-4818.
- Jenne, D., C. Rey, D. Masson, K. K. Stanley, J. Herz, G. Plaetinck, and J. Tschopp. 1988b. cDNA cloning of granzyme C, a granule-associated serine protease of cytolytic T lymphocytes. *J. Immunol.* 140:318-323.

- Jenne, D. E. 1994. Structure of the azurocidin, proteinase 3, and neutrophil elastase genes. Implications for inflammation and vasculitis. *Am. J. Respir. Crit Care Med.* 150:S147-S154.
- Jenne, D. E., D. Masson, M. Zimmer, J. A. Haefliger, W. H. Li, and J. Tschopp. 1989. Isolation and complete structure of the lymphocyte serine protease granzyme G, a novel member of the granzyme multigene family in murine cytolytic T lymphocytes. Evolutionary origin of lymphocyte proteases. *Biochemistry* 28:7953-7961.
- Jenne, D. E., M. Zimmer, J. A. Garcia-Sanz, J. Tschopp, and P. Lichter. 1991. Genomic organization and subchromosomal in situ localization of the murine granzyme F, a serine protease expressed in CD8+ T cells. *J. Immunol.* 147:1045-1052.
- Johnson, H., L. Scorrano, S. J. Korsmeyer, and T. J. Ley. 2003. Cell death induced by granzyme C. *Blood* 101:3093-3101.
- Kagan, V. E., B. Gleiss, Y. Y. Tyurina, V. A. Tyurin, C. Elenstrom-Magnusson, S. X. Liu, F. B. Serinkan, A. Arroyo, J. Chandra, S. Orrenius, and B. Fadeel. 2002. A role for oxidative stress in apoptosis: oxidation and externalization of phosphatidylserine is required for macrophage clearance of cells undergoing Fas-mediated apoptosis. *J. Immunol.* 169:487-499.
- Kagi, D., B. Ledermann, K. Burki, P. Seiler, B. Odermatt, K. J. Olsen, E. R. Podack, R. M. Zinkernagel, and H. Hengartner. 1994. Cytotoxicity mediated by T cells and natural killer cells is greatly impaired in perforin-deficient mice. *Nature* 369:31-37.
- Kam, C. M., D. Hudig, and J. C. Powers. 2000. Granzymes (lymphocyte serine proteases): characterization with natural and synthetic substrates and inhibitors. *Biochim. Biophys. Acta* 1477:307-323.
- Keefe, D., L. Shi, S. Feske, R. Massol, F. Navarro, T. Kirchhausen, and J. Lieberman. 2005. Perforin triggers a plasma membrane-repair response that facilitates CTL induction of apoptosis. *Immunity* 23:249-262.
- Kelly, J. M., N. J. Waterhouse, E. Cretney, K. A. Browne, S. Ellis, J. A. Trapani, and M. J. Smyth. 2004. Granzyme M mediates a novel form of perforin-dependent cell death. *J. Biol. Chem.* 279:22236-22242.
- Kelly, K. J., R. M. Sandoval, K. W. Dunn, B. A. Molitoris, and P. C. Dagher. 2003. A novel method to determine specificity and sensitivity of the TUNEL reaction in the quantitation of apoptosis. *Am. J. Physiol Cell Physiol* 284:C1309-C1318.
- Kothakota, S., T. Azuma, C. Reinhard, A. Klippel, J. Tang, K. Chu, T. J. McGarry, M. W. Kirschner, K. Koths, D. J. Kwiatkowski, and L. T. Williams. 1997. Caspase-3-generated fragment of gelsolin: effector of morphological change in apoptosis. *Science* 278:294-298.
- Kramer, M. D. and M. M. Simon. 1987. Are proteinases functional molecules of T lymphocytes. *Immunol. Today* 8:140-142.

- Kuhn, J. R. and M. Poenie. 2002. Dynamic polarization of the microtubule cytoskeleton during CTL-mediated killing. *Immunity*. 16:111-121.
- Kummer, J. A., A. M. Kamp, M. van Katwijk, J. P. Brakenhoff, K. Radosevic, A. M. van Leeuwen, J. Borst, C. L. Verweij, and C. E. Hack. 1993. Production and characterization of monoclonal antibodies raised against recombinant human granzymes A and B and showing cross reactions with the natural proteins. *J. Immunol. Methods* 163:77-83.
- Kurschus, F. C., R. Bruno, E. Fellows, C. S. Falk, and D. E. Jenne. 2005. Membrane receptors are not required to deliver granzyme B during killer cell attack. *Blood* 105:2049-2058.
- Kurschus, F. C., M. Kleinschmidt, E. Fellows, K. Dornmair, R. Rudolph, H. Lilie, and D. E. Jenne. 2004. Killing of target cells by redirected granzyme B in the absence of perforin. *FEBS Lett.* 562:87-92.
- Laemmli, U. K. 1970. Cleavage of structural proteins during the assembly of the head of bacteriophage T4. *Nature* 227:680-685.
- Lassus, P., X. Opitz-Araya, and Y. Lazebnik. 2002. Requirement for caspase-2 in stress-induced apoptosis before mitochondrial permeabilization. *Science* 297:1352-1354.
- Lauber, K., S. G. Blumenthal, M. Waibel, and S. Wesselborg. 2004. Clearance of apoptotic cells: getting rid of the corpses. *Mol. Cell* 14:277-287.
- Lauber, K., E. Bohn, S. M. Krober, Y. J. Xiao, S. G. Blumenthal, R. K. Lindemann, P. Marini, C. Wiedig, A. Zobywalski, S. Baksh, Y. Xu, I. B. Autenrieth, K. Schulze-Osthoff, C. Belka, G. Stuhler, and S. Wesselborg. 2003. Apoptotic cells induce migration of phagocytes via caspase-3-mediated release of a lipid attraction signal. *Cell* 113:717-730.
- Li, L. Y., X. Luo, and X. Wang. 2001. Endonuclease G is an apoptotic DNase when released from mitochondria. *Nature* 412:95-99.
- Lieberman, J. 2003. The ABCs of granule-mediated cytotoxicity: new weapons in the arsenal. *Nat. Rev. Immunol.* 3:361-370.
- Lieberman, J. and Z. Fan. 2003. Nuclear war: the granzyme A-bomb. *Curr. Opin. Immunol.* 15:553-559.
- Lobe, C. G., B. B. Finlay, W. Paranchych, V. H. Paetkau, and R. C. Bleackley. 1986. Novel serine proteases encoded by two cytotoxic T lymphocyte-specific genes. *Science* 232:858-861.
- Loh, J., D. A. Thomas, P. A. Revell, T. J. Ley, and H. W. Virgin. 2004. Granzymes and caspase 3 play important roles in control of gammaherpesvirus latency. *J. Virol.* 78:12519-12528.

- Lu, H., Q. Hou, T. Zhao, H. Zhang, Q. Zhang, L. Wu, and Z. Fan. 2006. Granzyme M directly cleaves inhibitor of caspase-activated DNase (CAD) to unleash CAD leading to DNA fragmentation. *J. Immunol.* 177:1171-1178.
- MacDonald, G., L. Shi, V. C. Vande, J. Lieberman, and A. H. Greenberg. 1999. Mitochondria-dependent and -independent regulation of Granzyme B-induced apoptosis. *J. Exp. Med.* 189:131-144.
- MacIvor, D. M., C. T. Pham, and T. J. Ley. 1999. The 5' flanking region of the human granzyme H gene directs expression to T/natural killer cell progenitors and lymphokine-activated killer cells in transgenic mice. *Blood* 93:963-973.
- Mahrus, S. and C. S. Craik. 2005. Selective chemical functional probes of granzymes A and B reveal granzyme B is a major effector of natural killer cell-mediated lysis of target cells. *Chem. Biol.* 12:567-577.
- Martin, S. J., D. M. Finucane, G. P. Amarante-Mendes, G. A. O'Brien, and D. R. Green. 1996. Phosphatidylserine externalization during CD95-induced apoptosis of cells and cytoplasts requires ICE/CED-3 protease activity. *J. Biol. Chem.* 271:28753-28756.
- Martinvalet, D., P. Zhu, and J. Lieberman. 2005. Granzyme A induces caspase-independent mitochondrial damage, a required first step for apoptosis. *Immunity.* 22:355-370.
- Masson, D., P. J. Peters, H. J. Geuze, J. Borst, and J. Tschopp. 1990. Interaction of chondroitin sulfate with perforin and granzymes of cytolytic T-cells is dependent on pH. *Biochemistry* 29:11229-11235.
- Masson, D., M. Zamai, and J. Tschopp. 1986. Identification of granzyme A isolated from cytotoxic T-lymphocyte-granules as one of the proteases encoded by CTL-specific genes. *FEBS Lett.* 208:84-88.
- Matsumoto, R., A. Sali, N. Ghildyal, M. Karplus, and R. L. Stevens. 1995. Packaging of proteases and proteoglycans in the granules of mast cells and other hematopoietic cells. A cluster of histidines on mouse mast cell protease 7 regulates its binding to heparin serglycin proteoglycans. *J. Biol. Chem.* 270:19524-19531.
- McGuire, M. J., P. E. Lipsky, and D. L. Thiele. 1993. Generation of active myeloid and lymphoid granule serine proteases requires processing by the granule thiol protease dipeptidyl peptidase I. *J. Biol. Chem.* 268:2458-2467.
- Metkar, S. S., B. Wang, M. Aguilar-Santelises, S. M. Raja, L. Uhlin-Hansen, E. Podack, J. A. Trapani, and C. J. Froelich. 2002. Cytotoxic cell granule-mediated apoptosis: perforin delivers granzyme B- serglycin complexes into target cells without plasma membrane pore formation. *Immunity* 16:417-428.
- Metkar, S. S., B. Wang, M. L. Ebbs, J. H. Kim, Y. J. Lee, S. M. Raja, and C. J. Froelich. 2003. Granzyme B activates procaspase-3 which signals a mitochondrial amplification loop for maximal apoptosis. *J. Cell Biol.* 160:875-885.



- Meyer, T. S. and B. L. Lamberts. 1965. Use of coomassie brilliant blue R250 for the electrophoresis of microgram quantities of parotid saliva proteins on acrylamide-gel strips. *Biochim. Biophys. Acta* 107:144-145.
- Michallet, M. C., F. Saltel, X. Preville, M. Flacher, J. P. Revillard, and L. Genestier. 2003. Cathepsin-B-dependent apoptosis triggered by antithymocyte globulins: a novel mechanism of T-cell depletion. *Blood* 102:3719-3726.
- Moffatt, B. A. and F. W. Studier. 1987. T7 lysozyme inhibits transcription by T7 RNA polymerase. *Cell* 49:221-227.
- Mullbacher, A., K. Ebnet, R. V. Blanden, R. T. Hla, T. Stehle, C. Museteanu, and M. M. Simon. 1996. Granzyme A is critical for recovery of mice from infection with the natural cytopathic viral pathogen, ectromelia. *Proc. Natl. Acad. Sci. U. S. A* 93:5783-5787.
- Mullbacher, A., P. Waring, H. R. Tha, T. Tran, S. Chin, T. Stehle, C. Museteanu, and M. M. Simon. 1999. Granzymes are the essential downstream effector molecules for the control of primary virus infections by cytolytic leukocytes. *Proc. Natl. Acad. Sci. U. S. A* 96:13950-13955.
- Naito, M., K. Nagashima, T. Mashima, and T. Tsuruo. 1997. Phosphatidylserine externalization is a downstream event of interleukin-1 beta-converting enzyme family protease activation during apoptosis. *Blood* 89:2060-2066.
- Nakajima, H., H. L. Park, and P. A. Henkart. 1995. Synergistic roles of granzymes A and B in mediating target cell death by rat basophilic leukemia mast cell tumors also expressing cytolysin/perforin. *J. Exp. Med.* 181:1037-1046.
- Neumann, H., I. M. Medana, J. Bauer, and H. Lassmann. 2002. Cytotoxic T lymphocytes in autoimmune and degenerative CNS diseases. *Trends Neurosci.* 25:313-319.
- Ortaldo, J. R., A. Mason, and R. Overton. 1986. Lymphokine-activated killer cells. Analysis of progenitors and effectors. *J. Exp. Med.* 164:1193-1205.
- Pao, L. I., N. Sumaria, J. M. Kelly, S. van Dommelen, E. Cretney, M. E. Wallace, D. A. Anthony, A. P. Uldrich, D. I. Godfrey, J. M. Papadimitriou, A. Mullbacher, M. A. Degli-Esposti, and M. J. Smyth. 2005. Functional analysis of granzyme M and its role in immunity to infection. *J. Immunol.* 175:3235-3243.
- Pereira, R. A., M. M. Simon, and A. Simmons. 2000. Granzyme A, a noncytolytic component of CD8(+) cell granules, restricts the spread of herpes simplex virus in the peripheral nervous systems of experimentally infected mice. *J. Virol.* 74:1029-1032.
- Perfettini, J. L. and G. Kroemer. 2003. Caspase activation is not death. *Nat. Immunol.* 4:308-310.
- Pham, C. T., R. J. Armstrong, D. B. Zimonjic, N. C. Popescu, D. G. Payan, and T. J. Ley. 1997. Molecular cloning, chromosomal localization, and expression of murine dipeptidyl peptidase I. *J. Biol. Chem.* 272:10695-10703.

- Pham, C. T., J. L. Ivanovich, S. Z. Raptis, B. Zehnbauser, and T. J. Ley. 2004. Papillon-Lefevre syndrome: correlating the molecular, cellular, and clinical consequences of cathepsin C/dipeptidyl peptidase I deficiency in humans. *J. Immunol.* 173:7277-7281.
- Pham, C. T., D. M. MacIvor, B. A. Hug, J. W. Heusel, and T. J. Ley. 1996. Long-range disruption of gene expression by a selectable marker cassette. *Proc. Natl. Acad. Sci. U. S. A* 93:13090-13095.
- Phillips, J. H. and L. L. Lanier. 1986. Dissection of the lymphokine-activated killer phenomenon. Relative contribution of peripheral blood natural killer cells and T lymphocytes to cytotoxicity. *J. Exp. Med.* 164:814-825.
- Pinkoski, M. J., M. Hobman, J. A. Heibein, K. Tomaselli, F. Li, P. Seth, C. J. Froelich, and R. C. Bleackley. 1998. Entry and trafficking of granzyme B in target cells during granzyme B-perforin-mediated apoptosis. *Blood* 92:1044-1054.
- Pipkin, M. E. and J. Lieberman. 2007. Delivering the kiss of death: progress on understanding how perforin works. *Curr. Opin. Immunol.* 19:301-308.
- Podack, E. R. and P. J. Konigsberg. 1984. Cytolytic T cell granules. Isolation, structural, biochemical, and functional characterization. *J. Exp. Med.* 160:695-710.
- Proskuryakov, S. Y., V. L. Gabai, A. G. Konoplyannikov, I. A. Zamulaeva, and A. I. Kolesnikova. 2005. Immunology of apoptosis and necrosis. *Biochemistry (Mosc.)* 70:1310-1320.
- Raja, S. M., B. Wang, M. Dantuluri, U. R. Desai, B. Demeler, K. Spiegel, S. S. Metkar, and C. J. Froelich. 2002. Cytotoxic cell granule-mediated apoptosis. Characterization of the macromolecular complex of granzyme B with serglycin. *J. Biol. Chem.* 277:49523-49530.
- Rao, N. V., G. V. Rao, B. C. Marshall, and J. R. Hoidal. 1996. Biosynthesis and processing of proteinase 3 in U937 cells. Processing pathways are distinct from those of cathepsin G. *J. Biol. Chem.* 271:2972-2978.
- Revell, P. A., W. J. Grossman, D. A. Thomas, X. Cao, R. Behl, J. A. Ratner, Z. H. Lu, and T. J. Ley. 2005. Granzyme B and the downstream granzymes C and/or F are important for cytotoxic lymphocyte functions. *J. Immunol.* 174:2124-2131.
- Riedl, S. J., P. Fuentes-Prior, M. Renatus, N. Kairies, S. Krapp, R. Huber, G. S. Salvesen, and W. Bode. 2001. Structural basis for the activation of human procaspase-7. *Proc. Natl. Acad. Sci. U. S. A* 98:14790-14795.
- Riedl, S. J., W. Li, Y. Chao, R. Schwarzenbacher, and Y. Shi. 2005. Structure of the apoptotic protease-activating factor 1 bound to ADP. *Nature* 434:926-933.
- Robertson, J. D., V. Gogvadze, A. Kropotov, H. Vakifahmetoglu, B. Zhivotovsky, and S. Orrenius. 2004. Processed caspase-2 can induce mitochondria-mediated apoptosis independently of its enzymatic activity. *EMBO Rep.* 5:643-648.

- Rodriguez, A., P. Webster, J. Ortego, and N. W. Andrews. 1997. Lysosomes behave as  $\text{Ca}^{2+}$ -regulated exocytic vesicles in fibroblasts and epithelial cells. *J. Cell Biol.* 137:93-104.
- Rosenberg, A. H., B. N. Lade, D. S. Chui, S. W. Lin, J. J. Dunn, and F. W. Studier. 1987. Vectors for selective expression of cloned DNAs by T7 RNA polymerase. *Gene* 56:125-135.
- Rossi, C. P., A. McAllister, M. Tanguy, D. Kagi, and M. Brahic. 1998. Theiler's virus infection of perforin-deficient mice. *J. Virol.* 72:4515-4519.
- Rozman-Pungercar, J., N. Kopitar-Jerala, M. Bogyo, D. Turk, O. Vasiljeva, I. Stefe, P. Vandenabeele, D. Bromme, V. Puizdar, M. Fonovic, M. Trstenjak-Prebanda, I. Dolenc, V. Turk, and B. Turk. 2003. Inhibition of papain-like cysteine proteases and legumain by caspase-specific inhibitors: when reaction mechanism is more important than specificity. *Cell Death. Differ.* 10:881-888.
- Rudolph, R. and H. Lilie. 1996. In vitro folding of inclusion body proteins. *FASEB J.* 10:49-56.
- Sanger, F., G. M. Air, B. G. Barrell, N. L. Brown, A. R. Coulson, C. A. Fiddes, C. A. Hutchison, P. M. Slocombe, and M. Smith. 1977. Nucleotide sequence of bacteriophage phi X174 DNA. *Nature* 265:687-695.
- Sarin, A., M. S. Williams, M. A. Alexander-Miller, J. A. Berzofsky, C. M. Zacharchuk, and P. A. Henkart. 1997. Target cell lysis by CTL granule exocytosis is independent of ICE/Ced-3 family proteases. *Immunity.* 6:209-215.
- Savill, J., I. Dransfield, C. Gregory, and C. Haslett. 2002. A blast from the past: clearance of apoptotic cells regulates immune responses. *Nat. Rev. Immunol.* 2:965-975.
- Sayers, T. J., A. D. Brooks, J. M. Ward, T. Hoshino, W. E. Bere, G. W. Wiegand, J. M. Kelly, and M. J. Smyth. 2001. The restricted expression of granzyme M in human lymphocytes. *J. Immunol.* 166:765-771.
- Schechter, I. and A. Berger. 1967. On the size of the active site in proteases. I. Papain. *Biochem. Biophys. Res. Commun.* 27:157-162.
- Sedelies, K. A., T. J. Sayers, K. M. Edwards, W. Chen, D. G. Pellicci, D. I. Godfrey, and J. A. Trapani. 2004. Discordant regulation of granzyme H and granzyme B expression in human lymphocytes. *J. Biol. Chem.* 279:26581-26587.
- Sharif-Askari, E., A. Alam, E. Rheaume, P. J. Beresford, C. Scotto, K. Sharma, D. Lee, W. E. DeWolf, M. E. Nuttall, J. Lieberman, and R. P. Sekaly. 2001. Direct cleavage of the human DNA fragmentation factor-45 by granzyme B induces caspase-activated DNase release and DNA fragmentation. *EMBO J.* 20:3101-3113.
- Shi, L., R. P. Kraut, R. Aebersold, and A. H. Greenberg. 1992. A natural killer cell granule protein that induces DNA fragmentation and apoptosis. *J. Exp. Med.* 175:553-566.

- Shresta, S., T. A. Graubert, D. A. Thomas, S. Z. Raptis, and T. J. Ley. 1999. Granzyme A initiates an alternative pathway for granule-mediated apoptosis. *Immunity*. 10:595-605.
- Shresta, S., J. W. Heusel, D. M. MacIvor, R. L. Wesselschmidt, J. H. Russell, and T. J. Ley. 1995. Granzyme B plays a critical role in cytotoxic lymphocyte-induced apoptosis. *Immunol. Rev.* 146:211-221.
- Simon, M. M., M. Hausmann, T. Tran, K. Ebnet, J. Tschopp, R. ThaHla, and A. Mullbacher. 1997. In vitro- and ex vivo-derived cytolytic leukocytes from granzyme A x B double knockout mice are defective in granule-mediated apoptosis but not lysis of target cells. *J. Exp. Med.* 186:1781-1786.
- Smyth, M. J., M. J. McGuire, and K. Y. Thia. 1995. Expression of recombinant human granzyme B. A processing and activation role for dipeptidyl peptidase I. *J. Immunol.* 154:6299-6305.
- Smyth, M. J., T. J. Sayers, T. Wiltout, J. C. Powers, and J. A. Trapani. 1993. Met-ase: cloning and distinct chromosomal location of a serine protease preferentially expressed in human natural killer cells. *J. Immunol.* 151:6195-6205.
- Smyth, M. J., S. E. Street, and J. A. Trapani. 2003. Cutting edge: granzymes A and B are not essential for perforin-mediated tumor rejection. *J. Immunol.* 171:515-518.
- Spaeny-Dekking, E. H., A. M. Kamp, C. J. Froelich, and C. E. Hack. 2000. Extracellular granzyme A, complexed to proteoglycans, is protected against inactivation by protease inhibitors. *Blood* 95:1465-1472.
- Stinchcombe, J. C., G. Bossi, S. Booth, and G. M. Griffiths. 2001. The immunological synapse of CTL contains a secretory domain and membrane bridges. *Immunity*. 15:751-761.
- Stinchcombe, J. C. and G. M. Griffiths. 2006. Secretory Mechanisms in Cell-Mediated Cytotoxicity. *Annu. Rev. Cell Dev. Biol.*
- Stoka, V., B. Turk, S. L. Schendel, T. H. Kim, T. Cirman, S. J. Snipas, L. M. Ellerby, D. Bredesen, H. Freeze, M. Abrahamson, D. Bromme, S. Krajewski, J. C. Reed, X. M. Yin, V. Turk, and G. S. Salvesen. 2001. Lysosomal protease pathways to apoptosis. Cleavage of bid, not pro-caspases, is the most likely route. *J. Biol. Chem.* 276:3149-3157.
- Studier, F. W. 1991. Use of bacteriophage T7 lysozyme to improve an inducible T7 expression system. *J. Mol. Biol.* 219:37-44.
- Suck, G., D. R. Branch, M. J. Smyth, R. G. Miller, J. Vergidis, S. Fahim, and A. Keating. 2005. KHYG-1, a model for the study of enhanced natural killer cell cytotoxicity. *Exp. Hematol.* 33:1160-1171.
- Sugawara, S. 2005. Immune functions of proteinase 3. *Crit Rev. Immunol.* 25:343-360.

- Sutton, V. R., J. E. Davis, M. Cancilla, R. W. Johnstone, A. A. Ruefli, K. Sedelies, K. A. Browne, and J. A. Trapani. 2000. Initiation of apoptosis by granzyme B requires direct cleavage of bid, but not direct granzyme B-mediated caspase activation. *J. Exp. Med.* 192:1403-1414.
- Sutton, V. R., D. L. Vaux, and J. A. Trapani. 1997. Bcl-2 prevents apoptosis induced by perforin and granzyme B, but not that mediated by whole cytotoxic lymphocytes. *J. Immunol.* 158:5783-5790.
- Thiele, D. L., M. J. McGuire, and P. E. Lipsky. 1997. A selective inhibitor of dipeptidyl peptidase I impairs generation of CD8<sup>+</sup> T cell cytotoxic effector function. *J. Immunol.* 158:5200-5210.
- Thomas, D. A., C. Du, M. Xu, X. Wang, and T. J. Ley. 2000. DFF45/ICAD can be directly processed by granzyme B during the induction of apoptosis. *Immunity.* 12:621-632.
- Towbin, H., T. Staehelin, and J. Gordon. 1979. Electrophoretic transfer of proteins from polyacrylamide gels to nitrocellulose sheets: procedure and some applications. *Proc. Natl. Acad. Sci. U. S. A* 76:4350-4354.
- Trapani, J. A. 2001. Granzymes: a family of lymphocyte granule serine proteases. *Genome Biol.* 2:REVIEWS3014.
- Trapani, J. A., D. A. Jans, P. J. Jans, M. J. Smyth, K. A. Browne, and V. R. Sutton. 1998. Efficient nuclear targeting of granzyme B and the nuclear consequences of apoptosis induced by granzyme B and perforin are caspase-dependent, but cell death is caspase-independent. *J. Biol. Chem.* 273:27934-27938.
- Trapani, J. A. and M. J. Smyth. 2002. Functional significance of the perforin/granzyme cell death pathway. *Nat. Rev. Immunol.* 2:735-747.
- Trapani, J. A. and V. R. Sutton. 2003. Granzyme B: pro-apoptotic, antiviral and antitumor functions. *Curr. Opin. Immunol.* 15:533-543.
- Tschopp, J., D. Masson, and K. K. Stanley. 1986. Structural/functional similarity between proteins involved in complement- and cytotoxic T-lymphocyte-mediated cytolysis. *Nature* 322:831-834.
- Turk, B., D. Turk, and V. Turk. 2000. Lysosomal cysteine proteases: more than scavengers. *Biochim. Biophys. Acta* 1477:98-111.
- Tyurina, Y. Y., F. B. Serinkan, V. A. Tyurin, V. Kini, J. C. Yalowich, A. J. Schroit, B. Fadeel, and V. E. Kagan. 2004. Lipid antioxidant, etoposide, inhibits phosphatidylserine externalization and macrophage clearance of apoptotic cells by preventing phosphatidylserine oxidation. *J. Biol. Chem.* 279:6056-6064.
- van den Broek, M. E., D. Kagi, F. Ossendorp, R. Toes, S. Vamvakas, W. K. Lutz, C. J. Melief, R. M. Zinkernagel, and H. Hengartner. 1996. Decreased tumor surveillance in perforin-deficient mice. *J. Exp. Med.* 184:1781-1790.

- Waley, I., S. C. Bhakdi, F. Hofmann, N. Djonder, A. Valeva, K. Aktories, and S. Bhakdi. 2001. Delivery of proteins into living cells by reversible membrane permeabilization with streptolysin-O. *Proc. Natl. Acad. Sci. U. S. A* 98:3185-3190.
- Waterhouse, N. J., V. R. Sutton, K. A. Sedelies, A. Ciccone, M. Jenkins, S. J. Turner, P. I. Bird, and J. A. Trapani. 2006. Cytotoxic T lymphocyte-induced killing in the absence of granzymes A and B is unique and distinct from both apoptosis and perforin-dependent lysis. *J. Cell Biol.* 173:133-144.
- Wilharm, E., M. A. Parry, R. Friebe, H. Tschesche, G. Matschiner, C. P. Sommerhoff, and D. E. Jenne. 1999. Generation of catalytically active granzyme K from *Escherichia coli* inclusion bodies and identification of efficient granzyme K inhibitors in human plasma. *J. Biol. Chem.* 274:27331-27337.
- Williams, M. S. and P. A. Henkart. 2005. Do cytotoxic lymphocytes kill via reactive oxygen species? *Immunity*. 22:272-274.
- Wolf, B. B., M. Schuler, F. Echeverri, and D. R. Green. 1999. Caspase-3 is the primary activator of apoptotic DNA fragmentation via DNA fragmentation factor-45/inhibitor of caspase-activated DNase inactivation. *J. Biol. Chem.* 274:30651-30656.
- Woodard, S. L., S. A. Fraser, U. Winkler, D. S. Jackson, C. M. Kam, J. C. Powers, and D. Hudig. 1998. Purification and characterization of lymphocyte chymase I, a granzyme implicated in perforin-mediated lysis. *J. Immunol.* 160:4988-4993.
- Woodard, S. L., D. S. Jackson, A. S. Abuelyaman, J. C. Powers, U. Winkler, and D. Hudig. 1994. Chymase-directed serine protease inhibitor that reacts with a single 30-kDa granzyme and blocks NK-mediated cytotoxicity. *J. Immunol.* 153:5016-5025.
- Xia, Z., C. M. Kam, C. Huang, J. C. Powers, R. J. Mandle, R. L. Stevens, and J. Lieberman. 1998. Expression and purification of enzymatically active recombinant granzyme B in a baculovirus system. *Biochem. Biophys. Res. Commun.* 243:384-389.
- Yang, J., X. Liu, K. Bhalla, C. N. Kim, A. M. Ibrado, J. Cai, T. I. Peng, D. P. Jones, and X. Wang. 1997. Prevention of apoptosis by Bcl-2: release of cytochrome c from mitochondria blocked. *Science* 275:1129-1132.
- Zagury, D. 1982. Direct analysis of individual killer T cells: susceptibility of target cells to lysis and secretion of hydrolytic enzymes by CTL. *Adv. Exp. Med. Biol.* 146:149-169.
- Zajac, A. J., J. M. Dye, and D. G. Quinn. 2003. Control of lymphocytic choriomeningitis virus infection in granzyme B deficient mice. *Virology* 305:1-9.
- Zhang, D., P. J. Beresford, A. H. Greenberg, and J. Lieberman. 2001. Granzymes A and B directly cleave lamins and disrupt the nuclear lamina during granule-mediated cytolysis. *Proc. Natl. Acad. Sci. U. S. A* 98:5746-5751.
- Zhao, H., J. Joseph, H. M. Fales, E. A. Sokoloski, R. L. Levine, J. Vasquez-Vivar, and B. Kalyanaraman. 2005. Detection and characterization of the product of hydroethidine

- and intracellular superoxide by HPLC and limitations of fluorescence. *Proc. Natl. Acad. Sci. U. S. A* 102:5727-5732.
- Zhao, H., S. Kalivendi, H. Zhang, J. Joseph, K. Nithipatikom, J. Vasquez-Vivar, and B. Kalyanaraman. 2003a. Superoxide reacts with hydroethidine but forms a fluorescent product that is distinctly different from ethidium: potential implications in intracellular fluorescence detection of superoxide. *Free Radic. Biol. Med.* 34:1359-1368.
- Zhao, M., F. Antunes, J. W. Eaton, and U. T. Brunk. 2003b. Lysosomal enzymes promote mitochondrial oxidant production, cytochrome c release and apoptosis. *Eur. J. Biochem.* 270:3778-3786.
- Zhao, T., H. Zhang, Y. Guo, and Z. Fan. 2007a. Granzyme K directly processes bid to release cytochrome c and endonuclease G leading to mitochondria-dependent cell death. *J. Biol. Chem.* 282:12104-12111.
- Zhao, T., H. Zhang, Y. Guo, Q. Zhang, G. Hua, H. Lu, Q. Hou, H. Liu, and Z. Fan. 2007b. Granzyme K cleaves the nucleosome assembly protein SET to induce single-stranded DNA nicks of target cells. *Cell Death. Differ.* 14:489-499.
- Zhivotovsky, B. and S. Orrenius. 2005. Caspase-2 function in response to DNA damage. *Biochem. Biophys. Res. Commun.* 331:859-867.
- Zong, W. X. and C. B. Thompson. 2006. Necrotic death as a cell fate. *Genes Dev.* 20:1-15.
- Zou, H., Y. Li, X. Liu, and X. Wang. 1999. An APAF-1.cytochrome c multimeric complex is a functional apoptosome that activates procaspase-9. *J. Biol. Chem.* 274:11549-11556.

**VIII - Abbreviations and Initialisms**

$\Delta\Psi$	Membrane potential
$\varepsilon$	Absorption coefficient
<b>A</b>	
A	Absorbance
a.a	Amino acid
A.A	Acrylamide
Ab	Antibody
AFC	7-Amino-3-trifluoromethylcoumarine
AMC	7-Amino-4-Methylcoumarin
ATP	Adeninetriphosphate
AV	Annexin V
<b>B</b>	
b	path length
Bid	<b>B</b> H3 interacting domain death agonist
t-Bid	Truncated <b>Bid</b>
BSA	Bovine Albumin
bp	<b>B</b> ase <b>p</b> air
<b>C</b>	
c	concentration
CAD / ICAD	<b>C</b> aspase <b>a</b> ctivated <b>D</b> Nase / <b>I</b> nhibitor of <b>CAD</b>
CG	<b>C</b> athepsin <b>G</b>
CD	<b>C</b> luster of <b>D</b> ifferentiation
cDNA	<b>C</b> omplementary <b>DNA</b>
CML	<b>C</b> hronic <b>M</b> yelogenous <b>L</b> eukemia
CTH	<b>C</b> hymotrypsin
CTL	<b>C</b> ytotoxic <b>L</b> ymphocyte
Cyt.c	<b>C</b> ytochrome <b>c</b>
<b>D</b>	
DBP	<b>DNA</b> <b>B</b> inding <b>P</b> rotein
DCI	3,4- <b>D</b> ichloroisocoumarin
DHE	<b>D</b> ihydroethidium, hydroethidine
DNA	<b>D</b> eoxyribonucleic acid
DPPI	<b>D</b> i-peptidyl-peptidase <b>I</b>
DTE	<b>D</b> ithioerythritol
DTT	<b>D</b> ithiothreitol
DTNB	5,5'-Dithio-bis(2-Nitrobenzoic acid)
dNTP	<b>D</b> eoxynucleotide triphosphates
DMSO	<b>D</b> imethyl sulfoxide
<b>E</b>	
E	Enzyme
EDTA	<b>E</b> thylenediamine tetraacetic acid
ELISA	<b>E</b> nzyme-linked immunosorbant assay
<b>F</b>	
FACS	<b>F</b> luorescence-Activated <b>C</b> ell <b>S</b> orter
FBS	<b>F</b> etal <b>B</b> ovine <b>S</b> erum
FCS	<b>F</b> etal <b>C</b> alf <b>S</b> erum
FITC	<b>F</b> luorescein (reactive isothiocyanate form)
FMK	<b>F</b> luoromethyl ketone
FPLC	<b>F</b> ast <b>P</b> rotein <b>L</b> iquid <b>C</b> hromatography



---

<b>G</b>	
GdmCl	<b>Guanidinium chloride</b>
GSH	Glutathione (reduced)
GSSH	Glutathione (oxydised)
<b>H</b>	
H <sub>2</sub> O <sub>2</sub>	Hydrogen peroxide
HL60	Human caucasian promyelocytic leukaemia cell line
HPLC	<b>H</b> igh <b>P</b> ressure <b>L</b> iquide <b>C</b> hromatography
HRP	<b>H</b> orseradish <b>P</b> eroxydase
<b>I</b>	
I	<b>I</b> nhibitor
IB	<b>I</b> nclusion <b>B</b> ody
IL-2	<b>I</b> nterleukin- <b>2</b>
IPTG	<b>I</b> sopropyl-β-D-thiogalaktosid
<b>J</b>	
JC-1	5,5',6,6'-tetrachloro-1,1',3,3'-tetraethylbenzimidazolyl-carbocyanine iodide
<b>K</b>	
K562	Erythroleukemia cell line
kDa	<b>K</b> ilodalton
<b>L</b>	
LB	<b>L</b> uria- <b>B</b> ertani (medium)
<b>M</b>	
ME	β- <b>M</b> ercaptoethanol
MES	2-Morpholinorthansulphonic acid
MIMP	<b>M</b> itochondrial <b>I</b> nter- <b>M</b> embrane-space <b>P</b> rotein
MMP	<b>M</b> itochondrial <b>M</b> embrane <b>P</b> ermeability
<b>N</b>	
NFPM	<b>N</b> on <b>F</b> at <b>P</b> owered <b>M</b> ilk
NK	<b>N</b> atural <b>K</b> iller (cell)
NP-40	<b>N</b> onidet <b>P</b> - <b>40</b>
<b>O</b>	
OD	<b>O</b> ptical <b>D</b> ensity
OMe	Esterified
<b>P</b>	
p	Fragment
PAGE	<b>P</b> olyacrylamide <b>G</b> el <b>E</b> lectrophoresis
PBMC	<b>P</b> eripheral <b>b</b> lood <b>m</b> ononuclear <b>c</b> ells
PBS	<b>P</b> hosphate <b>B</b> uffered <b>S</b> aline
PBS-T	<b>P</b> hosphate <b>B</b> uffered <b>S</b> aline - <b>T</b> ween
PCD	<b>P</b> rogrammed <b>C</b> ell <b>D</b> eath
PCR	<b>P</b> olymer <b>C</b> hain <b>R</b> eaction
PEG	<b>P</b> olyethylenglycol
PFN	<b>P</b> erforin
PI	<b>I</b> soelectric <b>P</b> oint / <b>P</b> ropidium <b>I</b> odide
PMSF	<b>p</b> henyl <b>m</b> ethanesulphonyl <b>f</b> luoride
pNA	<b>P</b> aranitroanilid
PS	<b>P</b> hosphytidyl <b>s</b> erine
PS-SCL	<b>P</b> ostion <b>s</b> canning <b>s</b> ynthetic <b>c</b> ombinatorial <b>l</b> ibraries
PVDF	Immunobilon-PSQ
RF	<b>R</b> efolding
ROS	<b>R</b> eactive <b>o</b> xygen <b>s</b> pecies
RNA	<b>R</b> ibonucleic <b>a</b> cid
RNase	<b>R</b> ibonuclease

rpm	<b>R</b> evolutions <b>p</b> er <b>m</b> inute
RPMI	<b>R</b> oswell <b>P</b> ark <b>M</b> emorial <b>I</b> nstitute
RT	<b>R</b> oom <b>T</b> emperature
<b>S</b>	
SB	<b>S</b> olubilisation
SD	<b>S</b> tandard <b>D</b> eviation
SDS	<b>S</b> odium <b>D</b> odecyl <b>S</b> ulphate
SBzl	<b>T</b> hioester
SET	<b>S</b> uppressor of variegation, <b>e</b> nhancer of zeste and <b>T</b> rithorax
SLO	<b>S</b> treptolysin <b>O</b>
Suc	<b>S</b> uccinyl
<b>T</b>	
T <sub>m</sub>	Annealing temperature
TEMED	<b>N,N,N',N</b> - <b>T</b> etraethyl <b>m</b> ethylendiamin
TMB	<b>3,3',5,5'</b> - <b>t</b> etramethyl <b>b</b> enzidine
Tris	<b>T</b> ris(hydroxymethyl)aminomethan
<b>U</b>	
U	<b>U</b> nit
U937	Human leukemic monocyte lymphoma cell line
<b>V</b>	
V	<b>V</b> olt
<b>W</b>	
WT	<b>W</b> ild type
<b>Z</b>	
Z	Benzyloxycarbonyl

## IX - Appendix

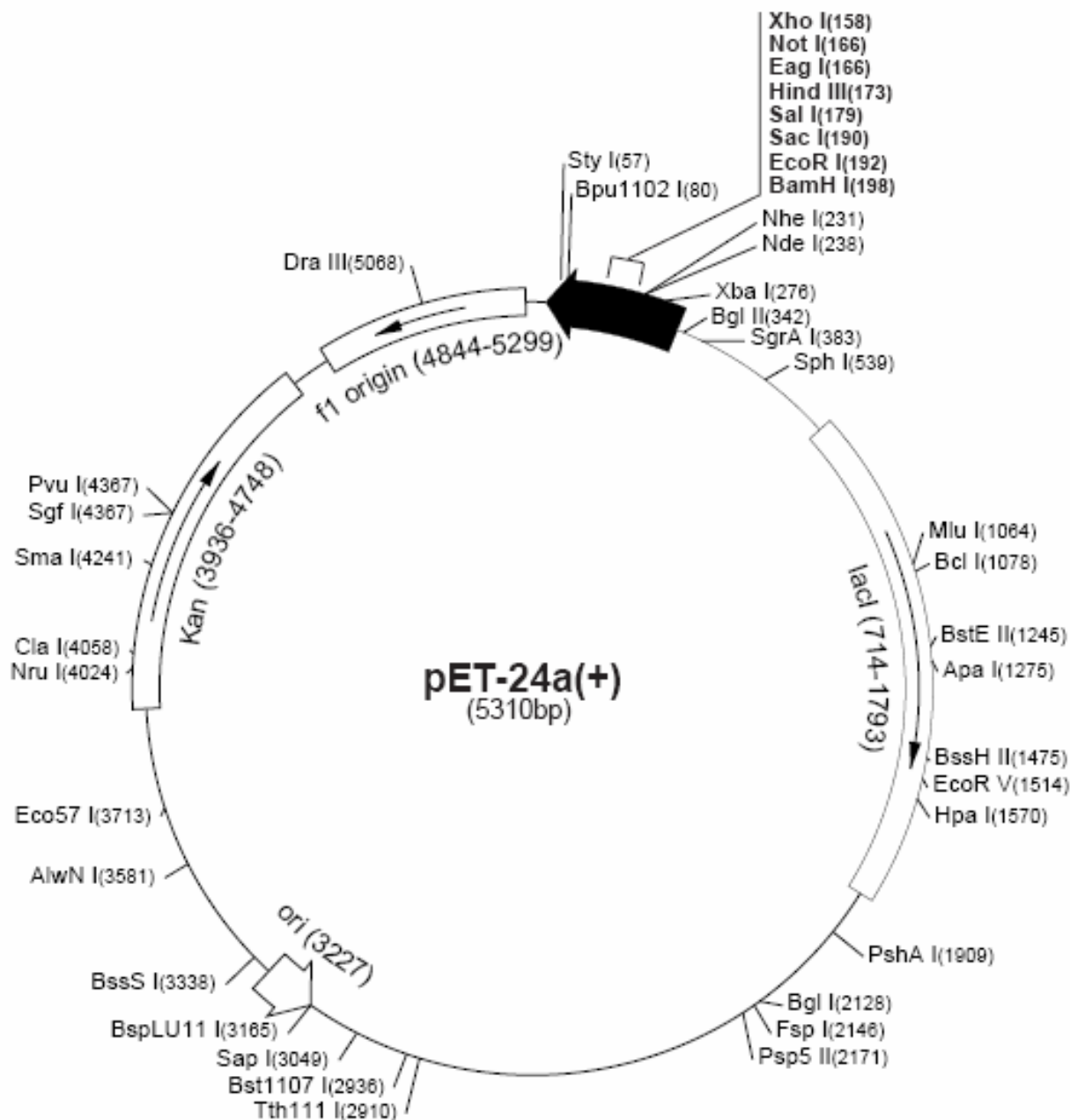


**Figure VIII.1 - Vector pET-24c(+).** The pET24c(+) vector contains kanamycin resistance. Unique sites are shown on the map. The sequence is numbered by the pBR322 convention, so that the T7 expression region is reversed on the map. The cloning/expression region of the coding strand transcribed by T7 RNA polymerase is shown. Refer to the Novagen pET-24a-d(+) vectors for full details. The pET24c(+)MKH<sub>6</sub>GzmH vector was constructed by cloning the MKH<sub>6</sub> codon sequence (introducing the *Pml* I site) into the vector's multiple cloning site, cleaved at restriction sites *Nde* I and *Bam* HI. GzmH cDNA was then cloned, directly upstream from the MKH<sub>6</sub> tag, into the *Pml* I and *Hind* III (173) cut pET24c(+)MKH<sub>6</sub> vector (see results section).

```

          9      18      27      36      45      54
1 catatcatcggtggccatgaggccaagccccactcccgccttacatggcctttgttcag
1  I  I  G  G  H  E  A  K  P  H  S  R  P  Y  M  A  F  V  Q
   (16)
      63      72      81      90      99      108      117
Tttctgcaagagaagagtcggaagaggtgtggcgccatcctagtgagaaaggactttgtg
20 F  L  Q  E  K  S  R  K  R  C  G  G  I  L  V  R  K  D  F  V

      126      135      144      153      162      171      180
ctgacagctgctcactgccaggggaagctccataaatgtcaccttgggggcccacaatatc
41 L  T  A  A  H  C  Q  G  S  S  I  N  V  T  L  G  A  H  N  I
   (57)
      189      198      207      216      225      234
aaggaacaggagcggacccagcagtttatccctgtgaaaagacccatcccccatccagcc
61 K  E  Q  E  R  T  Q  Q  F  I  P  V  K  R  P  I  P  H  P  A

      243      252      261      270      279      288      297
tataatcctaagaacttctccaacgacatcatgctactgcagatggagagaaaggccaag
81 Y  N  P  K  N  F  S  N  D  I  M  L  L  Q  M  E  R  K  A  K
   (99)      (102)
      306      315      324      333      342      351      360
tggaccacagctgtgcggcctctcaggctacctagcagcaaggccaggtgaagccaggg
101 W  T  T  A  V  R  P  L  R  L  P  S  S  K  A  Q  V  K  P  G

      369      378      387      396      405      414
cagctgtgcagtgtggctggctgggttatgtctcaatgagcacttttagcaaccacactg
121 Q  L  C  S  V  A  G  W  G  Y  V  S  M  S  T  L  A  T  T  L

      423      432      441      450      459      468      477
caggaagtgttgctgacagtgcagaaggactgccagtgtgaacgtctcttccatggcaat
141 Q  E  V  L  L  T  V  Q  K  D  C  Q  C  E  R  L  F  H  G  N

      486      495      504      513      522      531      540
tacagcagagccactgagatttgtgtgggggatccaaagaagacacagaccggtttcaag
161 Y  S  R  A  T  E  I  C  V  G  D  P  K  K  T  Q  T  G  F  K
   (189)
      549      558      567      576      585      594
ggggactccggggggcccctcgtgtgtaaggacgtagcccaaggatattctctcctatgga
181 G  D  S  G  G  P  L  V  C  K  D  V  A  Q  G  I  L  S  Y  G
   (195)      (216)
      603      612      621      630      639      648      657
aacaaaaaagggaacacctccaggagtctacatcaagggtctcacacttctgccttgatc
201 N  K  K  G  T  P  P  G  V  Y  I  K  V  S  H  F  L  P  W  I
   (226)
      666      675
Aaacgtaccatgaaacgcctctaaagct
221 K  R  T  M  K  R  L  -

```

**Figure VIII.2 - Human granzyme H (GzmH) nucleic- and amino-acid sequences in pET24c(+).**

The amino acid sequence is displayed in the single letter code, each representative letter positioned under the middle nucleic acid of each codon. The MKH<sub>6</sub> tag is not included but would precede the mature N-terminus sequence Ile-Ile-Gly-Gly. The amino acids in bold are conserved critical residues (bovine chymotrypsinogen A numbering) that determine the specificity of GzmH at the P1 (Thr189, Gly216 and Gly226) and P2 (Phe99) positions. Also highlighted are the three residues that constitute the catalytic triad (His57, Asp102 and Ser195). Ile16 is marked in bold as once the MKH<sub>6</sub> tag is removed, it proceeds to form a salt bridge with Asp194. The numbering above the cDNA sequence applies to the first nucleic acid of the codon. The red letters designate the nucleic acids after which restriction enzymes *Eco* RV (5'-End) and *Hind* III (3'-End) cut respectively. The stop codon is marked by a dash (-).

## ***X - Curriculum Vitae***

### **EDWARD FELLOWS**

11<sup>th</sup> June 1977 - Wesel, Germany

**Max Planck Institute of Neurobiology, Martinsreid, Germany**  
**Ph.D student, department of Neuroimmunology.**  
**Group of Dr. E. Jenne**

**Apr. 2003 –Present**

- Production and characterisation of recombinant granzyme H and investigation into the protease's role in cell death induction.
- Thesis title: Determination of granzyme H as a cell death inducing serine protease

#### **Pre PhD Period**

**May 2002 – Apr. 2003**

- Project title: Production of recombinant Granzyme B, study of its inhibition with serpins and assessment of its ability induce target cell death.

**University of Bath, U.K**  
**BSc in Molecular and Cellular Biology**  
Graduated with **Second Class, First Division Honours**

**Sept. 1996 – Jul. 2000**

- Industrial Placement Year (1998-1999): Research Project at Bayer AG, Monheim, Germany.  
Research Project: Transformation of the fungus *Botrytis cinerea* with GFP (*Aequorae victorea*).
- Final Year Research Project, 2000: Study of the murine *Cdx-1* homeobox gene promoter and the construction of reporter vectors for the detection of *its* expression.

**The European School, Culham, nr Oxford, U.K**  
**European Baccalaureate**

**Sept. 1994 – Jul. 1996**

School leaving qualification: The European Baccalaureate (Language of instruction: French).  
Subjects included: Biology, Chemistry, Maths, French, Philosophy, German, English, Geography and History.

**Lycee Viala-Lacoste, Salon de Provence, France**  
French secondary school

**Sept. 1993 – Jun. 1994**

**Collège de la présentation de Marie, Salon de Provence, France**  
**Brevêt des Collèges**  
School leaving qualification: **Brêvet des collèges.**

**Sept. 1989 – Jun. 1993**

## ***XI - Publications and Meetings***

### ***Publications***

Edward Fellows, Shirley Gil-Parado, Dieter E. Jenne and Florian C. Kurschus. Natural Killer cell-derived human granzyme H induces an alternative, caspase independent cell death program. *Blood*. 2007 Jul 15; 110(2):544-52.

Felipe Andrade, Edward Fellows, Dieter E. Jenne, Antony Rosen and C. S. H Young. Granzyme H destroys the function of critical adenoviral proteins required for viral DNA replication and granzyme B inhibition. *EMBO J*. 2007, 26(8):2148-57

Florian C. Kurschus, Roxana Bruno, Edward Fellows, Christine S. Falk, Dieter E. Jenne. Membrane receptors are not required to deliver Granzyme B during killer cell attack. *Blood*. 2005 Mar 1; 105(5):2049-58.

Florian C. Kurschus, Martin Kleinschmidt, Edward Fellows, Klaus Dornmair, Rainer Rudolph, Hauke Lilie, Dieter Jenne. Killing of target cells by redirected granzyme B in the absence of perforin. *FEBS Letters* 562 (2004) 87-92.

### ***Meetings***

Edward Fellows and Dieter E. Jenne. Recombinant Granzyme H, the road to characterisation. Oral presentation at the 21<sup>st</sup> Winter School on proteases and their inhibitors. February 25<sup>th</sup>-29<sup>th</sup>, 2004, Tiers, Italy.

Edward Fellows, Florian C. Kurschus, Shirley Gil Parrado and Dieter E. Jenne. Cell death induced by Granzyme H. Oral Presentation at the 22<sup>nd</sup> Winter School on proteases and their inhibitors. March 2<sup>nd</sup>-6<sup>th</sup>, 2005, Tiers, Italy.

Edward Fellows, Florian C. Kurschus and Dieter E. Jenne. Granzyme H, a killer in innate immunity. Poster presentation at the 1<sup>st</sup> joint meeting of European national societies of immunology. September 6<sup>th</sup>-9<sup>th</sup> 2006, Palais des Congrès Paris, France.

Edward Fellows, Florian C. Kurschus and Dieter E. Jenne. Granzyme H, a killer in innate immunity. Poster presentation at the the 14th FEBS Summer School on Immunology. September 10<sup>th</sup>-17<sup>th</sup> 2007, Hvar, Croatia.